

**Regulation of the floral transition
at the shoot apical meristem of
Arabidopsis as studied by genetics and
next generation sequencing**

Inaugural-Dissertation

zur

Erlangung des Doktorgrades

der Mathematisch-Naturwissenschaftlichen Fakultät

der Universität zu Köln

vorgelegt von

Stefano Torti

aus Narni (Italien)

Köln, April 2010

Die vorliegende Arbeit wurde am Max-Planck-Institut für Pflanzen Züchtungsforschung in Köln, in der Abteilung für Entwicklungsbiologie der Pflanzen (Direktor Prof. Dr. George Coupland) angefertigt.

Prüfungsvorsitzender: Prof. Dr. Martin Hülskamp

Berichterstatter: Prof. Dr. George Coupland
Prof. Dr. Wolfgang Werr

Tag der mündlichen Prüfung: 9. Juni 2010

Abstract

The floral transition is the process by which flowering plants switch from vegetative growth to the production of flowers. Consistent with the importance of this developmental transition, flowering is highly regulated through several genetic pathways, some of which respond to environmental cues. *Arabidopsis thaliana* flowers earlier under long-days (LD) of spring than under short-days (SD) of winter, and day-length, or photoperiod, is one of the most important environmental stimuli influencing the flowering response. Photoperiod is perceived in the leaves, while the floral transition occurs at the shoot apical meristem (SAM). In LD, a genetic cascade is activated in the leaf vasculature, so that a key transcriptional regulator called CONSTANS activates the genes *FLOWERING LOCUS T* (*FT*) and its homolog *TWIN SISTER OF FT* (*TSF*). FT protein is then transported through the phloem, eventually reaching the SAM, where it triggers the floral transition. By forming a complex with FD, a bZIP transcription factor, FT activates target genes, such as *SUPPRESSOR OF OVEREXPRESSION OF CO* (*SOC1*), *FRUITFULL* (*FUL*) and later *APETALA1* (*API*), all of which encode MADS-box transcription factors. However, the floral transition involves a dramatic transcriptional reprogramming of the shoot meristem, and a complete picture of the global changes in gene expression occurring specifically in the SAM is still missing. Therefore, in the first part of this work, SAMs were specifically collected by the use of laser microdissection from plants experiencing a shift from SD to LD. RNA isolated from the meristems was converted to cDNA and gene expression quantified through next-generation sequencing by RNA-seq. Genes were grouped according to those increased or reduced in expression, with a particular focus on novel genes that were up-regulated similarly to *SOC1* or *FUL*. Among them, the expression of a selected set of genes was tested by *in situ* hybridisation on wild-type apices to confirm their activation at the SAM, and to uncover their spatial pattern of mRNA expression. Several novel genes were confirmed to be induced by transferring plants to LD and they showed specific spatial patterns of expression in various regions of the SAM. Moreover, apices of *ft tsf* double mutants were also hybridised, to reveal whether those genes are induced by the photoperiodic cascade downstream of *FT/TSF*. Surprisingly, while many genes were induced only in the presence of *FT/TSF*, similarly to *SOC1*, some of them still respond to photoperiod in the *ft tsf* double mutants, suggesting that additional unknown signals may play a role in response to inductive day-length independently of *FT* and *TSF*. Further preliminary studies on a set of these novel genes are described in this study.

In the second part, genetic approaches were employed to address the function of *SHORT VEGETATIVE PHASE* (*SVP*), which encodes a floral repressor of the MADS-box family,

demonstrating new interactions with floral promoter genes and distinct roles of the *SVP* gene in the leaves and in the meristem.

Zusammenfassung

Der Vorgang bei welchem Angiospermen von vegetativem Wachstum zur Bildung von Blüten übergehen wird als Übergang zur Blüte („floral transition“) bezeichnet. Dieser entwicklungsbiologische Vorgang ist von großer Bedeutung und wird streng durch ein genetisches Netzwerk reguliert, wobei einige Komponenten des Netzwerkes auf Umweltfaktoren reagieren. *Arabidopsis thaliana* blüht früher unter Langtagbedingungen (LD) des Frühlings als unter den Kurztagbedingungen (SD) des Winters. Die Tageslänge oder Photoperiode ist einer der wichtigsten Umweltfaktoren welcher die Blühantwort beeinflusst. Die Photoperiode wird über die Blätter wahrgenommen während der Übergang zur Blüte im apikalen Sprossmeristem (SAM) stattfindet. Unter Langtagbedingungen wird eine genetische Kaskade im Leitgewebe des Blattes angestoßen, woraufhin ein Schlüsseltranskriptionsregulator mit dem Namen CONSTANS das Gen mit dem Namen *FLOWERING LOCUS T (FT)* und sein Homolog *TWIN SISTER OF FT (TSF)* aktiviert. Das FT Protein wird daraufhin durch das Phloem transportiert und erreicht schlussendlich das SAM wo es den Übergang zur Blüte auslöst. Durch Bildung eines Komplexes mit FD, einem bZIP Transkriptionsfaktor, aktiviert FT Zielgene wie *SUPPRESSOR OF OVEREXPRESSION OF CO (SOC1)*, *FRUITFULL (FUL)* und später *APETALA1 (API)*, welche für MADS-Box Transkriptionsfaktoren codieren. Der Übergang zur Blüte erfordert jedoch im SAM eine dramatische Neuprogrammierung der Transkriptionsvorgänge. Ein vollständiges Bild der Genexpression welche spezifisch im SAM stattfindet fehlt bislang. Daher wurden im ersten Teil dieser Arbeit apikale Sprossmeristeme durch Lasersezierung aus Pflanzen ausgeschnitten, welche von SD nach LD überführt worden waren. RNA, welche aus den Meristemen isoliert worden war, wurde in cDNA umgeschrieben und die Genexpression durch Next-Generation Sequencing durch RNA-seq quantifiziert. Die Gene wurden nach gesteigerter oder verringerter Expression sortiert, wobei ein besonderes Augenmerk auf neue Gene gelegt wurde deren Expression ähnlich der von *SOC1* und *FUL* gesteigert wurde. Ein Teil dieser Gene wurde über *in situ* Hybridisierung in Wildtyp-Apizes getestet um ihre Aktivierung im SAM zu bestätigen und ihr räumliches Expressionsmuster aufzuklären. Für mehrere neue Gene konnte die Induktion durch Transfer der Pflanzen in LD bestätigt werden; auch zeigten sie spezifische räumliche Expressionsmuster in zahlreichen Regionen des apikalen Sprossmeristems. Es wurden auch Apizes von *ft tsf* Doppelmutanten hybridisiert um aufzudecken ob die neuen Gene an der von der Photoperiode abhängige Kaskade folgend auf *FT/TSF* beteiligt sind. Während viele Gene ähnlich wie *SOC1* nur in Anwesenheit von *FT/TSF* induziert wurden, fanden sich erstaunlicherweise auch Gene welche auch in *ft tsf* Doppelmutanten noch auf die Photoperiode reagierten. Dies legt nahe, dass zusätzliche

unbekannte Signale eine Rolle in der Antwort auf eine induzierende Tageslänge unabhängig von *FT* und *TSF* spielen. In der vorliegenden Arbeit werden auch weitere Untersuchungen neuer Gene beschrieben.

Im zweiten Teil der vorliegenden Arbeit wurden genetische Ansätze verwendet um die Funktion von *SHORT VEGETATIVE PHASE (SVP)*, einem Blührepressor aus der MADS-Box Familie, zu untersuchen. Hierbei wurden neue Interaktionen mit die Blüte fördernden Genen und spezifische Rollen des *SVP* Gens in Blättern und Meristem aufgedeckt.

Table of contents

Abstract	I
Zusammenfassung	III
Table of contents	V
1. Introduction	
1.1 Plant development and the floral transition.....	1
1.2 Flowering pathways.....	2
1.2.1 Vernalisation pathway	
1.2.2 Autonomous pathway	
1.2.3 Gibberellin pathway	
1.3 Photoperiodic pathway and activation of flowering.....	7
1.3.1 Circadian clock	
1.3.2 The photoperiodic cascade	
1.3.2.1 <i>GIGANTEA</i>	
1.3.2.2 <i>CONSTANS</i>	
1.3.2.3 <i>FT</i> and <i>TSF</i>	
1.4 The repression of flowering by <i>FLC</i>	13
1.5 The repression of flowering by <i>SVP</i>	14
1.6 The early floral transition: from vegetative meristem to inflorescence meristem.....	17
1.6.1 The floral pathway integrators: classical and new members	
1.6.1.1 <i>FT</i> as an integrator	
1.6.1.2 <i>FT</i> and <i>FD</i>	
1.6.1.3 <i>SOCI</i>	
1.6.1.4 <i>AGL24</i>	
1.6.1.5 <i>LFY</i> as an integrator	
1.6.2 <i>FUL</i> in the floral transition	
1.6.3 <i>SPL</i> genes: another chapter in the floral transition?	
1.7 The later phase of the floral transition: from inflorescence meristem to floral meristem.....	27
1.7.1 Floral meristem identity genes	
1.7.1.1 <i>LFY</i>	
1.7.1.2 <i>API</i> and <i>CAL</i>	

1.7.1.3 <i>FUL</i>	
1.7.2 <i>TFL1</i>	
1.7.3 Flower development and the ABC model	
1.7.4 Flowering time genes regulate floral patterning	
1.8 The shoot apical meristem: balance between stem cell maintenance and organ production.	33
1.9 Genomics approaches to study the floral transition.....	35
1.9.1 “Single cell” technology	
1.9.2 Next-generation-sequencing technologies and gene expression analysis	
1.9.3 Recent genomics studies on SAM	
Objectives.....	41
2. Materials and methods.....	42
3. Global gene expression analysis of the floral transition at the SAM collected by LCM using next-generation sequencing.....	55
3.1 Defining the floral transition in <i>Arabidopsis thaliana</i>	55
3.1.1 Shift and double shift experiments to study the floral transition	
3.1.2 <i>In situ</i> hybridisation on marker genes	
3.1.3 Double shift experiments to link expression of flowering time genes to floral commitment	
3.2 Laser microdissection of shoot apical meristems.....	65
3.2.1 Calculation of the material needed and choice of the techniques	
3.2.2 Optimization of the protocol	
3.2.3 Collection of the SAMs	
3.2.4 RNA extraction from the captured material and RNA amplification	
3.2.5 Single strand cDNA synthesis to test the RNA extracted from the meristems	
3.2.6 Double strand cDNA synthesis for sequencing	
3.3 Next-generation sequencing for gene expression analysis in the SAM.....	77
3.3.1 Deep sequencing with Illumina-Solexa and mapping of the short-sequence reads	
3.3.2 Quality controls and reliability of the replicates	
3.3.3 Use of housekeeping genes for the normalization	
3.3.4 Expression values for known genes	
3.3.5 Data analysis: identification of differentially expressed genes	

3.3.6 GO term enrichment analysis

4. Characterization of novel genes induced during the floral transition selected from gene expression analysis	93
4.1 Selection of the genes.....	93
4.2 Validation of the gene expression data: <i>in situ</i> hybridisations on candidate genes.....	95
4.3 The use of mutants to test the response of the candidate genes to flowering pathways.....	101
4.4 <i>D13</i> : a lipid desaturase induced by photoperiod independently of <i>FT</i> and <i>TSF</i>	103
4.4.1 On the expression pattern of <i>D13</i> : possible interactions with <i>TFL1</i>	
4.4.2 On the signal inducing <i>D13</i> : triggering flowering without LD	
4.4.3 Modulation of <i>D13</i> expression with transgenic approaches	
4.5 <i>C11</i> : a homeo-domain transcription factor which is dependent on <i>FT/TSF</i>	111
4.5.1 <i>C11</i> has close homologues which might play redundant roles with it	
4.6 <i>C19</i> : a LRR protein responding to <i>FT/TSF</i>	113
4.6.1 Loss of function of <i>C19</i> may influence flowering	
4.7 Some bZIP transcription factors partially respond to <i>FT/TSF</i>	116
4.8 Several genes are related to the growth of the meristem in response to <i>FT/TSF</i>	118
4.9 An unknown protein induced in the center of the SAM by <i>FT/TSF</i>	119
5. The role of <i>SVP</i> in leaf and meristem and the control of flowering time	121
5.1 Loss of function of single floral promoter genes does not overcome the early flowering phenotype of <i>svp</i> mutants.....	121
5.2 <i>SVP</i> and the leaf: genetic and spatial interactions.....	123
5.2.1 Role of <i>SVP</i> in the leaf and its relationship to <i>FT</i> and <i>TSF</i>	
5.2.2 <i>SOCI</i> in relation to <i>SVP</i> , <i>FT</i> and <i>TSF</i> .	
5.2.3 Mis-expression of <i>SVP</i> in the leaf vasculature	
5.3 <i>SVP</i> and the meristem: genetic and spatial interactions.....	133
5.3.1 Role of <i>SVP</i> in the SAM and relation to <i>SOCI</i> and <i>FUL</i>	
5.3.2 Mis-expression of <i>SVP</i> in the meristem	
5.3.3 Double shift experiments with mutants in flowering time genes	
5.4 Dual role of <i>SVP</i> : leaf and meristem.....	144
5.4.1 Quintuple mutant	
5.4.2 Combined effect of mis-expression	
5.5 Mis-expression of <i>SVP.2</i> in different tissues.....	147

6. Discussion	149
6.1 Known genes and novel mechanisms that regulate the floral transition.....	149
6.2 Next-generation sequencing for global gene expression analysis.....	151
6.2.1 Comparison with available microarray data	
6.2.2 General features of the data	
6.3 Classification of the genes selected from the dataset.....	154
6.4 Time of the response to the inducing photoperiod.....	154
6.5 Spatial pattern of expression.....	155
6.6 Biological and molecular functions of the genes up-regulated during the floral transition...	157
6.6.1 Transcription factors and proteins involved in signaling	
6.6.1.1 <i>C19</i>	
6.6.1.2 <i>C11</i>	
6.6.2 Additional layers of regulation	
6.6.3 Genes involved in metabolism	
6.6.4 Growth is a key process for the floral transition	
6.6.4.1 Meristem growth	
6.6.4.2 <i>FT</i> , “florigen”, and growth	
6.7 Response to FT/TSF and responsiveness of <i>ft tsf</i>	167
6.8 A novel signal identified in response to shift in photoperiod.....	168
6.9 <i>SVP</i> represses many genes.....	170
6.10 Is <i>SVP</i> a general repressor or is it downstream of photoperiodic induction?.....	171
6.11 Double action leaf-meristem.....	172
6.12 <i>SVP</i> and <i>FLC</i>	172
6.13 A quintuple mutant reveals additional targets of <i>SVP</i>	174
Conclusions	175
Perspectives	177
References	179
Appendix I	196
Appendix II	201
Appendix III	209
Acknowledgments	211
Erklärung	212
Lebenslauf	213

1. Introduction

1.1 Plant development and the floral transition

Plants differ from animals in many aspects of their biology and have evolved different strategies to adapt to the environment. For example, plants cannot move and therefore have evolved an extraordinary variety of mechanisms to respond to diverse environmental stimuli and to adapt to changes in their surroundings. Moreover, plants use a distinct developmental strategy, because while animals undergo major developmental changes during embryogenesis, plants can also undertake dramatic changes in their morphology post-embryonically (Weigel and Jürgens, 2002).

One of the best examples of post-embryonic plant developmental changes is the floral transition, which drives a switch from vegetative growth to reproductive development. This process is regulated by a number of different components, including not only internal changes but also environmental factors, because plants need to synchronize the production of flowers with the most favorable conditions and season of the year.

This switch in development involves a structure that is located at the apex of the plant shoot, called the shoot apical meristem (SAM). This is a group of undifferentiated cells formed during embryogenesis that is ultimately responsible for producing all above-ground organs of the plant. The SAM must change its identity and shift from the stage of a vegetative meristem, which produces leaves, to the stage of an inflorescence meristem, which produces flowers. This change in identity is a prerequisite for reproductive development to occur.

The timing of flowering is clearly very important to ensure the production of seeds and the perpetuation of a plant species. It is also important in agriculture as for many crop plants the seeds are harvested. Therefore a large effort has been made in recent years to understand the mechanisms of regulation of flowering processes and flowering time in plants. Most of this knowledge has been obtained by studying the model plant *Arabidopsis thaliana* (*Arabidopsis*), through genetic analyses, biochemical and physiological approaches. *Arabidopsis* is a particularly suitable system to study flowering. The life cycle of many accessions of this plant is fast, around three months in total. After germination, a seedling starts the cycle with an initial phase called “vegetative”. When the plant is old enough it is then able to respond to inductive stimuli and to switch to a phase called “reproductive” in which it develops flowers. These in turn produce fruits, in this case called siliques. Fruits contain and finally release the seeds, while the plant becomes senescent and then dies. The seeds generate new plants, re-starting the cycle from the beginning. *Arabidopsis* is an

Introduction

annual plant, completing its life cycle within one year, and upon floral transition all the shoot meristems which are generated in the individual plant are induced to flower so that the entire plant starts the senescence process and cannot survive to the following year.

Arabidopsis has a number of additional features which are especially useful for dissecting the genetics of flowering and of other processes in general (Koorneef and Meinke, 2010), such as a relatively small genome size compared to most of the other higher plant species. The genome has been fully sequenced (The *Arabidopsis* genome initiative, 2000). Also, natural variation within the species regarding flowering time produced an even richer scenario to study the genetic basis of flowering regulation. For some accessions, also the genome sequences are becoming available (Ossowski et al. 2008a). *Arabidopsis* is a diploid organism, is self pollinating, and relatively easy to use for genetic crosses. It is also easy to transform in a stable manner with exogenous DNA. Several collections of mutants were generated, and several genetic and genomic tools are also available (O' Malley and Ecker, 2010).

On the other hand, some aspects of development at the level of the shoot apical meristem have been hindered so far by the small size of this organ in *Arabidopsis*. Therefore, this disadvantage resulted in a delay of the study of this particular aspect within flowering, and the developmental biology of the floral transition, especially at the genomic level, still needs to be elucidated.

1.2 Flowering pathways

Five major genetic pathways controlling flowering have been described in *Arabidopsis* (Boss et al., 2004): the photoperiodic pathway, the vernalisation pathway, the autonomous pathway, the gibberellin pathway and the age-related pathway (Fornara and Coupland, 2009) (**Fig. 1** and **Fig. 2**). In addition other factors and less characterized pathways also play a role in the regulation of flowering, such as ambient temperature (Blázquez et al., 2003; Halliday et al., 2003; Lee et al., 2007b), light quality (Cerdan and Chory, 2003) and several other hormones (Davis, 2009). Interestingly, while new aspects of flowering time regulation are continuously uncovered, rendering these networks more and more detailed and inter-connected, some of the key genes and mechanisms are shared even among distantly related species, whereas others are not conserved and give rise to important differences between plant species.

Arabidopsis is a facultative long-day plant, which means it flowers earlier in long day (LD) and later in short days (SD). The mechanism by which plants flower in response to day-length, or photoperiod, resides in the so-called photoperiodic pathway.

Introduction

Another pathway responding to an external stimulus, in this case extended exposure to low temperature for several weeks, is the vernalisation pathway. Vernalisation is a prolonged period of cold that some plant species and some winter-annual accessions of *Arabidopsis* have to experience in order to be able to flower. Together with the photoperiod, this pathway enables a plant to initiate the flowering process soon after winter, and it prevents premature flowering which would cause the reproductive structures to be damaged by the cold.

The other three pathways respond to endogenous signals. The autonomous pathway controls flowering via fundamental mechanisms of gene expression such as 3'-end site selection, the gibberellin pathway in relation to endogenous hormonal levels, and the ageing pathway through a microRNA whose level falls as the plant gets older. Importantly, the pathways are not entirely separate, but they have some genes in common, and they finally converge in a small set of key floral-promoting genes, which for that reason are called “floral pathway integrators” (Fig. 1).

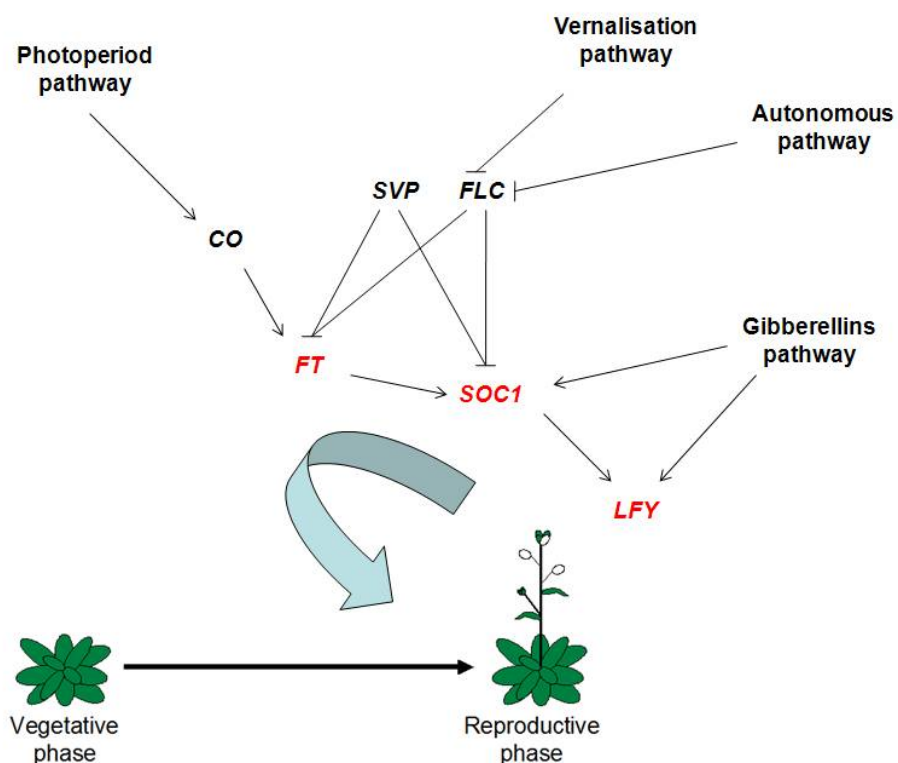


Fig. 1. Flowering pathways in *Arabidopsis thaliana*. A general scheme of the most characterized genetic pathways influencing flowering is shown in the figure. Genes marked in red color are “floral pathway integrators”.

1.2.1 Vernalisation pathway

The vernalisation pathway allows flowering after the plant is exposed to an extended period of low temperature (vernalisation), preventing flowering during the unfavourable winter season. In *Arabidopsis*, winter-annual accessions respond to vernalisation because they carry active alleles at two loci, *FRIGIDA* (*FRI*) and *FLOWERING LOCUS C* (*FLC*). Commonly used *Arabidopsis* ecotypes Columbia (Col) and Landsberg *erecta* (*Ler*) are null mutants of *FRI*.

FRI encodes a nuclear protein present only in plants (Johanson et al., 2000), and it increases *FLC* expression by a mechanism that remains unclear (Michaels and Amasino, 1999; Michaels and Amasino, 2001). In plants having an obligate vernalisation requirement *FLC* is expressed at high level and strongly delays flowering because it represses key floral promoter genes, such as *FLOWERING LOCUS T* (*FT*) and *SUPPRESSOR OF OVEREXPRESSION OF CONSTANS* (*SOCI*). When the plant experiences vernalisation, *FLC* mRNA expression is reduced (Michaels and Amasino, 1999) and thus flowering is permitted.

The reason for this reduction in expression is related to chromatin modifications at the *FLC* locus. Indeed, the *FLC* gene is under epigenetic regulation, so after proper exposure to cold it is stably maintained in a silent state, and even after a return to warm temperature this gene is not re-activated in *Arabidopsis*. This phenomenon requires the activity of proteins such as VERNALIZATION INSENSITIVE 3 (*VIN3*), VERNALIZATION1 (*VRN1*), *VRN2*, *VRN5/VIN3-LIKE1* (*VIL1*) (Kim et al, 2009 for a review). *VIN3*, which encodes a PHD protein, is expressed during vernalisation, but its expression drops once plants are returned to warm temperature, so that it seems to be involved in the first part of the repression mechanism of *FLC* (Sung and Amasino, 2004). Vernalisation results in the increase in methylation of lysine 9 and lysine 27 of histone H3, which are repressive histone modifications, at the *FLC* locus (Bastow et al., 2004; Sung and Amasino, 2004). In *vin3* and *vrn2* mutants, and partially in *vrn1* mutants, these methylation events do not occur at the *FLC* locus, and the *FLC* gene is not repressed upon vernalisation (Bastow et al., 2004; Sung and Amasino, 2004). *VRN2* encodes a component of Polycomb repression complex 2 (*PRC2*) (Gendall et al., 2001), while *VRN1* is a DNA-binding protein with B3 domains. *VRN5/VIL1*, another PHD protein, is also required for these modifications (Greb et al., 2007; Sung et al., 2006).

Other specific chromatin modifications are associated with *FLC* activation (Kim et al., 2009).

Interestingly, in the related perennial species *Arabis alpina* the orthologue of *Arabidopsis FLC*, *PEP1*, is also repressed by vernalisation but this repression is not stably maintained when plants return to warm temperature the following year (Wang et al., 2009b). This mechanism is related to

the different life strategy of this plant. In *pepl* mutants, indeed, both the requirement for vernalisation and the seasonal flowering behavior are lost.

1.2.2 Autonomous pathway

A group of mutants not belonging to the other pathways were grouped into a so-called autonomous pathway. Their common feature is being later flowering than wild-type both in LD and SD (Koornneef et al., 1991). The late flowering behavior of these mutants is similar to *FRI*-active accessions (Michaels and Amasino, 2001), because they present a high *FLC* expression level, and they are accelerated in flowering-time upon vernalisation treatment. Indeed, the autonomous pathway promotes flowering by decreasing the level of the mRNA of the *FLC* transcriptional repressor. Rather than a linear pathway, this pathway is a collection of at least eight genes, *FCA*, *FY*, *FPA*, *FVE*, *FLOWERING LOCUS D (FLD)*, *FLK*, *LUMINIDEPENDENS (LD)* and *RELATIVE OF EARLY FLOWERING 6 (REF6)*, which converge on *FLC* regulation (Simpson, 2004; Noh et al., 2004). They encode mainly proteins associated with chromatin structure or RNA-binding proteins.

FLD encodes a protein homologous to a member of a human histone deacetylase complex, which would be involved in deacetylation of *FLC* chromatin to prevent its transcription and promote flowering (He et al., 2003). *FVE* encodes a WD-repeat protein, also associated with histone deacetylation (Ausin et al., 2004). *REF6* encodes a jumonji/zinc-finger-class transcription factor, also required for histone deacetylation of *FLC* locus (Noh et al., 2004).

FCA (Macknight et al., 1997), *FPA* (Schomburg et al., 2001) and *FLK* (Lim et al., 2004; Mockler et al., 2004) proteins contain putative RNA binding domains. *FY* encodes a protein homologous to Pfs2p, a poly-adenylation and 3'-end processing factor in yeast. *FCA* has a complex but well studied regulation. Its transcripts have alternative forms, and *FCA* itself negatively regulates its own expression, promoting the inactive splicing form with an internal poly-adenylation site (Quesada et al., 2003; Macknight et al., 2002). This mechanism is *FY*-dependent, and *FY* and *FCA* proteins physically interact (Simpson et al., 2003).

LD encodes a homeodomain protein with unknown function (Lee et al., 1994).

1.2.3 Gibberellin pathway

Gibberellins (GAs) are plant hormones required for plant growth. They act through promotion of cell division and elongation, and they also promote developmental switches, including flowering.

Introduction

The effect of GAs on flowering is more pronounced in SD, and the GA pathway has been shown to be particularly important in the absence of the activation of the photoperiodic pathway (Reeves and Coupland, 2001). Indeed, for example *gal* mutants, which lack the first step of GA biosynthesis, never flower in SD. *gai* mutants, which instead are insensitive to GA, are also late flowering in SD (Wilson et al., 1992). *gal-3*, a highly GA-deficient mutant (Koornneef and Van der Veen, 1980), is severely dwarfed, regardless of photoperiod, since bolting in *Arabidopsis* is absolutely dependent on GA signaling (Mutasa-Göttgens and Hedden, 2009). Conversely, *spindly* mutants, which have constitutively active GA signaling, are early flowering (Jacobsen and Olszewski, 1993).

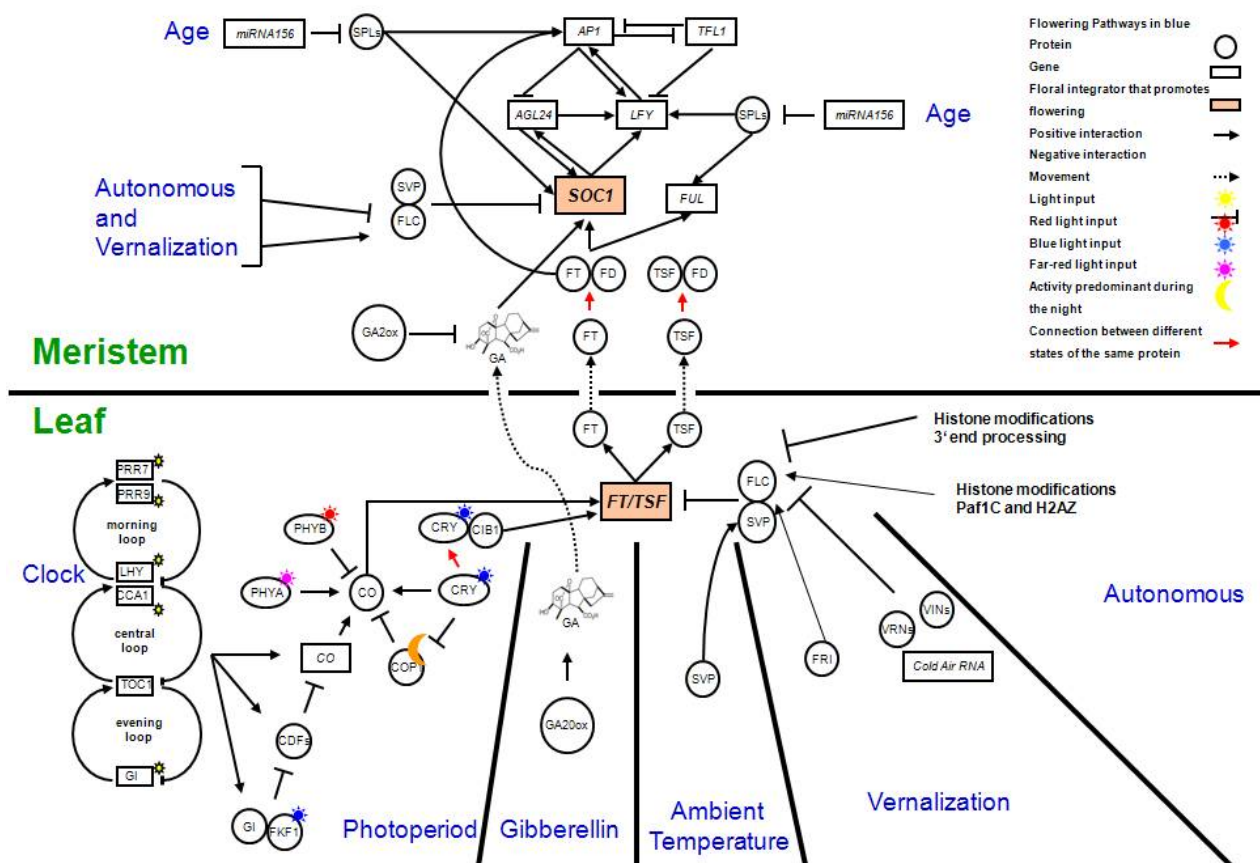


Fig. 2. Genes involved in the control of the floral transition. Some relevant genes involved in flowering and their relationships are shown. Details are given in the text. The scheme was kindly provided by Fabio Fornara.

1.3 Photoperiodic pathway and activation of flowering

The “photoperiodic pathway” acts in response to the photoperiod, or day length. Day length is one of the major environmental factors regulating flowering time. Indeed, the characteristic of many plant species to flower in response to changes in photoperiod synchronises flowering with the favourable season. For example *Arabidopsis* flowers in response to increased day lengths of spring, whereas rice flowers in response to short days to avoid drought periods.

Interestingly, the perception of photoperiod in plants takes place in the leaves, while the floral transition happens in the SAM, where the floral structures will arise, and although this has been known for a long time, the molecular mechanism underlying this phenomenon have been revealed only recently (Turck et al., 2008 for a review).

The ability of plants to measure day length and respond to its changes is based on the interaction of light with an internal housekeeping mechanism that plants use to measure time, the so-called “circadian clock”.

1.3.1 Circadian clock

Plants are able to generate circadian rhythms, with a period of approximately 24 hours. This system is composed of the clock core or central oscillator, which generates the timing, of input pathways that synchronise the clock oscillator to daily cycles of light and dark, and of output pathways regulating various specific processes that are under circadian influence (Salome and McClung, 2004; Strayer and Kay, 1999). One of the rhythmic outputs generated by the circadian clock is the photoperiodic regulation of flowering (Imaizumi, 2010 for a review). Input pathways synchronising the clock are mediated for example by the photoreceptors. Some of the families of photoreceptors participating in clock entrainment are phytochromes, cryptochromes and the ZTL family (Ausin et al., 2005). Proteins that have been shown to be at the centre of the circadian oscillator are CCA1, LHY, TOC1, which create a feedback loop of approximately 24 hours (Alabadi et al., 2001). Their mRNAs are expressed in a circadian rhythm, but *LHY* and *CCA1* mRNA levels peak at dawn, while *TOC1* mRNA level peaks at dusk. *CCA1* and *LHY* repress the expression of *TOC1*. *TOC1* activates *LHY* and *CCA1*. Mathematical models postulated additional loops to account for the real complexity of the data (Locke et al., 2005). Experimental studies supported this hypothesis. Another loop includes *TOC1*, *CCA1*, *LHY* and a Y component, which has been suggested to be the *GI* gene (Locke et al., 2005). Finally, *PRR7* and *PRR9*, two proteins similar to *TOC1* containing a CCT motif, form together with *CCA1* and *LHY* an additional loop (Zeilinger et al., 2006). Therefore the

plant circadian clock is composed of three interlocked transcriptional feedback loops (**Fig. 2**), and additional regulation is provided to the clock at the post-transcriptional level (Harmer, 2009 for a review).

1.3.2 The photoperiodic cascade

Classically, the three key genes *GIGANTEA* (*GI*), *CONSTANS* (*CO*) and *FLOWERING LOCUS T* (*FT*) were all assigned to the photoperiodic pathway in *Arabidopsis*. This was shown by genetic analysis (Redei, 1962; Koornneef et al., 1991; Koornneef et al., 1998), since the loss-of-function of these genes delays flowering under long days (LD) but not in short days (SD). Other studies demonstrated that the hierarchy of activation is *GI-CO-FT* (Kardailsky et al., 1999; Kobayashi et al., 1999; Samach et al., 2000; Suárez-López et al., 2001).

Nowadays a linear model *GI-CO-FT* is only a simplified version of a more complex situation. This main branch still accounts for the major contribution to the photoperiodic pathway, but at the molecular level many other details and players have been revealed (**Fig. 2**).

1.3.2.1 *GIGANTEA*

A gene called *GIGANTEA* (*GI*) plays a role both in the circadian system itself, and in controlling flowering as an output of the circadian clock, and it has been shown that these functions are distinct (Mizoguchi et al., 2005). *gi* mutants for example are altered in period length of the circadian rhythm, they have reduced amplitude of *LHY* and *CCA1* mRNA (Fowler et al., 1999; Park et al., 1999; Mizoguchi et al., 2002) and some alleles cause a long hypocotyl in deetiolated seedlings particularly under red light, because they are impaired in *phyB* signaling (Huq et al., 2000).

GI, as an output of the clock, is circadian regulated with a peak of expression of its mRNA 10 hours after dawn (Fowler et al 1999, Park et al 1999). *gi* mutants are late flowering in LD, and in this background the mRNA of *CO* is reduced (Suárez-López et al., 2001). Conversely, plants over-expressing *GI* from the *35S* promoter are early flowering both in LD and SD (Mizoguchi et al., 2005) and express *CO* and *FT* mRNA at higher level. *GI* promotes the transcription of *CO*, and connects in this way the circadian clock to the photoperiodic pathway. Nevertheless, in *co* or *ft* background *35S::GI* can still partially accelerate flowering, possibly through other pathways independent of *CO* and *FT* (Mizoguchi et al., 2005). For example, a mechanism in which *GI* controls *FT* independently of *CO* was reported, where a microRNA, miR172, is involved in the pathway (Jung et al., 2007).

Introduction

GI encodes a nuclear protein (Huq et al., 2000), with a large size, composed of 1173 amino acids. Though the molecular and biochemical functions of *GI* remained for a long time unknown, lately some progress has revealed new aspects of this protein. Interaction of *GI* protein with the F-box protein ZEITLUPE (*ZTL*) is necessary to establish and sustain circadian oscillations of *ZTL*, through a post-translational mechanism (Kim et al., 2007). *ZTL* protein then sustains the circadian clock by mediating the ubiquitination and degradation of *TOC1*.

One mechanism that has been proposed to explain the promotion of *CO* transcription is based on the interaction of *GI* protein with the FLAVIN-BINDING, KELCH REPEAT, F-BOX1 (*FKF1*) and CYCLING DOF FACTOR1 (*CDF1*) proteins, which associate on *CO* chromatin (Sawa et al., 2007). Interaction of *GI* protein with *FKF1* protein would promote the *FKF1*-dependent degradation of *CDF1* protein, which is a repressor of *CO*, leading to *CO* transcription (Sawa et al., 2007). Recently, other members of the DOF transcription factor family were shown to redundantly repress *CO* expression. The abundance of *CDF2* protein is also regulated by *GI* (Fornara et al., 2009). *CDF1*, *CDF2*, *CDF3* and *CDF5* when over-expressed in phloem companion cells delay flowering and decrease *CO* expression, while a quadruple mutant lacking all four genes is early flowering both in LD and SD and photoperiodic-insensitive, with *CO* expressed at higher level but still following the circadian pattern (Fornara et al., 2009). Interestingly, when also *GI* is mutated in this background, both the response to photoperiod and the circadian pattern of *CO* are restored in the quintuple mutant (Fornara et al., 2009). Therefore, it seems that *GI* is not essential for the transcription and for the diurnal oscillation of *CO*, but rather required to enhance it by removing the repression exerted by the *CDF* proteins.

1.3.2.2 *CONSTANS*

CO encodes a nuclear protein containing two zinc-finger domains (Putterill et al., 1995; Samach et al., 2000; Robson et al., 2001). According to expression studies based mainly on *GUS* reporter constructs, *CO* mRNA is expressed in vascular tissue, in hypocotyl, cotyledons and leaves, and also at the apex (Takada and Goto, 2003; An et al 2004). However, it has been shown that *CO* acts in the phloem companion cells, activating its target gene *FT* in a cell-autonomous manner, and then resulting in activation of floral development at the apex (An et al., 2004). A systemic signal activated by *CO* crosses graft junctions, and does not require movement of *CO* protein, as shown by analysis of *CO*:GFP fusion (An et al., 2004).

CO is a central regulator of flowering time, and not only the gene itself is finely regulated at the

Introduction

transcriptional level (see previous paragraph) but also the protein is regulated at the post-transcriptional level through multiple mechanisms (**Fig. 2**).

CO expression is under circadian regulation, with a marked peak of its mRNA level at the end of the day (Suarez-Lopez et al., 2001) (**Fig. 3**). In this way, this gene mediates between the circadian clock and photoperiodic control of flowering time. Nevertheless, CO protein level depends not only on the relative RNA pattern but also on the light condition, because exposure to light is necessary to activate CO protein function (Valverde et al., 2004). If the plants grow in SD, the peak of *CO* falls in the dark period (night), when CO protein is not stabilized and it is degraded. In LD, this peak is at dusk (Suarez-Lopez et al., 2001; Yanovsky and Kay, 2002; Imaizumi et al., 2003). In this condition CO protein, in response to light, is stabilized, and it directly activates the expression of *FT* (Kardailsky et al., 1999; Kobayashi et al., 1999; Samach et al., 2000; Valverde et al., 2004) thus triggering flowering.

The so-called “external coincidence model” was formulated decades ago (Bünning, 1936; Pittendrigh and Minis, 1964), before knowing any molecular mechanisms underlying flowering, to explain the photoperiodic response. This model seems to fit with the current model of *CO* regulation. In this view, a coincidence of the peak of expression of *CO* mRNA with the exposure to an external condition (light), has to be fulfilled to have an active function and activate flowering (**Fig. 3**).

White light, blue light and far-red light stabilize CO protein, while red light and dark promote its degradation through the proteasome (Valverde et al., 2004). CRYPTOCHROME1 (CRY1), CRY2 and PHYTOCHROME A (PHYA) photoreceptors are involved in the stabilization of CO protein (Yanovsky and Kay, 2002; Valverde et al., 2004). The two cryptochromes (CRY1 and CRY2) stabilize CO in blue light and both at the beginning and at the end of the day. PHYA stabilizes CO in far-red light, and similarly to the cryptochromes during the day. Conversely, PHYB photoreceptor is responsible for the reduction of CO protein level, in red light and during the morning (Valverde et al., 2004). In *35S::CO* background, *cry1 cry2* and *phyA* mutations delay flowering while *phyB* mutation accelerates flowering, in agreement with the previous observations on the effects of the various photoreceptors on CO abundance and with the relative levels of *FT* expression, as an output of CO activity (Valverde et al., 2004). Recently, SUPPRESSOR OF PHYA (SPA) proteins have been implicated in the control of stability of CO protein (Laubinger et al., 2006). *spa1* mutants are early flowering in SD, and *spa1 spa3 spa4* even earlier, because of a dramatic up-regulation of *FT* expression. The *co* mutation suppresses the early flowering of *spa1*

Introduction

mutation. However, in absence of *SPA1* the expression of *CO* mRNA is not altered, but there is a high increase of CO protein abundance. Moreover, SPA proteins have been shown to physically interact with CO protein, both *in vitro* and *in vivo* (Laubinger et al., 2006). More recently, it has been shown that an ubiquitin ligase called CONSTITUTIVE PHOTOMORPHOGENIC 1 (COP1) promotes the degradation of CO protein in the dark (Jang et al., 2008). Indeed, *cop1* mutants are early flowering, they also show an increase in *FT* expression, and they are even able to flower in darkness. Mutation in *CO* partially suppresses the early flowering of *cop1*. Indeed, in *cop1* mutant CO protein is stabilized in the night period, but not in the morning. Moreover, CO and COP1 proteins have been shown to physically interact (Jang et al., 2008). This provides additional molecular details on how flowering response to day length is achieved.

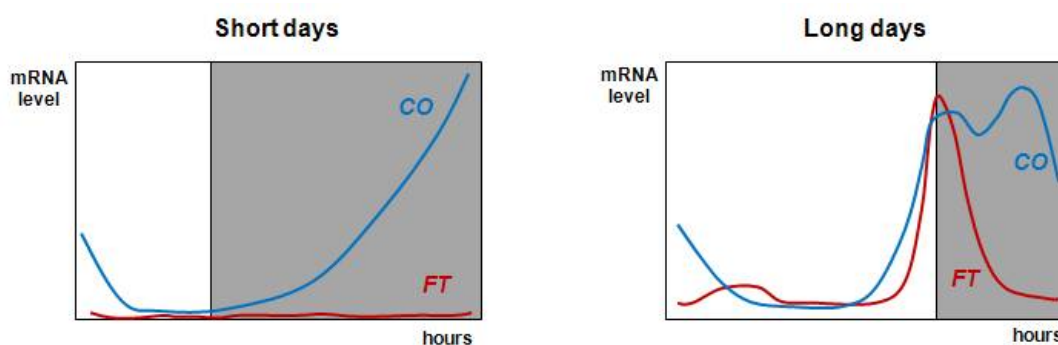


Fig. 3. Expression patterns of *CO* and *FT* mRNA. A schematic representation shows the expression pattern of the mRNAs of these two genes during a 24 hours daily cycle.

1.3.2.3 *FT* and *TSF*

FT encodes a small protein with similarity to RAF-kinase inhibitor proteins in animals (also known as phosphatidyl ethanolamine-binding proteins) (Chardon and Damerval, 2005).

Over-expression of *FT* causes a dramatic early flowering, both in LD and SD (Kardailsky et al., 1999; Kobayashi et al., 1999), while *ft* loss of function mutants are late flowering in LD (Koorneef et al., 1991). Under LD this gene is activated by CO and it is transcribed in the vascular tissue of leaves (Kardailsky et al., 1999; Kobayashi et al., 1999; An et al., 2004; Wigge et al., 2005; Samach et al., 2000). As an output of *CO*, *FT* is also diurnally regulated, with a peak toward the end of the day, around ZT16 (Suarez-Lopez et al., 2001) (**Fig. 3**).

Over-expressing *CO* in phloem companion cells with *SUC2* promoter causes early flowering through the activation of *FT*. *SUC2::FT*, similarly, results in early flowering. Using *KNAT1*

Introduction

promoter to express *FT* in the shoot apical meristem also causes early flowering, while using this promoter to drive expression of *CO* does not accelerate flowering (An et al., 2004). So, although both *CO* and *FT* genes are expressed in leaves, CO protein acts in the phloem while FT protein acts in the apical meristem to induce gene expression and promote flowering in this tissue. Since the 1930s it was proved that photoperiod is perceived by the leaf, whereas flowering takes place in the shoot apical meristem (Knott, 1934; Zeevaart, 1976). It was also demonstrated that an hypothetical long-distance signal, the so-called “florigen”, has to be transferred from the leaf to the apical meristem to promote flowering. It was then postulated for long time that FT is a plausible candidate for the “florigen”, although it was not clear whether this signal would travel as *FT* mRNA or FT protein. Convincing experiments coming from different groups recently solved the debate (reviewed by Kobayashi and Weigel, 2007; Turck et al., 2008). It has been proposed that FT protein is the molecule moving from the leaf to the SAM inducing flowering in *Arabidopsis* (Corbesier et al., 2007). In plants containing a *SUC2::FT:GFP* construct, which is also able to cause early flowering, FT:GFP signal was detected not only in the vascular tissue of the shoot, but also in the provascular tissue at the shoot apex and at the base of the SAM, while no *FT:GFP* mRNA was detected (Corbesier et al., 2007). FT:GFP was also graft-transmissible through the phloem to a *ft-7* mutant shoot receiver, accelerating its flowering. *GAS1* promoter was also used to drive the expression of *FT* in the phloem companion cells of the minor veins of leaves. In the *ft-7* background, *GAS1::FT* causes early flowering, while *GAS1::GFP:FT* does not accelerate flowering, although the protein is still active in the leaf and there promotes up-regulation of *FT* target genes (Corbesier et al., 2007). Therefore, the GFP fusion prevents flowering because it does not allow the export of the FT protein from the minor veins of the leaf to the apex. Other groups supported the same conclusions with complementary experiments (Jaeger and Wigge, 2007; Mathieu et al., 2007). In one report, an epitope-tagged version of FT was constructed fusing Myc-tags to *FT*. Using specific antibodies, Myc:FT protein was detected on the route from the vasculature to the organ primordia through the provascular tissue (Jaeger and Wigge, 2007). Then, a nuclear localization signal (NLS) was used to target FT protein constitutively to the nucleus. Myc:NLS:FT expressed in the *ft-10* mutant background causes early flowering when expressed with 35S promoter, while it does not accelerate flowering when expressed with *SUC2* promoter, because the FT protein is blocked in the leaf nuclei and cannot traffic to the SAM anymore (Jaeger and Wigge, 2007). Similarly, another group made use of FT fused to three copies of YFP and a NLS, and a recognition site for a virus protease between FT and the rest of the tag. Expression of this

Introduction

tagged version of *FT* with *35S* or *FD* (specific for the SAM) promoters promoted flowering, while expression with *SUC2* promoter did not promote flowering because the protein was trapped into the companion cells, preventing FT to reach the meristem (Mathieu et al., 2007). Releasing FT protein through a construct expressing the specific protease was sufficient to cause early flowering. Moreover, artificial microRNA (amiRNA) against *FT* mRNA expressed by *SUC2* promoter caused late flowering, while by *FD* promoter did not delay flowering demonstrating that the mRNA is not required at the meristem (Mathieu et al., 2007).

Similar results were found also in rice for the homologue of *FT* (Tamaki et al., 2007), and in Cucurbits (Lin et al., 2007). However, the “florigen” might be a set of additive signals, and FT protein would be one part of this set (Corbesier and Coupland, 2005; Corbesier and Coupland, 2006; Giakountis and Coupland, 2008).

A gene with similar features to *FT* is *TWIN SISTER OF FT (TSF)*. *FT* in *Arabidopsis* is part of a gene family which includes six members (Chardon and Damerval, 2005), and *TSF* is the closest to *FT*. *35S::TSF* promotes early flowering like *FT* (Kobayashi et al., 1999). *tsf* mutant is not late flowering, but enhances the late flowering of *ft* mutant in the *ft tsf* double mutant (Michaels et al., 2005; Yamaguchi et al., 2005), so that these two related genes have overlapping roles, but *FT* is predominant. *TSF* is regulated by *CO*, as its expression is lower in *co* mutants and induced by LD and by CO activation through an inducible system (Yamaguchi et al., 2005). In agreement with that, the early flowering phenotype of *SUC2::CO* is only partially suppressed by the *ft* mutation (An et al., 2004), while it is completely suppressed in a *ft tsf* double mutant background (Jang et al., 2009). Also the diurnal pattern of *TSF* is similar to the one of *FT*, with a peak at dusk in LD (Yamaguchi et al., 2005). However, the spatial expression patterns of *TSF* and *FT* do not seem to completely overlap in young seedlings, since *TSF* was shown to be expressed in the vascular tissue of hypocotyl and petiole, in the basal part of cotyledons and near the SAM. Later in the development their expression patterns are more similar (Yamaguchi et al., 2005). Over-expression of *TSF* in the phloem with *SUC2* promoter causes early flowering also in the absence of *FT*, and the same effect is obtained by *SUC2::FT* in *tsf* mutant (Jang et al., 2009). Anyway, it is not yet clear whether TSF is part of the florigen signal as movement of the protein has not been tested (Turck et al., 2008).

1.4 The repression of flowering by *FLC*

FLOWERING LOCUS C (FLC) encodes a MADS-box transcription factor that is a potent floral

Introduction

repressor, with a central role in flowering, because, as discussed previously, the vernalisation and autonomous pathways converge on this gene (see paragraphs 1.2.1 and 1.2.2).

To repress flowering, FLC reduces the expression of floral promoter genes, like *SOC1*, *FT*, *FD* and possibly *TSF* (Yamaguchi et al, 2005). Loss-of-function mutations in *FLC* cause early flowering (Michaels and Amasino, 1999), while over-expression of this gene causes late flowering (Michaels and Amasino, 2001).

Ectopic expression of *FLC* with the *35S* promoter causes down-regulation of *SOC1* and *FT* in seedlings (Hepworth et al., 2002; Michaels et al., 2005). *FLC* represses also *FD* expression (Searle et al., 2006). Indeed, FLC protein directly binds, in specific CArG boxes, *SOC1* promoter (Hepworth et al., 2002), the first intron of *FT* (Helliwell et al., 2006) and *FD* promoter (Searle et al., 2006). In this way, it has been demonstrated that *FLC* acts by repressing both systemic flowering signals produced in the leaves (such as *FT*) and the response to these signals at the meristem (*SOC1* and *FD*), until vernalisation reduces *FLC* expression in both tissues and allows flowering to occur (Searle et al., 2006).

Recently, some reports revealed new interesting aspects of the FLC transcription factor. One aspect is the physical and functional interaction with SVP, another potent floral repressor (see next paragraph). Another one is the possible involvement of *FLC* in the regulation of seed germination (Chiang et al., 2009). Finally, the role of antisense transcripts of *FLC* in the regulation of this gene and its impact on flowering time regulation showed an additional mechanism that plants use to finely regulate gene expression (Swiezewski et al., 2009; Liu et al., 2010).

1.5 The repression of flowering by SVP

Another gene that acts as a floral repressor is *SHORT VEGETATIVE PHASE (SVP)*. SVP belongs to the MADS-box transcription factor family. Loss of function of this gene in *Arabidopsis* causes an early flowering phenotype, both in LD and SD (Hartmann et al., 2000). *svp* mutants are still sensitive to photoperiod, which means that in SD they are earlier flowering than wild-type but still later than the mutant in LD. Moreover, plants heterozygous for *svp* mutation show an intermediate phenotype between wild-type and homozygous, suggesting a dosage effect for the product of this gene. *SVP* expression is present during the vegetative phase in young leaves and apical meristems, until the early stages of bolting. Then it is not present in the inflorescence meristem, and it rises again in flower primordia (Hartmann et al., 2000). This pattern suggests a role for this gene in maintaining the vegetative phase, before flowering occurs, and another distinct, later function in the

flower.

Several reports proved that SVP represses the expression of *FT*. The *FT* mRNA level is elevated in *svp* mutants, and *FT::GUS* shows ectopic expression in the leaf (Lee et al., 2007b). Expression of *FT* is up-regulated in *svp* mutants during the whole diurnal cycle of 24 hours, and the same happens to *TSF* (Jang et al., 2009, and this study). Another gene that is repressed by SVP is *SOCI*. *SOCI* expression is higher in *svp* mutant and lower in *35S::SVP*, compared to wild-type (Li et al., 2008). In addition, *SOCI* mRNA increases in *svp* largely independently of *FT* and *AGL24* (Li et al., 2008). *ft* or *soc1* mutations partially delay flowering in *svp* mutant background (Lee et al., 2007b), and also when combined in the *ft soc1* double mutant still cannot completely suppress the effect of *svp* mutation (Li et al., 2008; Fujiwara et al., 2008). The *svp* mutation in *ft tsf* double mutant background again causes early flowering. In this triple mutant *SOCI* is still transcribed as in wild-type (Jang et al., 2009, and this study). Therefore, *SVP* plays a role in repressing *SOCI* transcription strongly in the shoot apex, independently of *FT* and *TSF*, while it modulates also *FT* and *TSF* expression in the leaf (Li et al., 2008; Jang et al., 2009, and this study).

Direct binding of SVP protein to both *FT* and *SOCI* loci has been reported. By ChIP, SVP protein was shown to bind to a CARG motif in the promoter of *FT* in protoplasts (Lee et al., 2007b), and to bind to the promoter of *SOCI* (Li et al., 2008). This last observation was confirmed also by mutating the putative binding site in the *SOCI* promoter, which abolished *SOCI* repression (Li et al., 2008).

The targets of *SVP* tightly links this gene to another MADS-box gene, *FLC*. Both *SVP* and *FLC* are floral repressors, and both *FT* in the leaf and *SOCI* in the SAM are also directly regulated by *FLC*, as discussed in the previous section. Mutations in *FLC* or increase in its expression by the use of *FRI FLC* alleles does not affect *SVP* expression level, and also altering the expression of *SVP* does not change *FLC* expression level (Lee et al., 2007b). Conversely, late flowering of plants carrying active *FRI FLC* is largely suppressed by *svp* mutation, suggesting that *FLC* needs *SVP* as a partner to exert its repressing function (Lee et al., 2007b), while loss of *FLC* does not completely rescue the late flowering of *35S::SVP* (Li et al., 2008). Moreover, *flc svp* flowers earlier than *svp* (Li et al., 2008), although the difference is very subtle. Finally, it has been shown that *FLC* and *SVP* proteins physically interact, both *in vitro* and *in vivo* (Li et al., 2008; Fujiwara et al., 2008). However, *SVP* mRNA transcription does not change with vernalisation treatment (Li et al., 2008). *SVP* expression level is not affected in photoperiodic mutants, while it has been shown that this gene responds to endogenous signals from the autonomous pathway and from the gibberellin pathways, since it is

Introduction

reduced by gibberellin treatment and increased in *fve* and *gal* mutants (Li et al., 2008). In a previous report it was also proposed that *SVP* mediates ambient temperature signalling in *Arabidopsis* (Lee et al., 2007b). *svp* mutants do not alter their flowering time in response to different temperatures, which suggests a role for this gene in response to temperature changes. *SVP* was indeed proposed to act in the thermosensory pathway, downstream of the genes *FCA* and *FVE*, which are in this pathway (Blázquez et al., 2003), since the *svp* mutation was also epistatic to both *fca* and *fve* mutations (Lee et al., 2007b). Very recently a study reported a miRNA responsive to temperature changes, miR172, to be more expressed in *svp* mutant compared to wild-type, and some of the miRNA targets to be consequently decreased in expression (Lee et al., 2010). Since miR172 promotes flowering, this provides a possible link between *SVP* and miRNAs to regulate flowering in response to changes in ambient temperature. Therefore, *SVP* is a floral repressor controlling floral pathway integrators in response to various endogenous and environmental signals. Finally, an additional further role for *SVP* was recently discovered. This role would be downstream of two genes involved in the regulation of the circadian clock: *LHY* and *CCA1*. *lhy cca1* double mutants accumulate SVP protein, and a role for these genes was proposed in reducing the abundance of SVP protein, which would result in flowering acceleration (Fujiwara et al., 2008). This effect could be mediated by *ELF3*, since ELF3 protein interacts in yeast two-hybrid experiments both with CCA1 and SVP proteins (Yoshida et al., 2009). Moreover, SVP protein abundance increases in *ELF3* over-expressors, while *elf3* mutants show a delayed phase of SVP protein accumulation (Yoshida et al., 2009).

The closest paralogous gene to *SVP* is *AGAMOUS-LIKE 24 (AGL24)*. Nevertheless, despite the close relationship between them in term of sequence similarity, they have opposite effects on flowering time, and *svp* mutation is epistatic to *agl24* mutation (Gregis et al., 2006).

Another MADS-box gene that represses flowering is *FLOWERING LOCUS M (FLM)*. Mutation in *FLM* results in early flowering, both in LD and SD, while over-expression of *FLM* by the 35S promoter causes late flowering, similarly to the *SVP* gene (Scortecci et al., 2001). The expression pattern of *SVP* and *FLM* is also similar. *flm svp* double mutants flower like the single mutants, both in LD and SD, and both the effect of 35S::*FLM* and 35S::*SVP* are suppressed by mutations in *SVP* and *FLM* respectively, although *FLM* expression levels do not affect *SVP* expression levels, suggesting that *SVP* and *FLM* act as partners in the same pathway (Scortecci et al., 2003). Although *FLM* is closer to *FLC* in terms of sequence similarity, it is not affected by *FRI*, vernalisation

treatment, and mutations in genes of the autonomous pathway (Scortecci et al., 2001; Scortecci et al., 2003). *FLM* could be involved in the modulation of the sensitivity to temperature, as was shown in a recent report (Balasubramanian et al., 2006).

1.6 The early floral transition: from vegetative meristem to inflorescence meristem

1.6.1 The floral pathway integrators: classical and new members

Signals from the different flowering pathways converge to a restricted group of genes that for this reason have been classically named “floral pathway integrators” (Simpson and Dean, 2002). Therefore, they are somehow responsible for the final part of the decision to undergo the floral transition. These genes are all floral promoters and include *FT*, *LEAFY (LFY)* and *SOC1*.

1.6.1.1 *FT* as an integrator

FT has a central role in the induction of flowering in response to photoperiod. However, also several other factors control *FT* expression. The balance between the main activator *CO* and the various repressors determines the activation of flowering by *FT*. The role of some repressors of *FT* transcription belonging to the MADS-box family, like *FLC* and *SVP*, has been already discussed (see above).

Some other transcription factors that have been shown to repress *FT* activity are comprised in a family containing one or more DNA-binding AP2-domains. *TEMPRANILLO1 (TEM1)* and *TEM2* genes encode two related RAV transcription factors, with one AP2/ERF domain and one B3 domain, and they have been shown to repress *FT* expression (Castillejo and Pelaz, 2008). *FT* and *TEM1* have an opposite trend of expression during development. Over-expressing *TEM1* results in lower *FT* mRNA level and late flowering, while the *tem1* mutant shows higher *FT* expression, and the *tem1 tem2* double mutant is early flowering. Additionally, TEM1 protein was shown to directly bind a region at the 5'UTR of the *FT* locus (Castillejo and Pelaz, 2008). Based on the effects on *FT* mRNA level of manipulating the relative expression levels of *CO* and *TEM1*, it was proposed that the balance of expression levels of these two genes contributes to determining *FT* expression and the time to flower (Castillejo and Pelaz, 2008).

Another six related transcription factors contain two AP2-domains, and they are targets of miR172 (Aukerman and Sakai, 2003; Schmid et al., 2003): *APETALA2 (AP2)*, *TARGET OF EAT1-3 (TOE1-3)*, *SHLAFMÜTZE (SMZ)* and *SCHNARCHZAPFEN (SNZ)*. Within this family, only *toe1* mutant has a phenotype, which results in early flowering, and which is enhanced in *toe1 toe2*

Introduction

double mutants (Aukerman and Sakai, 2003). *TOE1* function has been associated with repression of *FT* (Jung et al., 2007). Also *SMZ* has been proposed to be a repressor of *FT* (Mathieu et al., 2009). Plants over-expressing *SMZ* are late flowering (Schmid et al., 2003), and although both *smz* single mutants and *smz snz* double mutants do not have a phenotype, *smz snz toe1 toe2* is earlier flowering than *toe1 toe2* (Mathieu et al., 2009). *FT* transcription is repressed by over-expression of *SMZ*. Interestingly, both the late flowering and the *FT* mRNA decrease were suppressed by *flm* mutation, suggesting that *FLM* is needed for *SMZ* activity and maybe participates in the regulation of *FT* repression (Mathieu et al., 2009).

TERMINAL FLOWER 2 (TFL2), a protein involved in epigenetic repression, is also a repressor of *FT*. Loss of function mutants of this gene are early flowering (Larsson et al., 1998). The increased level of *FT* mRNA in *tfl2* mutants is the main cause of early flowering, since the *ft* mutation completely suppresses the early flowering phenotype (Kotake et al., 2003). *co tfl2* double mutants flowered as early as *tfl2*, although the *CO*-independent *FT* up-regulation was present only in the basal part of leaves, while *FT* expression in the apical part requires *CO* (Takada and Goto, 2003). The *tfl2* mutation further accelerated the flowering time of *35S::CO* and increased the level of *FT* mRNA, suggesting that *TFL2* counteracts the activity of *CO* on *FT* expression (Takada and Goto, 2003).

Like *FT*, *TSF* has also been shown to be induced by vernalisation and negatively regulated by *FLC* (Yamaguchi et al., 2005), by *SVP* (Jang et al., 2009, and this study), and repressed by over-expression of *SMZ* (Mathieu et al., 2009), so that it could also be considered as an integrator. *TSF* is not repressed by *TFL2* (Yamaguchi et al., 2005).

1.6.1.2 *FT* and *FD*

Once *FT* is transcribed at high enough level and its protein is transported to the SAM, a series of downstream genes are activated to trigger flowering at the SAM (**Fig. 4**). In the current model *FT* protein directly interacts with a bZIP transcription factor encoded by a gene called *FLOWERING LOCUS D (FD)*, forming a protein complex which is able to directly activate the gene *APETALA1 (API)* (Abe et al., 2005; Wigge et al., 2005). *API* is a floral meristem identity gene which encodes a MADS-box transcription factor involved in flower formation, and which marks the beginning of floral meristem formation (Bowman et al., 1993; Irish and Sussex, 1990; Mandel et al., 1992). Two main reports suggested this model on the basis of very similar results (Abe et al., 2005; Wigge et

Introduction

al., 2005). First of all, loss of function of *FD* results in late flowering and strongly suppresses the early flowering phenotype of *35S::FT* over-expression. Interaction between FT and FD proteins was also detected in yeast-two hybrid and other methods (Abe et al., 2005; Wigge et al., 2005). In one report, FD was found to interact also with the FT-homolog TFL1 (Wigge et al., 2005), while in the other the interaction was barely detectable (Abe et al., 2005). FD protein was localized in the nucleus of cells at the shoot apex (Abe et al., 2005). *FD* mRNA is expressed in the SAM, and part of this domain overlaps with *API* expression domain (Abe et al., 2005). In agreement with that, *API* mRNA appearance in the apex is delayed in the *fd* single mutant (Wigge et al., 2005). Moreover, *ft lfy* double mutants show a very similar phenotype to *fd lfy* double mutants, and the expression of *API* mRNA is in both cases strongly reduced (Abe et al., 2005; Wigge et al., 2005). *35S::FD* causes ectopic expression of *API* and *FUL*, which does not occur under SD or in *ft* mutant background (Abe et al., 2005; Wigge et al., 2005). Finally, ChIP experiments using *35S::FD* and antibodies for FT showed that *API* promoter sequences were enriched in LD but not in SD (Wigge et al., 2005).

Interestingly, *FD* expression seems to decrease in floral primordia once *API* is expressed in that domain (Wigge et al., 2005), suggesting that *FD* is not longer required once *API* has been already activated.

Clearly, *API* is not the only target of *FT*, since *apl* mutants do not suppress the early flowering of *35S::FT* (Kardailsky et al., 1999). *SOCI* has been demonstrated to be downstream of *FT* in several reports (Yoo et al., 2005; Searle et al., 2006), and is an earlier acting gene than *API*. In addition, two other two MADS-box genes shown to be induced by *FT* are *FUL* and *SEP3*, although this was not investigated in the meristem so far. In leaves, *FUL* and *SEP3* are up-regulated in *35S::FT* and down-regulated in *ft* mutant, compared to wild-type (Teper-Bamnolker and Samach, 2005). The *fd* mutation resulted in reduction in expression level of these genes similarly to *ft* mutation. Moreover, *ful* slightly delayed the early flowering of *35S::FT* (Teper-Bamnolker and Samach, 2005). Moreover, *FUL* is induced by shift to LD (Hempel et al., 1997) but this increase is strongly delayed in *ft* mutants (Schmid et al., 2003).

Also TSF protein has been shown to physically interact with FD protein by yeast two-hybrid (Jang et al., 2009). Indeed, *fd ft* double mutants flower later than *ft*, and similarly to *ft tsf* and *fd ft tsf*, suggesting that both the FT-FD and TSF-FD protein interactions are biologically relevant (Jang et al., 2009). However, *ft tsf* is remarkably later flowering than *fd* mutant. Therefore, *FT* and *TSF* must act also independently of *FD* to promote flowering.

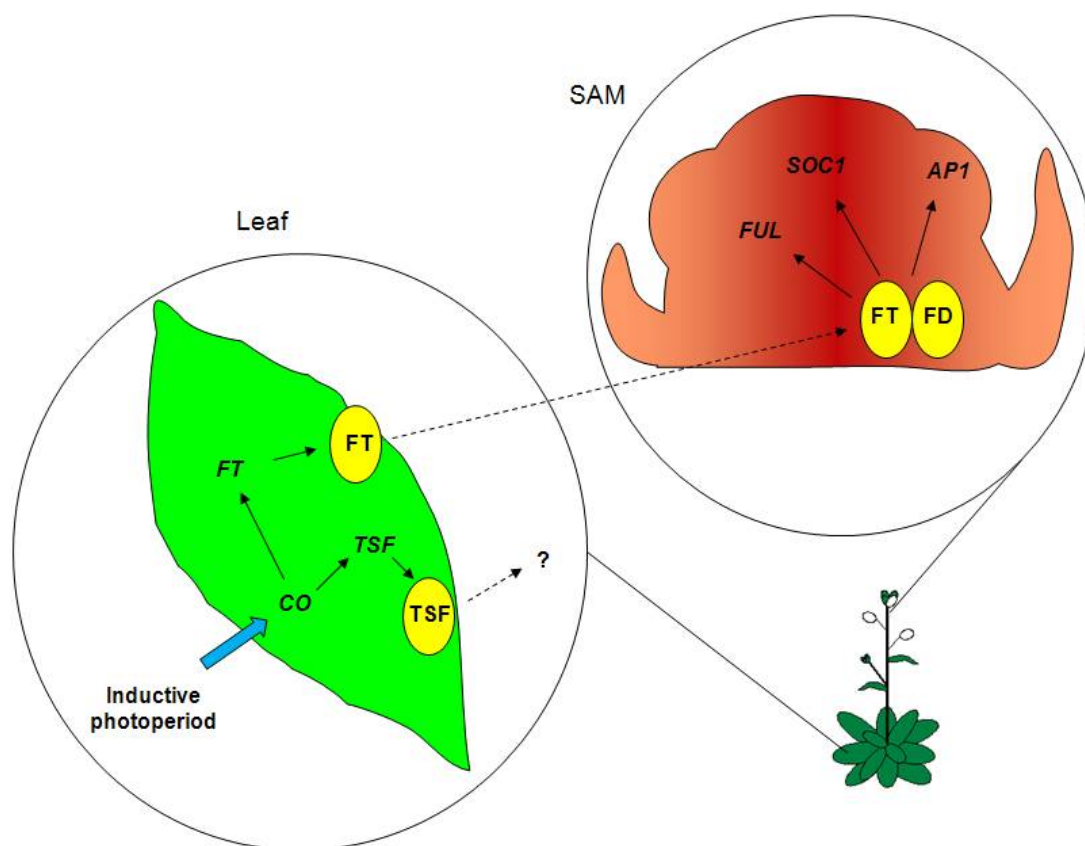


Fig. 4. FT protein moves to the shoot apical meristem to induce flowering. Genes acting to promote flowering in the early phases of the floral induction are indicated.

1.6.1.3 *SOC1*

SOC1 or *AGAMOUS-LIKE 20 (AGL20)* encodes a MADS-box transcription factor promoting flowering. It was isolated in a mutagenesis screen where *soc1* mutation partially suppressed the early flowering caused by over-expression of *CO* with 35S promoter (Onouchi et al., 2000). Coherently, *SOC1* expression was strongly increased by inducing *CO* activity with a 35S::*CO:GR* inducible system (Samach et al., 2000). The *soc1* mutation alone delays flowering, both under LD and SD, and the mutant is still sensitive to photoperiod (Samach et al., 2000; Lee et al., 2000). Over-expression of *SOC1* through 35S promoter causes early flowering (Samach et al., 2000; Borner et al., 2000). *SOC1* responds to photoperiod, as its expression is remarkably lower in SD than in LD (Lee et al., 2000; Borner et al., 2000). It is induced at the SAM and leaf primordia, already 16 hours after shift from SD to continuous light (Samach et al., 2000) or to LD (Borner et al., 2000). It is expressed in the inflorescence meristem, but excluded from floral primordia, and

Introduction

reappears in flowers at stage 2 and 3 of flower development (Samach et al. 2000; Borner et al., 2000).

The activation of *SOCI* by *CO* is mediated by *FT* (Yoo et al., 2005). Indeed, not only *SOCI* is up-regulated in *35S::FT* and down-regulated in *ft* mutant, but also the *ft* mutation suppresses the induction of *SOCI* by *35S::CO* (Yoo et al., 2005). Up-regulation of *SOCI* at the meristem is dependent on both *FT* and *FD*, since in *ft* and *fd* mutants *SOCI* increase is strongly delayed (Searle et al., 2006). *TSF*, like *FT*, also promotes *SOCI* transcription (Michaels et al., 2005; Yamaguchi et al., 2005). However, *SOCI* over-expression in the meristem is not sufficient to overcome the effect of the *co* and *ft* mutation (Searle et al., 2006). Moreover *soc1* mutation, which indeed does not result in a strong late flowering in LD, only partially suppresses the early flowering of *35S::FT* (Yoo et al., 2005), confirming that *FT* has additional target genes other than *SOCI*.

In addition to the photoperiod, *SOCI* integrates also the signals from the other pathways.

Its expression increases with the age of the plant, and it is influenced by the autonomous pathway (Samach et al. 2000; Borner et al., 2000; Lee et al., 2000). This gene indeed was also isolated with another screen by activation-tagging in which over-expressed *SOCI* suppressed the late flowering phenotype of a *FRI*-introgressed line (Lee et al., 2000). The repression exerted by *FLC*, which is direct, and mediates the effect of the autonomous and vernalisation pathway, has been already discussed (see paragraph 1.4). Interestingly, *SOCI* increases upon vernalisation also independently of *FLC* (Moon et al., 2003). The repression exerted by *SVP* has also been mentioned (see paragraph 1.5).

Finally, *SOCI* integrates the signals from the gibberellin pathway (Moon et al., 2003). *SOCI* expression increases upon GA treatments (Borner et al., 2000), and the over-expression of *SOCI* overcomes the late flowering of *ga1-3*, a mutant in the gibberellin pathway, while the *soc1* mutant is less responsive to GA (Moon et al., 2003).

Not so much is known about how *SOCI* activates flowering, and so far the only well documented target is *LFY* (see next paragraphs). Surprisingly, over-expression of *SOCI* by the *35S* promoter, which causes early flowering, also results in an increase of *FT* (Michaels et al., 2005). Indeed, the over-expression of *SOCI* causes early flowering not only when is targeted in the meristem through *KNAT1* promoter, but also when is targeted in phloem companion cell through *SUC2* promoter, although with a very small difference in terms of leaf number (Searle et al., 2006).

A possible explanation for this phenomenon comes from a recent report, in which a role of *SOCI* in reducing *FLC* mRNA level is proposed (Seo et al., 2009), which could explain the promotive effect

of *SOCI* on *FT*. Microarray analysis comparing wild-type, loss of function and over-expressor of *SOCI* revealed that this gene negatively regulates a set of cold-regulated (*COR*) genes (Seo et al., 2009). This repression is not direct, but acts through the CRT/DRE binding factors (*CBFs*), which are key regulators of the cold response pathway in *Arabidopsis* and positively regulate the *COR* genes (Thomashow, 1999). *SOCI* protein binds to the promoters of the *CBF1-3* genes, as shown by ChIP (Seo et al., 2009). On the other hand, over-expression of the *CBFs* with *35S* promoter causes an increase in *FLC* expression. Therefore, there is a feedback loop, so that transient cold would promote *CBFs*, and consequently *FLC* expression and *SOCI* repression, while floral induction would activate *SOCI* that represses the cold-response and *FLC*, further promoting flowering.

1.6.1.4 *AGL24*

AGAMOUS-LIKE24 (*AGL24*) encodes another MADS-box transcription factor that promotes the floral transition. Its expression is also regulated by different floral pathways, such as photoperiod, gibberellin, autonomous and vernalisation pathways, so that it has been proposed as another floral pathway integrator (Yu et al., 2002; Michaels et al., 2003; Liu et al., 2008).

agl24 mutants are moderately late flowering, both in LD and SD, so that they are still photoperiod-sensitive. The effect of this gene is dosage-dependent, since plants heterozygous for the mutation present an intermediate flowering phenotype (Michaels et al., 2003), and the late flowering degree in plants harboring RNAi against *AGL24* depends on the remaining expression level of this gene (Yu et al., 2002). It is expressed in many tissues, but especially in inflorescence meristems, in young floral primordia until stage 2 (Michaels et al., 2003), and in other floral organs (Yu et al., 2002). *AGL24* is affected by photoperiod. In *co* mutants its expression level is decreased compared to wild-type, although not affected in *ft* mutant (Yu et al., 2002).

AGL24, like *SOCI*, increases in expression during development (Liu et al., 2008), and it is also up-regulated upon vernalisation (Yu et al, 2002), although its mRNA level is not regulated by *FLC* (Michaels et al., 2003). Moreover, the late flowering of *agl24* is not suppressed by vernalisation, and it is not dependent on *FLC* (Michaels et al., 2003).

SOCI and *AGL24* directly activate each other, and they are mutually dependent. In *35S::SOCI* there is an increase in *AGL24* mRNA, and in *35S::AGL24* an increase in *SOCI* mRNA (Yu et al., 2002; Michaels et al., 2003). *SOCI* is activated directly by *AGL24*, as shown by an inducible system, and in *agl24* mutants less *SOCI* mRNA is present at the SAM during floral transition (Liu et al, 2008). Moreover, over-expression of *AGL24* with *35S* promoter causes early flowering,

although *soc1* mutation partially suppresses this effect, so that *AGL24* should promote flowering in part through *SOC1*. Similarly, over-expression of *SOC1* with 35S promoter is also partially suppressed by *agl24* mutation (Yu et al., 2002; Michaels et al., 2003). Indeed, ChIP experiments confirmed that *AGL24* binds to *SOC1* promoter and that *SOC1* binds to *AGL24* promoter (Liu et al., 2008). Binding sites in the identified CArG boxes were mutated and proved to be biologically relevant for the transcriptional activation (Liu et al., 2008).

Interestingly, GA treatment induces both *SOC1* and *AGL24*, but in *agl24* and *soc1* mutants the expected up-regulation of *SOC1* and *AGL24* respectively are abolished (Liu et al., 2008). Moreover, GA does not accelerate flowering on *soc1 agl24* double mutant, while it still can accelerate flowering in the single mutants (Liu et al., 2008).

1.6.1.5 *LFY* as an integrator

LFY encodes a plant-specific transcription factor, which does not belong to a gene family (Parcy et al., 1998).

It is expressed in young leaf primordia and its mRNA increases until a maximum in young floral meristems, gradually under SD condition or more sharply upon shift to LD (Hempel et al., 1997; Blázquez et al., 1997). *LFY* is a pathway floral integrator, it specifies floral identity and it also promotes determinacy (Weigel et al., 1992). As a floral integrator, a correlation was shown between the number of copies of *LFY* introduced in *Arabidopsis* and an effect on acceleration of flowering time (Blázquez et al., 1997). It is activated not only by the photoperiodic pathway, but also by the gibberellin pathway. It has been also shown that regions of *LFY* promoter that are activated by gibberellins are distinct from the ones that respond to photoperiod (Blázquez and Weigel, 2000). Moreover, recent findings proposed *SPL3* to be directly upstream of *LFY* (Yamaguchi et al., 2009; see paragraph 1.6.3). It was already shown that activation of CO protein through an inducible system driven by 35S promoter leads to rapid up-regulation of *LFY* (Simon et al., 1996). This effect is probably not direct, and the activation by the photoperiodic pathway is mediated via *SOC1* (Lee et al., 2000; Moon et al., 2003; Samach et al., 2000). ChIP analysis showed that SOC1 protein directly binds to the *LFY* promoter (Liu et al., 2008; Lee et al., 2008). *LFY* expression level is also reduced in *agl24* mutants (Yu et al., 2002), and even in this case, binding of AGL24 protein to the *LFY* promoter has been proven by ChIP, also in regions that overlap with SOC1 binding sites (Lee et al., 2008). Recently it has been proposed that a physical interaction between SOC1 and AGL24 proteins would be relevant for the direct activation of *LFY* (Lee et al., 2008b) (**Fig. 5, A**). SOC1

protein expressed in protoplasts was localized in the cytoplasm, while AGL24 protein in the nucleus. When AGL24 was co-transfected with SOC1 in protoplasts, they both co-localized in the nucleus (Lee et al., 2008b).

LFY is also activated by gibberellins (Blázquez et al., 1998). In the *gal* mutant, which has dramatic reduction of endogenous GA level, *LFY* promoter activity is strongly reduced, and treatment with GA₃ restores the activity of *LFY* (Blázquez et al., 1998). *35S::LFY* in *gal* recovers the ability to flower in SD, but does not completely complement for the early flowering phenotype, suggesting that GAs regulate not only *LFY* expression but also the competence to respond to *LFY* (Blázquez et al., 1998). Another report proved also GA₄ to be able to induce flowering and to activate *LFY* promoter (Eriksson et al., 2006). At the same time, a sharp increase of GA₄ was observed during floral transition at the apex. This, together with the fact that the expression of several GA biosynthetic enzymes did not change at the apex, and with some evidence of transport of GA₄ from leaves to apex, suggests that gibberellins may also act as a transported signal (Eriksson et al., 2006). A factor that could mediate the activation of *LFY* by gibberellins is AtMYB33, a transcriptional activator of a large gene family (Gocal et al., 2001). AtMYB33 has a very similar pattern of expression to the one of *LFY* in response to GA, and its protein product binds to the *LFY* promoter *in vitro* (Gocal et al., 2001).

1.6.2 *FUL* in the floral transition

Several functions of the *FUL* gene have been described. *FUL* has a key role in carpel and fruit development, since loss of function of this gene largely affects development of the siliques, which fail to elongate (Gu et al., 1998). It has a further role in the floral transition, although the *ful* mutant has only a very subtle late flowering phenotype, depending on the conditions (Ferrándiz et al., 2000). Finally it has been shown to be involved in some aspects of meristem determinacy (Melzer et al, 2008).

The mRNA of this gene accumulates in two distinct phases. In the first phase, it is very similar to *SOC1*, as it is present in inflorescence meristems, where it shows a sharp increase during the floral transition (Mandel and Yanofsky, 1995a; Hempel et al., 1997), and not in flower primordia at stages 1 and 2, while it reappears in stage 3. *API* represses *FUL* in stages 1 and 2, since in *apl* mutant *FUL* is also expressed in those stages (Mandel and Yanofsky, 1995a). In the second phase, it is expressed in the carpel walls, reflecting its function in carpel development (Mandel and Yanofsky, 1995a). *FUL* is also expressed in cauline leaves, and the *ful* mutant presents also wider

cauline leaves, due to problems in their development and their cellular organization (Gu et al., 1998). *FUL* and *SOCI* induction by LD at the shoot apex is strongly decreased in *ft* and *co* mutants (Schmid et al., 2003), delayed in *fd* mutant and increased in *35S::FD* (Wang et al., 2009a).

A clearer function for *FUL* in the floral transition has been uncovered through the use of *soc1 ful* double mutants (Melzer et al., 2008). Indeed, *ful* mutation enhances the late flowering of *soc1* mutation, and while the single mutants only partially suppress the early flowering of *35S::FT* constructs, the double mutant almost completely suppresses the effect of *FT* over-expression. This suggests that *SOCI* and *FUL* have a redundant and crucial role downstream of *FT* during the floral transition (Melzer et al., 2008).

Unexpectedly, over-expression of *FUL* causes early flowering not only when it is driven by *35S* and *FD* promoter, but also when *SUC2* promoter is used (Wang et al., 2009a). Moreover, *ft* mutation suppresses the early flowering of *SUC2::FUL*, suggesting that the early flowering may be caused by an increase in *FT* mRNA, similarly to the cases of *SOCI* (Michaels et al., 2005; Searle et al., 2006) and *SPL3* (Wang et al., 2009a). However, the major effect of *FUL* on floral transition seems to be through the meristem, since *amiR-FUL* constructs driven by *SUC2* promoter have a minor effect on flowering in *soc1* mutant, while under the *FD* promoter they render the *soc1* mutant as late flowering as *soc1 ful* double mutants (Wang et al., 2009a).

1.6.3 *SPL* genes: another chapter in the floral transition?

A family of transcription factors that are named SQUAMOSA PROMOTER BINDING PROTEIN-LIKE (*SPL*) is characterized by the presence of a SBP-box domain (for SQUAMOSA PROMOTER BINDING PROTEIN), and is encoded by 16 genes in *Arabidopsis*. Among them, 10 members of this family are regulated by miRNA156 (Rhoades et al., 2002). This family of genes has been implicated in several processes, particularly plant phase transitions (Cardon et al., 1997; Cardon et al., 1999; Chuck et al., 2007; Schwartz et al., 2008; Wu and Poethig, 2006; Xie et al., 2006).

Plants experience several developmental transitions during their life cycle (Bäurle and Dean, 2006; Poethig, 2003). The vegetative phase change is the transition from the juvenile to the adult vegetative stage, and it has to be achieved to undergo the subsequent reproductive phase change (or floral induction), which is the transition from the vegetative to reproductive phase. MicroRNAs miR156 and miR172 play a role in these transitions. miR156 is expressed highly early in development and decreases with time (Wu and Poethig, 2006), while miRNA172 shows the opposite trend (Aukerman and Sakai 2003; Jung et al., 2007). Over-expressing miRNA156 results

Introduction

in longer expression of juvenile vegetative traits and delay in flowering (Wu and Poethig, 2006; Schwab et al., 2005). Over-expressing miRNA172 results in acceleration of flowering (Aukerman and Sakai 2003; Chen 2004; Jung et al., 2007).

Some of the targets of these miRNAs have also been involved in floral transition. For example, some of the SPL factors whose mRNAs are targeted by miRNA156, such as *SPL3*, *SPL4*, and *SPL5*, are also involved in the floral transition, since their over-expression results in early flowering, especially when the regions targeted by the miRNA are eliminated or mutated (Cardon et al., 1997; Wu and Poethig, 2006). A specific sequence at the 3'UTR of *SPL3* mediates translational inhibition of the miRNA (Gandikota et al., 2007). These three related genes act downstream of *CO* and *FT* at the shoot apex, because they increase in expression upon transfer to LD, but the induction is reduced in the *co* and *ft* mutants (Schmid et al., 2003).

Recently, a set of reports shed more light on the involvement of the SPLs in the floral transition and into their complex regulation. *SPL3* was shown to activate directly the genes *LFY*, *FUL* and *API* (Yamaguchi et al., 2009). Transgenic plants carrying *35S::miR156* showed reduced level of *LFY*, *FUL*, and *API* mRNAs, while in *35S::SPL3Δ* plants (*SPL3* mRNA without the miRNA target site at the 3' UTR) the expression of *LFY*, *FUL*, and in some condition *API*, is increased. Moreover, single loss of function mutations in *LFY*, *FUL*, and *API* were, to different extents and each for different aspects, all partially epistatic to *35S::SPL3Δ* (Yamaguchi et al., 2009). ChIP experiments proved direct binding of SPL3 protein to *LFY*, *FUL*, and *API* genomic loci (Yamaguchi et al., 2009). Another report confirmed the same results for SPL3 protein with the *FUL* gene (Wang et al., 2009a). *35S::SPL4Δ* and *35S::SPL5Δ* resulted in a similar phenotype, suggesting redundant roles for *SPL3-4-5* (Yamaguchi et al., 2009).

Surprisingly, SPLs act both in the phloem and in the SAM. Plants carrying *FD::MIR156* flower very late, carrying *SUC2::MIR156* slightly late, and the combination of the two transgenes cause an additive effect (Wang et al., 2009a). Also the non-targeted version of *SPL3* driven by *SUC2* or *FD* promoters causes early flowering. Interestingly, *ft* mutation suppresses the effect of *SPL* expressed in the phloem (Wang et al., 2009a). When *FD::MIR156* is introduced into the *fd* mutant, so that *LFY* and *API* mRNA levels are strongly decreased (Wang et al., 2009a), the resulting phenotype resembles *ft lfy*, *fd lfy* and *lfy api* double mutants (Ruiz-Garcia et al., 1997; Abe et al., 2005; Wigge et al., 2005).

SPL9 was shown to be involved, redundantly with *SPL15*, in the juvenile-to-adult transition, and the loss of function of one of these genes also slightly delays flowering, while *spl9 spl15* double

Introduction

mutants enhance this late flowering (Schwartz et al., 2008). *SPL9* is expressed stronger in apices exposed to LD, and it is localized at the provascular strands below the meristem and in floral anlagen and early floral primordia (Wang et al., 2008; Wang et al., 2009a). Interestingly, *SPL9* still increased during floral transition in *ft tsf* double mutants, so that in addition to photoperiod, an age-dependent pathway independent of photoperiod regulates *SPL9* (Wang et al., 2009a). Similarly, the level of *SPL3* expression was increased in *35S::FT:GFP* plants, but *35S::miR156* was not epistatic to *35S::FT:GFP* and *35S::SPL3A* enhanced its effect, suggesting both a response to *FT* and another pathway parallel to *FT* (Yamaguchi et al., 2009). In addition, over-expressing *SPL3* accelerates flowering of *fd* mutants, and *FD::MIR156* increases the late flowering of *35S::amiR-FT/TSF* (Wang et al., 2009a), so that *FD* and *SPL3* would act also in parallel.

Given the redundancy of SPL factors, one of the reports showed that several MADS-box genes, particularly *FUL*, *SOCI* and *AGL42* were increased in *35S::MIM156* (a target mimic of miR156), in which *SPLs* levels are higher, and decreased in *35S::MIR156* (Wang et al., 2009a). While induction of *SPL9* by a GR inducible system led to a strong increase of *FUL* expression, ChIP experiments showed that *SPL9* binds to *SOCI* and *AGL42* loci (Wang et al., 2009a).

Recently it was also reported that miR156 acts upstream of miR172 to regulate its expression (Wu et al., 2009). This control is achieved via *SPL9* that, redundantly with *SPL10*, promotes transcription of miR172. Since *SPL9* and other *SPLs* promote miR156 transcription, a negative loop is established, in which the miRNAs are positively regulated by the transcription factors they target, which could be a way to keep a certain developmental phase more stable and avoid abrupt changes (Wu et al., 2009).

1.7 The later phase of the floral transition: from inflorescence meristem to floral meristem

1.7.1 Floral meristem identity genes

Upon integration of the flowering signals, the floral pathway integrators eventually induce a set of genes called “floral meristem identity genes”, which initiate a developmental patterning program for the generation of floral organs (Long and Barton, 2000). This group comprises the genes *LEAFY (LFY)*, *APETALA1 (API)*, *CAULIFLOWER (CAL)*, and to a certain extent also *FRUITFULL (FUL)* (Blázquez et al., 2006). During the transition to the reproductive phase a reprogramming of the primordia takes place at the apex, and these genes are responsible for establishing a robust network which irreversibly starts to confer floral identity on the meristem.

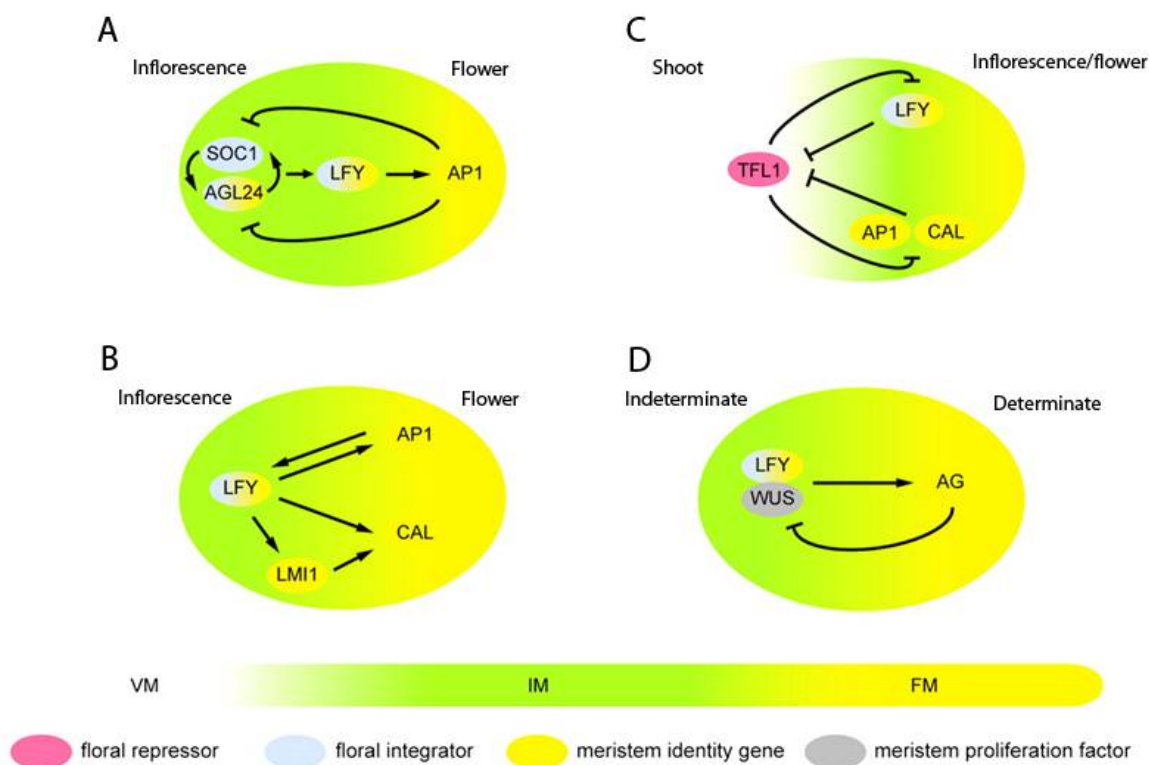


Fig. 5. Transcriptional loops mediating floral commitment. VM: vegetative meristem. IM: inflorescence meristem. FM: floral meristem. See text for details.

1.7.1.1 *LFY*

LFY as a floral pathway integrator has been discussed in previous paragraphs. Upon floral transition, this gene has also two essential functions in conferring floral meristem identity and determining floral organ patterning (Weigel et al., 1992), and these two functions are distinct (Parcy et al., 1998).

Loss of function of *LFY* causes conversion of the floral meristem into inflorescence shoots (Schultz and Haughn, 1991; Weigel et al., 1992). Conversely, ectopic expression of *LFY* causes conversion of the inflorescence meristem into a terminal flower (Weigel and Nilsson, 1995). The mechanism by which *LFY* determines floral meristem identity and organ patterning is based on the induction of floral homeotic genes.

To define floral meristem identity *LFY* directly activates *API* and *CAULIFLOWER (CAL)* (Mandel and Yanofsky, 1995b; Wagner et al., 1999; William et al., 2004). Moreover, *LFY* activates the gene encoding the homeodomain-zipper transcription factor *LATE MERISTEM IDENTITY 1 (LMI1)*,

which is also a positive regulator of *CAL*, since loss of function of *LMII* in weak *lfy* alleles reduces *CAL* expression and enhances the *lfy* phenotype (Saddic et al., 2006). Both LFY and LMI1 proteins directly bind to the promoter of *CAL* (William et al., 2004; Saddic et al., 2006) (**Fig. 5, B**).

To define floral patterning, *LFY* activates genes such as *AP3* and *AGAMOUS (AG)* (Parcy et al., 1998). The activation of *AP3* needs *UNUSUAL FLORAL ORGANS (UFO)* as a co-activator (Parcy et al., 1998), while the activation of *AG* needs the homeodomain transcription factor *WUSCHEL (WUS)* as a co-activator (Lenhard et al., 2001; Lohmann et al., 2001).

1.7.1.2 *API* and *CAL*

API is a floral meristem identity gene which encodes a MADS-box transcription factor.

API and *CAL* are expressed in young flower primordia that rise from the inflorescence meristem, and they act in a redundant way to specify floral meristem identity (Mandel et al., 1992; Kempin et al., 1995). *API* expression rises later than *LFY*, and it is an indicator of floral determination (Hempel et al., 1997). *CAL* is the closest relative of the *API* gene, and it plays redundant functions with it (Kempin et al., 1995). Loss of *API* gene causes defects in floral meristem identity and floral organ identity (Irish and Sussex, 1990), while *cal* mutation does not show a phenotype, but it strongly enhances the *apl* mutation, so that in *apl cal* double mutants the floral meristems are completely transformed into inflorescence meristems, and instead of flowers produce new meristems that re-iterate the pattern (Bowman et al., 1993). Later in development even these structures achieve floral identity. Over-expression of *API* causes conversion of the inflorescence meristem into a terminal flower (Mandel and Yanofsky, 1995b).

API and *CAL*, which are activated by LFY, also positively regulate *LFY* (Bowman et al., 1993; Liljegren et al., 1999) creating a feedback loop that establish a stable floral determination (**Fig. 5, B**).

1.7.1.3 *FUL*

As a floral meristem identity gene, *FUL* is maybe responsible for the residual floral fate that *apl cal* double mutants eventually show, because *apl cal ful* triple mutants never acquire floral fate, they fail to flower and produce leafy shoots (Ferrándiz et al., 2000). However, it could also be that the up-regulation of *FUL* in the *apl* background (Mandel and Yanofsky, 1995a) would lead this gene to partially take over the function of the *API* and *CAL* in their absence, since these three genes are closely related in terms of sequence (Mandel and Yanofsky, 1995a). Alternatively, *FUL* could

have a function in positively regulating *LFY* activation, because in the *apl cal ful* triple mutant *LFY* expression is reduced compared to *apl cal* double mutants, and *35S::LFY* partially overcomes the loss of floral determination of the triple mutants (Ferrándiz et al., 2000).

Finally, a recent report suggests a new perspective in which *SOCI* and *FUL* affect meristem determinacy (Melzer et al., 2008). The *soc1 ful* double mutant shows a peculiar “inflorescence reversion” phenomenon (see Tooke et al., 2005, for a definition), which allows further vegetative growth after flowering, which again proceeds to another flowering phase. This cycle is repeated several times. This behaviour, together with the marked secondary growth and the extreme longevity of these double mutants, resembles the perennial plant life style (Melzer et al., 2008).

1.7.2 *TFL1*

A gene with an opposite role to genes like *LFY* or *API*, and which conversely specifies inflorescence shoot identity, is *TERMINAL FLOWER1 (TFL1)*. Loss of function of this gene causes the inflorescence shoot to be converted into a floral meristem, with resulting terminal flowers (Shannon and Meeks-Wagner, 1991).

TFL1 is expressed in the center of the SAM (Bradley et al., 1997), where it prevents the expression of *API* and *LFY*, and consequent termination of the floral meristem (**Fig. 5, C**). Indeed, the transformation of the inflorescence meristem into a floral meristem in *tfl1* mutant is caused by ectopic expression of *API* and *LFY* (Weigel et al., 1992; Bowman et al., 1993; Gustafson-Brown et al., 1994; Bradley et al., 1997). Over-expression of *TFL1* with *35S* promoter causes late flowering, enhanced in SD, by delaying the expression of *LFY* and *API*, but without a direct block on them (Ratcliffe et al., 1998). In contrast, *LFY* represses *TFL1* (Ratcliffe et al., 1999; Parcy et al., 2002), while *API* and *CAL* negatively regulate *TFL1* (Liljegren et al., 1999; Ratcliffe et al., 1999). Moreover, TFL1 protein was shown to be mobile, and to spread beyond the site where its mRNA is synthesized. A signal from *LFY* would promote the movement of TFL1 protein, as in *lfy* mutant the protein localization is restricted similarly to one of the mRNA (Conti and Bradley, 2007).

TFL1 plays a role also in flowering time as a repressor of the floral transition, since *tfl1* mutants are early flowering (Shannon and Meeks-Wagner, 1991; Bradley et al., 1997). However, the two functions in shoot identity and flowering do not seem to be separate, but rather based on a general mechanism this gene employs to regulate the transition at the SAM (Ratcliffe et al., 1998).

TFL1 does not encode a transcription factor, but has homology to phosphatidyl ethanolamine-

binding proteins (Bradley et al., 1997), like *FT*. It is quite surprising that, despite the high sequence similarity (about 59% amino acid sequence identity) and almost an identical three-dimensional structure between these proteins (Ahn et al., 2006), they have opposing functions. In one report, an external loop was proposed to be responsible for the antagonistic activity between the two proteins (Ahn et al., 2006). In another report, it has been shown that even a single amino acid is important for their distinct roles, since exchanging this residue between the two proteins results in almost a complete switch between the activities of FT and TFL1 proteins (Hanzawa et al., 2005). This similarity would suggest common biochemical properties and similar molecular function, such as the interaction with the same partners. TFL1 may then interact with FD to compete with FT. However, a recent report suggested that TFL1 protein has a function in the transport of proteins to the protein storage vacuoles, proposing an alternative biochemical function for TFL1 (Sohn et al., 2007).

1.7.3 Flower development and the ABC model

Flowers in *Arabidopsis*, as in other eudicots, are composed of four whorls of organs: sepals, petals, stamens and carpels (from the outermost whorl to the center of the flower). The stamens are the male reproductive organs, while the carpels are the female structures that once fertilized will produce the fruit. Genetic studies in *Arabidopsis* and *Antirrhinum majus* led to the proposal of a model for flower development called the ABC model (Coen and Meyerowitz, 1991). The combination of the different A, B, and C activities give the specific organs of the flower whorls: A for the sepals, A and B together for the petals, B and C for the stamens and C for the carpels (Krizek and Fletcher, 2005, for a review). The homeotic genes belonging to the ABC functions are all MADS-box genes, except for *AP2*. In *Arabidopsis* the A function genes are *AP1* and *AP2*, B function genes *AP3* and *PISTILLATA (PI)*, and the C function gene is *AGAMOUS (AG)*. Modifications of the model were included with the discovery of *SEPALLATA (SEP)* genes, which are necessary for the development of all the four whorls of organs. It has been suggested that A, B, C and SEP proteins act as multimeric complexes to activate downstream genes (Jack, 2001; Theißen and Saedler, 2001, for reviews).

1.7.4 Flowering time genes regulate floral patterning

AP1 as a transcription factor has an additional role as a repressor, and it was demonstrated that it controls *AGL24* (Yu et al., 2004), *SVP*, *SOC1* (Liu et al., 2007) and *FUL* (Mandel and Yanofsky,

Introduction

1995a) genes by repressing their transcription in floral meristems. This sort of feedback loop is probably needed to repress these genes in the floral meristem once the floral transition has occurred. At that point reversion to an inflorescence or vegetative meristem must be avoided, and repression of flowering time genes by *API* is believed to be one of the mechanisms that avoids floral reversion (**Fig. 5, A**). All these four genes are ectopically expressed in *ap1* mutant, and the three genes *SVP*, *AGL24* and *SOCI* are down-regulated upon activation of AP1 (Liu et al., 2007; Yu et al., 2004). It has been demonstrated by use of ChIP that AP1 protein binds to *cis*-regulatory regions of all these three genes (Liu et al., 2007). This, together with the fact that over-expression of *SVP* (Masiero et al., 2004), *AGL24* (Yu et al., 2004), or *SOCI* in combination with one of the other two, leads to partial reversion of the floral meristem into inflorescence shoots, and that mutations in *SVP*, *AGL24* or *SOCI* alleviates the inflorescence character of the flowers of *ap1* mutants, suggests they have a role in inflorescence identity (Liu et al., 2007). However, recently an additional role for *AGL24*, *SVP* and *SOCI* in floral meristem determination has been hypothesized (Liu et al., 2009a for a review).

AGL24 and *SVP* redundantly control flower meristem identity with *API* (Gregis et al., 2006; Gregis et al., 2008). After floral transition, *AGL24* and *SVP* proteins, in agreement with the mRNA pattern, are localized in floral meristems during stages 1 and 2 of flower development, and disappear at stage 3 (Gregis et al., 2009). AP1-*AGL24* and AP1-*SVP* protein dimers interact with the LUG-SEU co-repressor complex (Gregis et al., 2006), which regulates *AG* (Sridhar et al., 2004). Indeed, in *agl24 svp* double mutant, which has a temperature-dependent floral phenotype, the class B and C genes *AP3* and *AG* are deregulated (Gregis et al., 2006), and *LUG* down-regulation in *agl24 svp* enhances the floral defects of the double mutant (Gregis et al., 2009). *ap1* mutation enhances the floral phenotype of the double mutant, and *ap1 svp agl24* triple mutants resemble *ap1 cal* double mutants (Kempin et al., 1995, Bowman et al., 1993; Gregis et al., 2006). In the triple mutant *FUL* is up-regulated, and in the *ap1 agl24 svp ful* quadruple mutants the vegetative characters are increased, so that *FUL* may take over a function in flower formation in the triple mutant (Gregis et al., 2008). A role for *SOCI* has also been proposed in the context of floral development. *soc1 agl24 svp* triple mutant has more floral defects than the *svp agl24* double mutant, so that *SOCI*, *AGL24* and *SVP* would redundantly regulate flower development (Liu et al., 2009b). However, in *agl24 svp* double mutant *SOCI* is ectopically expressed in floral meristems at stage 1-2 floral development, where it should not be expressed (Gregis et al., 2009), therefore *SOCI* could take over a function in the flower when the other two MADS-box genes are missing. In

Introduction

the *soc1 agl24 svp* triple mutant, class B (*AP3* and *PI*) and C (*AG*) genes are deregulated (Liu et al., 2009b). By ChIP, both SVP and AP1 proteins has been shown to bind genomic regions of *AG*, *AP3*, *PI* and *SEP3* in the same fragments, and AGL24 protein binds when *SVP* is not present. SOC1 protein binds to *AG*, *AP3* and *PI* when *AGL24* and *SVP* are not present (Gregis et al., 2009).

AGL24, *SVP* and *SOC1* redundantly repress *SEP3*, which is up-regulated in *svp* mutant and even more in combinations of double or triple mutants of these genes, depending on the developmental stage (Liu et al., 2009b). In an another report, SVP protein was also shown to bind *SEP3* promoter by ChIP, and again AGL24 and SOC1 also bind but only in absence of *SVP* (Liu et al., 2009b). Interestingly, SVP could recruit TFL2 protein to *SEP3* genomic region. The interaction between SVP and TFL2 proteins was detected by yeast two-hybrid, and with other methods *in vitro* and *in vivo* (Liu et al., 2009b). Moreover, they bind to the same region of *SEP3*, and TFL2 binding is decreased in the *svp* mutant (Liu et al., 2009b).

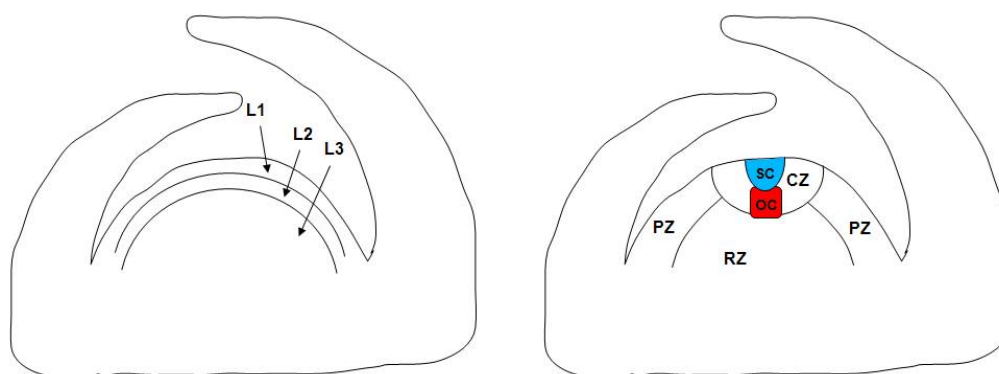


Fig. 6. The cellular structure of the shoot apical meristem. The division in layers (L1, L2 and L3) is depicted on the left side. The division in domains is depicted on the right side. CZ: central zone. PZ: peripheral zone. RZ: rib zone. SC: stem cells. OC: organizing center.

1.8 The shoot apical meristem: balance between stem cell maintenance and organ production

Plant meristems are the source of new cells for the plant growth. Almost all the growth of a plant after embryogenesis is due to the action of two apical meristems: the shoot apical meristem (SAM), which is responsible for the formation of the aerial part of the plant, or above-ground part, and the root apical meristem (RAM), which forms the below-ground structures.

At the SAM, three layers of cells can be distinguished: the L1, at the very tip of the apex, in which cells only divide in anticlinal plane, gives rise to the epidermis; the L2, in which the cells also divide in anticlinal plane, gives rise to mesophyll cells; the L3, in which the cells divide in more

Introduction

random planes, anticlinally and periclinally, gives rise to the central tissue of the leaf and stem (**Fig. 6**). Moreover, three zones have been classically described based on functional and cyto-histological point of view: the central zone (CZ), which contains pluripotent stem cells; the peripheral zone (PZ), where the differentiation into lateral organs takes place; the rib zone (RZ), which provides multipotent cells for the differentiating stem that supports the SAM (**Fig. 6**).

The SAM is responsible to keep the balance between a pool of stem cells that are maintained in that state and the production of differentiated tissues incorporated into the organs.

The mechanism by which meristems remain undifferentiated is based on a pathway in which the main actors are the gene *WUSCHEL* (*WUS*) and the *CLAVATA* (*CLV*) family genes (Carles and Fletcher, 2003; Dodsworth, 2009, for a review). The homeodomain transcription factor *WUS* promotes stem cell production through a non-cell-autonomous signal to activate cell division (Laux et al., 1996). In *wus* mutants, after formation of a few organs premature termination of the SAM and floral meristem occurs (Laux et al., 1996; Mayer et al., 1998). *CLV1*, *CLV2* and *CLV3* genes are components of an extracellular signaling pathway that acts to limit the expansion of the undifferentiated stem cell population in the SAM and floral meristems (Clark, 2001). *WUS* is expressed in the so-called organizing center (OC) while *CLV3* is expressed by the stem cells region (SC) (**Fig. 6**). *WUS* activates *CLV3*, and the *CLV* pathway represses *WUS* restricting its expression and therefore negatively regulates stem cell production (Schoof et al, 2000). The result of this loop is a balance in the meristem homeostasis so that the loss of cells going to new organs is counteracted by the gain of new stem cells.

SHOOTMERISTEMLESS (*STM*) is another gene expressed in the SAM that plays a role in maintaining the meristem in an indeterminate state (Long et al., 1996). It acts independently of the *WUS/CLV* pathway, preventing cell differentiation in the meristem. *STM* encodes a homeodomain transcription factor, and it is part of the family of *KNOX* (*KNOTTED1-like HOMEODOMAIN*) genes, a group including also *KNAT1*, *KNAT2*, and *KNAT6*, which are also expressed in the SAM and play redundant functions with *STM* (Carles and Fletcher, 2003; Dodsworth, 2009).

The floral transition, which marks the critical passage from vegetative to reproductive phase, and eventually commits the plant to the production of flowers, is reflected in a change in the apical meristem identity (**Fig. 7**). Initially, the meristem at the shoot apex of a plant functions as a vegetative meristem, which is responsible for the vegetative growth of the plant and produces leaves and shoots. When the decision to flower has been taken, the meristem undergoes the floral transition and becomes an inflorescence meristem, which in turn produces floral meristems. Floral

Introduction

meristems arise on the flanks of the inflorescence meristem, and all the floral organs composing the flowers are ultimately derived from this meristem. In *Arabidopsis*, both vegetative and inflorescence meristems are indeterminate meristems, which means that they are maintained through a pool of self-renewing cells. Conversely, floral meristems are determinate meristems. They produce flowers, which are predetermined structures, and they eventually terminate the stem-cell activity (Sablowski, 2007).

Interaction between *LFY* and the *WUS* pathway eventually causes termination of the meristem. *LFY*, together with *WUS*, activates the floral homeotic gene *AGAMOUS* (*AG*) by direct binding to its regulatory sequences (Lenhard et al. 2001; Lohmann et al. 2001; Hong et al. 2003). Upon activation, *AG* mediates termination of the meristem by repression of *WUS*, thus blocking indeterminate growth of the floral meristem (Lohmann et al. 2001; Lehnard et al., 2001) (**Fig. 5, D**). Indeed, *WUS* is expressed in the floral meristem in early phases, but decreases when *AG* is activated and disappears when carpel primordia initiate (Mayer et al. 1998). Therefore, in *ag* mutants *WUS* is expressed constitutively and a stem cell population is produced in the flower, resulting in continuous production of leaf-like organs (Lenhard et al. 2001; Lohmann et al. 2001). Conversely, *wus* mutants show premature termination of floral meristems similar to the over-expression phenotype of *AG* (Laux et al. 1996; Mizukami and Ma 1997; Mayer et al. 1998).

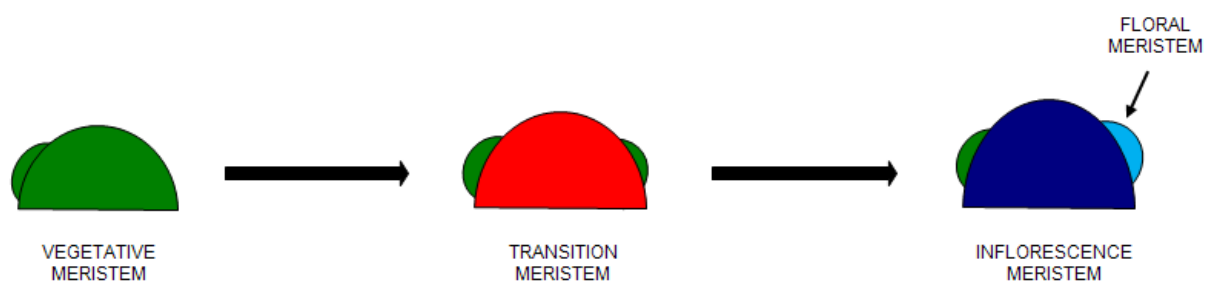


Fig. 7. Phase transition at the shoot apical meristem. A schematic representation of the change in identity of the meristem during the floral transition is indicated in the figure. Green color represents vegetative tissues (vegetative meristem and leaves), red color the transition meristem, light blue the floral meristem and dark blue the inflorescence meristem.

1.9. Genomics approaches to study the floral transition

The transition from vegetative to reproductive growth is a dramatic change requiring a stepwise reprogramming of the shoot apical meristem. Upon inductive conditions, in a few days a set of

Introduction

molecular events transforms a vegetative meristem into an inflorescence meristem and eventually floral meristems arise. Given the biological importance of this switch, several groups reported studies on global gene expression during the floral transition at the shoot apex. Pioneer work was performed already in the 90s on the plant *Sinapis alba* (Melzer et al., 1990). At that time microarray technology was not available, and subtraction hybridisation was used to enrich the extracted RNA in transcripts specifically isolated from the shoot apical meristems. cDNA libraries from apical meristems before the induction (vegetative), during the transition (inflorescence), and after the transition (floral) were compared. This approach successfully led to the identification of new genes involved in the floral transition in *Sinapis* (Melzer et al., 1990).

More recently (Schmid et al., 2003), a global gene expression study at the shoot apex using microarray analysis focused on the floral transition of *Arabidopsis thaliana* (both Landsberg and Columbia ecotypes). Expression levels of the whole transcriptome were followed and analysed in plants that were shifted from SD to LD to induce floral transition. Loss of function mutants were included in this study (*co*, *ft*, and *lfy*) and compared to wild-type. These experiments provided a systematic and complete expression dataset for SAM-enriched apices during floral transition. The expression pattern of known genes was largely consistent with previously published data. The only limitation of these experiments was the use of entire shoot apices. Indeed, meristems were isolated using a razor under a microscope, leading to unavoidable contamination by surrounding leaf tissues, so that genes that are expressed in leaves were also analyzed. Moreover, genes expressed at low level in the meristem or in small subsets of it could be diluted in the whole apical tissue, while a highly specific collection of meristem tissue would enhance the sensitivity to detect these genes (Jiao et al., 2009, for an example in leaf cell types).

1.9.1 “Single cell” technology

Many techniques are available to collect and work on specific cells, without contamination from the surrounding tissues. In some cases, a level of “single cell technology” has been reached (Kehr, 2003). Among these approaches Laser Capture Microdissection (LCM) is particularly powerful (**Fig. 8**). LCM was developed for research in the human and medical field, and the application to plant science followed later (Nelson et al., 2006, for a review). Particularly, some specific features of plant cells have led to the necessity of some modifications, resulting in a further delay. Fortunately, there was a growing interest in recent years for the use of LCM in plants, and there are several reports to which it is possible to refer to set up experiments (Asano et al., 2002; Nakazono et

Introduction

al., 2003; Kerk et al., 2003; Inada and Wildermuth, 2005; Yu et al, 2007). LCM technology allows to collect specific tissues or cell types. With dedicated protocols the tissue material is prepared in order to retrieve nucleic acids or even proteins from the collected tissue. It is then possible to study the presence of specific molecules in the tissue under study.

In order to enhance the power of the tissue specificity with the characterization of the global gene profiling of specific tissues or cell types, LCM has been also often coupled to microarray analysis, with very good results in terms of detailed gene expression of several tissues with extraordinary specificity, even in the case of very small and hidden tissues. This has been successful also in the case of plant tissues (Nakazono et al., 2003; Zhang et al., 2007; Jiao et al., 2009), and because in these experiments normally the amount of tissue recovered is very low, special procedures of RNA amplification have been often associated with the RNA extracted from samples processed with LCM. For example, the RNA linear amplification with the T7 polymerase has been shown not to affect relevantly the proportion of the different transcripts, that means that the amplification, defined “linear amplification”, is balanced (Nygaard and Hovig, 2006; Ginsberg, 2005). So, in the case of critically small amounts of RNA extracted from small tissues, this is normally the best choice so far.

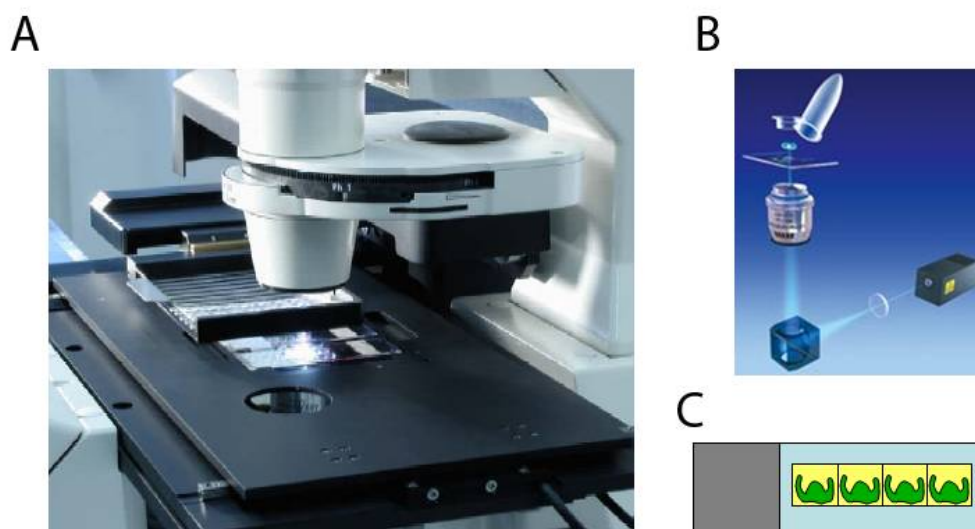


Fig. 8. Laser capture microdissection technology. The LMPC (Laser Microdissection optionally coupled to laser Pressure Catapulting) device form P.A.L.M. is shown in panel A. A scheme of how the sample is collected by the use of a catapulting laser beam is shown in panel B. A scheme of the samples adhered to the glass slides that are used for the laser microdissection is shown in panel C.

1.9.2 Next-generation-sequencing technologies and gene expression analysis

Recently new technologies have been introduced for DNA sequencing. These so-called next-generation sequencing methods are based on massive scale DNA sequencing (see Mardis, 2008, for a review). Besides the application for sequencing or re-sequencing genomes, and to reveal the sites where proteins bind to DNA at the genomic level (“Chip-Seq”), these techniques have been successfully applied to sequence cDNA derived from RNA samples (also called “RNA-Seq”), in order to characterize gene expression at a certain stage and/or in a certain tissue. There are already several variations on this method, and different platforms are available on the market, with features and costs depending on the requirements of the investigator. Two examples are technologies developed by 454 (Margulies et al., 2005) and Illumina (formerly Solexa sequencing) (Bennet et al., 2005). The Illumina Genome Analyzer for example has been used to sequence cDNA from different organisms, including plants (Danilevskaya et al., 2008; Peiffer et al., 2008). An example of an application is the so-called MPSS (massively parallel signature sequencing) (Brenner et al., 2000) coupled with Illumina sequencing, which uses 17-20 nucleotide signatures, and allows the identification of the different transcripts in a cDNA library of a given sample. This approach has been used to perform large-scale gene expression analyses in *Arabidopsis* (Meyers et al., 2004), for example for the floral transcriptome (Peiffer et al., 2008).

Methods are being developed to quantify the number of transcripts for all the genes and to compare these numbers in different experiments, giving rise to an alternative to microarray analyses for global comparisons of gene expression (Cloonan et al., 2008; Mortazavi et al., 2008; Marioni et al., 2008). Studies comparing the results from microarray and sequencing platforms confirmed that the two methods are highly comparable, and the general trend of the gene expression data is very similar (Marioni et al., 2008). Nevertheless, sequencing methods have several advantages compared to microarray methods. Indeed, available microarrays do not contain complete transcriptomes, they suffer from artifacts of hybridisation, and they need several replicates (normally 3 replicate series). Sequencing methods allow a complete identification of the genetic material contained in the biological sample, they have no hybridisation artifacts and they do not imply a strict need of technical replicates since the repetition of sequencing has been shown to be extremely reliable (Marioni et al., 2008). Sequencing allows also discrimination of different splicing variants of genes and permits the discovery of new un-annotated genes or the correction of mis-annotated gene models. Moreover, microarray experiments can be very demanding in terms of quantity of RNA to perform hybridisations. Some sequencing technologies require quantities well below one

microgram of DNA. Moreover, next-generation sequencing methods open up the possibility to characterize the gene expression profile of other organisms in addition to model species. Indeed, microarrays can be performed only when the corresponding chips are produced, while RNA-Seq can be applied in principle to all organisms, even when the genome sequence is not available.

1.9.3 Recent genomics studies on SAM

Very recently, a series of reports were published in which these new technologies described above were used in various combinations. These studies are applied also to other plants than *Arabidopsis*, taking advantage of the fact that sequencing technologies are less dependent on fully-sequenced genomes or availability of dedicated microarray chips. Some of these studies using global gene expression analysis are related to the floral transition, or simply to the specific gene expression patterns of the shoot apical meristem. In all cases, other techniques have been used to validate some of the genes identified by these high-throughput analysis, like RT-PCR and *in situ* hybridisation.

In garden pea, cDNA libraries specific for the shoot apical meristem were generated, and a microarray has been designed based on these libraries which has been used to compare global gene expression between SAM and non-meristematic tissues (Wong et al., 2008a).

In maize, several reports describe how, by means of LCM and amplification of the extracted RNA, shoot apical meristem gene expression has been characterized by microarray. In one case, wild-type and a mutant for a specific homeobox gene have been compared by means of a specifically designed microarray (Zhang et al., 2007). In another one, both microarray analysis and 454 sequencing technology have been used to compare the gene expression between SAM and entire seedlings (Ohtsu et al., 2007). Finally, a global gene expression comparison has been done between two sub-compartments of the SAM, leading to the identification of a novel gene involved in maize shoot and leaf development (Brooks III et al., 2009). Moreover, another group collected SAMs from maize in vegetative and early reproductive stages, compared their gene expression through MPSS, identified two MADS-box genes that were up-regulated upon floral transition, and proved with further experiments the involvement of one of these genes in the floral transition (Danilevskaya et al., 2008).

In soybean, two papers report global gene expression analysis of shoot apical meristem using soybean GeneChip microarrays. In one case, a comparison of the global gene expression profile was performed among SAM, non meristematic tissues and axillary meristems (Haerizadeh et al., 2008). In the other one, SAMs were collected before and during the floral transition, induced by shifting

Introduction

the plants from LD to SD (flowering in soybean is induced by SD), and global gene expression analysis has been performed, with the resulting data suggesting a possible role of auxin and abscisic acid in floral induction (Wong et al., 2008b).

Altogether, these reports testify that we are gradually moving into a new scenario, in which a global knowledge of the gene expression profiles occurring at the shoot apical meristem will unravel a more complete understanding of the floral transition in plants.

OBJECTIVES

Flowering is a complex trait and many studies using several different approaches uncovered a large number of genes involved in this process and also a large number of interactions among these genes. From a spatial point of view, leaves perceive the change in photoperiod whereas shoot apical meristems produce flowers, so that these two tissues are responsible for triggering distinct genetic cascades. While most of the mechanisms regulating the gene cascade responding to the photoperiod in the leaves has been elucidated during the past years, the gene cascade which responds early to the florigenic signal at the SAM is less well known. This has been caused by the technical problem of reaching enough specificity to collect only cells from the apical meristems, which limited the study of gene expression on this tissue. We chose two main approaches to characterize the genes involved in the floral transition at the meristem.

One approach is to make use of Laser Capture Microdissection (LCM) technique to achieve the spatial tissue specificity on SAM and to avoid contamination of other surrounding tissues. We want to set up a system which allows collection of specifically cells from the SAM, and a protocol to extract RNA out of this tissue and to perform global gene expression analysis to study the gene expression during floral transition induced by photoperiod. This would lead to identification of the genes that show a significant increase or decrease in expression during this process, and new genes that would be likely involved in the switch from the vegetative to the inflorescence meristem. We want to confirm the expression pattern of these genes by means of independent expression studies and then place them in the flowering network using other genetic analysis.

The other approach aims at the characterization of *SHORT VEGETATIVE PHASE (SVP)*, a gene involved in repressing the floral transition. Because not too much is known about its spatial regulation, we want to test the hypothesis that *SVP* has different functions, regulating transcription not only in leaves but also in meristems. Because loss of function of this gene leads to early flowering, we want to find which genes are de-regulated in this mutant and are responsible for the premature floral transition at the SAM, in order to identify the possible direct targets of *SVP* transcriptional repressor. Finally, analysis of the genetic interactions of *SVP* with other flowering time genes together with tissue-specific mis-expression studies of this gene will help to clarify and separate the functions of *SVP* in different tissues and to place it in the flowering network.

2. Materials and methods

Plant material

Plants used in this study were *Arabidosis thaliana* accession Columbia (Col), or Landsberg *erecta* (*Ler*) in some cases where specified in the text. The alleles carrying the mutations for *SOC1*, *CO*, *FT*, *TSF*, *FUL*, *SVP* and *TFL1* in Col background were: *soc1-2*, *co-10*, *ft-10*, *tsf-1*, *ful-2*, *svp-41*, *svp-31*, *svp-32*, *tfl1-18*.

The alleles carrying the mutations for *SOC1*, *FT*, *FUL*, and *SVP* in *Ler* background were: *soc1-1*, *ft-1*, *ful-1*, *svp-3*.

35S::*SVP* line in Col background is from Peter Huijser (described in Masiero et al., 2004).

35S::*CO:GR* line (described in Simon et al, 1996) is in *co-2* background (in *Ler*).

Insertion lines from the SALK collection were: SALK_093764 for the *C19* candidate gene; SALK_070018 for *D13* candidate gene.

Plants were genotyped using specific primers (see the list of primers in **Appendix I**).

Growth conditions

Seeds before the experiments were treated with stratification on soil at 4°C for 3 days in the dark. Plants for the experiments were grown in growth cabinets (unless specified in the greenhouse). Long days (LD) were 16 hours of light and 8 hours of dark, short days (SD) were 8 hours of light and 16 hours of dark. The temperature in the growth cabinet was 18°C.

Flowering time measurements

Flowering time was scored as number of leaves at the bolting time. The number of rosette leaves was counted until the bolting shoot reached around 1 cm of length. Cauline leaves were counted when they were all visible on the shoot.

Formula to calculate the percentage of induction

For each population (a distinct genotype or a population with a certain time of vegetative growth in SD) the following formula was used to calculate the degree of induction in the double shift experiments:

Materials and methods

$$\text{percentage of induction (X)} = \frac{NSD - X}{NSD - NLD} \times 100$$

Where NSD is the number of leaves at flowering for the plants in SD, NLD is the number of leaves at flowering for the plants shifted from SD to LD, and X is the number of leaves at flowering of the plants for which the percentage of induction is calculated. NSD, NLD and X are total leaf number (rosette plus cauline leaves), calculated as average of the population grown in the same condition.

Vectors and constructs

To express the gene products of *SVP*, *FT* and *D13*, their complete coding sequence was specifically amplified from cDNA by PCR, using primers with Gateway extensions, and it was inserted into Gateway p201 (for *SVP*) or p207 (for all the others) pDONR vectors by BP reaction, to generate ENTRY vectors.

An ENTRY clone with *SVP.2* was already obtained from the REGIA collection in the pDONR.

The coding sequence was then inserted into different Gateway pDEST vectors by LR reaction. The pDEST vectors were:

- pSUC2 Gateway, with the *SUC2* promoter, which carries the resistance for spectinomycin in bacteria and for BASTA *in planta*.
- pKNAT1 Gateway, derived from pGREEN with *KNAT1* promoter
- pFD Gateway, derived from pGREEN with *FD* promoter
- pLEELA, with Gateway and *35S* promoter

The last three vectors carry the resistance for Ampicillin in *E. coli*, for Carbenicillin in *Agrobacterium*, and for BASTA *in planta*.

For the knock-down constructs using double-strand RNA interference, a region of mRNA from the gene of interest (*SVP* or *D13*) of around 200 bp was amplified from cDNA with specific primers (see List of primers) including Gateway extensions and was cloned into a Gateway p207 DONOR, and then transferred through LR reaction into different pDEST vectors derived from pJawohl17-RNAi 2000 containing *SUC2*, *KNAT1*, and *UFO* promoters in the case of *SVP*, and pJawohl8.2 containing *35S* promoter in the case of *D13*. The *35S* vector contains resistance to BASTA while the others to Kanamycin *in planta*. In this vector the fragment is cloned in two opposite orientations, with an intron in between, in order to create a hairpin loop of a specific region of the gene of interest that triggers the RNA interference processes and silence specifically the target mRNA (Ossowski et al., 2008b).

Materials and methods

For artificial microRNA (amiRNA) (Schwab et al., 2006) constructs the MIR319a precursor was engineered replacing the original miR319a with an artificial sequence (21mer) specific for the target genes and the miR319a* with a sequence that pairs to the amiRNA. The amiRNA was designed with the WMD tool (Ossowski et al., 2008b), and primers were generated with this tool and used for the site-directed mutagenesis PCR reactions using pRS300 plasmid as template. The amiRNA precursors were then cloned into a Gateway p207 DONOR, and then transferred through LR reaction into the pDEST vector pLeela containing the 35S promoter.

Agrobacterium (strain GV3101 pMP90 RK) was transformed with the various pDEST vectors described above.

***E. coli* transformation**

Use DH5 α competent cells.

- Add DNA to the cells (aliquot of cells: 50 μ l)
- put on ice for 30 minutes
- 42°C in waterbath for 90 seconds
- put on ice for 1-2 minutes
- add 400 μ l LB medium
- put at 37°C in the shaker for 1 hour
- spin at 5000g for 2 minutes to collect the cells
- discard the supernatant and replace it with 100 μ l of fresh LB. Resuspend the pellet
- transfer to agar plates (LB+antibiotic)
- leave at room temperature until there is no liquid on the plate
- incubate 37°C, overnight

***Agrobacterium* transformation (heat shock)**

Use *Agrobacterium* GV3101 pMP90 RK, which requires Gentamycin, Rifampicin, Kanamycin antibiotics to be selected.

- Use 3-5 μ l (500 ng-3 μ g) of plasmid in a 2 ml tube.
- put DNA in competent cells
- mix with the tip of the pipette

Materials and methods

- leave on ice for 30 min
- heat shock: 1 minute liquid nitrogen, then 5 min 37°C
- add 500 µl of LB
- put at 37°C in the shaker for 2 hours
- plate on LB agar plates + the 3 antibiotics + antibiotic to select the vector, at 28°C, for 3 days
- grow small liquid cultures of the colonies
- make glycerol stocks

***Agrobacterium* transformation (electroporation)**

Use *Agrobacterium* GV3101 pMP90 RK, which requires Gentamycin, Rifampicin, Kanamycin antibiotics to be selected.

- Thaw competent cells on ice (50 µl)
- add plasmid DNA (1 µl of *E. coli* miniprep) to the cells, and mix on ice
- transfer to a pre-chilled electroporation cuvette. Use the following conditions:
 - capacitance: 25 µF
 - voltage: 2.4 kV
 - resistance: 200 Ω
 - pulse length: 5 msec
- immediately after electroporation, add 1 ml of LB to the cuvette, and transfer the bacterial suspension to a 15 ml culture tube.
- incubate for 4 hours at 28°C with gentle agitation
- collect the cells by centrifugation, and spread them on LB agar plate containing the 3 antibiotics + antibiotic to select the vector
- incubate for 3-4 days at 28°C
- grow small liquid cultures of the colonies
- make glycerol stocks

Plant transformation

Plants were transformed with *Agrobacterium* strain GV3101 pMP90 RK by floral dipping (Clough and Bent, 1998). Plants carrying the transgene were selected in two steps: first either with BASTA or kanamycin, according to the resistance in the vector, and then the insertion of the transgene was checked with specific primers by PCR on genomic DNA extracted from single leaves from the

Materials and methods

independent lines. Finally, the T2 progeny was screened, and only plants segregating 3:1 for the resistance (plants carrying only one single insertion of the transgene) were kept for further analysis. These lines were segregated again in the T3 to select the plant with the insertion in homozygosis.

Sample collection and fixation for *in situ* hybridisation and LCM experiments

Seedlings were collected and fixed with 4% (w/v) paraformaldehyde (in PBS, plus 0.1% Tween-20 and 0.1% Triton X-100) for *in situ* hybridisation or Ethanol:Acetic acid in 3:1 ratio for laser capture. The vials with the samples were continuously kept on ice during the harvesting to preserve the RNA. To allow penetration of the fixative, after collection the tissue was vacuum infiltrated using a pump. The fixative was replaced with a fresh one, and the samples left at 4°C on ice overnight. The following day the fixative was replaced with a stepwise Ethanol: Water series, at 4°C.

For *in situ* hybridisation samples:

- 30% Ethanol, 1 hour
- 40% Ethanol, 1 hour
- 50% Ethanol, 1 hour
- 60% Ethanol, 1 hour
- 70% Ethanol, 1 hour
- 85% Ethanol, over-night
- 95% Ethanol, 4 hours
- 100% Ethanol, over-night
- 100% Ethanol, fresh.

For the LCM samples:

- 85% Ethanol, 4 hours
- 95% Ethanol, 4 hours
- 100% Ethanol, over-night
- 100% Ethanol, fresh

The samples were stored at 4°C in 100% ethanol

Embedding and microtome sectioning

Samples were stained with eosin (0.1% Eosin Y in 100% Ethanol) prior to embedding in paraffin. Embedding was performed with an automated system, the ASP300 tissue processor (Leica). The machine replaces the solution in which the samples are immersed (100% Ethanol) with liquid wax

Materials and methods

at 60°C through a stepwise procedure. Paraplast Plus (McCormick) was used as embedding wax material. Wax blocks with eosin-stained samples were manually prepared with fresh wax at 60°C, cooled down in water at room temperature, and then stored at 4°C.

The embedded plants were sectioned using a rotary microtome (Leitz 1512) at 7 micrometers thickness for *in situ* hybridisation and 10 micrometers thickness for laser capture. After microtome sectioning the tissue was distended on water on the glass slides, above a heatplate, and once the water was removed the samples were adhered on the slides overnight. Superfrost Plus (from Menzel Gläser) or Histobond (from Marienfeld) glass slides were used for *in situ* hybridisation, and PALM MembraneSlides (PEN-membrane, 1 mm) from P.A.L.M. were used for LCM.

***In situ* hybridisation**

Templates for the RNA probes were amplified by PCR using specific primers (see List of primers). For *API* a plasmid (from Mandel et al., 1992) was used to synthesize a probe of 720bp (map n. 45) For *TFL1* the pJAM2045 plasmid (map n. K4, in pGEM-T) was used to synthesize a probe of 0,5Kb of *TFL1*.

Probe synthesis. Reaction mix: 2.5 µl 10x RNA polymerase buffer, 1 µl RNase inhibitor, 2.5 µl 5mM ATP, 2.5 µl 5mM GTP, 2.5 µl 5mM CTP, 2.5 µl 1mM DIG-UTP, x µl DNA template (50 ng of PCR product), 1 µl T7 polymerase, dH₂O to 25 µl. Incubate for 60 min. at 37°C. To stop reaction add 75 µl 1X MS (10mM Tris-HCl pH 7.5, 10mM MgCl₂, 50mM NaCl), 2 µl tRNA (100 mg/mL), 1 µl DNase (RNase free). Incubate for 10 min. at 37°C. Precipitate with 100 µl 3.8M NH₄Ac, 600 µl EtOH (ice cold). Leave at -80°C for 15 min. Spin down 15 min. at 4°C at 14000 rpm. Wash pellet with 200 µl 70% EtOH (ice cold). Spin again, remove supernate and air dry. Resuspend in 50 µl TE.

Tissue pretreatment. Place slides in stainless steel racks and pass through the solutions in the following order: HistoClear 1 (10'), HistoClear 2 (10'), 100% ethanol 1 (1'), 100% ethanol 2 (30''), 95% ethanol (30''), 85% ethanol, 0.85% NaCl (30''), 50% ethanol, 0.85% NaCl (30''), 30% ethanol, 0.85% NaCl (30''), 0.85% NaCl (2'), PBS 1 (2'), Proteinase K (1µg/ml) in 100 mM Tris pH 8, 50 mM EDTA (30' at 37°C), Glycine 0.2% in PBS (2'), PBS 1 (2'), PBS 2 (2'), 4% paraformaldehyde in PBS (10'), PBS 2 (2'), PBS 3 (2'), acetic anhydride (3 ml in drops) in 0.1M triethanolamine pH 8 (10'), PBS 3 (2'), 0.85% saline (2'). Dehydrate through the ethanol series up to 100% ethanol, wash in fresh 100% ethanol.

Hybridization. Prepare hybridization buffer 50% formamide (32 µl per slide with 22 x 50 mm

Materials and methods

coverslip + 8µl probe mix with 50% formamide) for 48 slides: 240 µl 10x salts (3M NaCl, 0.1M Tris-HCl pH 6.8, 0.1M NaPO₄ buffer, 50mM EDTA), 960 µl deionized formamide, 24 µl tRNA 100 mg/ml, 48 µl 50 x Denhardt's, 160 µl H₂O, 480 µl 50% dextran sulphate. Vortex the hybridization buffer, spin down and leave at room temperature. Take the slides out of the rack, allow ethanol to evaporate completely. Heat the probe/50% formamide mix for 2' at 95°C, cool on ice and spin down. Mix the probe with hybridization buffer in a 4:1 buffer : probe ratio. Vortex, spin down and leave at room temperature. Draw around sections with a Pap pen and add buffer/probe to slide. Lower coverslip onto slides. The coverslips have to be previously washed 15 minutes in acetone and baked. Place the slides in sealed boxes (kept humid inside) and leave in 50°C waterbath overnight.

Washing. Place the slides in wash buffer 0.1 X SSC (15 mM NaCl, 1.5 mM Na₃Citrate) and let the coverslips to fall from the slides. Incubate at 50°C for 30' in wash buffer. Change wash buffer and incubate for 45' at 50°C. Change wash buffer and incubate for a further 45' at 50°C again. Wash in wash buffer 1 h at 50°C, then in PBS 5' at room temperature.

Antibody staining. Incubate the slides for 5' in Buffer 1 (100 mM TRIS-HCl, 150 mM NaCl. Transfer the slides to square Petri dishes, flood with Buffer 2 (0.5% (w/v) blocking reagent in buffer 1) and incubate for 30' on a rocking platform. Incubate for 30' in Buffer 3 (1% BSA, 0.3% Triton X-100 in Buffer 1). Incubate in Buffer 4 (Anti-digoxigenin-AP FAB fragment 1:3000 in Buffer 3) for 1 h 30' on a rocking platform. Wash in Buffer 3 (20' 4 times), Buffer 1 (5'), Buffer 5 (100 mM Tris pH 9.5, 100 mM NaCl, 50mM MgCl₂) (5'). Transfer slides to new Petri dishes and flood with Buffer 6 (150 µg/ml NBT, 75 µg/ml BCIP, 24 µg/ml levamisole, in Buffer 5). Cover the trays with a lid and leave in the dark. Check after 12 hours under a dissecting microscope.

Washing and counter staining. To stop the enzyme reaction and to wash off background, put slides back in racks and wash for 30' with: distilled H₂O, 70% ethanol, 95% ethanol, 100% ethanol, 95% ethanol, 70% ethanol, distilled H₂O. Time of washes will depend on intensity of signal and background; if the background is high, wash for longer. Wash briefly in distilled H₂O. Air dry slides, add 3 drops of 50% Glycerol, cover with coverslip and let it dry.

Preparation of slides for LCM samples

The slides for LCM were treated to remove possible RNase contamination, with dry heat at 180°C for 4 hours. This was followed by UV treatment, by irradiation with UV light at 254 nm for 30 minutes using a cross-linker UV Stratalinker 1800 (Stratagene). This allows a further sterilisation

and also the membranes to become more hydrophilic.

Preparation of slides before LCM

To dissolve the paraffin, the slides were exposed to histoclear solvent, and then to a series of ethanol/water solutions with increasing concentration of water:

- 100% histoclear, 2 minutes
- 100% histoclear, 2 minutes
- 100% Ethanol, 1 minute
- 96% Ethanol, 1 minute
- 70% Ethanol, 1 minute
- 50% Ethanol, 1 minute
- Water, 1 minute. Let it dry.

LCM

LMPC (Laser Microdissection optionally coupled to laser Pressure Catapulting) was used, which is modification of the conventional LCM machine. This device is composed by a microscope connected to a computer interface, and a laser beam that can cut the samples that are horizontally stuck on a glass slide. The machine used was "HAL 100" model (230 VZ) from P.A.L.M., equipped with "Axiovert 200 M" from Zeiss. Dedicated software directly controls the beam, and enables to draw the shape of the line that the laser will cut. After microdissection of the tissue, a laser catapult-system can pull the sample into a small collection tube (PALM AdhesiveCaps from P.A.L.M.).

Recovery of RNA after laser capture

The samples were dissolved from the caps of the collection tubes, to extract the RNA.

- Add RLT buffer (from RNeasy kit, Qiagen) + β -mercapto-ethanol (10 μ l for 1 ml of buffer), 100 μ l each tube.
- set the tube upside-down
- 5-10 minutes at room temperature
- vortex for 10 minutes
- spin with microfuge at 13400 ref for 5 minutes
- store at -80°C to avoid RNA degradation

RNA extraction

For the samples processed by laser capture the total RNA has been extracted with PicoPure extraction kit (Arcturus). For all the other samples total RNA has been extracted with RNAeasy kit (Qiagen). The procedures were followed according to the manufacturer's manuals.

RNA amplification

RNA amplification was performed with RiboAmp HS amplification kit (Arcturus). The procedure was followed according to the manufacturer's manual. A general scheme of the procedure is provided in **Fig. 16**.

RNA quality assessment

The RNA quality tests were performed with the Agilent 2100 Bioanalyzer (Agilent Technologies). The kit used for the analysis of the RNA samples with the Bioanalyzer was the RNA 6000 Pico Assay (Agilent Technologies).

cDNA synthesis

cDNA synthesis was performed with SuperScript II kit (Invitrogen).

In the case of the samples processed by laser capture the cDNA synthesis was done using the RiboAmp kit where mentioned in the text.

PCR

The PCR were carried out with the following program:

94°C for 3 min.
 {94°C for 30 s
 55-60°C (depending on the annealing T of the primers) for 45 seconds
 68°C for 30 s - 2.5 min. (depending on the size of the fragment)
 } repeated 25-40 cycles (depending on the level of expression of the gene)
68°C for 5 min.
4°C for 10 min.

PCR mix:

template DNA 3 µl

Materials and methods

primer F (10 μ M)	0.5 μ l
primer R (10 μ M)	0.5 μ l
dNTPs (10 mM)	0.5 μ l
Brown Taq	
buffer (10X)	2 μ l
Brown Taq	
polymerase	0.2 μ l
water	13.3 μ l

Quantitative real time PCR

After total RNA extraction the DNA contamination was removed from the RNA samples with DNaseI treatment (DNaseI from Ambion). A total quantity of 3 μ g of RNA per sample was used to synthesize cDNA for quantitative real time PCR. The synthesized cDNA was diluted to 150 μ l with water, and 3 μ l were used in the PCR reaction. Amplified products were detected using SyBR green I in a IQ5 (Bio-Rad) thermal cycler. *ACTIN2* has been used as a housekeeping gene to normalize the expression of the genes investigated.

Buffer for real-time:

10X buffer (from Invitrogen)	1.2 ml
MgCl ₂ 1M	24 μ l
TRITON X-100	18 μ l
SyBR green 19.6 mM	
(1/10 diluted in TE pH 7.5)	2 μ l

DNA extraction from plant tissue

Genomic DNA was extracted from leaves using a modification of the Edwards method (Edwards et al., 1991).

- Place about 20 mg of plant tissue in a tube
- freeze it in liquid nitrogen
- grind tissue with pellet pestle
- add 400 μ l of extraction buffer (200 mM TRIS-HCl pH 7.5, 250 mM NaCl, 25 mM EDTA, 0.5% SDS)

Materials and methods

- Vortex for 30 seconds
- centrifuge in table-top microfuge for 10 minutes at maximum speed
- transfer supernatant to new tube (take around 250 µl)
- add 1 volume of ice cold isopropanol and incubate on ice for 5 minutes
- centrifuge in table-top microfuge at room temperature for 5 minutes at maximum speed
- discard supernatant and dry pellet
- add 500 µl of 70% ethanol
- centrifuge in table-top microfuge at room temperature for 5 minutes at maximum speed
- discard supernatant and dry pellet
- resuspend pellet in 100 µl of TE (Tris HCl 10 mM pH 7.5, EDTA 1 mM pH 8)
- store at -20°C

Use 3 µl for PCR reactions

DNA purification from gel

DNA for cloning purposes or for synthesizing RNA probes from DNA templates was extracted from agarose gels using Qiaex II gel extraction kit (Qiagen) or Nucleospin extract II kit (Macherey-Nagel).

Plasmids purification

Plasmids were extracted from bacteria and purified using Nucleospin plasmid kit (Macherey-Nagel).

Illumina-Solexa sequencing

The sequencing has been performed by FASTERIS Life Sciences (Geneva, Switzerland). The method used for the next-generation sequencing for the samples of replicates A and B was based on “genomic sample preparation” performed by this company (see **Fig. 21**).

For the samples of replicate C the method used was based on the protocol for mRNA-Seq transcriptome shotgun sequencing derived from Illumina, as performed by FASTERIS (see **Fig. 21**).

Analysis of short-sequence reads from Illumina-Solexa sequencing

Trimming and Filtering

The data were initially filtered using “Seqclean” (executable dated 2005-08-18). This program trims matches against user-specified target sequences (here: the primer sequences GACGGCCAGTGAATTGTAATACGACTCACTATAGGGAGATCTGTATGCTGG and CCAGCATACAGATCTCCCTATAGTGAGTCGTATTACAATTCCTGGCCGTC, and the UniVec_Core database (dated 2008-10-08), as well as poly-A tails and ends rich in undetermined bases. After trimming, a read may be trashed entirely for one of 3 reasons: (a) the sequence is shorter than the minimum length specified via the “-l” parameter (here, 30), (b) the percentage of undetermined bases is greater than 3%, and (c) less than 40nt of the sequence is left unmasked by the “dust” low-complexity filter.

Mapping the reads

Each dataset of reads was converted into a blast database using “formatdb”. Because interest was in matches to known genes, the TAIR8 cDNA collection (TAIR8_cdna_20080325) was then compared to the read databases using Megablast (settings: -v 2000 -b 500 -a 4 -W16 -p 0.6 -e 1 -D3)

The initial runs were performed using the (Mega)blast version BLASTN 2.2.13 [Nov-27-2005]; the last runs were done with BLASTN 2.2.21 [Jun-14-2009].

Determining raw expression counts of genes (loci)

The Megablast output was converted to an expression count by the following 4 steps, in this order:

- (1) discard a match if its bitscore is 5 or more below the best bitscore that is reached by the respective read
- (2) discard a match if it is shorter than 20 bp, or if its edit distance (number of gaps + number of mismatches) is 4 or more, or if the match does not start within the first 3 bases of the read (rationale for the last condition: sequencing quality is best at the 5' end, therefore a true match should cover the 5' end)
- (3) discard all matches involving reads that map to more than a single locus (note that a locus can encompass more than a single transcript (cDNA))
- (4) for each locus, count the number of different reads that map to it (a single read can map multiple

Materials and methods

times to a locus if the locus has multiple transcripts: yet, the read will be counted only once at this step)

The count of step (4) is output as a raw expression count.

P-value method for the identification of differentially expressed genes

For the identification of the differentially expressed genes based on a p-value, the values were calculated according to the hypergeometrical distribution (see Marioni et al., 2008), considering the replicates A and B. The method was implemented by Daniela Knoll.

In order to be considered as differentially expressed between two time points (here an example between +0LD and +3LD), a gene had to fulfill the following criteria:

$$P\text{-Value}(a_{0a3})/P\text{-value}(a_{0b0}) < 0,1$$

$$P\text{-value}(a_{0a3})/P\text{-value}(a_{3b3}) < 0,1$$

$$P\text{-value}(b_{0b3})/P\text{-value}(a_{0b0}) < 0,1$$

$$P\text{-value}(b_{0b3})/P\text{-value}(a_{3b3}) < 0,1$$

Where, for example, $P\text{-value}(a_{0a3})$ is the p-value calculated for a gene between +0LD in replicate A and +3LD in replicate A (“intra-replicate”), and $P\text{-value}(a_{0b0})$ is the p-value calculated for a gene between +0LD in replicate A and +0LD in replicate B (“inter-replicates”).

3. Global gene expression analysis of the floral transition at the SAM collected by LCM using next-generation sequencing

3.1 Defining the floral transition in *Arabidopsis thaliana*

In order to collect samples of the shoot apical meristem (SAM) in a time course during the floral transition, preliminary experiments were done to define the temporal boundaries of this transition. The initial phase of this process was of most interest, to find which genes act in the early stages of the response to long photoperiods. I did not want to include floral meristems which are produced at the flanks of the inflorescence meristem when the transition is completed, because these primordia trigger another developmental program, and they would represent a contaminating tissue (**Fig. 7** for a scheme of the tissues).

3.1.1 Shift and double shift experiments to study the floral transition

It is possible to induce flowering in *Arabidopsis* by shifting plants from short days (SD, 8 hours light) to long days (LD, 16 hours light). This approach represents a convenient way to induce flowering in a controlled and synchronized manner. With this approach it is possible to collect samples at the end of the SD period before induction, and then at different days after induction in LD, thereby placing events within a temporal framework. Moreover, “double shift” experiments were set up, in which plants were grown vegetatively in SD, then shifted transiently to LD, and shifted back to SD, to define the critical number of inductive long days required for the plants to be induced to flower. *Arabidopsis* from the Columbia ecotype (Col) were grown two weeks in SD, and then divided into 6 groups. 4 groups were each exposed to a different number of LD - in this case 1, 3, 5, or 7 LD - and then shifted back to SD. Another group was shifted from SD to LD and left in LD, as a positive control, and the last group was never shifted to LD, as a negative control. Flowering time was scored (**Fig. 9, A**). Both 7 LD and 5 LD of induction under these conditions were enough for the plants to be fully induced to flower, and these plants behave like plants shifted to LD permanently in terms of number of leaves produced before flowering. The condition in which a plant is fully induced, and irreversibly undergoes the floral transition, can be defined as “floral commitment”. Conversely, a transient exposure to 3 LD is not enough to induce a complete induction, but it nevertheless has a significant effect in accelerating flowering. Finally, 1 LD does not have a significant effect on floral induction, since it does not accelerate flowering compared to continuous SD exposure.

Results

Genetic background has a pronounced influence on the results of these experiments. Natural variation in *Arabidopsis thaliana* is present at the level of responsiveness to photoperiod. It is known that the Landsberg *erecta* (*Ler*) accession responds earlier than Col to the floral induction. A previous report showed that in the case of *Ler* when plants were grown for 2 weeks in SD and shifted transiently to LD they responded already after 3 LD with complete floral induction (Corbesier et al., 2007).

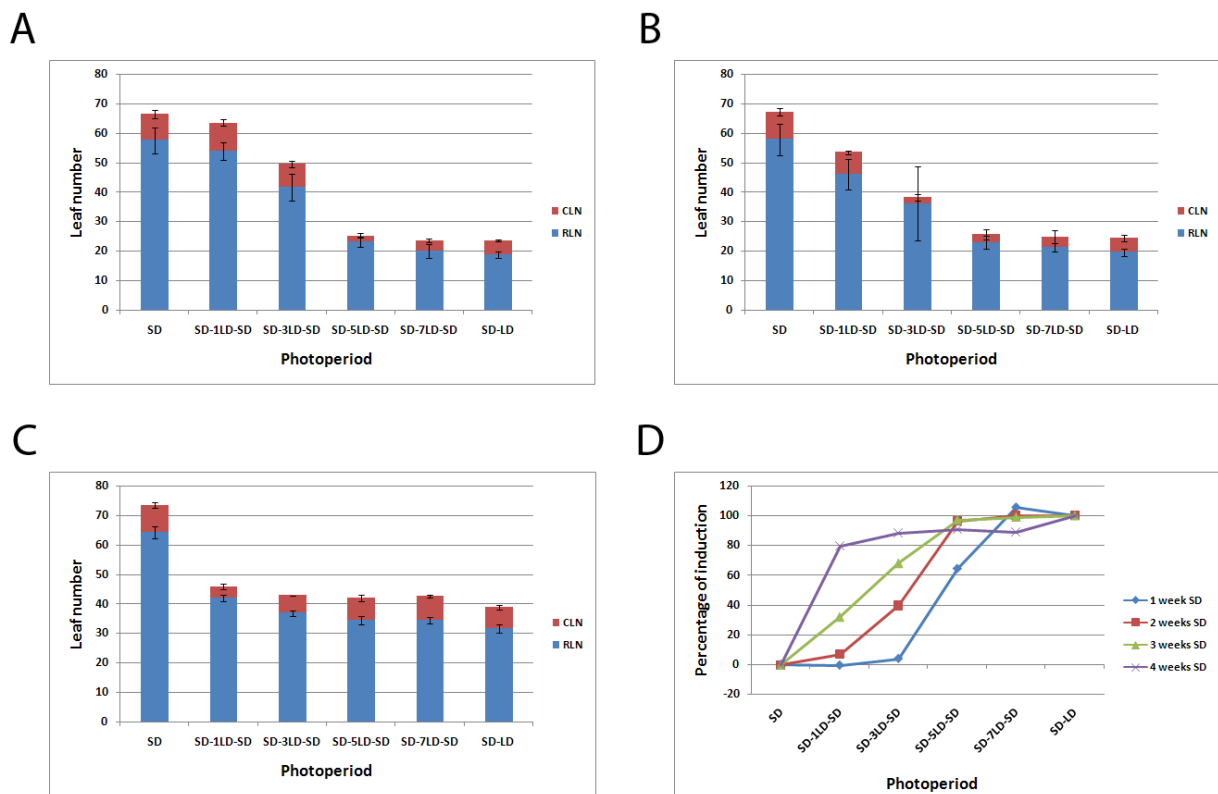


Fig. 9. Flowering time scored after “double shift” experiments. Plants were grown initially in short days (SD) for 2 weeks (Panel A), 3 weeks (Panel B) or 4 weeks (Panel C), shifted to long days (LD, the number of LDs is indicated in the X axis) and then shifted back to SD. Flowering time was scored as number of rosette leaves (RLN) plus number of cauline leaves (CLN). In panel D, experiment with plants initially grown in SD for 1, 2, 3 and 4 weeks are compared. Percentage of induction was calculated with a formula described in the Methods. All the shifts were performed at ZT8.

Several other parameters can also be changed, affecting the susceptibility to floral commitment, such as light quality (Hempel et al., 1997; King et al., 2008), a different number of hours of light in the LD or a different amount of time in which the plants are grown in SD before the shift to LD (Corbesier et al., 1996). In fact, there is a developmental process that drives *Arabidopsis* to flower eventually in SD, so that older plants are more sensitive to floral induction and more responsive to

LD. For example, in the case of Col, for plants that are grown 3 weeks in SD, still 5 LD are necessary to have a complete induction, but also 3 LD are able to induce flowering in some individuals (**Fig. 9, B**). The fact that some of these plants are not fully induced by 3 LD causes a variation in flowering time that is reflected by the large standard deviation. Moreover, also 1 LD has already an effect in accelerating flowering of 3 week old plants. When plants were grown for 4 weeks in SD, also plants transiently exposed to 3 LD were almost fully induced, as indicated by the number of leaves before bolting, and 1 LD had a strong effect in accelerating flowering (**Fig. 9, C**). We can define the “degree of induction” of plants exposed to these double shift experiments, and we can express how much quickly the plant responds to LD depending on how much it grew before in SD, using experimental data. This value was then plotted as “percentage of induction” following a formula (see Methods) which takes into account the flowering time of the plants in continuous SD, which would have 0% induction, the flowering time of plants shifted from SD permanently to LD, which would have 100% induction, and computes the values of the other treatments based on those two extremes. The plot (**Fig. 9, D**) shows that the more the plants were grown in SD, the more they rapidly responded to LD induction. This plot is useful to compare how much a plant can be easily induced among different conditions, and how much the time window of the floral transition can be lengthened or shortened depending on the initial growth time in SD.

In a previously reported study of global gene expression during floral transition in *Arabidopsis*, plants were grown 4 weeks in SD before induction in LD, both for Col and *Ler* ecotypes (Schmid et al., 2003). Based on our data, 2 weeks in SD were instead chosen because at this stage plants have not yet started the flowering process, and the time window in which floral induction occurs is longer, allowing a better detection of the temporal activation of the different processes and genes at the SAM.

3.1.2 *In situ* hybridisation on marker genes

In order to confirm the previous observations based on flowering time and to correlate them with the molecular events occurring at the SAM, *in situ* hybridisations were performed on wild-type *Arabidopsis* apices using probes for several flowering time genes. Known genes that can be used as markers were chosen, such as *SOC1*, *SVP*, *FD* and *API*, because they are expressed in meristems and they are associated with early events of the floral transition. Previous reports on the expression of some of these genes upon shifts to LDs in *Ler* and Col ecotypes (Searle et al., 2006; Wigge et al., 2005; unpublished data from our lab) were used as a guideline for our experiments in Col (**Fig. 10**).

Results

Plants were grown for 2 weeks in SD and shifted to LD, and samples for *in situ* hybridisation were collected at +0LD (before the shift), +1LD, +3LD, and +5LD. All the samples were collected eight hours after dawn (ZT8), which is also the time when all the shifts were done. The same experiment was repeated, and the biological replicates showed the same results.

As expected, *SOC1* mRNA is remarkably rapidly up-regulated upon exposure to LD. Before induction no signal was visible for this mRNA by *in situ* hybridisation (**Fig. 11, A**). *SOC1* mRNA starts to be clearly detectable already from the first day after induction in LD (**Fig. 11, B**). After 3 LD the expression level increases even more (**Fig. 11, C**). Conversely *SVP*, which encodes a floral repressor, is strongly expressed in SD before induction and then decreases in expression upon LD induction (**Fig. 11, D-F**).

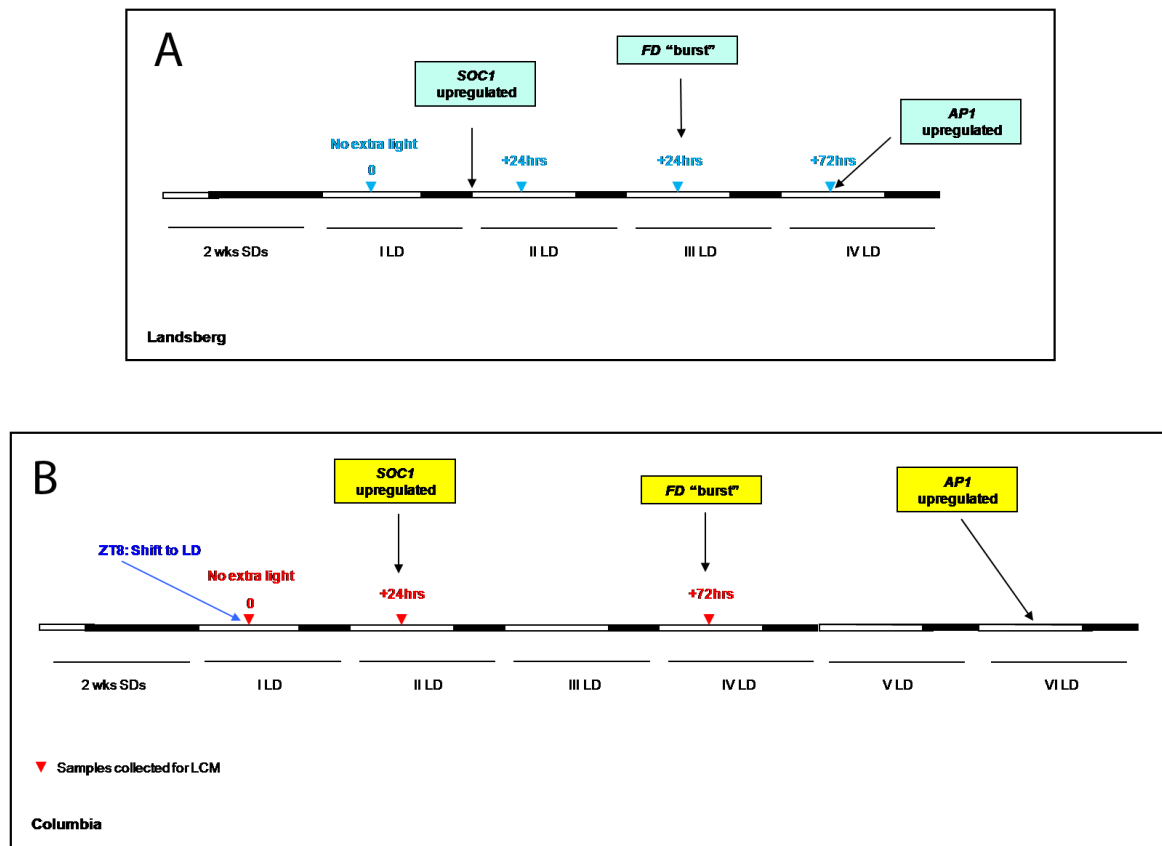


Fig. 10. Collection of the samples for *in situ* hybridisation and LCM.

Panel A: A general guideline for the temporal expression of flowering time genes is given by experiments previously performed on Landsberg *erecta* ecotype (see text).

Panel B: Schematic representation of the results of *in situ* hybridisations on wild-type Columbia ecotype for flowering time genes that can be used as markers of the floral transition.

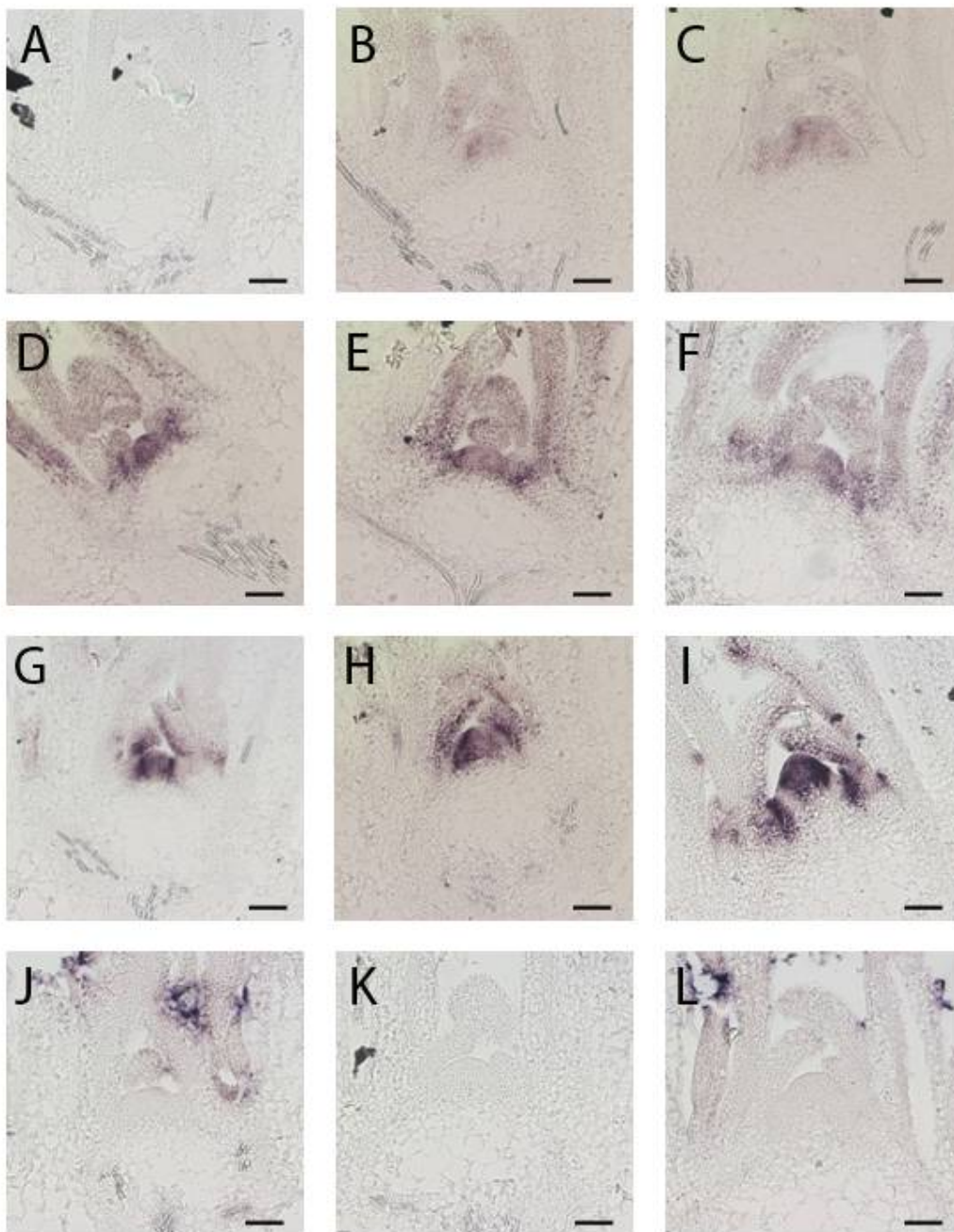


Fig. 11. *In situ* hybridisation of flowering time marker genes at the shoot apices of wild-type Columbia plants. RNA probes were used to detect *SOCI* (A, B, C), *SVP* (D, E, F), *FD* (G, H, I) and *API* (J, K, L) mRNAs. Plants were grown 2 weeks in SD and collected before induction at ZT8 (+0 LD) (A, D, G, J), after 24 hours (+1 LD) (B, E, H, K) and 72 hours (+3 LD) (C, F, I, L) of induction in LD. Scale bar is 50 μ m.

In the case of *FD*, there is strong expression all along the time course, as observed previously (**Fig. 11, G-I**). Following the current model, this suggests that when FT protein reaches the SAM it can

immediately interact with FD protein and activate the floral transition. Moreover, there is a small change in the expression pattern of *FD* during the floral transition. In terms of level of expression, although difficult to quantify, it seems that there is a reproducible increase in *FD* mRNA, as also reported previously (Wigge et al., 2005; Searle et al., 2006). Also the spatial pattern changes so that additional spots of strong expression appear in a region on the flanks of the SAM that is physically separated from it.

Plants grown two weeks in SD do not show *API* expression, and the same happens when they are shifted to LD after 1 and 3 LD of induction (**Fig. 11, J-L**). After 5 LD of induction *API* mRNA is clearly induced in the floral primordia, marking the beginning of floral development (see later, and **Fig. 14, C**). This correlates with the meristem being committed to flower at that stage, as demonstrated by the flowering time data of the double shift experiments (see above) and suggesting that the floral transition cannot be reverted once floral primordia are already present at the flanks of the SAM and *API* is induced.

Based on the results of *in situ* hybridisations and flowering time data of the “double shift” experiment, three time points were chosen for the global gene expression studies: two weeks SD + 0 LD (+0LD), two weeks SD + 1 LD (+1LD), and two weeks SD + 3 LD (+3LD). The first time point represents plants before photoperiodic induction; the second time point was included because although one transient LD does not affect flowering time it has been shown that *SOCI* is already up-regulated as a first marker of molecular events connected to floral induction; the third time point corresponds to the condition in which the meristem has progressed to flowering but without floral meristems present in the apical tissue. For the gene expression analysis seedlings were collected in the same experiment in which samples were collected and tested by *in situ* hybridisation. This already provided a control test for the stage in which the material used for LCM was collected.

3.1.3 Double shift experiments to link expression of flowering time genes to floral commitment

As it has been shown previously, when plants are shifted from SD to LD a set of genes changes expression level and pattern, at specific times and in specific places, and this is linked to molecular events triggering the floral transition at the SAM (Schmid et al., 2003; Searle et al., 2006; Wigge et al., 2005). Nevertheless, the expression response of these genes once the plants are shifted back to SD is not known. Presumably, this will depend not only on the specific function that each gene has in relation to the floral commitment, but also on how many days of induction in LD are given to the plants before shifting them back to SD, since different degrees of induction have a different

Results

consequence in terms of flowering time and floral commitment. A similar experiment was reported for *FT* gene expression in leaves, in which it has been shown that upon shift from SD to LD *FT* is turned on immediately and its expression increases with progressive exposure to LD. When plants are shifted back to SD the level of *FT* expression drops again to the typical basal level of SD condition (Corbesier et al., 2007). The authors concluded that once the floral commitment has been reached, *FT* expression is not required any longer, as flower development occurs in SD when *FT* is not expressed.

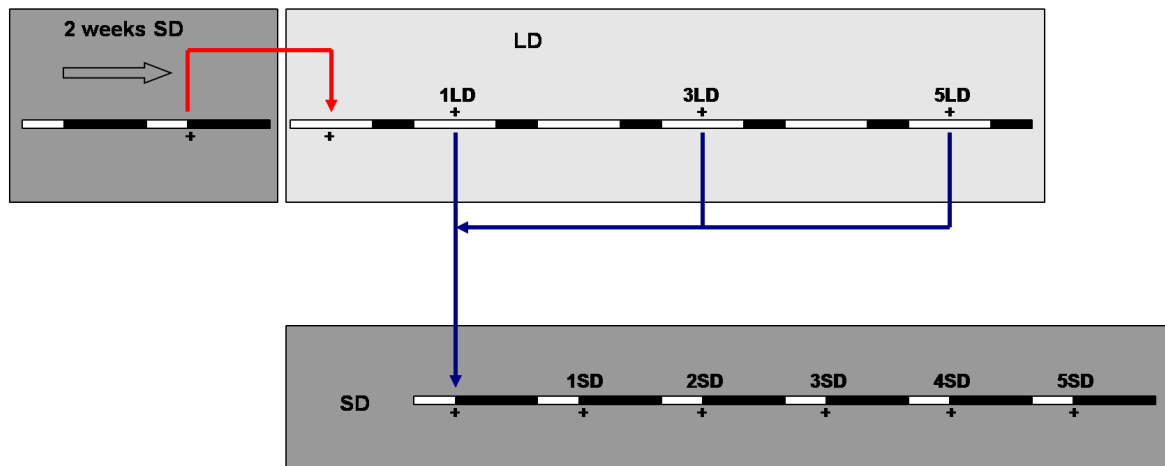


Fig. 12. Collection of samples for *in situ* hybridisation in “double shift” experiments. Shifts in photoperiod are represented in the figure. The red arrow represents the shift from SD to LD, the blue arrows shifts from LD to SD. + indicates 8 hours after dawn (ZT8).

Here, the focus is on the events which act downstream of *FT*, in the SAM. Therefore a time course was set up and samples were collected for *in situ* hybridisation at different time points. Wild-type Columbia plants were grown for two weeks in SD, then transferred to LD for 1 LD, 3 LD, and 5 LD and seedlings were collected. Plants were then transferred back to SD and seedlings collected after 1 SD, 2 SD, 3 SD, 4 SD, 5 SD (see **Fig. 12** for a scheme). Treated plants were given specific names so that for example a plant that is exposed to 3 LD of induction and then shifted back to SD for 2 days is named 3LD 2SD. A not induced control, 0LD 0SD, was also included. ZT8 was used as a reference point both for the time of the shifts and for time of collection of the seedlings. The analysis focused on the early part after the induction, represented by not more than 8 total days (LD+SD) after the first shift. Shoot apices from these plants were hybridised with different RNA

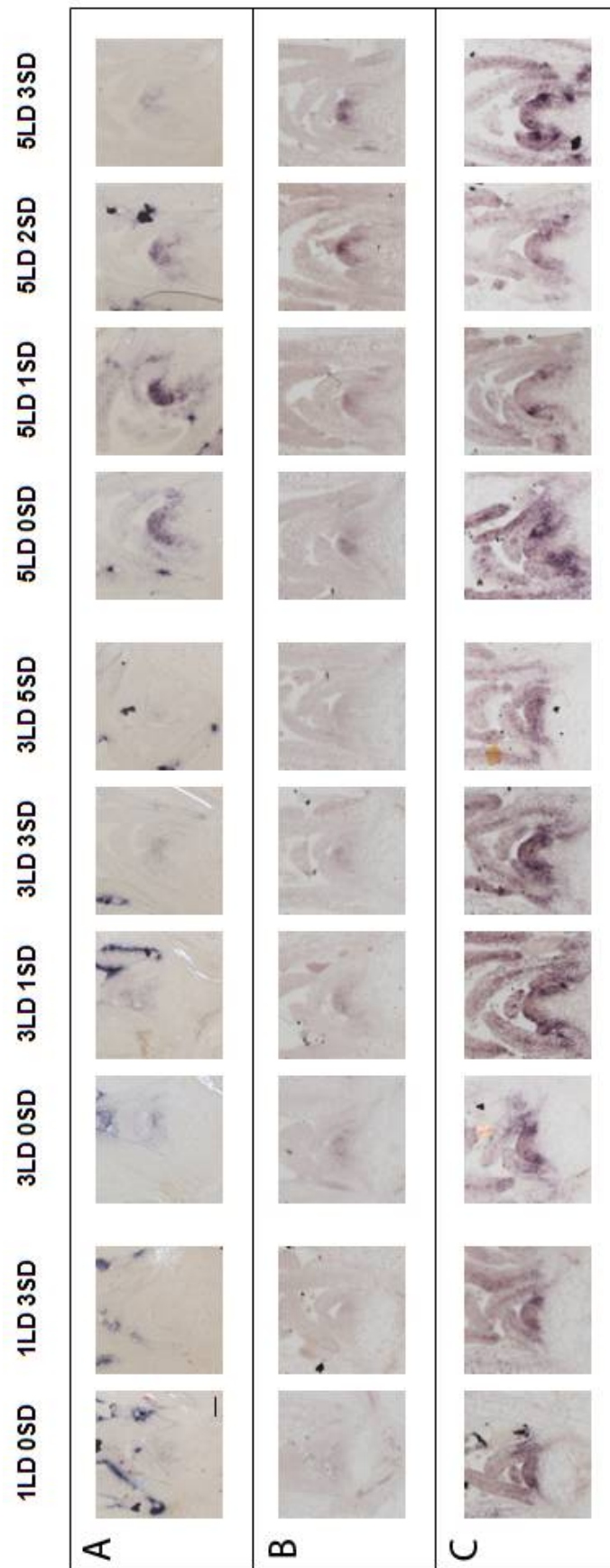
Results

probes. *In situ* hybridisation on a complete time course with probes for *SOCI*, *FUL* and *SVP* was carried out and it was also repeated. Additionally, some samples were hybridised with probes for *AGL24*, *API* and *FD*. It was not always easy to quantify changes in gene expression among different samples from this kind of experiment, because of small variations in individual plants, and because this technique has a limited power of quantification, especially when the signal is weak or weakly changed. Nevertheless, it is possible to observe a clear general trend in expression for the genes examined.

In situ hybridisation using *SOCI* probe (**Fig. 13, A**) confirmed that the mRNA of this gene is up-regulated at the SAM in response to LD and that the signal increases with the number of LD. When the plants are shifted back to SD the level of *SOCI* mRNA slowly decreases, regardless of the number of LD to which the plants were exposed and of the degree of induction of this gene. This is particularly evident in the 3 LD and in the 5 LD samples. Hence, although 3 LD and 5 LD represent not-committed and fully-committed meristems respectively, *SOCI* expression pattern follows the same decrease after return to SD. We can conclude that *SOCI* expression quickly responds not only to shifts in photoperiod from SD to LD but also from LD to SD, and that flowering could occur independently of the level of expression of *SOCI* once the meristem is committed to flower. Also, *SOCI* level of expression at the SAM follows the level of *FT* in the leaf (Corbesier et al., 2007).

The same time course was hybridised with a probe for another MADS box gene, *FUL*. This gene was chosen because its mRNA expression pattern during photoperiodic induction is similar to the one of *SOCI* and these genes are partially redundant in promoting the response to LD (Hempel et al., 1997; Melzer et al., 2008). In our experimental conditions *FUL* expression is activated upon photoperiodic induction by LD, and its expression increases with the number of LD, similar to *SOCI* (**Fig. 13, B**). *FUL* expression also drops when plants are shifted back to SD after exposure to 1 LD or 3 LD, but after 5 LD its induction becomes stable, even if the plants are shifted back to SD. So, in contrast to *SOCI*, the expression of *FUL* is stably maintained once the meristem is committed to flowering.

Fig. 13. (next page) Expression of flowering time genes at apices of wild-type plants during “double shift” experiments. *In situ* hybridisation was used to follow the expression of genes related to floral commitment at the SAM. RNA probes were used to detect *SOCI* (panel A), *FUL* (panel B) and *SVP* (panel C) mRNAs. Plants were initially grown for 2 weeks in SD. The number of LD and subsequent SD to which they were exposed before the sampling are indicated in the figure for each sample. Scale bar is 50 μ m, and magnification same for all panels.



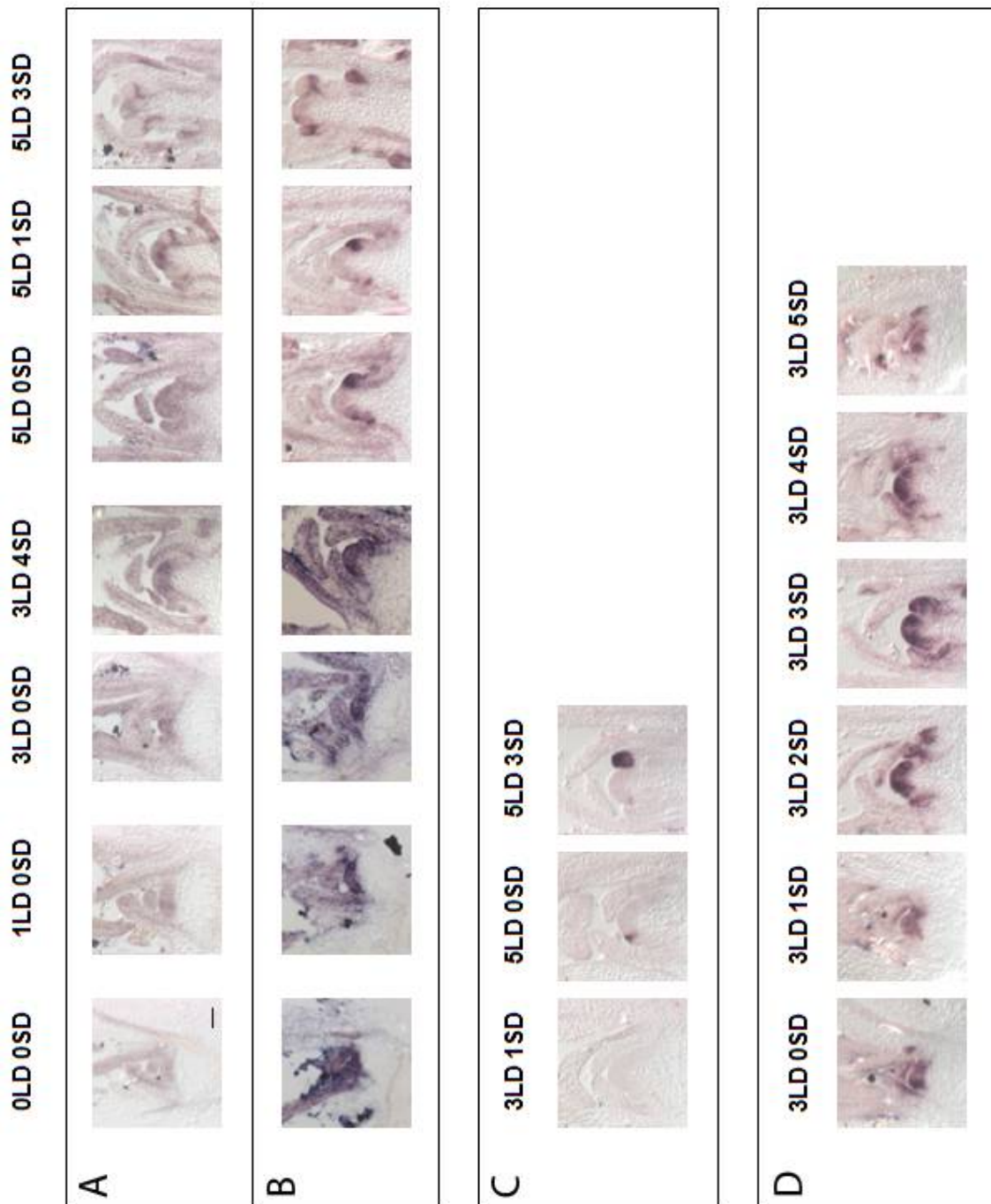


Fig. 14. Expression of flowering time genes at apices of wild-type plants during “double shift” experiments. *In situ* hybridisation was used to follow the expression of genes related to floral commitment at the SAM. RNA probes were used to detect *AGL24* (panel A), *SVP* (panel B), *API* (panel C) and *FD* (panel D) mRNAs. Plants were initially grown for 2 weeks in SD. The number of LD and subsequent SD to which they were exposed before the sampling are indicated in the figure for each sample. Scale bar is 50 μ m, and magnification same for all panels.

Results

The expression pattern of *SVP*, another marker of the floral transition, was also examined. In our experimental condition the expression of this MADS-box gene before LD exposure is very strong and broad in the whole SAM, while it decreases in the centre of the inflorescence meristem with progressive induction by LD (**Fig. 13, C**). This is in agreement with the role of this gene as a floral repressor. As it has also been shown previously (Hartmann et al., 2000), *SVP* is also strongly expressed in the floral primordia once they arise from the inflorescence meristem, after the transition. When plants induced by 1 LD or 3 LD are shifted back to SD the general level of expression of *SVP* does not dramatically decrease or increase, but seems to remain stable. After 5 LD of induction *SVP* expression clearly decreases, and does not rise again after shifting the plants to SD. This may indicate that after 5 LD floral commitment has been achieved, so that *SVP* mRNA and its floral repressing function are reduced, while after 3 LD, in which the floral commitment has not been completed, *SVP* mRNA is still expressed enough to prevent floral transition.

The closest *SVP* homologous gene is *AGL24*. The expression pattern of this MADS-box gene in our experimental conditions was not very clear (**Fig. 14, A**). *AGL24* mRNA seemed to be expressed both before and after shift from SD to LD, although in LD it appeared to get stronger in intensity and broader in terms of spatial distribution. Compared to *SVP* mRNA in the same condition (**Fig. 14, B**), it shows an overlapping pattern in the stages before and after the transition, while it has more a complementary pattern at the moment of floral commitment. This could be due to the proteins produced by these two genes physically interacting in certain developmental stages, while in others they have an opposite role (Gregis et al., 2006; Gregis et al., 2008; Liu et al., 2009).

In situ hybridisation using *API* probe showed that after 5 LD this gene is strongly expressed, confirming that the meristem is committed to flowering (**Fig. 14, C**). Even if the plant is shifted back to SD *API* remains strongly expressed. Finally *FD*, a gene that marks the competence of the meristem to receive the flowering signal (through interaction of *FD* with *FT*), is strongly expressed already after 3 LD when the meristem is not fully committed, and this is maintained when the plant is shifted back to SD (**Fig. 14, D**), leading to the conclusion that these shifts probably do not have much effect on the expression of the *FD* gene.

3.2 Laser microdissection of shoot apical meristems

3.2.1 Calculation of the material needed and choice of the techniques

Before starting the experiment, a calculation of the amount of material needed was done, in order to have a reasonable estimation of the number of plants to sample for each time point. Based on the

Results

expected number of cells in an average SAM, and on the quantity of RNA needed for analyzing global gene expression, the quantity of plants to be collected and dissected by laser capture microdissection (LCM) was calculated (see Fig. 15). Initially, a microarray chip experiment was planned for the global analysis of gene expression, which would need high quantities of high-quality RNA. So the calculations were based on these requirements.

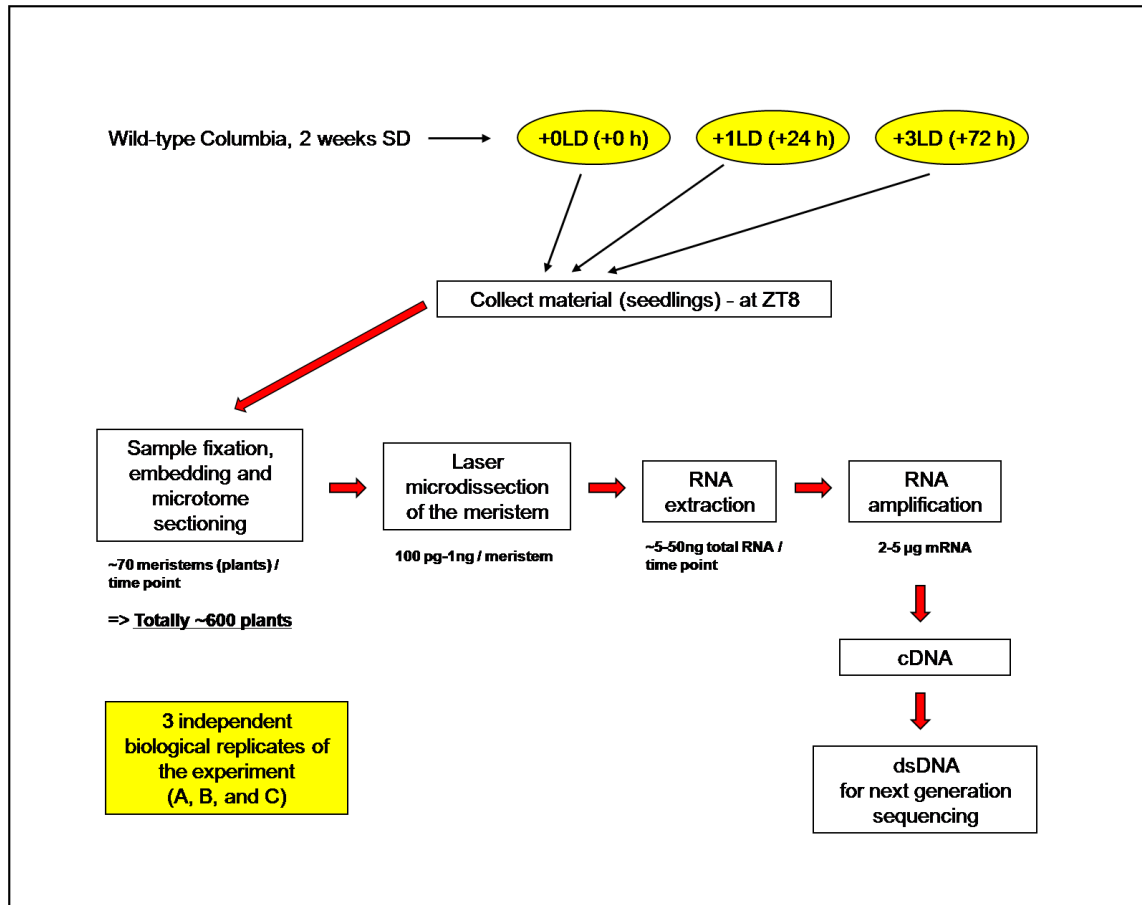


Fig. 15. Scheme of the general strategy followed to collect the samples for LCM. Apices from wild-type Col were collected and fixed according to LCM procedures indicated in the text. The amount of samples for LCM was estimated before the collection (see text for details). The experiment was done three times, and the samples were used as three independent biological replicates of the same experiment.

The SAM of *Arabidopsis* is very small (SAM diameter is about 50 micrometers for two-weeks old seedlings grown in SD, and almost double that after three long days of induction); thus not only many samples had to be laser-dissected, but also a step of RNA amplification had to be included, because of the low quantity of the starting material. To amplify the RNA extracted from SAM

tissue the so-called “linear RNA amplification” (based on T7 polymerase, with two rounds of amplification) was chosen (see **Fig. 16** for a scheme, and Methods; Ginsberg, 2005).

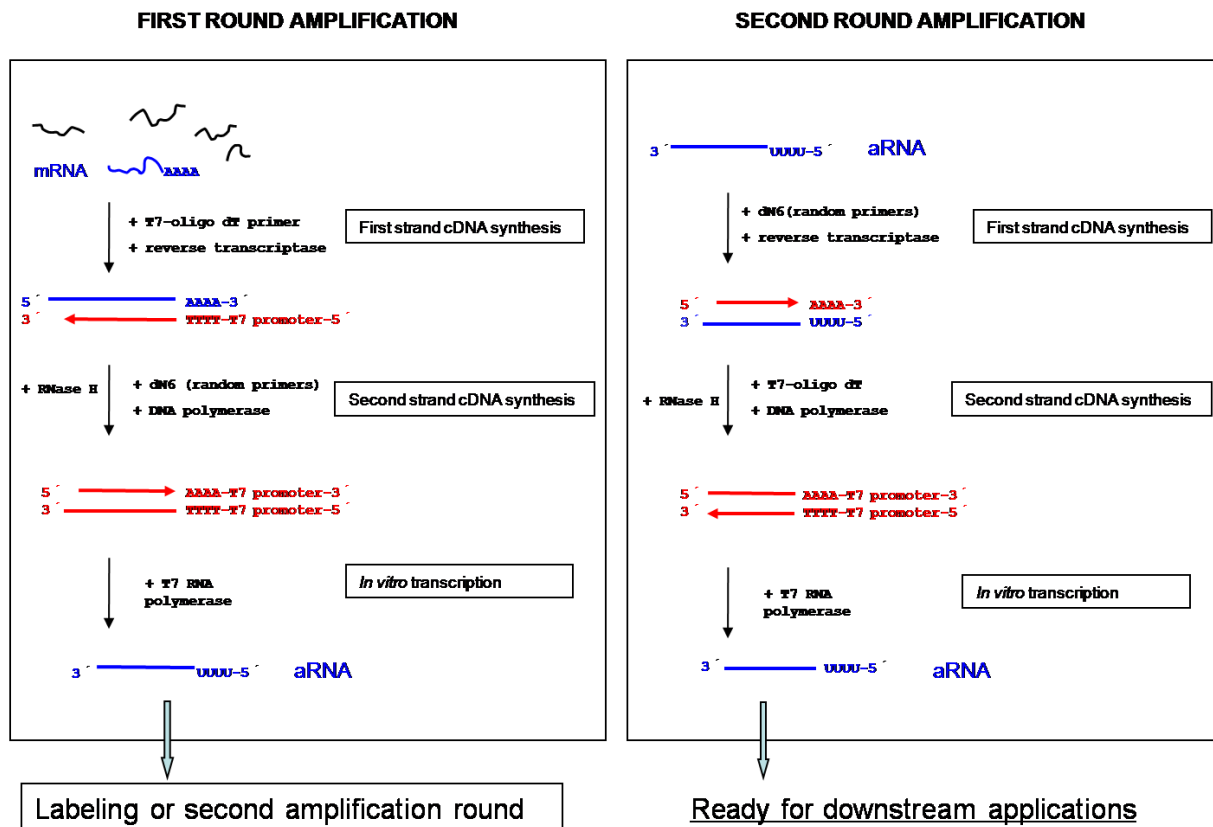


Fig. 16. RNA amplification process. This method performs RNA amplification of either one or two rounds, depending on the amount of the starting material. It is based on the use of a T7 RNA polymerase. It requires total RNA as input and generates amplified RNA (aRNA), which is the reverse complement of the mRNA.

The quantity of RNA required for an Affymetrix chip hybridisation is around 15 micrograms for each sample. Since the amplification step can give a yield ranging from one thousand to one million fold amplification, and the process starts with total RNA but specifically amplifies only the mRNA, it was estimated that before the RNA amplification step 5-50 ng of total RNA was required. If an average shoot apical meristem of *Arabidopsis* is composed of around 50-100 cells, the RNA contained should be around 100-1000 pg (for the calculations refer to: Nakazono et al., 2003; Kerk et al., 2003; Nygaard and Hovig, 2006; Ginsberg, 2005). Therefore, meristems from about 50 plants are needed for each time point, which consists of a total of around 2500 cells. This number,

compared with other experiments in the literature, seems to be more than sufficient for our purpose (Nakazono et al., 2003; Kerk et al., 2003). All of these calculations are obviously approximate, but they are important in providing a rough indication of the amount of material required.

A. thaliana Columbia wild type plants were grown for two weeks in SD, after +0 LD, +1 LD and +3 LD of induction samples were collected (see **Fig. 15**) at ZT8 (see **Fig. 10, B**). In order to have independent biological replicates, the experiment was done in triplicate, in controlled conditions in growth chambers. For each replicate about 100 plants per time point were collected, 70 for LCM and 30 for *in situ* hybridisation. Apices from the seedlings were fixed and embedded in wax blocks, and sectioned with microtome.

3.2.2 Optimization of the protocol

Before processing the meristem material, tests were carried out with other tissues, to set up and optimize the conditions for the LCM, RNA extraction, and the RNA amplification. To prevent the risk of compromising the valuable meristem material, some of the following trials were made with another tissue that was easier to collect. This permitted optimisation of the protocol for later procedure on the RNA and gave useful guidelines of how to proceed with the meristem samples. Therefore circular “leaf discs” were collected by LCM from the glass slides, both from young and mature leaves (**Fig 17, A**). Leaf tissue has different features than the meristematic tissue, which is composed of less differentiated cells that are smaller and more transcriptionally active. Leaf cells are less compact, due to larger vacuoles, and generally less rich in RNA, especially if compared with the meristems undergoing the floral transition. So, different quantities of leaf discs that could reasonably resemble the quantity of cells of the meristem samples were collected. Once leaf tissue was collected by LCM the RNA was extracted both with the “RLT buffer” of RNeasy kit (from Qiagen) and with the “XB” extraction buffer of Picopure kit (from Arcturus) and the RNA was purified both with the Qiagen and Arcturus kit (see Methods). To test the RNA extracted, it was converted into cDNA and RT-PCR was performed. Primers for *TUBULIN* were tested. With RNA extracted from 100 leaf discs no PCR product was visible on agarose gel after RT-PCR, but with RNA from 300 leaf discs a weak band appeared on the gel, which was more visible using 40 cycles in the PCR reaction instead of 35 (**Fig. 17, B**). The best yield of RNA estimated from the results of the RT-PCRs resulted from the RLT buffer from Qiagen as extraction buffer with the PicoPure kit from Arcturus.

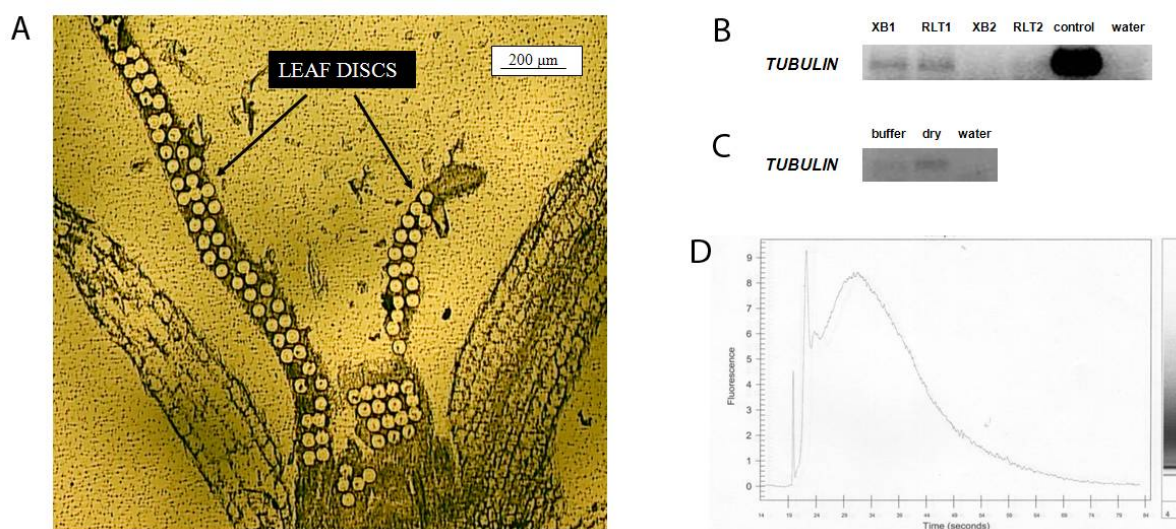


Fig. 17. Laser microdissection, RNA extraction and RNA amplification on a test tissue. Panel A: Circular leaf discs from *Arabidopsis* leaves were collected by laser microdissection on sectioned apices, and RNA extracted from the recovered tissue. Panel B and C: cDNA was produced from RNA, and it was tested with primers for *TUBULIN*. Panel B: Different buffers were compared. “XB1” and “XB2”: RNA extracted with XB buffer. “RLT1” and “RLT2”: RNA extracted with RLT buffer. XB1/RLT1 and XB2/RLT2 were collected in two independent experiments, and the second ones were then diluted 50% more compared to the first ones. “Control” was cDNA produced from high-amount RNA extracted with traditional methods. Water was used as a negative control. Panel C: Two different systems for the collection of the tissue catapulted from the laser beam were compared. “Buffer”: tissue collected on the RLT buffer. “Dry”: tissue collected directly on the matrix of the tube. “Water”: negative control with water. Panel D: Bioanalyzer analysis of the RNA that was extracted from leaf discs and then amplified with two-rounds of RNA amplification.

Two different methods for collecting the material catapulted from the slide by the laser into the collection tube were also tested. The “classical” method which employs special tubes from P.A.L.M., equipped with a matrix to which the tissue adheres, was compared to another method using normal tubes with the cap filled with RLT buffer where the tissue is catapulted. 300 leaf discs were collected with each of the two methods. RNA was extracted and converted into cDNA, and RT-PCR showed that the first method seems to give a better yield (**Fig. 17, C**). Therefore the “classical” method was used for the rest of the subsequent experiments.

Then RNA linear amplification was performed on RNA extracted from 200 leaf discs using the RNA amplification method (See **Fig. 16** and Methods). The RNA quantity after the first round of amplification was 0.804 micrograms, while after the second round it was 4.59 micrograms. The overall quality of the RNA was assessed by analysis with the Agilent Bioanalyzer (**Fig. 17, D**). The quantity was similar to that estimated above, and the quality was good in terms of RNA integrity. The second round gave an amplification of about 5.7 fold. The fold of amplification for the first

round could not be estimated because the quantity of the initial RNA before the amplification could not be measured due to its low concentration. Nevertheless, considering that the final amount is composed of only amplified mRNA, and that the initial material consisted of a few hundreds cells, we can conclude that this technique allows a useful amplification in mRNA quantity.

3.2.3 Collection of the SAMs

Once sure of the yields and quality of the amplified RNA, the meristem samples were processed in the same way explained above.

Making use of LCM, shoot apical meristems were collected from plants harvested in the time course described above, in order to proceed afterwards with RNA extraction. All the meristems were pooled in a total of 9 samples (+0LD, +1LD and +3LD, in triplicates A, B and C). A set of pictures of apices from the three time points before and after the capture of the meristems, demonstrate that the laser was able to cut out precisely the area of the whole meristem dome, avoiding the surrounding tissues, and especially leaf vasculature that is important not to take in this case (**Fig. 18**). It was checked by visual inspection with the microscope that most of the meristems were really catapulted in the cap of the LCM collection tubes.

3.2.4 RNA extraction from the captured material and RNA amplification

For each of the 9 samples the total RNA was extracted and two rounds of RNA amplification were performed on it. The RNA extractions and amplifications were carried out at three separate times for the three biological replicates. The resultant yields were in the range of 3-60 micrograms of amplified RNA (aRNA) depending on the sample (see **Table 1**). Remarkably, the quantity of RNA obtained was directly related to the level of floral induction, which probably reflects the larger size of florally-induced meristems. Indeed, in the case of replicates A and B, the second time point produced around double the amount of RNA of the first one, and the third time point produced around double the amount of the second one. Floral induction led to a visible growth of the meristem dome (**Fig. 11**, **Fig. 18**), resulting in both a larger area captured with the LCM and a higher number of sections captured per plant sample (about 2-4 sections for the +0LD, 4-6 for +1LD, and 6-9 for the +3LD). In addition to this increase in size, floral induction might contribute to a generally higher production of mRNA in the later meristems.

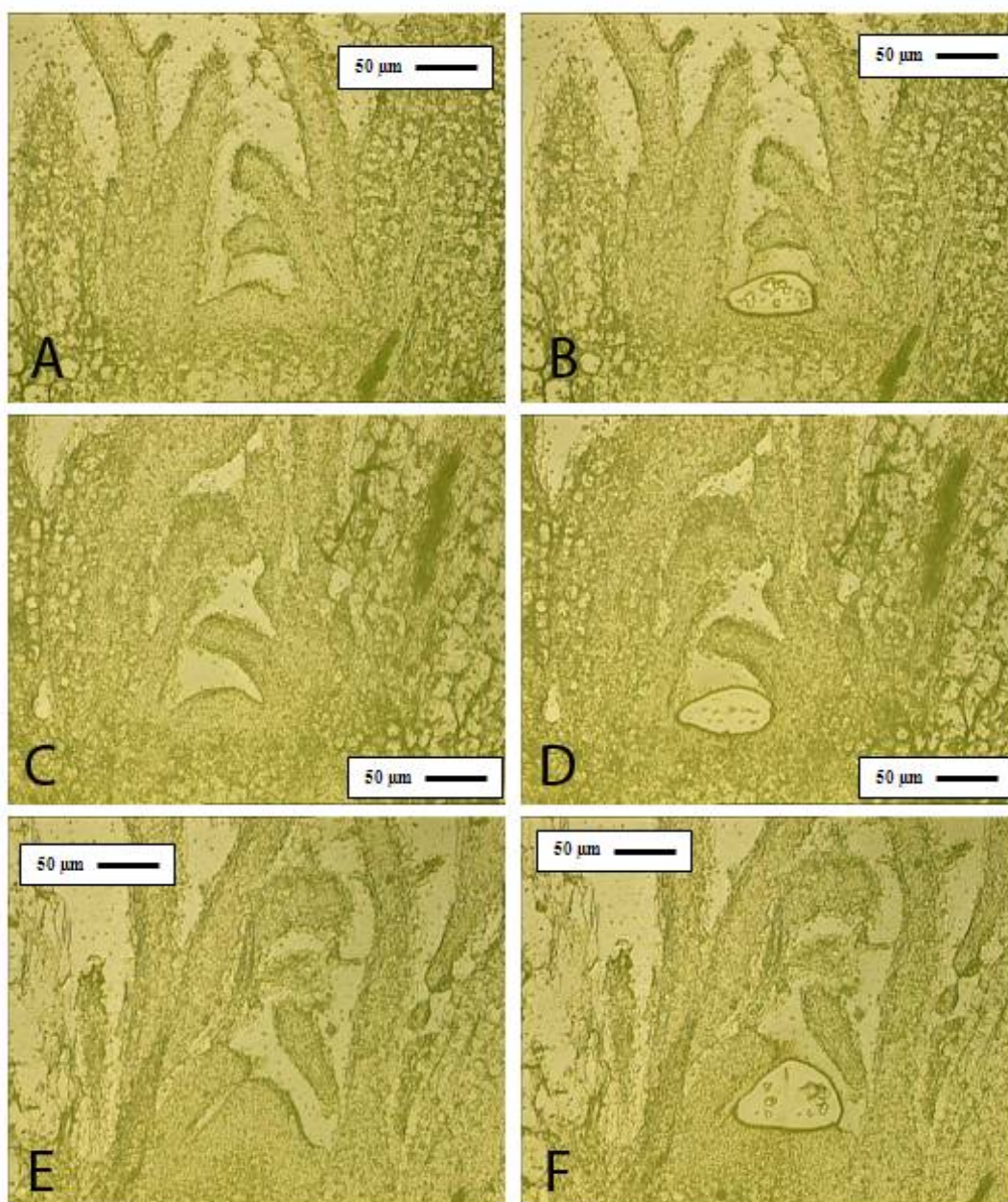


Fig. 18. Laser microdissection on shoot apical meristems. Apices of wild-type Columbia, which were sectioned and fixed on glass slides for LCM, are shown. Each sample is shown on the left before (A, C and E) and on the right after (B, D, and F) laser capture of the meristem. Samples shown were collected after 2 weeks in SD (A and B), and then shifted to LD for 1 LD (C and D) or 3 LD (E and F). Magnification: 20X.

Biological replicate	Time point	Number of plants	RNA after amplification	RNA for sequencing	DNA for sequencing
Replicate A	+0LD	~70	14.0 µg	1.0 µg	500 ng
	+1LD	~70	30.0 µg	1.5 µg	600 ng
	+3LD	~70	57.3 µg	1.0 µg	500 ng
Replicate B	+0LD	~70	5.6 µg	1.0 µg	500 ng
	+1LD	~70	28.1 µg	1.4 µg	600 ng
	+3 LD	~70	50.3 µg	1.6 µg	700 ng
Replicate C	+0 LD	~100	2.4 µg	0.6 µg	-
	+1 LD	~50	8.8 µg	2.4 µg	-
	+3 LD	~30	30.6 µg	8.0 µg	-

Table 1. RNA derived from the meristem collected by LCM and material used for the sequencing. Time points are from plants grown 2 weeks in SD and the collected at +0LD, +1LD or +3LD, as indicated in the table. RNA after amplification is aRNA. “RNA for sequencing” is the quantity of RNA used to prepare the cDNA sent for sequencing (replicates A and B) or the quantity of RNA sent directly for the RNA-seq protocol to FASTERIS (replicate C). “DNA for sequencing” is the quantity of DNA sent to make the library for the Solexa sequencing.

In the case of replicate C, the yields are slightly different than replicates A and B, because less material was collected for the larger meristems and more material for the smallest, in order to try to compensate for the different sizes of the meristems.

The quality of the aRNA was assessed using the Agilent Bioanalyzer. Also for this case, the distribution of transcript sizes demonstrates that the material is of an overall good quality (for replicate A and B, see **Fig. 19**), with only little RNA degradation, as for the leaf discs. Moreover, the size of the RNA molecules is in the range expected for mRNA transcripts in *Arabidopsis*, where the average transcript is around 1500 bp (The *Arabidopsis* genome initiative, 2000).

3.2.5 Single strand cDNA synthesis to test the RNA extracted from the meristems

Another method to assess the quality of the RNA is to check for the expression of some control genes by RT-PCR. Before proceeding to sequencing, some samples were tested in this way. Initially part of one of the aRNA samples (1,6 µg of RNA from induced +3LD, replicate B) was used to produce single stranded cDNA, using random primers. Random primers were used to prime the retro-transcription because the aRNA is a so-called cRNA, in other words the complementary strand of mRNA, which lacks the usual polyA (**Fig. 16**). RT-PCR was performed on this cDNA with

Results

primers for various genes, such as *ACTIN*, *TUBULIN*, *FD*, and *SOCI*. At first no PCR products were obtained, although this sample was produced by amplification and would be expected to contain cDNA from each of these genes. Also, a weak band (for *TUBULIN*) was obtained even from RNA before amplification, so the amplified RNA should give more product. However, the linear RNA amplification tends to shorten the RNA products in comparison with the initial templates, especially at the 5'-end (**Fig. 16**). After another subsequent cDNA synthesis with random primers, probably the fragments are even shorter. In this condition the primers for the PCR might have few DNA molecules long enough to anneal to primers at each end of the cDNA on the entire sequence. So, instead of primers that amplify a product of around 500 bp, primers for products of about 200 bp were introduced in the reaction. With these new primers, specific PCR products were obtained both for *ACTIN* and *SOCI* cDNA (see **Fig. 20, A**). This experiment therefore confirmed that the amplified cDNA after LCM did contain cDNAs of genes induced in expression during floral induction.

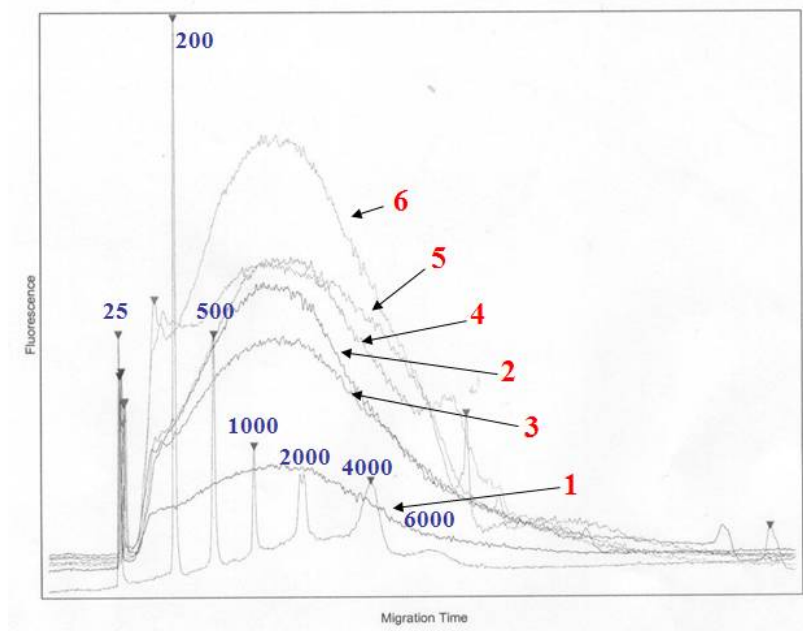


Fig. 19. Analysis of the RNA amplified from shoot apical meristems collected by laser microdissection. The outputs from Agilent BioAnalyzer from all the samples of replicates A and B were combined in a single graph, which includes the RNA ladder to easily compare the distribution of the size of the RNA molecules within the samples. Migration time is a function of the size of the molecule, fluorescence indicates the quantity of RNA for a particular size. 1: replicate A, + 0 LD. 2: replicate A, + 1 LD. 3: replicate A, + 3 LD. 4: replicate B, + 0 LD. 5: replicate B, + 1 LD. 6: replicate B, + 3 LD.

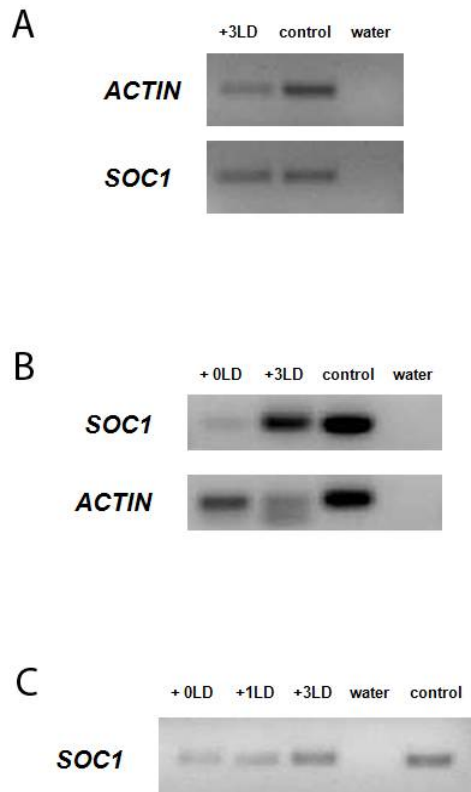


Fig. 20. Amplification of cDNA derived from the meristem samples collected by laser microdissection. RT-PCR was performed on cDNA produced from amplified RNA extracted from the shoot apical meristems. A: material from replicate B. B: material from replicate A. C: material from replicate C. “Control” was cDNA produced from a high-amount of RNA extracted from seedlings without laser microdissection.

3.2.6 Double strand cDNA synthesis for sequencing

Some difficulty was encountered in using the RNA extracted from the meristem by LCM to successfully hybridise Affymetrix *Arabidopsis* microarrays. Although several attempts were made and quality controls were performed in several steps, no signal was detected upon hybridisation of the labelled RNA on Affymetrix microarray (data not shown).

An alternative option to microarray hybridisation was based on next-generation sequencing technology. Short tags of DNA molecules derived from the cDNA of each time point separately, can be massively sequenced using Illumina-Solexa sequencing technology. Identifying which transcripts correspond to the short tags and counting how many times they occur in the sample, would give an output which is conceptually similar to a microarray expression profile. This technique has the advantage that a huge number of the molecules that are present in the sample are

Results

sequenced, with higher sensitivity compared to microarray technology and without the problems connected to hybridisation of nucleic acids (Wilhelm and Landry, 2009; Wang et al., 2009c). Moreover, whereas in the Affymetrix ATH1 array some genes of *Arabidopsis* are missing, by means of the sequencing method virtually all the expressed genes can be monitored.

Hence, the amplified RNA was used to produce DNA that can be sequenced through next-generation sequencing technology. The amplified RNA samples from meristems were converted into cDNA and then into double stranded DNA which is suitable for sequencing. Two different methods were used depending on the samples. For the replicates A and B (in total 6 samples) the aRNA was used for the synthesis of double stranded DNA. This was performed using part of the second round of RNA amplification, without subsequent *in vitro* transcription (Fig. 16).

In the case of A and B, 1-1.6 µg of aRNA were used to produce DNA (Table 1). The quality of the DNA was tested by RT-PCR using primers for *ACTIN* and *SOCI* on the samples +0LD and +3LD, replicate A. The cDNAs of these genes could clearly be detected in both samples, and the abundance of *SOCI* cDNA appeared higher in the +3 LD sample (Fig 20, B). A quantity of 0.5-0.7 µg of cDNA for each time point (Table 1), for a total of 6 samples (+0LD, +1LD and +3LD – biological replicate A, and +0LD, +1LD and +3LD – biological replicate B) was used for sequencing by the Illumina/Solexa method (“Genomic sample preparation”, Fig. 21, A and Methods).

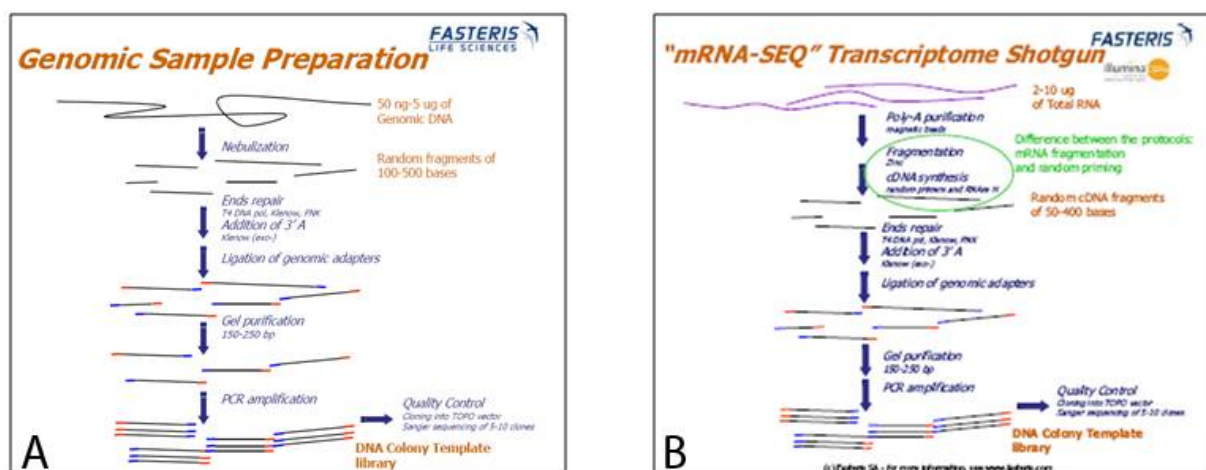


Fig. 21. Methods to prepare the libraries used for transcriptome profiling of the meristem by next-generation sequencing. The protocol was followed by the company Fasteris, for replicates A and B (Panel A) and replicate C (Panel B). The sequencing technology used was Solexa-Illumina.

Results

For replicate C (in total 3 samples), the RNA was sent directly to FASTERIS (Table 1), where it was converted into double-stranded cDNA and sequenced with the protocol for mRNA-Seq transcriptome shotgun sequencing derived from Illumina (see Methods) (Fig. 21, B). For replicate C, the quality of the RNA was previously checked by Bioanalyzer (data not shown), and by RT-PCR on cDNA derived from this RNA. The expression of *SOCI* appeared to increase upon exposure to LD (Fig. 20, C).

Biological replicate	Time point	Raw sequences from Solexa	MEGABLAST hits	BWA hits	BWA hits (paired-end)
Replicate A	+0LD	3,588,320	108,753	102,598	-
	+1LD (I)	3,499,827	38,561	44,934	-
	+1LD (II)	5,946,250	85,799	102,153	-
	+3LD	4,286,396	102,019	105,945	-
Replicate B	+0LD (I)	1,990,514	23,259	26,117	-
	+0LD (II)	3,026,184	73,894	82,895	-
	+1LD (I)	2,663,601	223,549	258,862	-
	+1LD (II)	5,263,622	487,814	561,999	-
	+3LD (I)	6,178,869	391,707	457,476	-
	+3LD (II)	6,174,436	906,665	1,049,321	-
Replicate C	+0LD (f)	12,855,783	1,121,040	1,164,146	944,386
	+0LD (r)	12,855,783	1,066,165	1,104,101	
	+1LD (f)	8,100,589	341,270	390,305	342,240
	+1LD (r)	8,100,589	373,289	398,705	
	+3LD (f)	11,422,486	5,634,735	6,327,817	5,905,511
	+3LD (r)	11,422,486	5,510,485	6,141,315	

Table 2. Data from the Solexa sequencing and mapping of the reads. Time points are from plants grown 2 weeks in SD and then collected at +0LD, +1LD or +3LD, as indicated in the table, for the three biological replicates. Raw sequences were received from FASTERIS, and then analyzed. “I” and “II” in brackets refer to samples that were sequenced twice, and indicate first and second sequencing run, respectively. These reads were pooled in order to have a larger single dataset for each biological sample. “f” and “r” refer to the samples that were sequenced by paired-end method, and indicate the forward and the reverse strands respectively.

3.3 Next-generation sequencing for gene expression analysis in the SAM

3.3.1 Deep sequencing with Illumina-Solexa and mapping of the short-sequence reads

The cDNA obtained was sequenced with “Solexa” sequencing technology (Illumina, Genome Analyzer I and II).

Short tag sequences were obtained as 35 base pair long reads. Each of the sequences was provided with another string which codes the quality scores for the relative sequence in each single position. A variable number of several millions of tags were obtained from the different samples (**Table 2**). Ulrike Göbel, Daniela Knoll and Heiko Schoof at MIPZ analyzed the raw data and converted them into a measure of gene expression for all the *Arabidopsis* transcripts. A brief scheme of the procedure used is indicated in **Fig. 22**.

A first filtering of the sequences was performed with SeqClean, a tool that removes vector sequences and some of the low quality sequences. Additionally, a large number of sequences were discarded because they corresponded to T7 polymerase primer sequence. Indeed, T7 polymerase primers were used during the RNA amplification procedure to prime the *in vitro* transcription (**Fig. 16**). For replicates A and B this occurred because the double-strand cDNA that was sequenced was produced with the kit for the RNA amplification, which includes the primers of the T7 promoter which are incorporated into the DNA sequences. These reads might correspond to primers that were not incorporated into cDNA or to transcripts that were sequenced from the starting point at the 3'-end where the primer sequence is present. Because the cDNA synthesis and especially the two rounds of RNA amplification tend to shorten the fragments (**Fig. 16**), many cDNAs may be relatively small and therefore not produce many fragments after the cDNA fragmentation prior to sequencing. In this case many of these fragments would contain the primer at the beginning. It would then be highly probable to sequence these type of fragments, and because of the short length of the Solexa reads, only the primer sequence would be obtained.

Removal of the primer sequences caused a loss of around 50 percent in the number of sequences present in replicates A and B. In replicate C, this problem was avoided by producing the double-stranded cDNA directly from the amplified RNA by another method (**Fig. 21, B**). This resulted in a larger number of cDNA sequences for replicate C. In addition, more sequences were retrieved from this last replicate compared to A and B because of the use of an improved Illumina Sequencer, resulting in a generally higher number of reads. Moreover, for replicate C “paired-end” sequencing was used, where each transcript is sequenced both from the 5' and 3' end. This method increased the quality of the data, because it helped to assign the corresponding gene to each cDNA, reducing

the number of ambiguities (Fullwood et al., 2009).

The remaining valid sequences were blasted against the *Arabidopsis* transcriptome (TAIR8 cDNA collection) with MEGABLAST (Altschul et al., 1997; Zhang et al., 2000), as described in Methods. During this process many sequences could not be assigned to any transcript and were removed from the analysis (**Table 2**). The origin of these non-aligned sequences could be due to poor sequence quality, contamination of DNA or artifacts created during the amplification process. Microarray hybridisation of RNA amplified by linear amplification showed reliable results in previous studies (Nygaard and Hovig, 2006), but there are not so far reports in the literature on RNA amplification procedures coupled with Solexa sequencing. So the amplification procedure could have affected the sequences, introducing for example point mutations. On the other hand, a large number of invalid tag sequences have been reported even with more “conventional” RNA preparations that do not involve amplification (Marioni et al., 2008).

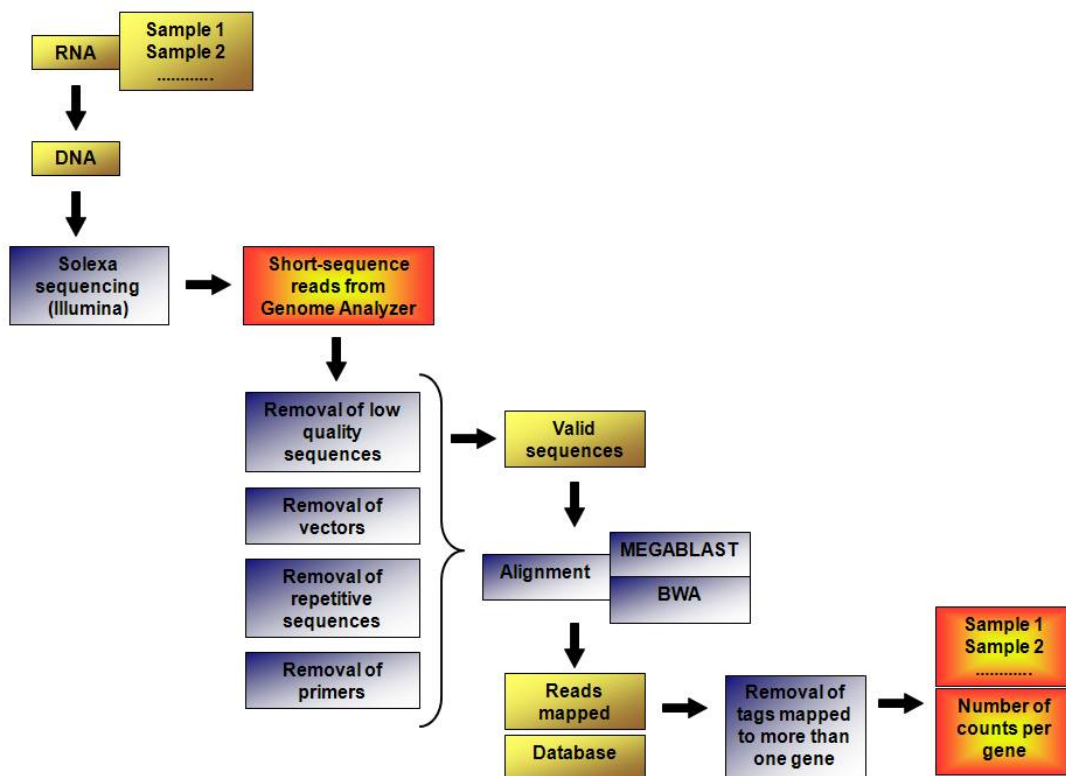


Fig. 22. Flow chart of the procedure used to analyze the short-sequence reads from Solexa sequencing. Blue boxes represent procedures, yellow boxes represent samples and data. Red boxes are the initial input and the final output of the analysis. Details are in the Methods section.

Results

Each of the reads remaining after the filtering processes were assigned to a gene. Only the reads that match a unique transcript were considered, while the ones matching more than one possible transcript, called “promiscuous tags”, were discarded and not included in these first analyses. The coverage of the expressed genes detected was evaluated for each sample, as transcripts detected at least one time. Relative to the whole set of *Arabidopsis* transcripts described in TAIR, between 50% and 75% were detected depending on the samples.

Another parallel approach employed another program, BWA (Li et al., 2009), to perform the alignment as an alternative to MEGABLAST. This program produced a slightly higher number of mapped reads, with the assigned parameters, with the exception of sample +0LD from replicate A. BWA is particularly useful in the case of the paired-end data. This program quantifies the number of expressed transcripts taking into account how the reads map on the exons of each gene. Therefore, in the case of paired-end data, because two independent reads coming from different positions of the same transcript give a more precise description of the distribution of the reads on the transcript, the full power of the BWA approach can be used.

For each of the 9 samples (time points +0LD, +1LD, and +3LD, repeated in three biological replicates A, B and C) a transcriptome has been obtained, composed of the number of reads derived from each *Arabidopsis* transcript. In the case of samples sequenced twice, the reads were pooled together to produce a single dataset for each biological sample and to increase the resolution for these samples by having more reads. The number of assigned valid reads greatly varied among the different samples (see **Table 2**), spanning two orders of magnitude from about 100000 total assigned reads to more than 5 million. Hence, in order to be able to compare the expression of a gene between the different time points and biological replicates, these data were normalized. The number of counts for each expressed gene in each sample was considered in relation to the total number of valid reads within that sample. Each sample was therefore normalized as number of counted “tags per million” (TPM). TPM for each sample was calculated by dividing the raw counts by the total number of tags mapped to the transcripts for the corresponding sample and then multiplying the answer by 1 million.

3.3.2 Quality controls and reliability of the replicates

A quality control was performed based on the quality score given as an output of the Genome analyzer. The quality was good enough for the short-sequence reads to be mapped to *Arabidopsis* genes. The quality of the reads decreases with the length of the read (data not shown). This is a

typical result for the current sequencing technology. Therefore, even if the entire length was considered, more weight was given to the initial bases of 35-mers of the reads (see Methods).

Scatter plots were produced comparing for each gene, the values as raw counts or TPM (depending on the cases) coming from two samples in all possible combinations. Some of them are shown in **Fig. 23**.

A scatter plot shows for each gene, as a dot in the graph, the relative expression for two compared datasets. Typically for microarray data, the distribution of the dots is expected to be as a cloud following a straight line (Gentleman et al., 2005). The majority of the genes should not show differential expression, while the outliers indicate the small percentage of genes that are expressed differently in the two samples. In the case of biological replicates of the same sample, the scatter plot should be distributed on a straight line, showing fewer deviations from the central line. Considering that microarray hybridisation data and RNA-seq data are highly correlated, the same kind of distribution is expected for both types of data. In our case, the scatter plots show a generally good distribution on a central straight line (**Fig. 23, A** for replicates A and B). However, for these biological replicates, a high number of genes deviate from the central line, especially for the earlier samples (+0LD and +1LD), while the correlation increases for the later samples (+3LD) (**Fig. 23, A**). This is well described by the correlation coefficient R , which is in the range 0.48-0.81 for the comparisons of +0LD, 0.33-0.62 for +1LD, and 0.59-0.94 for the +3LD. A comparison between different time points of the same replicate shows a situation similar to the one considering the same time points for different replicates, with correlation coefficient around 0.5.

In order to test whether the difference in the biological replicates is due to low accuracy of the Solexa technology, technical replicates were performed by re-sequencing a few samples. The re-sequenced samples look almost identical (**Fig. 23, B** for an example), even in the case of +0LD. The correlation coefficient R , between 0.94 and 1 for the different samples re-sequenced, confirms high reproducibility. This indicates that Solexa technology is highly reliable when performed on the same sample (see Marioni et al., 2008) and that the differences found in the biological replicates are probably due to differences in the different experiments. A likely reason for this difference is that the RNA amplification was not totally balanced for all the transcripts, especially if we consider the extremely low quantity of the starting material. Indeed, the lowest correlation is for samples derived from smaller meristems, while the best correlation is in the +3LD samples, those with the largest quantity of RNA material. Also the extremely high number of sequences identified as primers, if they were real transcripts of which the information was lost, could have biased the final result.

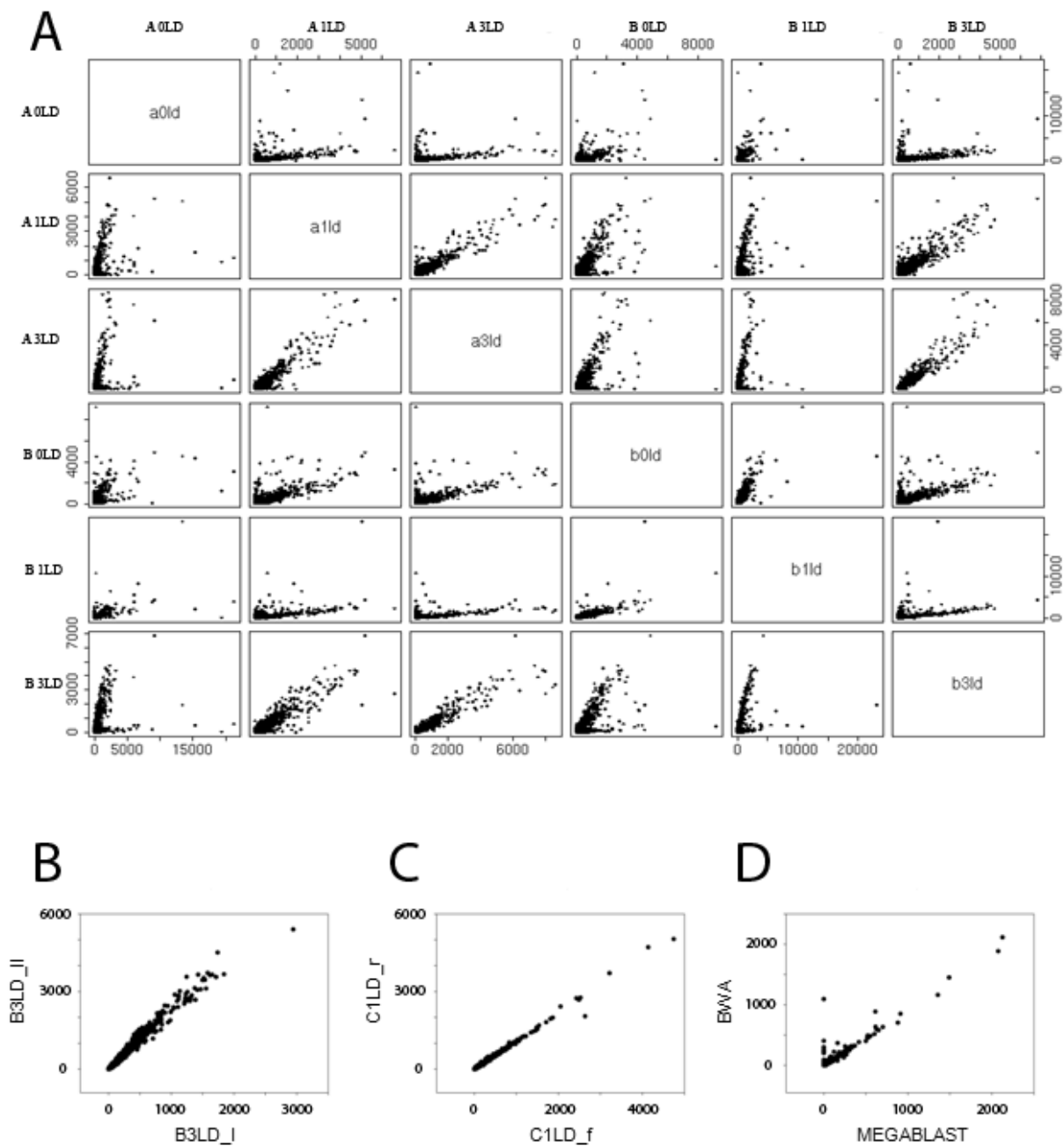


Fig. 23. Scatter plots for mapped reads. Panel A: All the different samples for replicates A and B are compared to each other as mapped with MEGABLAST. Panel B: comparison between two technical replicates of sample +3LD from replicate B as mapped with MEGABLAST. Panel C: comparison between the two strands of the paired-end sequences for sample +1LD from replicate C as mapped with MEGABLAST. Panel D: comparison between the reads mapped with MEGABLAST and BWA for sample +0LD from replicate A. The reads were in TPM (A) or raw counts (B, C, and D).

Results

A comparison was done to assess the performance of the paired-end sequencing in replicate C. In this case the transcripts were sequenced twice, from the two ends, and the two corresponding short sequences for each transcript are stored in separate files. Therefore, the two files were compared. Both scatter plots (**Fig. 23, C**) and R values (between 0.9 and 1) show that there is a very high correlation, so that the paired-end sequencing is a very accurate and reliable system to identify transcripts as both ends are highly likely to identify the same transcripts. Therefore, the values used for the further analysis of the data for replicate C were calculated as averages between the two sequenced strands. Another comparison was done between the reads obtained with the separated strands in replicate C and the reads obtained with BWA considering the two strands together. Also in this case the correlation was high (between 0.9 and 1 depending of the cases).

Finally, a comparison between MEGABLAST and BWA results was performed to assess whether there is a substantial difference between these two programs in mapping the reads onto the transcripts. From this comparison it emerged that the results are highly similar (**Fig. 23, D** for an example of a scatter plot). However there are large deviations in the case of a few genes, which render some of the R values lower than 0.7 in some cases. Because these genes show a large difference as outputs of the two programs (for example 0 counts with MEGABLAST and more than 4000 with BWA), while all the other genes have very similar numbers of counts, the increase of mapped reads with BWA is probably due to a few genes that were mapped as a result of an artifact. Therefore, the data mapped with MEGABLAST seemed more reliable and were used for further analysis.

3.3.3 Use of housekeeping genes for the normalization

An alternative possibility to normalize the results of next-generation sequencing is to use the expression of housekeeping genes as a standard. According to recent studies based on large sets of data from available microarrays, some classical *Arabidopsis* genes used in the past as reference genes, such as *ACTIN*, are not the best choice because they still show significant variation in expression under different environmental conditions (Czechowski et al., 2005). We chose *UBIQUITIN10* (*UBQ*), because it seemed to be the most constantly expressed gene among the classical genes used to normalize the mRNA levels of other genes in quantitative real-time PCR experiments. *UBQ* expression was then used to normalize the datasets generated by Solexa sequencing. For each independent sample, the number of counts for each gene was divided by the number of counts for *UBQ* in that sample, and then multiplied by 100. Therefore, the values for the

expressed genes were expressed as a percentage of the level for *UBQ*. This method cannot change the correlation coefficients between different samples, because it only changes a multiplicative factor applied to all the genes in the sample. Nevertheless, the average values of the genes and the variation of their values along the time points are affected. The value of some genes was checked, and although variation still occurred between the biological replicates, the trend of expression patterns for known genes was generally constant, and the variation was less compared to the data normalized only as TPM for the majority of genes that I tested (see next section), although for a few other genes the data expressed in TPM was instead more stable. Therefore different methods can be used to normalize RNA-seq data, and these generally improve the analysis in comparison to using raw reads, however the results of the different methods vary making it difficult to assess at this time which method is the most appropriate.

3.3.4 Expression values for known genes

As a first approach to assess the biological quality of the data, the number of tags (both in TPM and normalized with *UBQ*) for known meristem genes was checked in the dataset. In **Fig. 24** the values for some of these genes are shown, as TPM or normalized with *UBQ*. mRNAs of genes that should be expressed at the SAM, because they are important for its maintenance, such as *CLV1*, *CLV3*, *STM*, *WUS*, and *KNAT1* were detected in our gene expression datasets (**Fig. 24, A, B**, below). Particularly, mRNAs of genes that are expressed in a very restricted subset of the SAM tissue, like the *CLVs* and *WUS*, are easily detected. This demonstrates the value of specifically collecting SAMs, so the expression level of these genes was not diluted as would happen in entire apices, although *WUS* expression level is still low. *STM* and *KNAT1* are strongly expressed because they are present in the whole SAM, and the former seems to increase in expression upon the shift to LD, as already reported previously for apical samples (Schmid et al., 2003).

Another set of genes that are particularly important for this experiment comprises those involved in the floral transition at the SAM (**Fig. 24, A, B**, center). Particularly, *SOC1* mRNA shows a marked increase in the number of tags with the number of LD of induction in all three biological replicates (from 30 to 300 fold between +0LD and +3LD, in TPM). *FUL* mRNA also shows an increase, but much less than for *SOC1* (from 5 to 30 fold between +0LD and +3LD, in TPM) and it is delayed with respect to *SOC1*, which is also consistent with *in situ* hybridisation results (**Fig. 11, Fig. 13**). *FD* is already strongly expressed before the transition, and slightly increases after 3 LD, as is expected from our previous results. *SVP* is generally strongly expressed, and it appears to be

Results

slightly up-regulated after 3 LD. This seems in contradiction to its role as a floral repressor and the expression pattern shown by *in situ* hybridisation (see sections 3.1.2 and 3.1.3). This apparent contradiction might be reconciled because there is mainly a re-distribution of the mRNA of *SVP* within the meristem during the floral transition. Rather than a net decrease, there is a down-regulation of the mRNA in the central part of the inflorescence meristem, and an up-regulation on its flanks (**Fig. 11, Fig. 13, Fig. 14**). Therefore, such a complex pattern cannot be fully described by the quantification of the mRNA in the entire SAM. *AGL24* is another gene that has been shown to be expressed before floral induction by LD in our conditions, and increase in expression upon induction (Liu et al., 2008; Michaels et al., 2003; Yu et al., 2002). This is consistent with the data from RNA-seq gene expression dataset.

Genes involved in the floral transition, and controlled by miRNAs were also checked (**Fig. 24, A, B**, center). *SPL9* mRNA was absent before induction and increases upon transfer to LD, as recently reported and shown by *in situ* hybridisation at the SAM (Wang et al., 2009a). *SPL3* mRNA was not detected, while *SPL4* and *SPL5* mRNAs were detected at very low levels. This could be due to the fact that they are induced later, or to the similarity of their sequences, which creates ambiguities in the assignment of the reads to a unique gene causing the reads to be discarded. The two related genes *SMZ* and *SNZ* seem to decrease in expression, but their mRNAs were detected only in one sample. These two genes were identified by microarray analysis (Schmid et al., 2003) as down-regulated upon the shift to LD in shoot apices. Our approach, which is more specific for the meristematic tissue, suggests these genes are not expressed in the meristem, and this is in agreement with recent results indicating that they repress *FT* expression in the vascular tissue (Mathieu et al., 2009).

Another control that was performed was to test for the expression of genes whose mRNAs were not expected in these meristems (**Fig. 24, A, B**, on top). For example, mRNAs of meristem identity genes and floral genes should be absent or very lowly expressed, because they should be only expressed in later stages. *API* mRNA, as for *in situ* hybridisation, is barely detectable. Also *LFY* and *PI* mRNAs are not present at all or very lowly expressed. Conversely *TFL1*, which counteracts *LFY* and *API*, is expressed. Finally *TSF* mRNA is also not expressed in the collected SAMs, as expected because it is expressed in the leaf tissue.

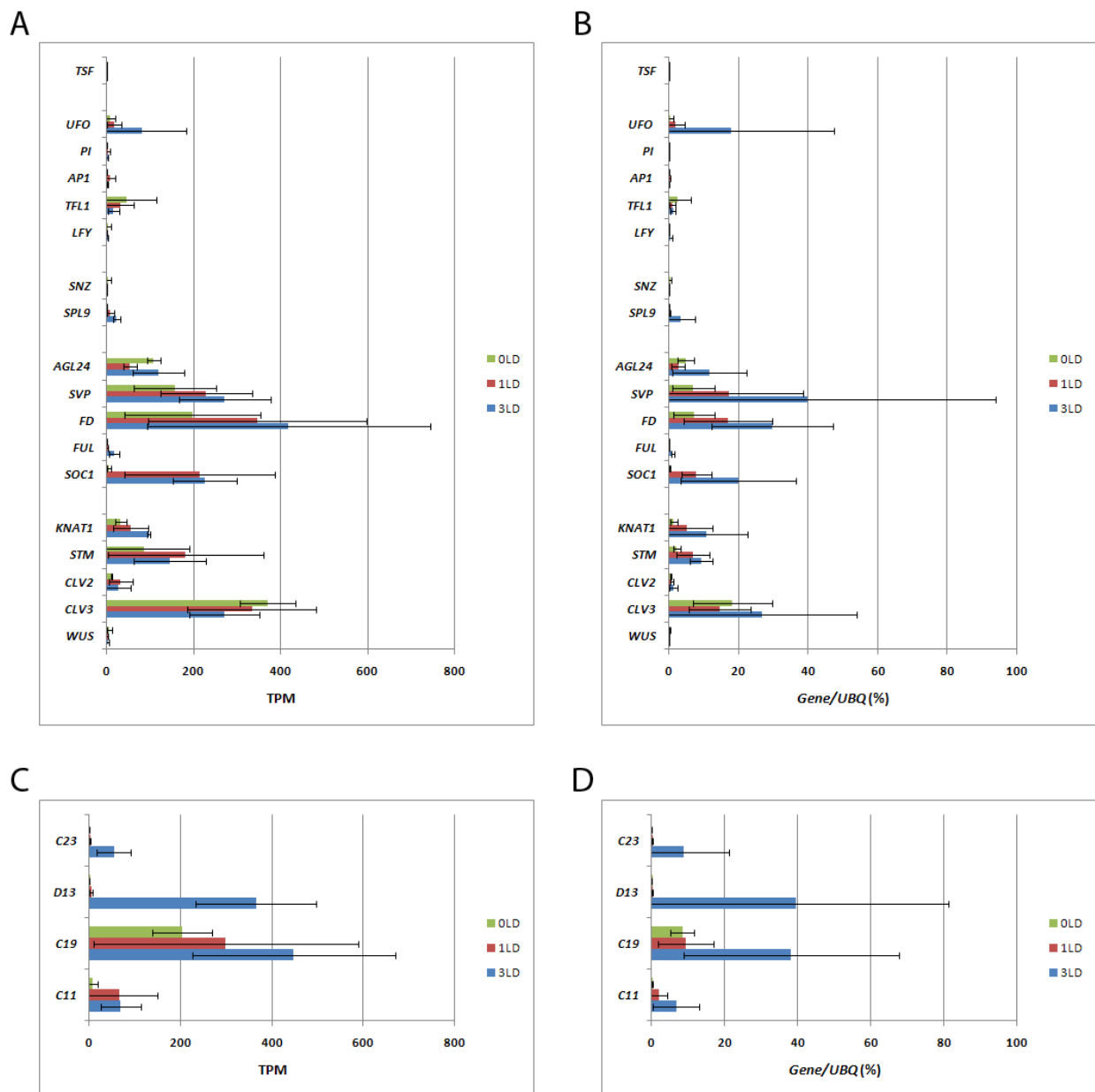


Fig. 24. Expression values of selected genes extracted from the gene expression dataset. The values are calculated as averages between the three biological replicates, as TPM (A and C) or normalized with *UBQ10* (B and D). The bar represents the standard deviation. In panels A and B, values for known meristem expressed genes are indicated. In panels C and D, values for candidate genes identified in the datasets are indicated. The corresponding candidate genes are listed in **Table 5**.

These controls provided important support for the RNA-seq method. Even although before sequencing the cDNA was tested by RT-PCR (for example for the presence of *SOCI* mRNA in the induced samples), it was not known whether the quantity of such mRNAs was still balanced in the

samples after RNA amplification. Also contamination by other tissues remained possible and that would disturb the general balance of the transcripts and include genes that should not be expressed. Based on these controls, we can conclude that next-generation sequencing applied as RNA-Seq on meristems collected by LCM produced a coherent dataset that detects several known mRNAs that are specifically expressed in the SAM, and does not include several mRNAs that are specifically expressed in floral meristems and leaves. Moreover, mRNAs of flowering time genes like *SOCI* and *FUL* seem to be up-regulated as they should be.

3.3.5 Data analysis: identification of differentially expressed genes

The general approaches for global gene expression analysis using microarrays make use of biological replicates to provide an estimate of the variation in gene expression for all the genes present on the array (Allison et al, 2006; Grant et al., 2007). Statistical tests are used to decide whether a gene is considered to be differentially expressed between different samples. In the RNA-Seq data, the variability was relatively high between samples and there are genes that have a relatively large difference in TPM not only between different time points, but also within the same time point for different biological replicates.

Therefore, different methods were applied to correct for the resulting noise and to identify genes differentially expressed between time points. Lists of genes considered up- or down-regulated during the shift to LD were generated with the different methods, and several candidates were tested for their expression levels by independent methods. This information was used also to validate and evaluate the different methods.

A first set of genes was made using only replicate A, before the other datasets were available. The genes were selected simply by the largest up- or down- regulation between +0LD and +3LD. These genes were named “C” candidates, from *C1* to *C20*.

Another set of genes was compiled using replicates A and B, before the third replicate was available. These were named “D” candidates, from *D1* to *D60*, and two approaches, a “p-value” approach and a “log₂ ratio” approach were used. To make possible some of the calculations of these methods (e.g. to calculate ratios and log₂ ratios), the 0 values (NULL) indicating the absence of expression of certain genes in certain time points, were converted to 1, which did not affect the general distribution of the data.

In the “p-value” approach, a particular statistical method was applied, using the hypergeometrical distribution. A formula was used (modification from Marioni et al., 2008, see Methods) to calculate

Results

for each gene a p-value, taking into account both its variation between time points and its variation between the two technical replicates. In this case the raw values (counts not normalized) were used to compute the calculations of the p-values. So for each gene a p-value is related to the probability that a gene is differentially expressed between two time points, for each comparison among the three time points +0LD/+1LD/+3LD (**Fig. 25, A**). The threshold has been set at 0.1 (p-value < 0.1), resulting in identification of 138 differentially expressed genes between +0LD and +1LD, 351 genes between +0LD and +3LD, and 232 genes between +1LD and +3LD (**Fig. 25, A**).

In the “log2 ratio” approach, using the normalized values as TPM, the log2 ratio between each pair of time points for each gene was calculated, and the genes were ranked. After ranking the top 1000 genes both for replicate A and replicate B separately, the genes which were present in both replicates and which had the same “trend” in expression (up- or down- regulation) were considered. The small number of genes in this list (37 genes between +0LD and +1LD, 46 genes between +0LD and +3LD, and 50 genes between +1LD and +3LD, see **Fig. 25, A**) indicates that it is difficult to compare the two replicates only in terms of up- or down- regulation without taking into account the variation of these genes in all the dataset.

A direct comparison between the two approaches was also done, and the majority of genes that are in the “log2 ratio” set are included in the “p-value” set for each comparison between time points (**Fig. 25, A**). *SOCI* up-regulation was detected between +0LD and +1LD, and between +0LD and +3LD, with both the approaches. If we consider the three groups of transitions (among +0LD, +1LD, and +3LD), it seems reasonable that some of the identified genes would belong to more than one group. Again, *SOCI* is a good example, since it is up-regulated between +0LD and +1LD, and between +0LD and +3LD. For all the differentially expressed genes the ones that are present in more than one group were identified. These genes should represent a set showing a coherent and constant expression pattern during the floral induction (**Fig. 25, A**). A total of 107 genes is present in more than one group, while only 2 of these genes are present in all three groups.

Finally, with a dataset including all three replicates, a “clustering” approach was used. When the data of all three replicates are compared, many genes show the same general trend in expression pattern (for example up- or down- regulation, or constant expression). However, the values expressed in TPM between replicates can be so different for certain genes that if the average is calculated, the standard deviation appears larger than the average. This could be due to the general distribution of the short-sequencing data, which does not follow the normal statistical distribution, or to the fact that the normalization in TPM is not accurate enough and another method is required.

Results

Moreover, the C replicate is qualitatively different to A and B, because more sequences were provided for the analysis giving rise to a deeper detection of transcripts, and also the paired-end approach generated a better-quality dataset. This could result in difficulties to compare directly the values for certain genes between replicates A and B and replicate C. While alternative statistical distributions for the short-sequence data and alternative methods for normalization have still to be well established, here a “clustering” method was used, which directly compared the data expressed in TPM.

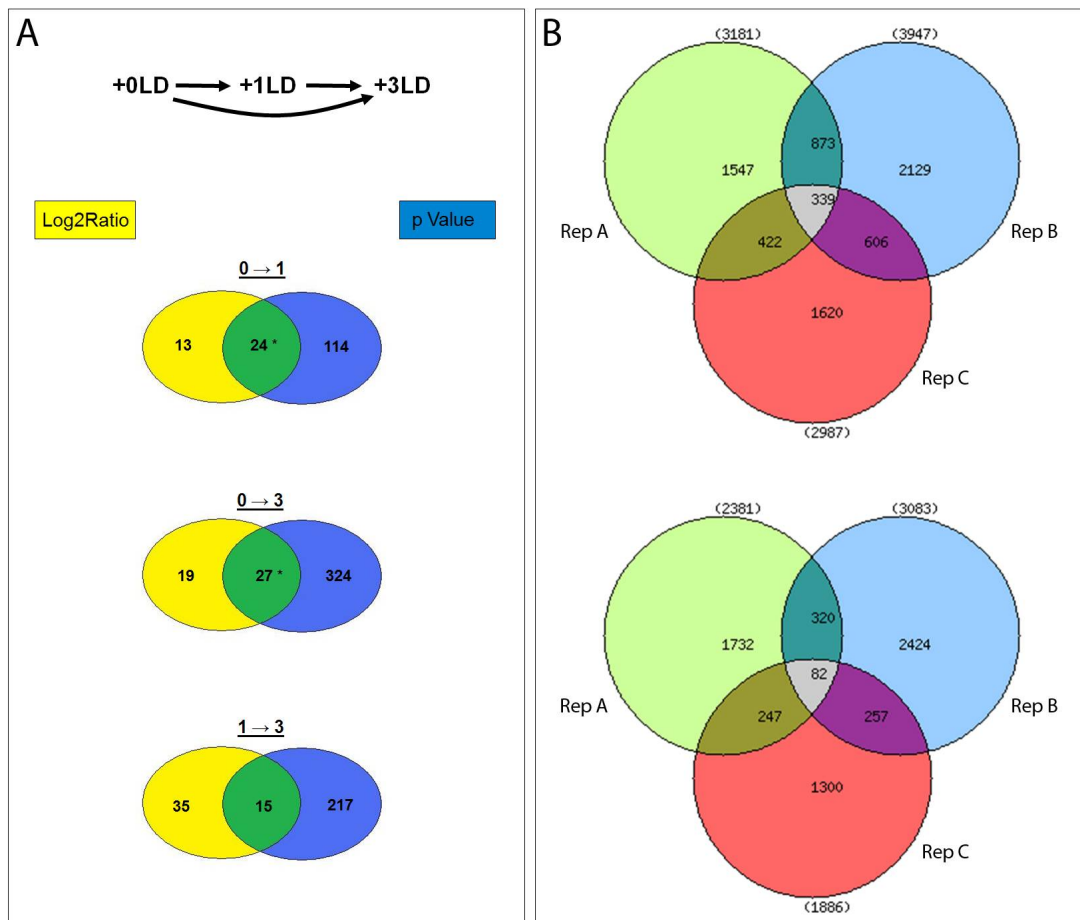


Fig. 25. Approaches used to identify differentially expressed genes in the global gene expression dataset from Solexa sequencing. Panel A: The 3 possible comparisons between time points are indicated above. For each of the comparisons, the number of genes identified by the “log2 ratio” and “p-value” methods and the number of common genes are shown in the Venn diagrams. Panel B: The clustering method identified genes that were up-regulated (upper Venn diagram) or down-regulated (lower Venn diagram) in all biological replicates and the number of genes identified is shown at the intersection of the three sets in each Venn diagram. “Rep A”, “B”, and “C” represent the three biological replicates.

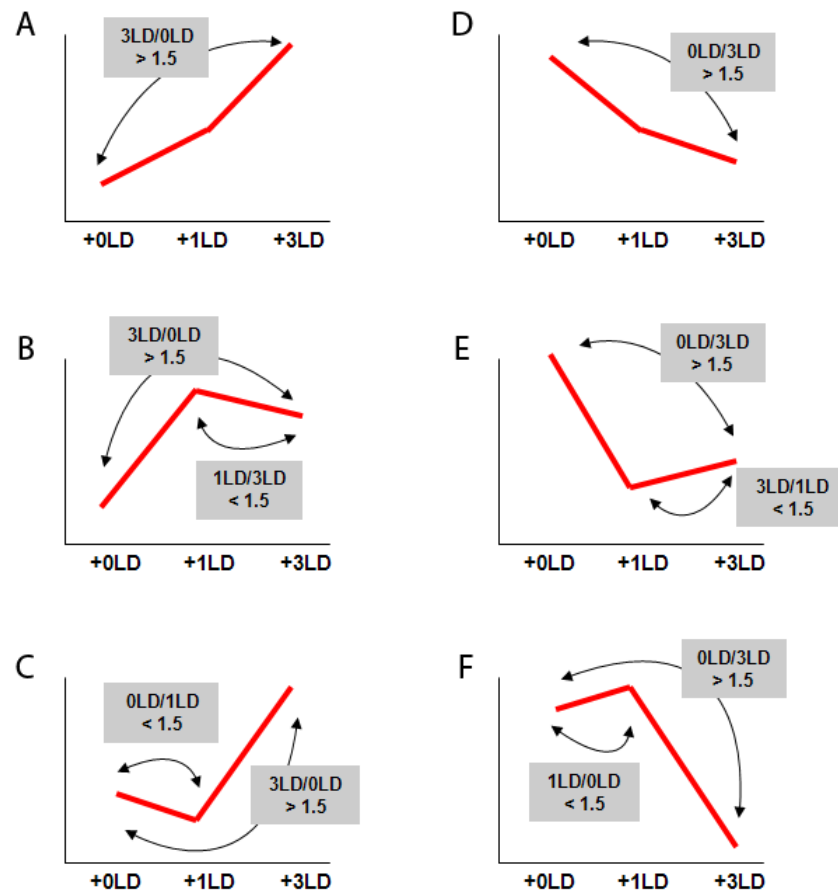


Fig. 26. A schematic representation of the possible relationships between the expression values of selected genes. +0LD, +1LD and +3LD represent the time points of the time course from the global gene expression dataset, for one hypothetical replicate. The red line represents the expression trend of a certain gene, up-regulated (A, B, C) or down-regulated (D, E, F). A gene is considered coherently up- or down-regulated if the expression values fulfill the conditions indicated in the figure.

The aim was to identify for each replicate the genes that are coherently up-regulated or down-regulated (from +0LD to +1LD and from +1LD to +3LD), and then among those to select the genes common to all three replicates (**Fig. 25, B**). These genes should represent a reliable set, because they are up- or down-regulated in 3 independent experiments. First of all, in order to set a threshold of detectable expression, all the values that were lower than 10 TPM were excluded by setting them to 0, resulting in the exclusion of genes considered to be too lowly expressed to be reliable. Then, for each replicate, a threshold for fold change was imposed to be $3LD/0LD > 1.5$ for the up-regulated genes. However, because of the slight variation of the data, I wanted to include not only the genes for which the value of the +1LD is located between +0LD and +3LD (**Fig. 26, A**, for a

schematic example), but also the genes for which this value is slightly higher than +3LD (**Fig. 26, B**) or slightly lower than +0LD (**Fig. 26, C**). Therefore, two additional conditions were allowed for the up-regulated genes: $1LD/3LD < 1.5$ and $0LD/1LD < 1.5$. A similar approach was considered for the down-regulated genes (**Fig. 26, D-F**), where the first condition to be respected was $0LD/3LD > 1.5$, and then two additional conditions were $3LD/1LD < 1.5$ and $1LD/0LD < 1.5$.

The use of these parameters resulted in the recovery of genes that are generally up- or down-regulated, without including genes that have a value in +1LD that is too deviating from the general trend. As an example, *SOCI* in replicate A is 0, 400 and 300 TPM respectively, and it fulfills these conditions.

The rationale to choose genes with this pattern was to have a set of genes that are co-expressed with *SOCI* (responding already after the first LD) and *FUL* (responding mainly after +3LD), in the case of the up-regulated genes. As an output of this analysis, the overlap between all replicates for the up-regulated genes was 339, while the overlap for the down-regulated genes was far lower (**Fig. 25, B**).

Another test was performed with the same method, but using the values of the genes normalized with *UBQ* (see above). The same criteria were applied for the fold ratios, while values lower than 1 (1% respect to *UBQ*) were considered 0. In this case, the common up-regulated genes were 447, although the down-regulated genes were 56, again very low. Moreover, the number of genes of the different replicates used for the intersection were very different to each other, in some case up to 3 fold. The overlap between the genes found starting with the TPM data and with the normalization with *UBQ* was 114 up-regulated genes and 29 down-regulated genes.

From all these lists of genes, a set of candidate genes were chosen to be tested by other experimental procedures, and they will be described in the following sections.

3.3.6 GO term enrichment analysis

The clustering approach identified differentially expressed genes using the data of three biological replicates, and therefore the lists of these up- and down-regulated genes were used for further analysis at the global gene expression level. In order to highlight the classes of processes characterizing the floral transition at a genomic level, GO term enrichment analysis was performed with the software FatiGO (Al-Shahrour et al., 2006). This program detects the GO terms that are over-represented in a sub-set of genes, in our case the up- or down-regulated genes, toward another list of genes, in our case composed of all the genes present in the list of transcripts used as a

Results

reference for the mapping of the reads. The output of the program provides also a p-value and an adjusted p-value for each of the terms, which gives a statistical significance to the different terms listed. For the up-regulated genes, several terms were found to be statistically significant (**Table 3**). Strikingly, for the biological processes, the set of classes found gave a coherent scenario, because they are all connected to general biosynthetic and metabolic processes. Going up to more specific classes (higher levels), other terms are more connected to protein metabolic processes, ribosomes biogenesis and assembly, and translation. The only molecular function found to be significantly enriched in this dataset was the one connected to the structural constituents of ribosomes.

For the down-regulated genes, a few terms were found to be statistically significant (**Table 4**), likely due to the fact that this list of genes is too restricted. Nevertheless, it seems that the category related to response to stress is over-represented, plus some processes related to specific metabolic pathways.

Index	Term	#1 vs #2	p value	adj. p v.
<u>GO biological process at level 3</u>				
	biosynthetic process (GO:0009058)	68.88% 31.12%	3.63e-14	2.14e-12
	macromolecule metabolic process (GO:0043170)	57.9% 42.1%	1.63e-6	4.82e-5
	cellular metabolic process (GO:0044237)	54.71% 45.29%	2.6e-5	5.12e-4
	primary metabolic process (GO:0044238)	55.18% 44.82%	5.55e-5	8.19e-4
	cellular component organization and biogenesis (GO:0016043)	62.53% 37.47%	5.91e-4	6.97e-3
<u>GO biological process at level 4</u>				
	cellular biosynthetic process (GO:0044249)	69.52% 30.48%	1.39e-14	1.95e-12
	ribonucleoprotein complex biogenesis and assembly (GO:0022613)	86.66% 13.34%	6.61e-12	4.62e-10
	protein metabolic process (GO:0019538)	62.5% 37.5%	2.74e-8	1.28e-6
	cellular macromolecule metabolic process (GO:0044260)	61.52% 38.48%	2.71e-7	9.48e-6
	organelle organization and biogenesis (GO:0006996)	72.38% 27.62%	2.11e-6	5.91e-5
<u>GO biological process at level 5</u>				
	macromolecule biosynthetic process (GO:0009059)	73.37% 26.63%	7.09e-15	2.2e-12
	ribosome biogenesis and assembly (GO:0042254)	90.58% 9.42%	1.67e-14	2.59e-12
	cellular protein metabolic process (GO:0044267)	61.39% 38.61%	3.86e-7	4e-5
<u>GO biological process at level 6</u>				
	translation (GO:0006412)	84.01% 15.99%	2.28e-27	8.9e-25
<u>GO molecular function at level 3</u>				
	structural constituent of ribosome (GO:0003735)	89.59% 10.41%	1.14e-34	15e-32

Table 3. GO term enrichment analysis for the 339 up-regulated genes identified by the clustering approach.

Index	Term	#1 vs #2	p value	adj. p v.
<u>GO biological process at level 3</u>				
	response to stress (GO:0006950)	74.6% 25.4%	5.9e-4	3.48e-2
<u>GO biological process at level 8</u>				
	fatty acid oxidation (GO:0019395)	97.17% 2.83%	13e-4	4.88e-2
<u>GO molecular function at level 4</u>				
	carbon-sulfur lyase activity (GO:0016846)	97.33% 2.67%	6.73e-6	1.29e-3

Table 4. GO term enrichment analysis for the 82 down-regulated genes identified by the clustering approach.

4. Characterization of novel genes induced during the floral transition selected from gene expression analysis

4.1 Selection of the genes

A set of genes expressed in the SAM is expected, which should already restrict the number of genes identified as induced during the floral transition. Moreover, only the early stage of the induction has been selected in the experiment, and this should further restrict the number of induced genes detected. A dataset is already available for the floral transition in the *Arabidopsis* shoot apex (Schmid et al., 2003), so a direct comparison with these available data is also useful. Of particular interest will be the genes that were not identified by the previous approach because their pattern of expression was masked by a dilution in the apical tissue, but were identified by our highly tissue-specific approach.

In situ hybridisation was selected to confirm the gene expression data. However, because this technique is not as sensitive as others such as RT-PCR, probing mRNA of genes that are not strongly expressed can lead to absence of a visible signal. Therefore a first filter was used to select genes that are strongly expressed at least in one of the time points. A general threshold was set based on the values of known genes that are detected by *in situ* hybridisation, of around 100 TPM. Moreover, the genes were selected on the basis of the highest degree of up/down regulation, because *in situ* hybridisation is also not always suitable to discriminate small differences in gene expression. Therefore, sometimes candidates were chosen even if the expression value was under the set threshold, as long as the difference in expression was high between time points.

Three lists of genes were selected using the three approaches described in the previous section:

- 1) *CI-20* from the first analysis based on replicate A.
- 2) *DI-60* from “p-value” and “log2 ratio” approaches, from replicates A and B. About one third of the genes were taken from the log2 ratio list, another third from the p-value list, and the remaining genes are present in both lists. This approach should give a chance to assess if one method is more reliable than the other (for the first 40 genes) and at the same time to screen the 20 genes that are in both lists, which should be the most reliable genes to test.
- 3) *C2I-30* from the “clustering” approach, from replicates A, B, and C.

The only gene that can be used as a positive control is *SOCl*, because it is known to be involved in the floral transition at the SAM and is clearly differentially expressed during the floral transition in

Results

our experimental conditions (Fig. 11). Up-regulated candidate genes were given emphasis because they showed a similar expression pattern to *SOC1*. Moreover, genes that are up-regulated only in the later phase, from +1LD to +3LD, were included in the set of genes to be analyzed. Indeed, these genes could be targets of *SOC1/FUL*, or of any other regulatory protein responding in the very early phase of the floral transition.

Code	AGI	Description	Fold 1LD/0LD	Fold 3LD/0LD	Method	Fold (Microarrays)
C4	AT2G18160	ATBZIP2	-	-	1	1.26
C11	AT1G14440	ATHB31	9.38	9.79	1 - 3	1.09
C15	AT4G36180	Leucine-rich repeat protein	1.80	2.41	1	1.05
C19	AT3G12145	FLOR1	1.47	2.20	1	-
C20	AT5G12330	LRP1	1.08	1.67	1	1.01
D3	AT4G19160	unknown	11.62	4.46	2	0.91
D13	AT1G43800	Stearoyl-ACP desaturase	26.78	2393.37	1 - 2 - 3	1.78
D19	AT4G29010	AIM1	2.37	1.25	2	0.95
D27	AT1G79920	ATP binding	2.76	2.47	2	0.98
D29	AT1G79530	GAPCP-1	2.93	2.50	3	1.13
D31	AT2G24150	HHP3	0.37	3.78	2	1.07
D35	AT1G37130	NIA2	0.35	11.66	2	0.88
D37	AT1G64620	Dof-type zinc finger	2.90	4.82	2	1.04
D55	AT1G80950	LPEAT1	1.21	9.79	3	1.01
C21	AT4G40060	ATHB16	20.07	76.46	3	1.55
C22	AT1G09390	Hydrolase/lipase	65.56	762.56	3	1.05
C23	AT1G03170	unknown	4.66	539.12	3	4.51
C25	AT3G54110	PUMP1	3.51	4.78	2 - 3	1.08
C26	AT3G55600	unknown	13.78	46.25	3	1.01
C27	AT1G49580	CDPK	27.62	151.99	3	1.01
C29	AT3G51080	GATA6	26.81	150.13	3	-
C30	AT3G54500	unknown	3.62	6.41	3	1.09
-	AT2G45660	SOC1	39.38	41.59	1 - 2 - 3	2.62
-	AT5G60910	FUL	4.61	55.15	-	3.55

Table 5. Candidate genes and their fold increase in expression after exposure to LDs. The fold changes 1LD/0LD and 3LD/0LD were calculated from the averages between the three replicates. In case of 0 values, they were converted to 0.1 to calculate the fold increase. The methods by which the genes were identified were the “first preliminary method” (1), “the p-value” and “log2 ratio” (2) and the “clustering” (3), described in the text. The fold change from microarray data is calculated from Schmid et al, 2003, considering the ratios between +3LD and +0LD in wild-type Col.

Some of the candidate genes were then analyzed by *in situ* hybridisation (see the following sections). A few of these genes are also plotted as they resulted originally from the global gene expression in the three replicates (see **Fig. 24, C and D**).

4.2 Validation of the gene expression data: *in situ* hybridisations on candidate genes

In situ hybridisation is a very powerful technique if coupled with the LCM and employed to confirm the results of the gene expression analysis. Indeed, we wanted to follow the expression of meristem-specific genes, therefore we cannot rely heavily on RT-PCR on apices because we would lose the resolution on expression level due to dilution of the meristem tissue in the whole apex. Moreover, *in situ* hybridisation gives not only an idea of the expression level by the strength of the signal, but it also shows the spatial expression pattern of a gene, revealing specific sub-compartments of the SAM in which that gene could exert a specific function.

In order to check the expression patterns of selected candidate genes by *in situ* hybridisation, DNA templates for *in situ* probes were synthesized by PCR using specific primers for the selected candidates, and the relative RNA probes tested on apices. The total number of genes tested was 60 (see **Appendix II** for the complete list). A list of 22 of these genes, which are discussed in the following sections because they show expression patterns consistent with the RNA-Seq gene expression data, are indicated in **Table 5**. Around half of the probes tested did not give any visible signal, while a few others showed signal but were not easy to interpret in terms of differential expression between samples.

In situ hybridizations with *SOC1* probe were repeated several times, to provide a positive control in our experiments with the candidate genes (**Fig. 27**).

1) First series.

The *C4* candidate gene showed an interesting expression pattern in wild-type, as it is expressed specifically only in the SAM and its signal increases with longer exposure to LD (**Fig. 27**). It is predicted to encode a bZIP transcription factor of unknown function. The *C11* candidate gene does not show visible expression before induction, is only weakly expressed after +1LD and more strongly expressed after +3LD (**Fig. 27**). It is a gene encoding a zinc finger-homeodomain protein. In terms of spatial distribution, *C11* mRNA is detected at the flanks of the SAM, in regions which correspond to the positions at which organ primordia will form. *C15* is expressed already before transition, but it seems to increase in expression upon transfer to LD. The pattern looks similar to genes like *AGL24* (see **Fig. 14**), although it is expressed more broadly also outside of the SAM.

Results

This gene encodes a leucine-rich repeat (LRR) family protein, with predicted kinase activity. *C19* is strongly expressed, especially at the SAM but also in the young leaves surrounding the meristem (**Fig. 27**), and it seems to increase during the floral transition. It encodes a LRR protein of unknown function. *C20* is strongly expressed in the apex, and particularly at the SAM. It is already present before induction in LD, and it seems to increase in intensity after induction, although the saturation of the signal makes the quantification quite difficult. It encodes a protein with RING finger-like zinc finger motif.

2) Second series.

D3, *D27* and *D29* seem to be expressed already before the shift, but they increase in intensity. Their expression is also not specific for the SAM, since they are expressed in other tissues in the apex (**Fig. 28** and **Fig. 29**). *D3* encodes a protein of unknown function, *D27* an ATP binding protein and *D29* a glyceraldehyde-3-phosphate dehydrogenase. *D19*, *D31*, *D35* and *D37* seem to be very specifically expressed in the meristem, although the mRNAs of the first three genes are very weakly detected. *D19* encodes a protein involved in the β -oxidation of fatty acids, *D31* a heptahelical transmembrane protein, *D35* a nitrate reductase that was found to be also involved in flowering (Seligman et al., 2008) and *D37* a Dof-type zinc finger protein. *D55* has a pattern similar to *SOC1*. It encodes for a phospholipid/glycerol acyl transferase.

D13 has an intriguing pattern of expression (**Fig. 28**). Before induction, it is expressed in the apex quite strongly and concentrated in the very young leaves near the meristem, on the most external cell layer of these leaves. After +3LD of induction another spot of expression appears in the center of the shoot apical meristem, spanning part of the “rib zone” and the “central zone” of the meristem, in a region that resembles *TFL1* expression pattern. *D13* encodes a stearyl-ACP desaturase.

3) Third series.

Most of the genes of this series were also tested. The ones shown (**Fig. 30**) are all up-regulated after +3LD, although for some of them the *in situ* hybridisation signal is very weak. All of them are expressed mainly in the whole SAM, except for *C23*, which is specifically expressed only in the central part of the SAM (**Fig. 30**). *C21* encodes a homeobox protein, which was shown to be involved in flowering (Wang et al., 2003), *C22* encodes a putative hydrolase/lipase, *C25* an uncoupling mitochondrial protein, *C27* a putative calcium-dependent protein kinase, and *C29* a GATA transcription factor. *C23*, *C26*, and *C30* all encode proteins with unknown function.

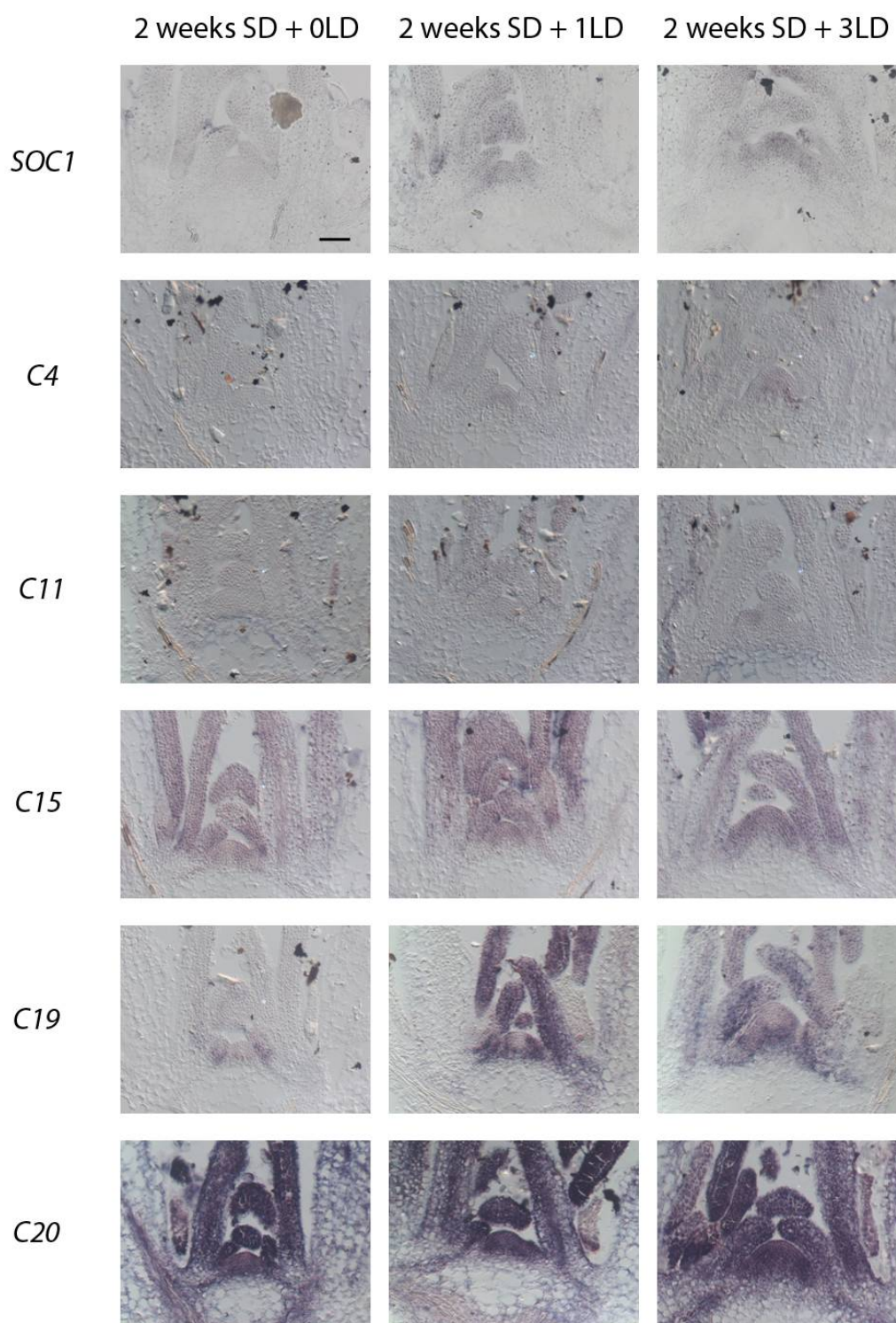


Fig. 27. *In situ* hybridisations with candidate genes. These genes were initially selected using only data from replicate A (see text for details). Plants were grown for 2 weeks in SD and shifted to LD, as indicated in the figure. Samples were collected at ZT8. *SOC1* is used as a positive control on the samples. The corresponding genes are listed in **Table 5**. Scale bar is 50 μ m.

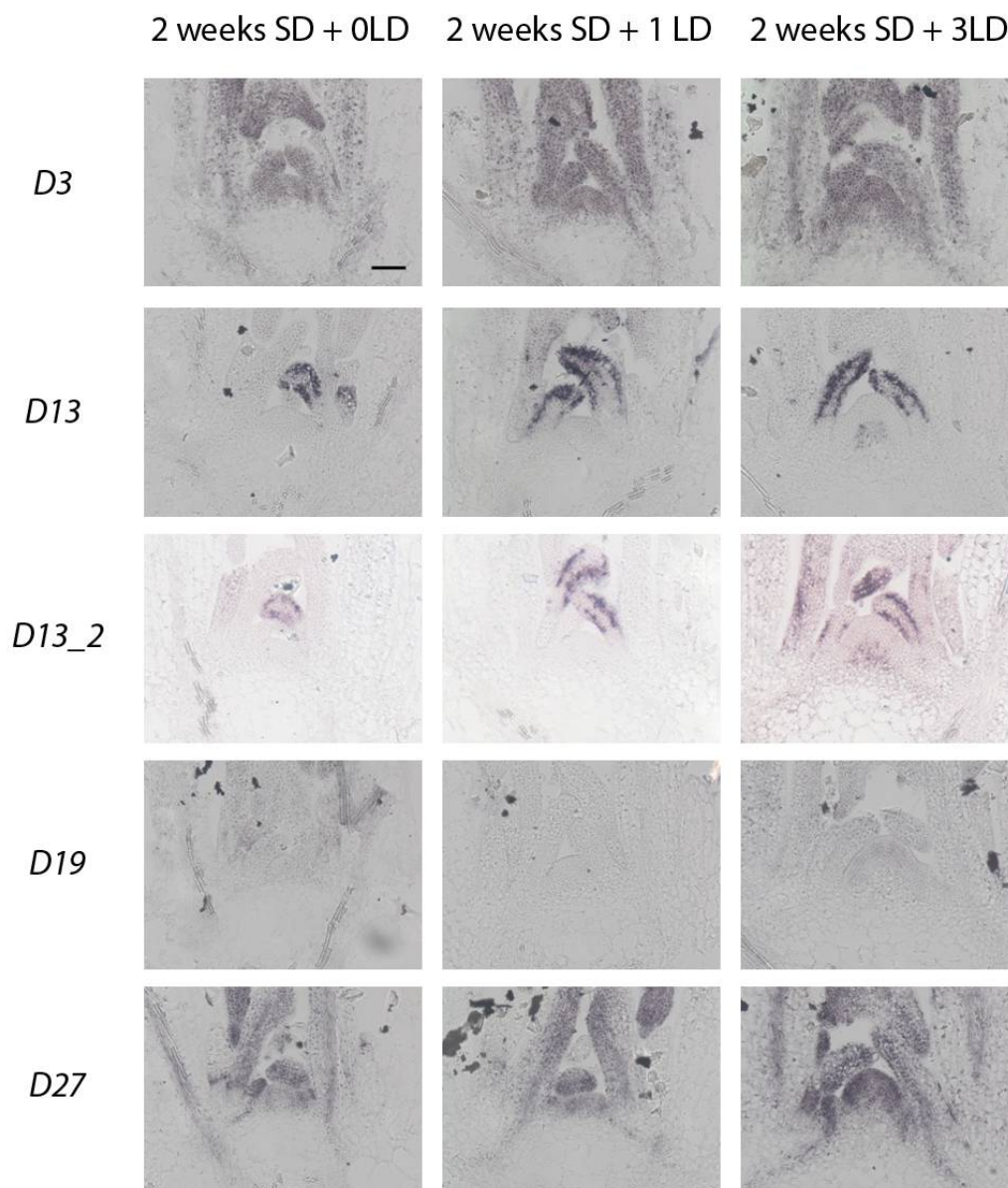


Fig. 28. *In situ* hybridisations with candidate genes. These genes were selected with the “p-value” and “log2 ratio” approaches using data from replicates A and B (see text for details). Plants were grown for 2 weeks in SD and shifted to LD, as indicated in the figure. Samples were collected at ZT8. *D13_2* is an alternative probe for detection of *D13* mRNA. The corresponding genes are listed in **Table 5**. Scale bar is 50 μ m.

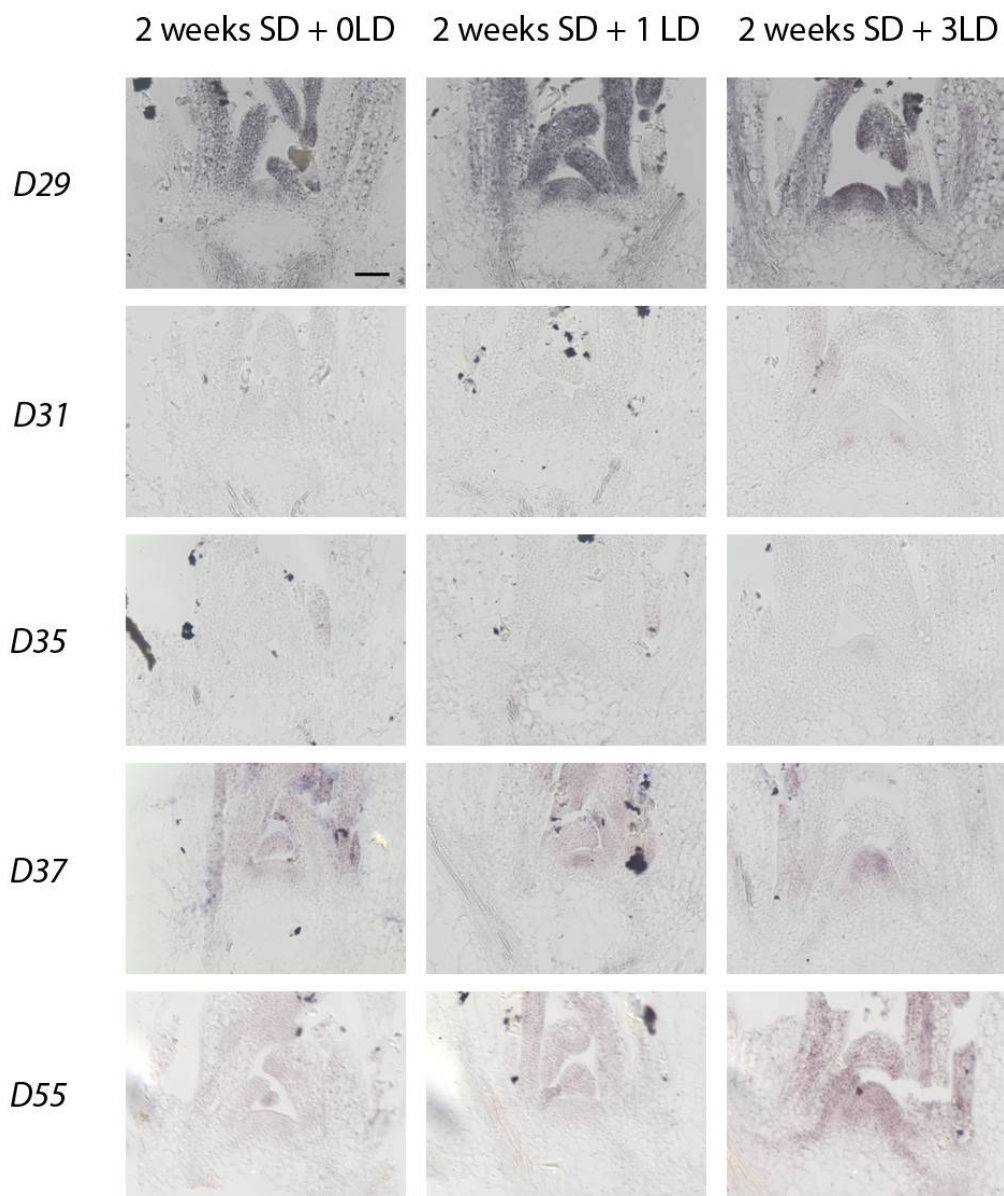


Fig. 29. *In situ* hybridisations with candidate genes. These genes were selected with the “p-value” and “log2 ratio” approaches using data from replicates A and B (see text for details). Plants were grown for 2 weeks in SD and shifted to LD, as indicated in the figure. Samples were collected at ZT8. The corresponding genes are listed in **Table 5**. Scale bar is 50 μ m.

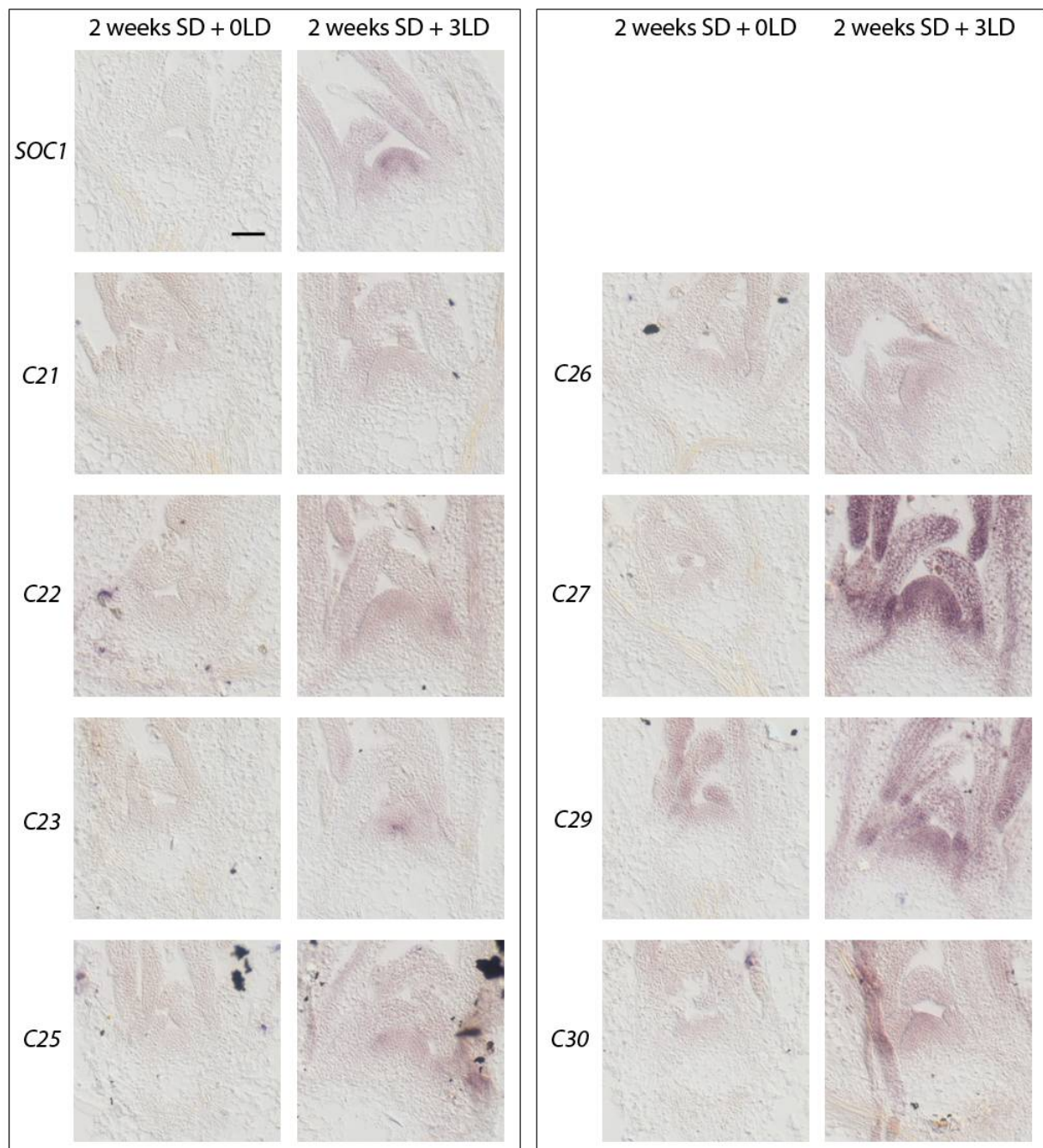


Fig. 30. *In situ* hybridisations with candidate genes. These genes were selected with the “clustering” approach, using data from replicates A, B and C (see text for details). Plants were grown for 2 weeks in SD and shifted to LD, as indicated in the figure. Samples were collected at ZT8. *SOC1* was used as a positive control and as a “reference gene”. The corresponding genes are listed in **Table 5**. Scale bar is 50 μ m.

All three methods of analysis lead to the identification of novel genes with interesting expression

patterns. However, the success rates of these methods were different. Although it is not easy to compare them directly, because a different number of genes was tested for each method. However, the most reliable method appears to be the third one, with a success rate of about 80% (8 positive genes out of 10 tested), followed by the first method with about 60% success rate (5 positive genes out of 8 tested), and finally the second method with about 21% (9 positive genes out of 42 tested). In the case of the second method, the “p-value” approach had more success than the “log₂ ratio” approach, since *D19*, *D27*, *D29*, *D31*, *D35* and *D37* were in the “p-value” list, while only *D55* was in the “log₂ ratio” list, and finally *D3* and *D13* were in both lists.

4.3 The use of mutants to test the response of the candidate genes to flowering pathways

In a first screen, *in situ* hybridisations were performed using probes for the candidate genes on apices from wild-type plants. To test whether the confirmed genes were activated by the photoperiodic flowering pathway they were analyzed by *in situ* hybridisation on a *ft-10 tsf-1* double mutant (grown in the same condition as wild-type plants) and repeated in parallel on wild-type. Indeed, up- or down-regulation of a gene at the SAM driven by a shift from SD to LD in wild-type could be caused by many different reasons, such as developmental changes at the meristem due to its growth, or simply a response to light, temperature or stress. A plant carrying null mutations in both *FT* and *TSF* is extremely late flowering in LD because it does not respond to photoperiod (Jang et al., 2009), as the SAM of these plants does not receive the floral stimulus from the leaf upon induction because both the FT mobile signal and its homologue TSF are absent. If a gene responds to the inductive FT/TSF signal at the SAM in wild-type plants, it should not respond to LD in the double mutant. This is indeed the case for *SOC1*, which was used as a control gene (see **Fig. 31**). So *ft tsf* can be used to identify genes that respond to this known signal. *In situ* hybridisations show that *SOC1* is not expressed in wild-type grown for two weeks in SD before induction (+0LD), starts to be up-regulated after +1LD and strongly increases at the SAM after +3LD (**Fig. 31, A-C**). In contrast, in the *ft-10 tsf-1* double mutant the level of expression of *SOC1* does not increase after induction, and remains at a very low level even after 3 LD (**Fig. 31, D-F**).

In principle, three behaviors in relation to *FT/TSF* can be expected: total dependence, partial dependence, independence.

D31 is an example of the first behavior. Indeed, expression of this gene is detected in wild-type in the whole SAM only after 3 LD, while it is absent in *ft tsf* (**Fig. 31, G-L**).

Results

D27 is an example of the second behavior. Although its expression depends sometimes on the tissue sections, in general it is expressed quite strongly and in particular after +3LD, in wild-type, while in the double mutant its expression is clearly lower, during the entire time course (**Fig. 32, A-F**). It is surprising that also before induction the double mutant shows less expression than wild-type, because it should look very similar since *FT* and *TSF* are generally believed not to be expressed in SD.

Surprisingly, the third behavior was also found. For *D13*, in the *ft tsf* double mutant the pattern appears similar to the one in wild-type both before and after induction (**Fig. 32**), which would imply that this gene is activated by a signal after 3 LD that is independent of *FT* or *TSF* action.

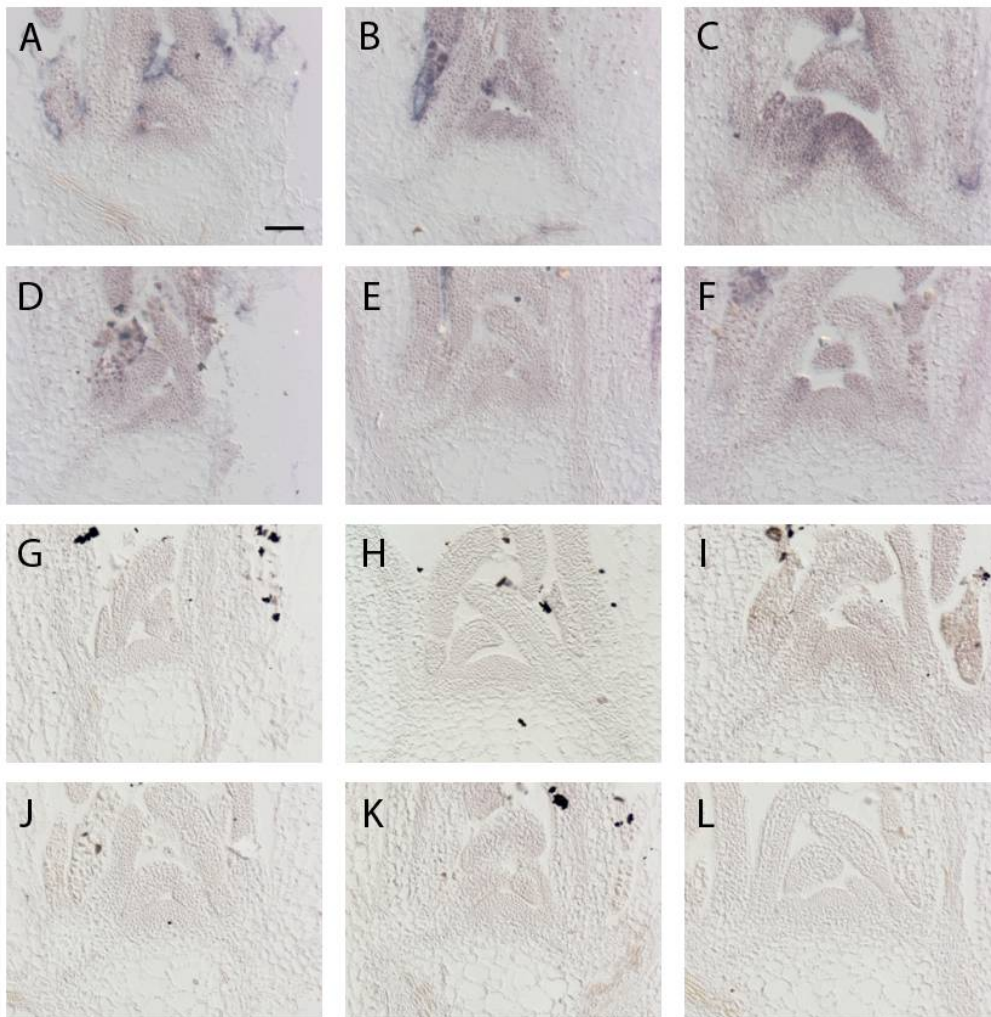


Fig. 31. *In situ* hybridisations with *SOCl* and a candidate gene. *In situ* hybridisations were carried out using probe for *SOCl* mRNA (A-F), or *D31* (G-L) on apices from wild-type Col (A, B, C, G, H, I) and *ft-10 tsf-1* (D, E, F, J, K, L). Plants were grown 2 weeks in SD and collected before induction at ZT8 as +0 LD (A, D, G, J), after +1 LD (B, E, H, K), after +3 LD (C, F, I, L) of induction in LD. Scale bar is 50 μ m.

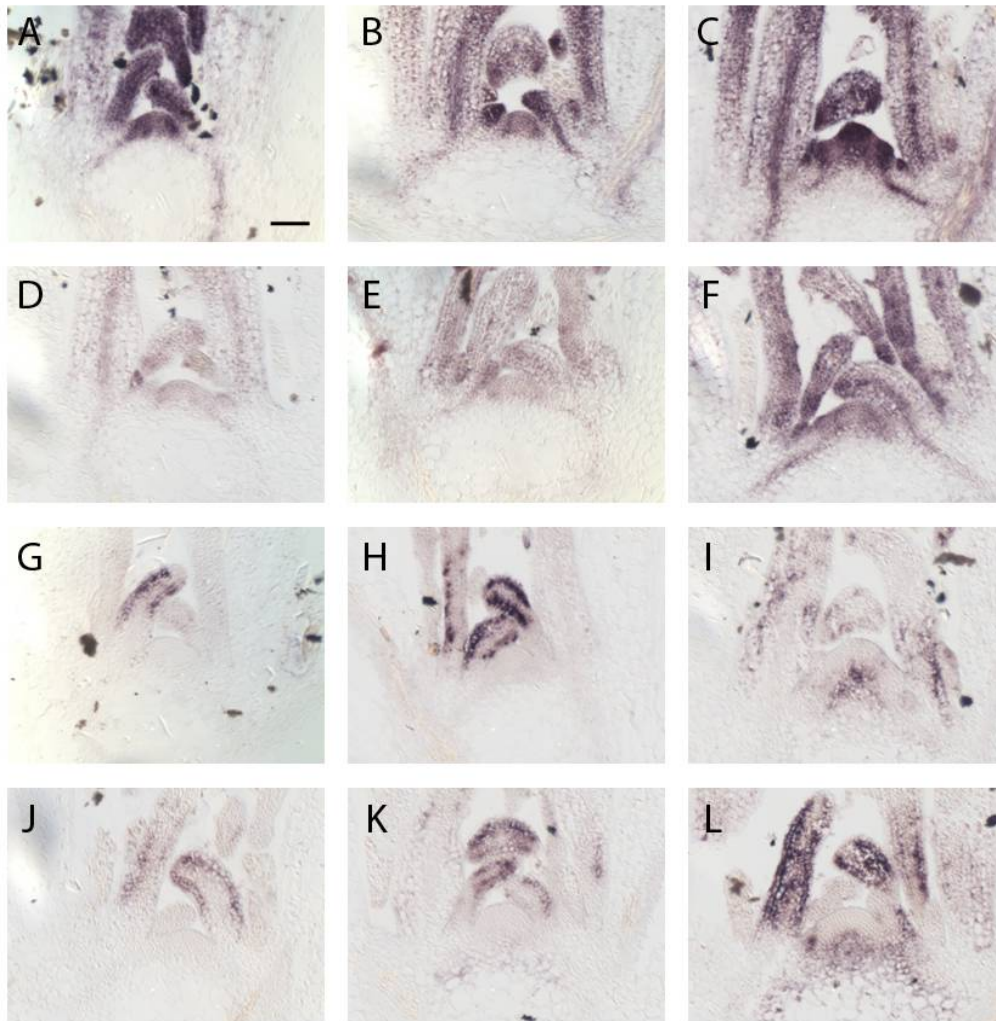


Fig. 32. *In situ* hybridisations with candidate genes. *In situ* hybridisations were carried out using probe for *D27* mRNA (A-F), or *D13* (G-L) on apices from wild-type Col (A, B, C, G, H, I) and *ft-10 tsf-1* (D, E, F, J, K, L). Plants were grown 2 weeks in SD and collected before induction at ZT8 as +0 LD (A, D, G, J), after +1 LD (B, E, H, K), after +3 LD (C, F, I, L) of induction in LD. Scale bar is 50 μ m.

4.4 *D13*: a gene encoding a lipid desaturase induced by photoperiod independently of *FT* and *TSF*

This gene was selected from the list of genes which were confirmed by *in situ* hybridisation for four main reasons. The first one is that its pattern of expression was unique among those tested. It is already expressed before induction, but only in the young leaves near to the meristem, specifically in the outer layer. Then upon exposure to LD it appears in the center of the inflorescence meristem with a strong signal after 3 days of induction (**Fig. 28**). The second reason is that in the global gene

Results

expression dataset from the meristem this gene has one of the highest levels of up-regulation (more than 500 times for the values in TPM between +0LD and +3LD), and this is reflected in a strong and clearly visible signal by *in situ* hybridisation. The third reason is that this gene encodes an enzyme (lipid desaturase), involved in a pathway that has not been linked so far to the floral transition. The fourth reason is that the expression pattern of this gene in *ft-10 tsf-1* double mutant is very similar to the one in wild-type plants (**Fig. 32, G-L**). This suggests that in the *ft-10 tsf-1* double mutant there is still a response to photoperiod, which triggers a signal, and eventually a response at the SAM, which is independent of *FT* and *TSF*, a fact that has not been described so far. Another interesting feature of this gene is that it is a member of a family of 7 genes, but while the others are expressed in several distinct tissues in the plant, *D13* expression could not be detected (Kachroo et al., 2007). This suggests that it may represent an isoform of this class of enzymes that is specific for the meristem.

The expression pattern initially found for this gene was reproducible, in different hybridisations and using samples collected in independent experiments. Also an alternative RNA probe for *in situ* hybridisation was synthesized, designed in another region of the mRNA, and using this second probe the pattern of expression for this gene was confirmed (**Fig. 28**). So the first probe was used for all the subsequent experiments, since it gave a slightly stronger signal.

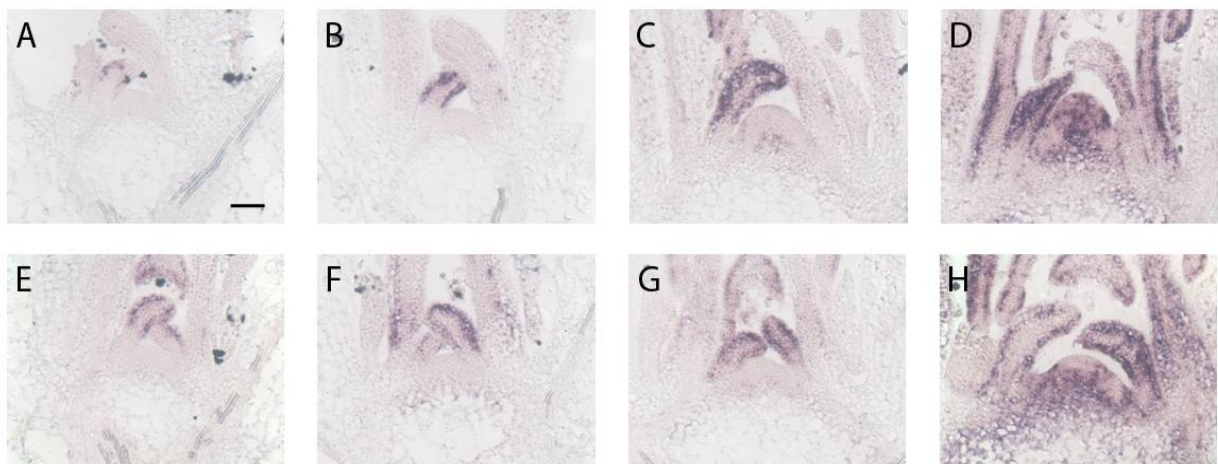


Fig. 33. Expression pattern of *D13* in wild-type and *ft tsf* double mutant until 5 LD after shift. *In situ* hybridisations were carried out using probe for *D13* mRNA, on apices from wild-type Col (A, B, C, D) and *ft-10 tsf-1* (E, F, G, H). Plants were grown 2 weeks in SD and collected before induction at ZT8 as +0 LD (A, E), after +1 LD (B, F), after +3 LD (C, G) and after +5LD (D, H) of induction in LD. Scale bar is 50 μ m.

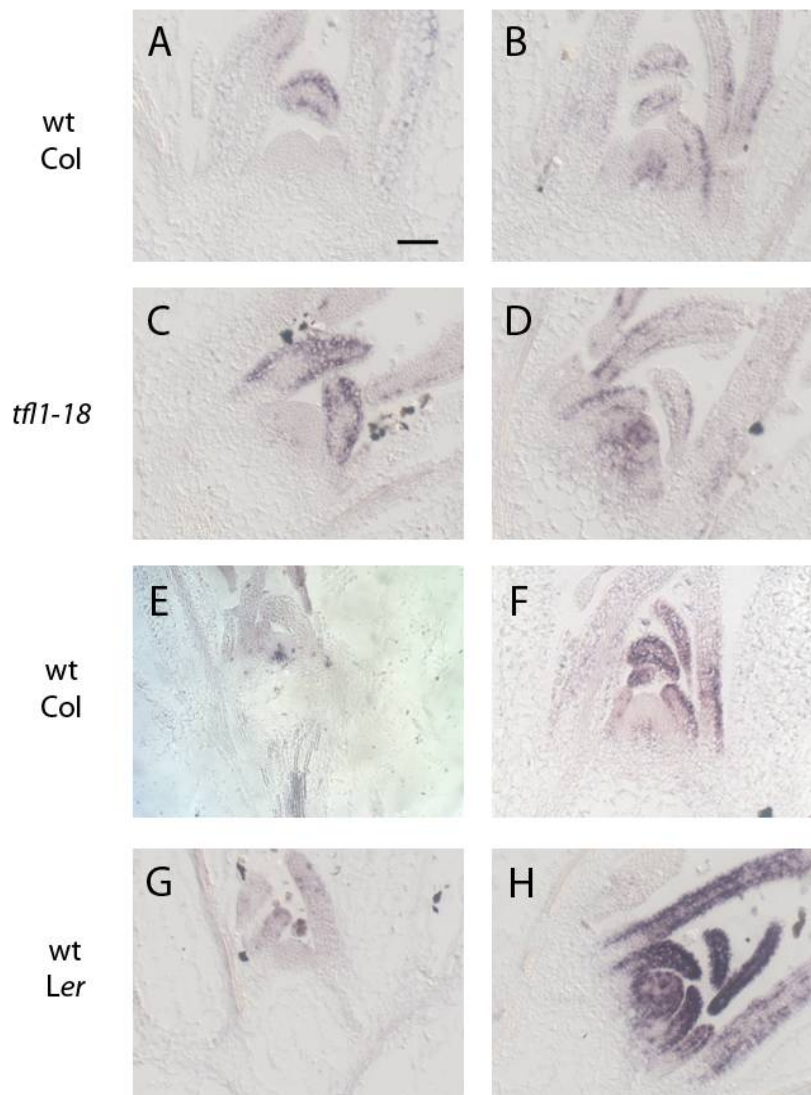


Fig. 34. Expression pattern of *D13* as induced by LD and in relation to *TFL1*. *In situ* hybridisations were performed using probes for *TFL1* (E) and *D13* (all the others). Plants were grown for 10 LD (A, C, E), 12 LD (B, D), 2 weeks SD +0LD (G), 2 weeks SD +3LD (H), and 2 weeks SD +3LD +2SD (F). Plants were collected at ZT8. Scale bar is 50 μ m. Picture E was kindly provided by Aimone Porri.

Another *in situ* hybridisation experiment showed again that *D13* is up-regulated after 3 LD in the central region of the inflorescence meristem, both for wild-type and *ft tsf* double mutants (**Fig. 33**). In this experiment the strength of the signal is slightly weaker for the double mutant, probably reflecting the biological variation of the sample (compare with **Fig. 32, G-L**). However, the signal is still clearly stronger than before the third LD. Moreover, after 5 LD of induction, the mRNA of *D13* is broadly expressed through all the inflorescence meristem, and this expansion of the

expression domain occurs both in wild-type and *ft tsf* double mutants (**Fig. 33**). In wild-type after 5 LD, there is a small domain in which *D13* is not expressed, which could be the floral meristem forming on the flanks of the inflorescence meristem (**Fig. 33**). This domain, indeed, is not present in *ft tsf* double mutants, which are strongly delayed in floral meristem formation.

4.4.1 On the expression pattern of *D13*: possible interactions with *TFL1*

Because the portion of the *D13* transcript which is expressed in the meristem after 3 LD of induction is similar to the pattern of expression of *TFL1* gene upon induction (**Fig. 34, E**), it was tested whether there is any interaction between these two genes.

A time courses of plants grown in LD, both for wild-type Col and *tfl-18* mutant, was collected and hybridised with *D13* probe. Meristems of *tfl1* mutants grow slightly faster in LD compared to wild-type due to the effect of a slightly earlier flowering of the mutant (**Fig. 34, A-D**). In both genetic backgrounds *D13* presents an increase of expression with the increasing number of LD in the florally-induced meristem. Nevertheless, *D13* shows a stronger signal in *tfl1* mutant compared to the corresponding wild-type control grown for the same number of LD (**Fig. 34, A-D**).

4.4.2 On the signal inducing *D13*: triggering flowering without LD

The expression of *D13* mRNA increases during floral induction triggered by LD, but is independent of *FT* and *TSF*, therefore it was of interest to separate floral induction from induction of flowering by photoperiod and assess whether *D13* was still induced during flowering. One way to separate these two processes is to use an inducible system, in which the flowering cascade can be triggered without shifting the plants to LD. Moreover, the fact that *D13* is increased in the absence of *FT* and *TSF* does not necessarily exclude that *FT* or *TSF* can also contribute to the induction of this gene and that they could induce it once they are strongly activated. Transgenic plants carrying a construct encoding the CO protein fused to the gluco-corticoid receptor (GR) ligand-binding domain driven by the *35S* promoter were used. In these lines, treatment with dexamethasone (DEX) leads to a strong activation of CO function and induction of flowering (Simon et al., 1996). This construct is in *co* genetic background (in *Ler*), so CO is activated only in response to DEX. Therefore, this system can be used to activate flowering in SD upon treatment with DEX and the response can be studied in terms of gene expression.

Plants were grown for 2 weeks in SD, and the ones carrying *35S::CO:GR* either treated with DEX or with the mock, only one time at ZT8, while wild-type *Ler* was shifted to LD, as a positive

Results

control for induction of floral promoting genes. Samples were collected at days +0, +1, +3, +5 after the treatment or the shift. Plants carrying *35S::CO:GR* were monitored and the ones treated with DEX flowered significantly earlier than the ones treated with the mock, confirming the effect of the treatment. Apices enriched in meristem tissue were collected by removing the leaves with small tweezers. These samples still contain small parts of leaves, so it is still possible to monitor an increase in *FT* expression under strong inductive condition, such as the activation of the CO:GR system. The expression of *FT* was measured and a strong up-regulation of this gene was found in the samples treated with DEX from the first day after treatment, while no increase was detected in the mock-treated samples (**Fig. 35, A**). Wild-type *Ler* shifted to LD did not show a large increase in *FT* mRNA, probably because there is not so much leaf tissue to detect the increase due to the shift in LD at this stage. *SOC1* was used as a marker for the relative induction at the meristem. *SOC1* induction upon DEX treatment reflects *FT* expression in these samples (**Fig. 35, B**), and it is even stronger than in wild-type shifted to LD, confirming that floral induction is being triggered in the samples treated with DEX. In wild-type samples there was no more increase of *SOC1* mRNA after the first long day. This could be due to the fact that after 3 LD *Ler* is already flowering, and there is not a significant increase of *SOC1* after this stage. Finally, expression level of *D13* was tested. First of all, because the expression pattern of *D13* was described in Col in our previous experiments, and for the RT-PCR *Ler* ecotype was used, *in situ* hybridisation was carried out on apices of wild-type *Ler* grown 2 weeks in SD and then shifted to LD. This experiment confirmed an up-regulation of *D13* upon exposure to LD (**Fig. 34, G, H**). The increase in the expression level of this gene seems even stronger in *Ler*, probably reflecting the faster induction occurring in this ecotype compared to Col. Therefore, expression level of *D13* could also be measured by RT-PCR. In wild-type samples this gene was strongly up-regulated upon shift to LD (**Fig. 35, C**), similarly to previous results from the sequencing data and from *in situ* hybridisation (see above). But in the case of plants carrying *35S::CO:GR*, no induction of *D13* was detected upon treatment with DEX. From this experiment we can conclude that *D13* is not influenced by the photoperiodic pathway activated by CO, and therefore that it is not activated by FT/TSF.

Additionally, since possible interactions between *D13* and *TFL1* are being tested, *TFL1* expression was also checked in those samples. *TFL1* expression level increased in wild-type upon shift to LD, similarly to *D13* (**Fig. 35, D**). In the case of plants carrying *35S::CO:GR*, no induction of *TFL1* expression was detected, as for *D13*. This last result seems to be in contradiction to what was published previously (Simon et al., 1996). Nevertheless, the general experimental and growth

Results

condition were probably very different, and it is not easy to compare our RT-PCR data with previous *in situ* hybridisation data. Moreover, the spatial expression pattern of *TFL1* is quite complex, because upon induction it starts to be expressed in different and separated zones of the SAM, and RT-PCR cannot take into account the contribution of these distinct parts on the general expression in the whole apex.

Expression of *D13* was also tested in plants that were grown 2 weeks in SD, shifted to LD for 3 LD and then shifted back to SD, in Col ecotype. *In situ* hybridisation shows that at 2 days after the shift back to SD, there is still strong expression (Fig. 34, F), comparable to that after 3 LD (Fig. 33, C). This would suggest that expression of *D13* is not only sustained by LD, but once expressed it can stay on even after return to SD. Nevertheless its expression does not increase to the levels detected in plants shifted to LD for 5 days.

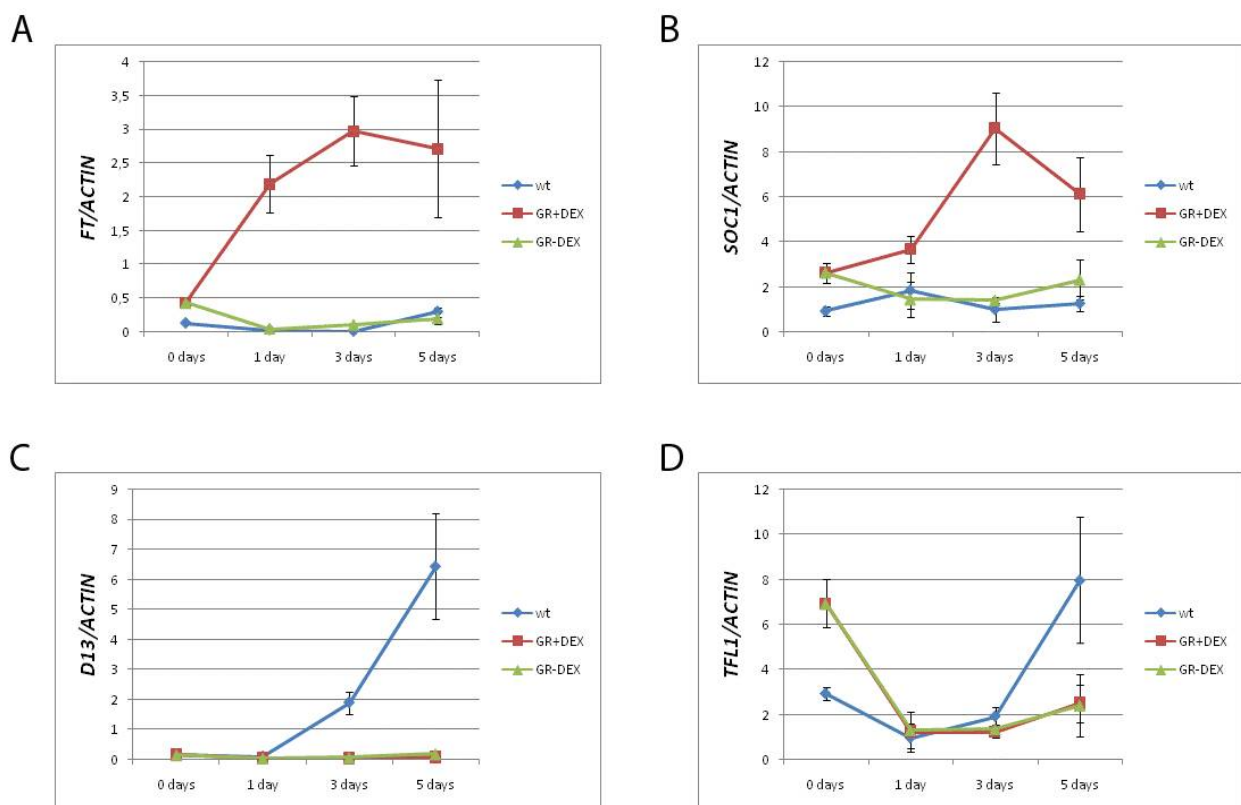


Fig. 35. Quantitative real time PCR on RNA extracted from plants in which the photoperiodic pathway has been induced. Levels of expression of *FT* (A), *SOCI* (B), *D13* (C), and *TFL1* (D) mRNAs are measured at ZT8 in apices of seedlings enriched in meristem tissue. Plants were previously grown for two weeks in SD, then wild-type *Ler* (wt) was shifted to LD, while *35S::CO:GR* in *co-2* (COGR) was kept in SD and treated with dexamethasone (+DEX) or with mock (-DEX).

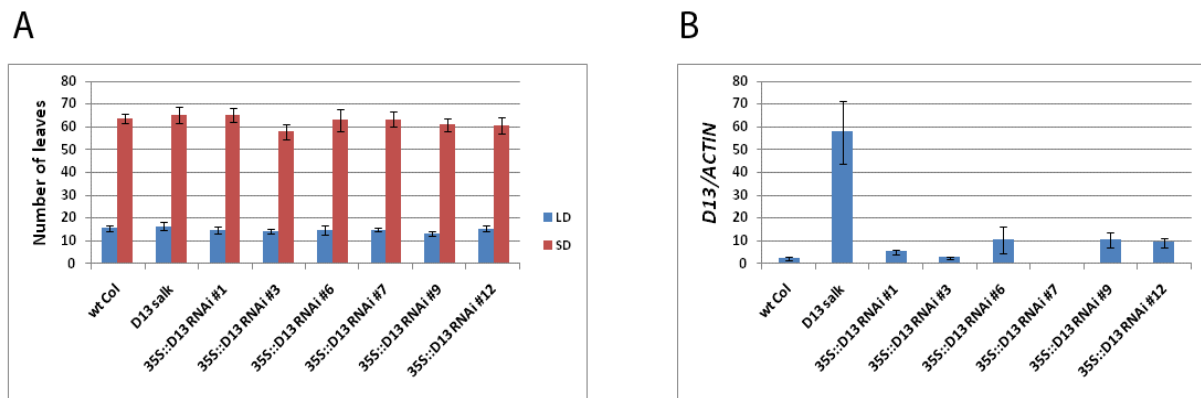


Fig. 36. Modulation of *D13* expression level with transgenic approaches. Wild-type Columbia, a T-DNA line (see text) with an insertion in the promoter of *D13*, and several independent lines expressing RNAi against *D13*, are compared. Panel A: flowering time data. Total number of leaves (rosette plus cauline leaves) are scored both in LD and SD. Panel B: quantitative real time PCR to measure *D13* RNA expression in apices (apices enriched in meristem tissue). Plants were grown in LD in growth chambers for 12 days and collected at ZT8.

4.4.3 Modulation of *D13* expression with transgenic approaches

The SALK collection of plants carrying T-DNA insertions (Alonso et al., 2003) was searched to find a line of *Arabidopsis* with an insertion at the *D13* locus. There was no line with a T-DNA insertion in exonic or intronic regions of this gene, but one with an insertion in the promoter region, just a few base pairs before the ATG start codon was detected. Therefore, it is not possible to predict the effect of this insertion. In parallel, the expression of this gene was modulated by transgenic approaches. Wild-type Col was transformed with a construct designed to target a specific region of the mRNA of *D13* by RNA interference (see Methods) driven by the 35S promoter. Six independent homozygous lines carrying one single insertion of the transgene were obtained. None of the RNAi lines nor the SALK line showed a flowering time phenotype or any other obvious phenotype (**Fig. 36, A**), except for a slight early flowering of line #3 (especially in SD) and line #9 (especially in LD). The RNA level of *D13* in all these lines was measured in apices (**Fig. 36, B**). Compared to wild-type, most of the lines did not show a significant decrease in *D13* expression. The only line with less detectable expression was line #7. Moreover, the SALK line showed higher *D13* expression, confirming that it is a line over-expressing *D13* presumably due to expression from a promoter within the T-DNA. However, there is no correlation between the resulting flowering time and level of expression of *D13* in those lines. It seems quite likely that the RNAi approach in this case did not result in a significant reduction of the mRNA of *D13*.

Results

Wild-type Col was also transformed with a construct expressing *D13* complete coding sequence, driven by *35S* promoter or *FD* promoter. T1 plants selected on BASTA did not show any obvious phenotype.

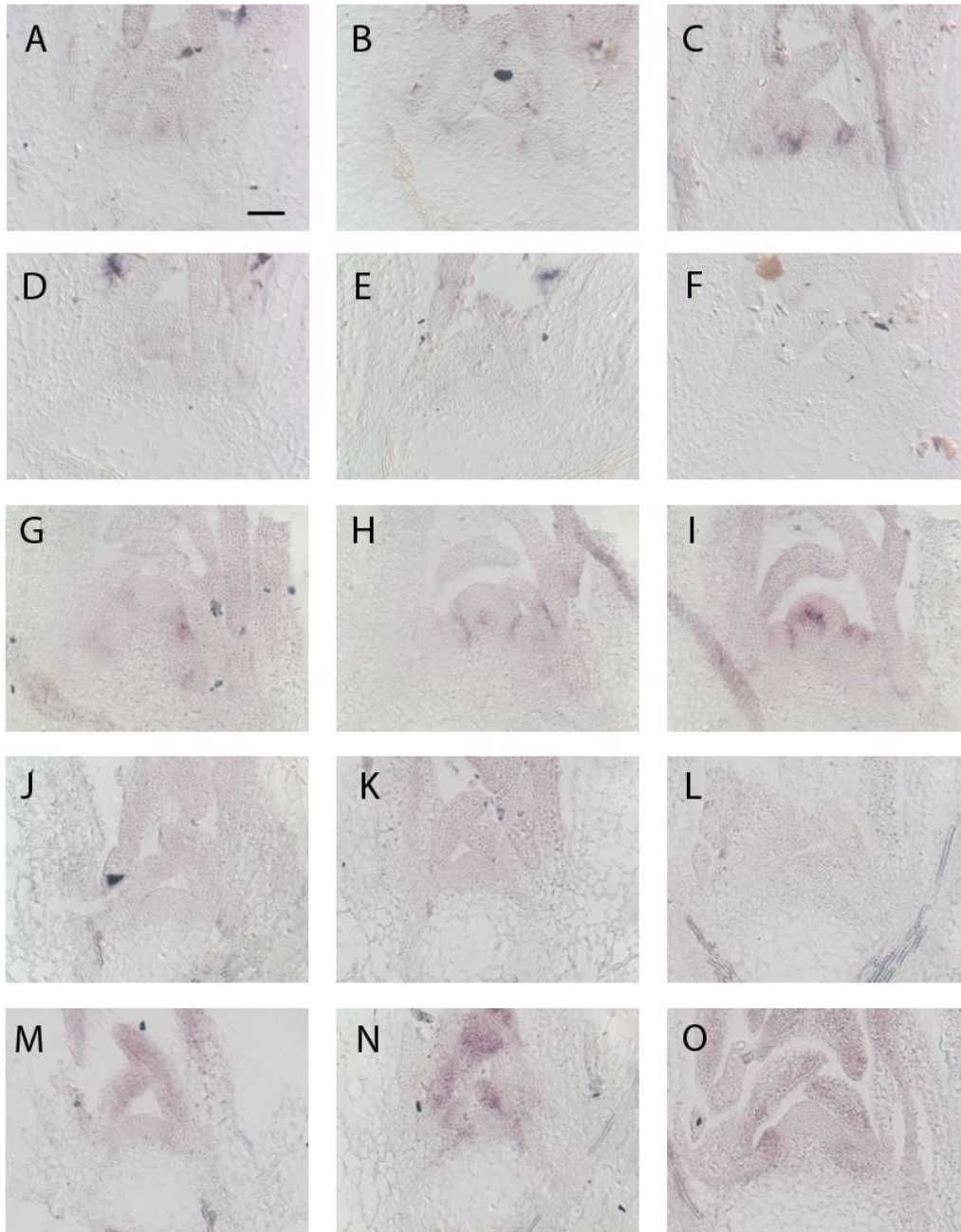


Fig. 37. Expression patterns of the *C11* candidate gene and close related genes. *In situ* hybridisations were carried out on shoot apices with probes for *C11* (A-I), *ATHB21* (J, K, L) and *ATHB25* (M, N, O). Apices were from wild-type Col (A, B, C, G-O) and *ft-10 tsf-1* (D, E, F). Plants were grown 2 weeks in SD and collected at +0LD (A, D, J, M), +1LD (B, E, K, N), +3LD (C, F, L, O) and +5LD (G, H, I). G, H and I are pictures from three sections of the same plant. Plants were collected at ZT8. Scale bar is 50 μ m.

4.5 C11: a homeodomain transcription factor which is dependent on *FT/TSF*

C11 is a gene encoding a homeodomain protein included in the zinc finger-homeodomain family. The gene that we identified as *C11* corresponds to *ATHB31*.

C11 mRNA is not detected by *in situ* hybridisation on apices of wild-type Col grown for 2 weeks in SD. Upon induction, it is weakly visible after 1 LD and more strongly expressed after 3 LD (**Fig. 27** and **Fig. 37, A-C**). The expression of this gene at +3LD seems to be restricted to regions at the flank of the SAM which correspond to the organ primordia. Although at this stage there are still leaf primordia, rather than floral primordia, this gene could be expressed just before the appearance of the floral primordium itself or during its formation. In addition, *ft tsf* double mutants do not express this gene at all during 3 LD of induction, demonstrating that it is downstream of the *FT/TSF* signal (**Fig. 37, D-F**). Furthermore, hybridisation on wild-type apices after 5 LD shows expression of *C11* specifically at the boundary between the meristem and the organ primordia (**Fig. 37, G-I**).

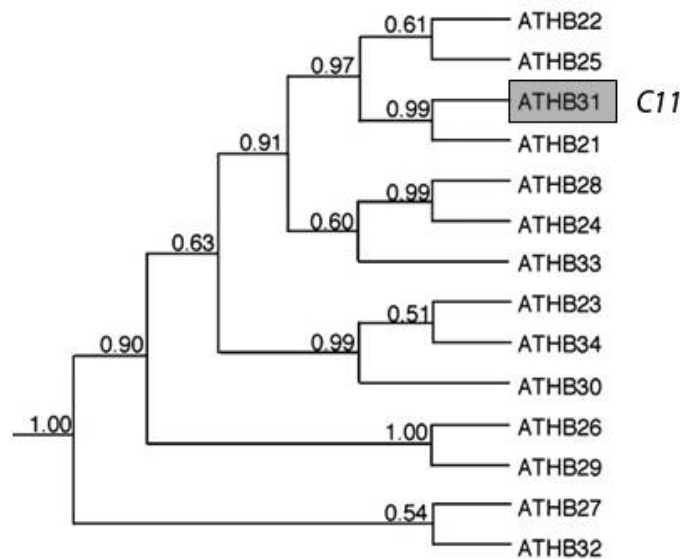


Fig. 38. Phylogenetic relationship in the *Arabidopsis* zinc finger-homeodomain gene family. The tree (from Tan and Irish, 2006) was constructed with Bayesian analysis, and posterior probabilities were indicated for each branch.

4.5.1 *C11* has close homologues which might play redundant roles with it

It was previously reported that loss of function alleles in each of the genes belonging to the same family as *C11* do not confer any visible phenotype (Tan and Irish, 2006). The authors concluded that this is probably due to functional redundancy between the members of this family, since they

Results

are quite similar in sequence. Also, in some cases the general expression pattern monitored by RT-PCR was similar for some of the members. In addition, protein-protein interaction among some members of this family was detected by yeast two-hybrid (Tan and Irish, 2006).

To study *C11* further, the members of the gene family that were closer to this gene were chosen, according to their phylogenetic relationship (**Fig. 38**). RNA probes for these genes were then synthesized, and wild-type apices were hybridised by *in situ* hybridisation.

The closest homologue to *C11*, which is *ATHB21*, did not show any visible signal (**Fig. 37, J-L**) in our conditions. These genes seem to be quite lowly expressed, so maybe it is difficult to detect the expression of some of them by *in situ* hybridisation. Indeed, in our dataset, *ATHB21* is detected only at +3LD, and is extremely lowly expressed (2.3 and 0.8 TPM for replicate B and C respectively) and not detected at all in replicate A. Another gene tested was *ATHB25*, which is the next closest homologue. This gene is not visible before induction by LD, but its expression becomes visible after 3 LD on the primordia at the flanks of the SAM (**Fig. 37, M-O**). This pattern is very similar to the the one of *C11*, further suggesting a possible redundant role with *C11*. In agreement with this possibility, a strong interaction in the yeast two-hybrid system was found between *ATHB31* and *ATHB25* proteins. In our dataset, *ATHB25* mRNA is detected (range 0-138 TPM), although not clearly up- or down- regulated.

Given the possible redundant function played by these genes, and the overlapping pattern of expression of some of them, the strategy of using artificial microRNA (amiRNA) to specifically knock down more than one gene of this family was chosen (Schwab et al., 2006). amiRNA constructs were designed (see Methods), and two constructs were generated: one targeting *ATHB31* and *ATHB21* (amiRNAh21/31), and the other one targeting *ATHB25* and *ATHB22* (amiRNAh22/25), both driven by the *35S* promoter.

At the stage of T1 several individuals, both from the first and the second construct, show a moderate later flowering time compared to the other individuals. A more precise screen, at the level of the homozygous T3 generation, including measuring RNA level for the targeted genes in comparison to wild-type plants, is needed to assign a possible function of this family of genes on flowering regulation.

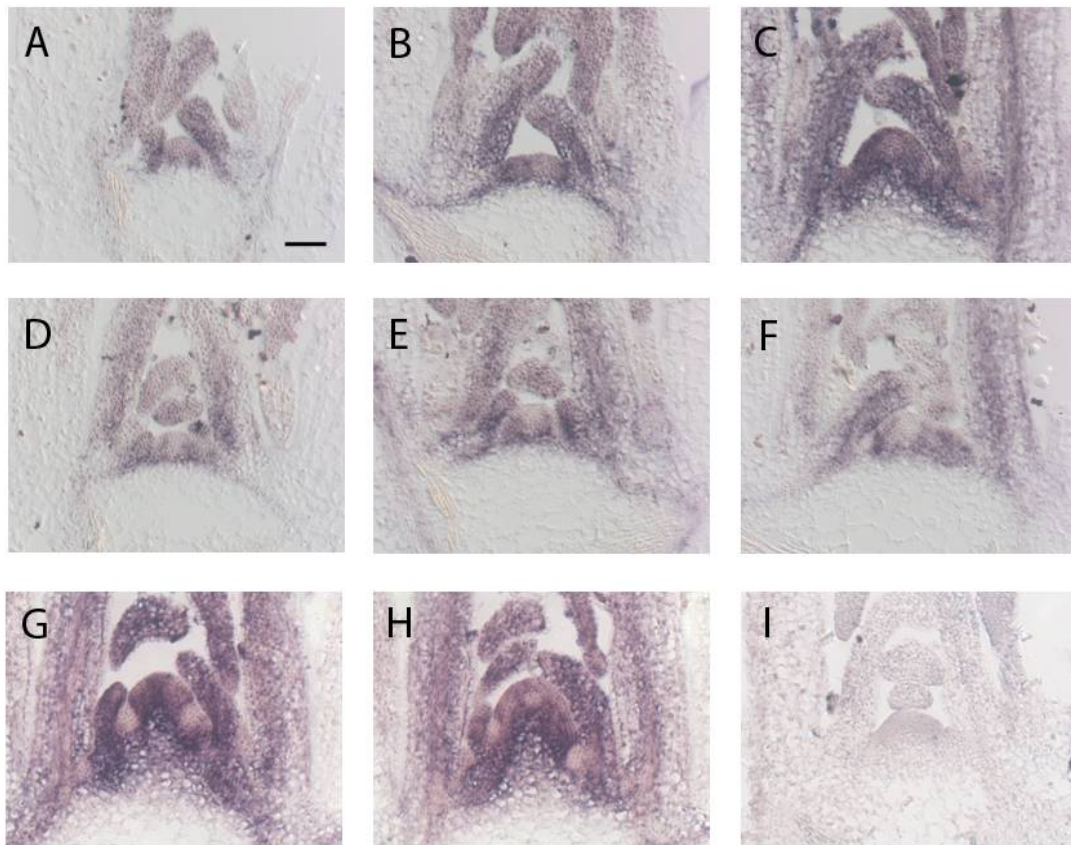


Fig. 39. Expression pattern of *C19* candidate gene. *In situ* hybridisations were carried out on shoot apices with probes for *C19* (A-H) and *PGIP2* (I). Apices were from wild-type Col (A, B, C, G, H, I) and *ft-10 tsf-1* (D, E, F). Plants were grown 2 weeks in SD and collected at +0LD (A, D), +1LD (B, E), +3LD (C, F, I) and +5LD (G, H). G and H are pictures from two sections of the same plant. Plants were collected at ZT8. Scale bar is 50 μ m.

4.6 *C19*: a LRR protein responding to *FT/TSF*

C19 encodes a protein that was previously named FLOR1, because it was discovered in an assay to isolate proteins putatively expressed in flowers. It was isolated as a possible interactor of AGAMOUS, and the physical interaction between them was tested and confirmed with various techniques (Gamboa et al., 2001). The protein is composed of 326 amino acids and contains a LRR domain. The predicted LRR domain is composed of 10 leucine-rich tandem repeats. It is also annotated as an enzyme inhibiting protein, because of its similarity with a class of inhibitors named polygalacturonase inhibiting protein (PGIP).

The signal detected for this gene by *in situ* hybridisation is very strong. It is present at the SAM, but also in young leaves surrounding the meristem (**Fig. 39**). The intensity of the signal clearly increases during the floral transition in wild-type plants (**Fig. 39, A-C**), while in *ft tsf* double

mutants it remains at a basal level that is comparable to the wild-type before induction (**Fig. 27** and **Fig. 39, D-F**). Interestingly, while in wild-type the expression spreads all over the meristem dome at the third LD (**Fig. 39, C**), in the double mutant it seems to be restricted in the lower part at the base of the meristem (**Fig. 39, F**), like in wild-type before induction (**Fig. 39, A**). This would suggest that the photoperiodic signal also changes the spatial distribution of the *C19* mRNA causing a broader expression over the central zone and reaching the L1 layer. Interestingly, in wild-type after 5 LD the expression is still strong all over the inflorescence meristem, but the signal is absent from the floral primordia (**Fig. 39, G, H**). This last feature is also found for *SOCI* and *FUL* transcripts (Samach et al. 2000; Mandel and Yanofsky, 1995a), which are excluded from the floral meristem and strongly expressed in the inflorescence meristem at this stage.

4.6.1 Loss of function of *C19* may influence flowering

A line which carries a T-DNA in the *C19* locus (SALK_093764) was found in the SALK collection (Alonso et al., 2003). The T-DNA is inserted in the intron between the two exons composing the gene locus (**Fig. 40, A**). This insertion was confirmed by PCR on genomic DNA and plants homozygous for the insertion were obtained by segregation. RNA was extracted for the homozygous T-DNA line and wild-type Col, and RT-PCR was used to test for the expression of *C19* transcript. When primers amplifying the segment of cDNA downstream of the T-DNA insertion were used, no transcript was detected, even with high number of PCR cycles, while a clear band is visible for wild-type (**Fig. 40, B**). Conversely, when primers amplifying the segment of cDNA upstream of the T-DNA insertion were used, a transcript was detected, with the same intensity of the product obtained for wild-type (**Fig. 40, C**). We can conclude that in this line the product of the *C19* gene is not entirely transcribed, but is truncated before the second exon. However, we cannot conclude on whether the putative product of this gene is functional in this mutant.

These plants do not have an obvious phenotype, although flowering occurs slightly later than wild-type Col, both in LD and SD. However, the difference is only approximately 1 leaf, and within the standard variation of the single individuals (**Fig. 41**), although reproducible in several experiments. The standard t-test was performed on three independent experiments, to test the statistical difference between the flowering time (as total number of leaves in LD) of wild-type and *c19* plants. In one case the difference was not significant (p-value=0.2), while in the other two cases it was either highly significant (p-value=0.02) or nearly significant (p-value=0.055).

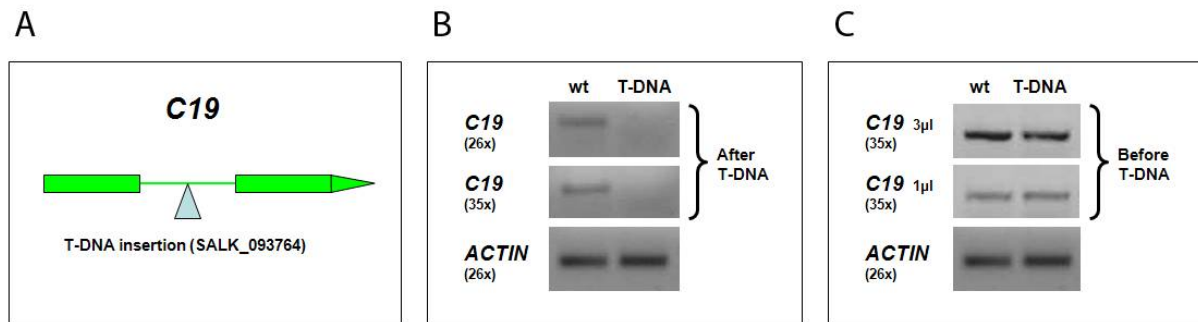


Fig. 40. A T-DNA insertion in the *C19* locus. Panel A: a scheme of the insertion site in the genomic DNA of *C19* locus for the line from the SALK collection. Panel B and C: Electrophoresis gels of products from RT-PCR reactions. “wt”: cDNA from wild-type Columbia. “T-DNA”: cDNA from the line homozygous for the insertion in *C19* locus. Number of cycles for the PCR reactions are within parenthesis. Primers used to amplify cDNA of *C19* were designed downstream of the T-DNA insertion (B) or upstream of the T-DNA insertion (C). Plants were grown in LD and seedlings were collected after 10 days at ZT8, for RNA extraction.

Because the pattern of expression of this gene by *in situ* hybridisation in the inflorescence meristem (**Fig. 39**) has similarities with the one of *SOC1* and *FUL*, and because the product of this gene has been shown to interact with *AGAMOUS*, another MADS-box transcription factor, *c19* putative mutant was crossed with *soc1-2 ful-2* to obtain *c19 soc1 ful* triple mutant and the other mutant combinations. Flowering time has been scored in LD (**Fig. 41**).

When combined with the loss of function of *SOC1* and *FUL*, *c19* mutant adds a slight delay in flowering time, so that *c19 soc1 ful* is slightly later flowering than *soc ful* in terms of number of rosette leaves at bolting. Again, this delay is small, but it appears to be enhanced compared to the one between *c19* and wild-type. There were few plants to score in this population and the experiment will be repeated to confirm the difference in flowering time. Additionally, flowering time of double mutants *c19 soc1* and *c19 ful* will be scored and compared to the ones of *soc1* and *ful* single mutants, to test whether an effect on flowering is already visible in one of these combinations.

A possible redundant function of this gene with homologue genes could mask a clear effect of the loss of function of *C19*. Nevertheless, *PGIP2* and *PGIP1*, the closest paralogs to *C19*, are barely detected in the SAM based on our gene expression dataset. This would be in agreement with the role of these genes in pathogen response (Ferrari et al., 2006), therefore not related to flowering. A test was carried out with a probe for *PGIP2* by *in situ* hybridisation on apices, which did not show a clear signal at the SAM (**Fig. 39, I**).

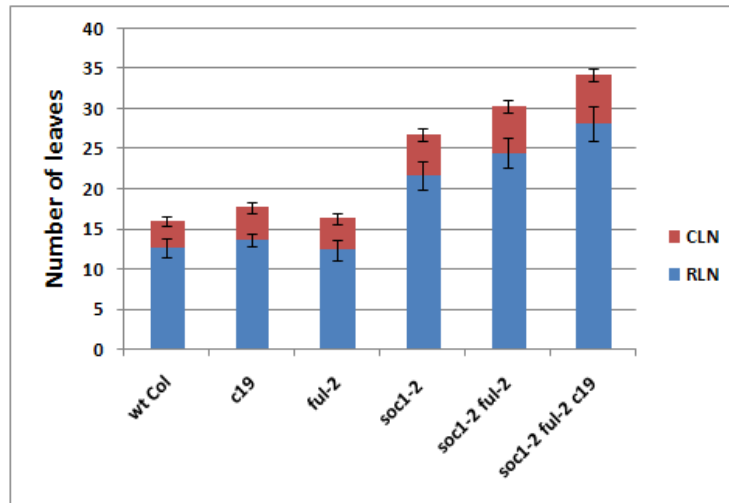


Fig. 41. Flowering times of Col wild-type and *soc1 ful* plants carrying *c19* T-DNA insertion. Flowering times were scored in LD. RLN: number of rosette leaves. CLN: number of cauline leaves.

4.7 Some bZIP transcription factors partially respond to *FT/TSF*

The candidate gene *C4* is annotated as a gene coding a bZIP transcription factor. Interestingly, the pattern of expression of this gene is very specific for the SAM. Upon shift to LD, its expression level increases, and it is visible not only in the central part of the SAM but also continues laterally toward the pro-vascular tissue (**Fig. 27** and **Fig. 42, A-C**). In *ft tsf* double mutants *C4* mRNA level does not show such an increase upon shift to LD, although there is a slight up-regulation (**Fig. 42, D-F**).

Another gene encoding a bZIP transcription factor, *FD*, is known to be important for the floral transition at the SAM, and it is also specifically expressed in this tissue. Therefore, *in situ* hybridisations were carried out in wild-type Col and *ft tsf* double mutant with a probe for *FD*. While in wild-type, as reported previously, there is an increase in expression of *FD* upon induction to LD (**Fig. 42, G-I**), in the double mutant the expression level of this gene remained almost constant (**Fig. 42, J-L**). It was previously shown that in the *ft* single mutant (in *Ler* ecotype) *FD* did not change its pattern compared to wild-type (Searle et al., 2006). It may be that *FT* and *TSF* redundantly contribute to up-regulation of *FD* at the SAM. However, the difference found between our experiment and the one in the *ft* mutant can be due to different experimental conditions, and to the different ecotype used.

Results

Taken together, these data suggest that some bZIP transcription factors are regulated in the meristem via *FT/TSF*.

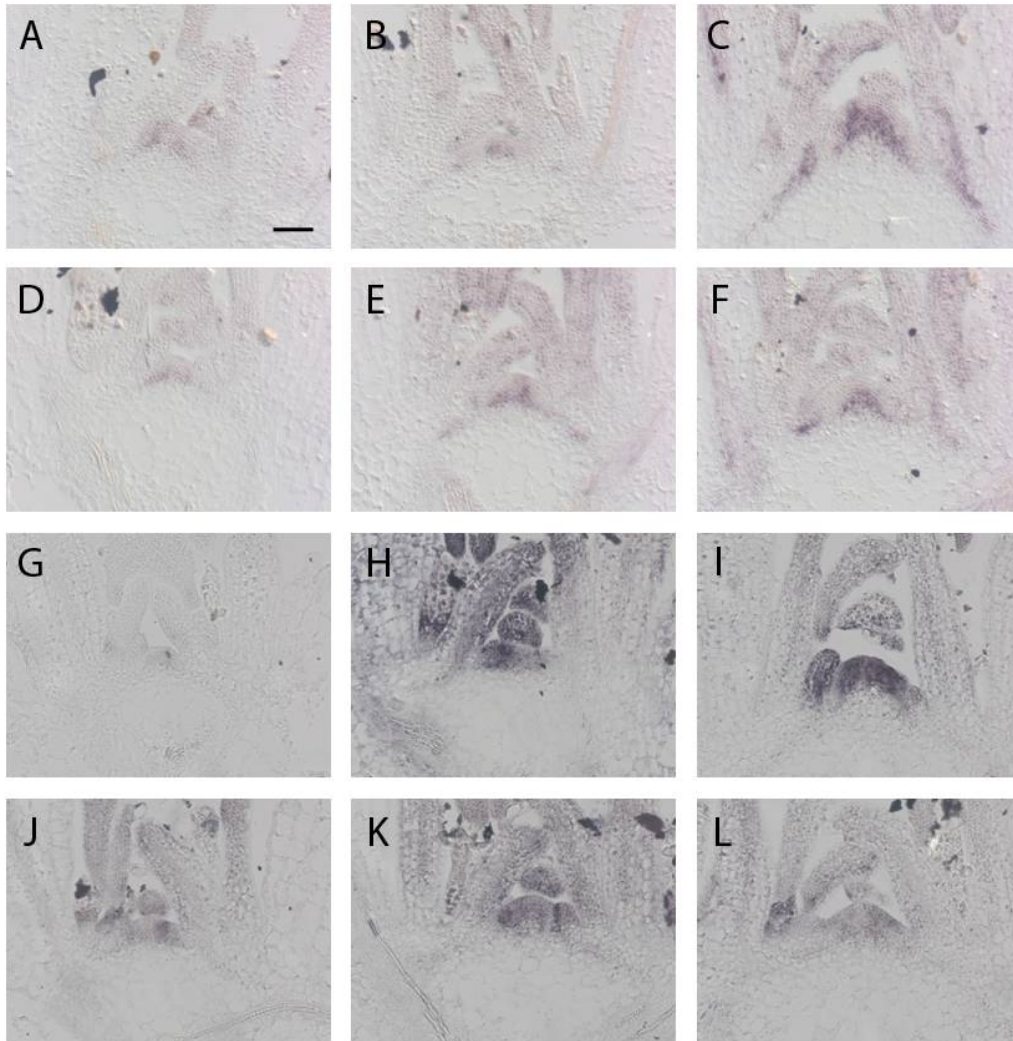


Fig. 42. Expression pattern of a bZIP candidate gene. *In situ* hybridisations were carried out on shoot apices with probes for *C4* (A-F) and *FD* (G-L). Apices were from wild-type Col (A, B, C, G, H, I) and *ft-10 tsf-1* (D, E, F, J, K, L). Plants were grown 2 weeks in SD and collected at +0LD (A, D, G, J), +1LD (B, E, H, K), and +3LD (C, F, I, L). Plants were collected at ZT8. Scale bar is 50 μ m.

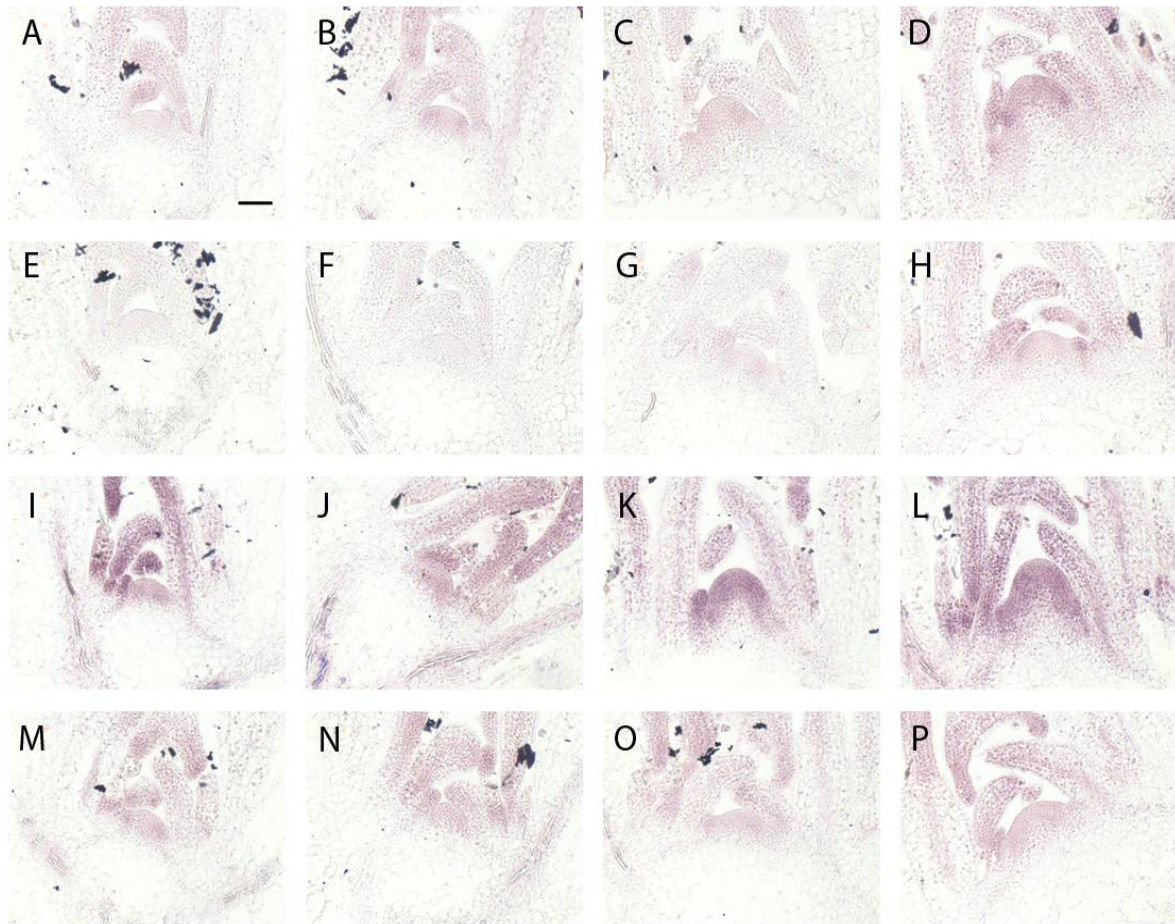


Fig. 43. *In situ* hybridisations with candidate genes. *In situ* hybridisations were carried out using probes for *C25* mRNA (A-H), or *C27* (I-P) on apices from wild-type Col (A-D, I-L) and *ft-10 tsf-1* (E-H, M-P). Plants were grown 2 weeks in SD and collected before induction at ZT8 as +0 LD (A, E, I, M), after +1 LD (B, F, J, N), after +3 LD (C, G, K, O), and after +5 LD (D, H, L, P) of induction in LD. Scale bar is 50 μ m.

4.8 Several genes are related to the growth of the meristem in response to *FT/TSF*

RNA probes for three genes from the series of candidate genes identified with the clustering approach (see previous sections) were tested again by *in situ* hybridisation in wild-type Col and *ft-10 tsf-1* double mutants: *C23* (described in the next section), *C25*, and *C27*. The time course was extended to +5LD for both genotypes. The expression patterns of *C25* and *C27* show some similarities. Indeed, upon shift they highly increase their expression progressively in LD, specifically at the SAM, in wild-type apices, while they show no or a very slight increase in the double mutant (Fig. 43). However, *C27* is already expressed in the whole apex before shift to LD, while *C25* is less expressed. As mentioned before, *C25* encodes for an uncoupling mitochondrial

protein (called PUMP1), while *C27* for a putative calcium-dependent protein kinase. Particularly, *C25* is involved in photosynthesis and the loss of function mutant is impaired in some of the processes related to photosynthesis (Sweetlove et al., 2006). We have shown already several genes tested from the lists of candidates increasing their expression, and many of those are involved in metabolic processes. This is also in strong agreement with our analysis for GO term enrichment on the up-regulated genes. Possibly many genes increase their expression upon shift to LD and then progressively during the LD induction, in relation to the marked growth of the meristem in this condition. In the case of *ft tsf*, this double mutant is impaired in the response to photoperiod, and its meristem does not grow as much as the wild-type one in response to LD, and thus shows no increase in the expression of those genes.

4.9 An unknown protein induced in the center of the SAM by *FT/TSF*

C23 showed an interesting pattern of expression, since its mRNA gives a very strong hybridisation signal only after +3LD of induction, in a specific region at the center of the SAM (see **Fig. 30**). This region seems to overlap with the one in which *WUSCHEL* is expressed (**Fig. 44, J, K**) (Schoof et al., 2000). *C23* probe was tested again by *in situ* hybridisation in wild-type Col and *ft-10 tsf-1* double mutants, in a time course extended to +5LD. This experiment confirmed that *C23* mRNA becomes strongly detectable at +3LD in wild-type (**Fig. 44, C, I**). At +5LD its expression is also very similar to +3LD, and additionally other regions, most probably axillary meristems forming at the flanks of the main shoot, show detectable expression (**Fig. 44, D**). Interestingly, in the double mutant no expression is detected, even after +5LD of induction (**Fig. 44, E-H**). This suggests that *C23* responds to a signal triggered by *FT/TSF*.

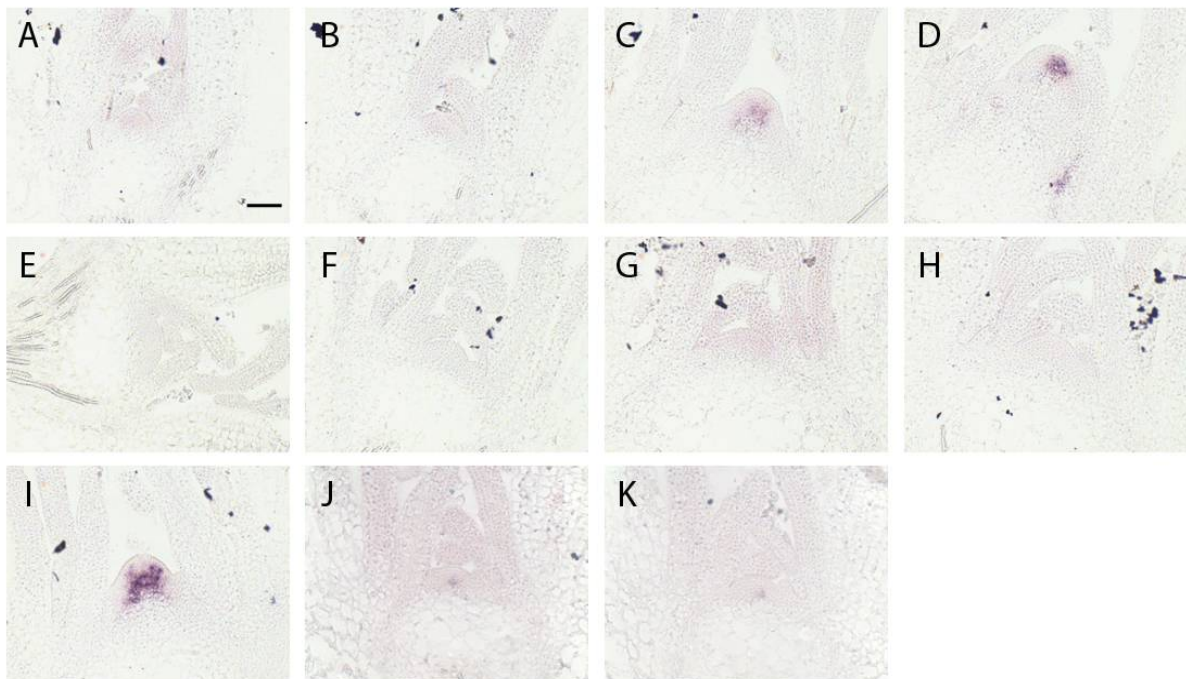


Fig. 44. *In situ* hybridisations with C23 candidate gene. *In situ* hybridisations were carried out using probes for *C23* mRNA (A-i), or *WUS* (J, K) on apices from wild-type Col (A-D, I-K) and *ft-10 tsf-1* (E-H). Plants were grown 2 weeks in SD and collected before induction at ZT8 as +0 LD (A, E), after +1 LD (B, F, J, K), after +3 LD (C, G, I), and after +5 LD (D, H) of induction in LD. D and I are pictures of the same plants in different sections. J and K are pictures of the same plants in different sections. Scale bar is 50 μ m.

5. The role of *SVP* in leaf and meristem and the control of flowering time

5.1 Loss of function of single floral promoter genes does not overcome the early flowering phenotype of *svp* mutants.

The first report of *SVP* was based on a mutant screen in which loss of function of this gene resulted in an early flowering phenotype (Hartmann et al., 2000). The *SVP* MADS-box transcription factor was therefore classified as a floral repressor. Later, it was proposed that *SVP* directly represses *FT* transcription (Lee et al., 2007b) and thereby prevents flowering. Because *FT* is transcribed in the leaf upon exposure to LD, *SVP* would then exert its function in the leaf. According to this hypothesis, mutations in *FT* should suppress the early flowering phenotype of *svp* mutants, but actually the effect of an *ft* mutation in a *svp ft* double mutant is very mild, and this was shown recently in Col (Li et al., 2008) and *Ler* (Fujiwara et al., 2008), although a previous report showed a larger effect (Lee et al., 2007b). This could be due to the use of different alleles for the mutants used by the different groups. I repeated these experiments with different and stronger alleles of the mutants. First of all, flowering time was scored for all the available mutants at the *SVP* locus, such as *svp-41*, *svp-31*, *svp-32* (in Col) and *svp-3* (in *Ler*), confirming that *svp-41* is the strongest allele in Col in terms of early flowering phenotype (**Fig. 45, A**). Then *svp-41* mutant was crossed with *ft-10* mutant, which carries the strongest loss of function allele for *FT* in Col, and this confirmed that *svp-41 ft-10* double mutants flower only slightly later than *svp-41* mutant (**Fig. 45, B**). This implies that there are other additional target genes regulated by *SVP*.

CO is a key gene in the induction of flowering in the leaf. Loss of function of *CO*, which causes very late flowering, does not have a strong effect in an *svp-41* mutant background (**Fig. 45, B**). The other plant tissue where *SVP* could have a role in controlling flowering in addition to the leaf is the shoot apical meristem (SAM). A suggestion that *SVP* could have a role outside of the leaf tissue comes from its expression pattern. Indeed *SVP* is also strongly expressed at the SAM, and its expression level in this tissue decreases upon floral transition (**Fig. 11**), raising the possibility of a role of *SVP* in blocking the floral transition at the meristem. *SOC1*, which induces flowering at the SAM, was also suggested to be target of *SVP* (Li et al., 2008). Nevertheless, loss of function of the *SOC1* gene in *soc1-2* background has a very mild effect of delaying flowering in the *svp-41* mutant, similar to the loss of function of *FT* (**Fig. 45, B**). Even a triple mutant *svp ft soc1*, although flowering later than wild-type, flowers earlier than *ft soc1* in *Ler* background (**Fig. 45, C**, and

Results

similarly Fujiwara et al., 2008), and remarkably earlier in Col background (Li et al., 2008). Therefore, the scenario is far more complex than SVP having a small number of known targets, and it is probably necessary to combine several mutations in genes promoting flowering in the *svp-41* mutant background to suppress its early flowering phenotype. Moreover, if *SVP* has a role not only in the leaf but also in the meristem, these two functions need to be clearly separated. Therefore, three parallel approaches were chosen: one is based on combining loss of function of *SVP* (in *svp-41* mutant background) with loss of function alleles of genes promoting flowering either in leaf or meristem; the second is performing expression analysis on specific genes in different mutant backgrounds; and the third is based on mis-expressing *SVP* in different tissues in the *svp-41* mutant background in order to study the direct effect of this gene on flowering in specific tissues.

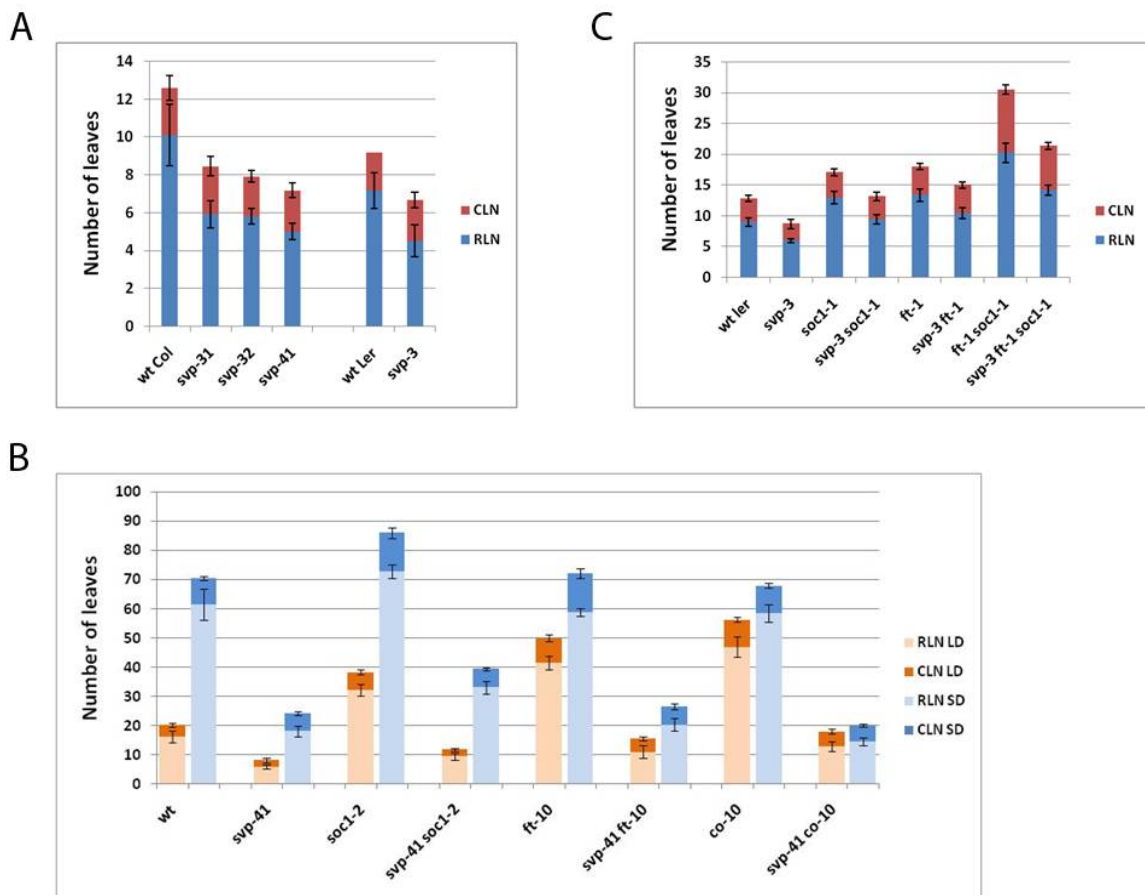


Fig. 45. Flowering times of plants carrying *svp* mutant alleles in Col or in combination with other mutations affecting flowering. Flowering time is scored as number of leaves. Col carrying different mutant alleles of *SVP* (A), *svp-41* in combination with *ft*, *soc1* or *co* in Columbia background (B) and *svp-3* in combination with *ft* and *soc1* in Landsberg *erecta* background (C). RLN: number of rosette leaves. CLN: number of cauline leaves.

5.2 *SVP* and the leaf: genetic and spatial interactions

5.2.1 Role of *SVP* in the leaf and its relationship to *FT* and *TSF*

As discussed before, *SVP* must have further targets in addition to *FT*. Particularly, if *SVP* has a role in repressing flowering in the leaf, an obvious candidate to test is *TSF*. This gene indeed shares many features with *FT*, as it is its closest homologue and it acts in part redundantly with *FT* (Michaels et al., 2005; Yamaguchi et al., 2005). It has been already reported that *FT* expression levels in *svp* mutants are higher than in wild-type (Lee et al., 2007b; Li et al., 2008). The levels of *FT* transcript were checked again by quantitative real-time PCR in the wild-type, *svp-41*, *co-10* and *co-10 svp-41* backgrounds using RNA from leaves collected from seedlings grown in LD condition for 12 days (**Fig. 46, A**). Then, also *TSF* transcript levels were measured (**Fig. 46, B**). In addition, a similar analysis was done for *SOCI*, because it is known that this gene is expressed in young leaves in addition to the shoot apical meristem (**Fig. 46, C**). In this case the levels of *SOCI* transcript were measured by quantitative real-time PCR in wild-type, *svp-41*, and *svp-41 ft-10* backgrounds, using RNA from leaves collected from 10 days-old seedlings grown in LD condition. In addition, the level of *FT* expression was measured by real-time PCR in meristems of wild-type and *svp* mutants grown in the same conditions, collecting apices enriched in SAM by manually removing as many leaves as possible, in order to check for the possibility of a direct effect in the meristem of *FT* up-regulation in *svp* mutants. Under these conditions, *FT* expression is barely detectable both in wild-type and *svp* apices (**Fig. 46, D**). This suggests that the up-regulation of *FT* in *svp* seedlings only occurs in the leaf tissue.

SOCI, *FT* and *TSF* show similar behavior in terms of their expression levels in the leaves (**Fig. 46**). In all cases, their expression decreases when genes promoting their expression are mutated: *FT* and *TSF* mRNAs decrease in *co* mutant background, *SOCI* mRNA decreases in *ft* mutant background. Moreover, their expression increases in *svp* mutants, compared to wild-type. In double mutants, where both the promoter gene and the repressor gene (*SVP*) are mutated, *FT*, *TSF*, and *SOCI* mRNAs have an intermediate level between wild-type Col and the *svp-41* mutant. These data are in agreement with the flowering time data of the corresponding genotypes.

Nevertheless, this expression analysis takes into account only one particular time during the day (around ZT8), and does not reflect the complex diurnal expression patterns that all these genes have and therefore describes only a simplified scenario of a more complex situation.

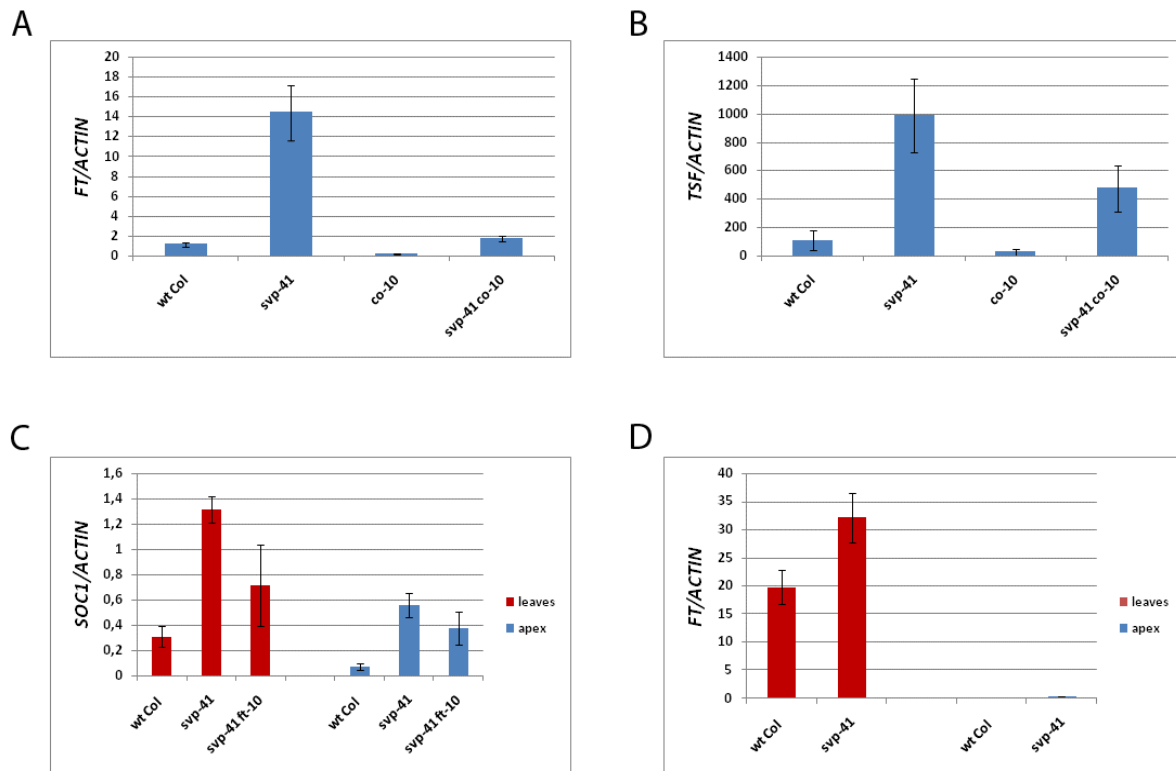
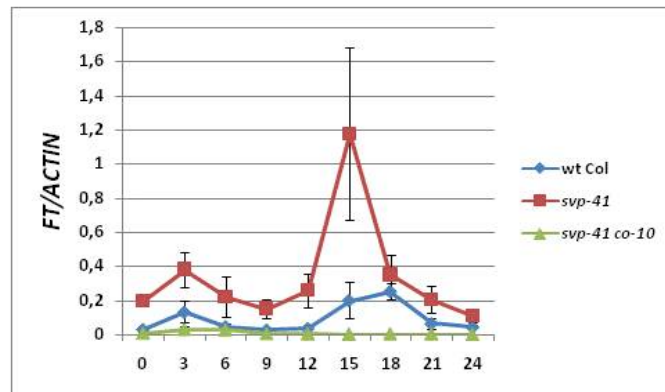


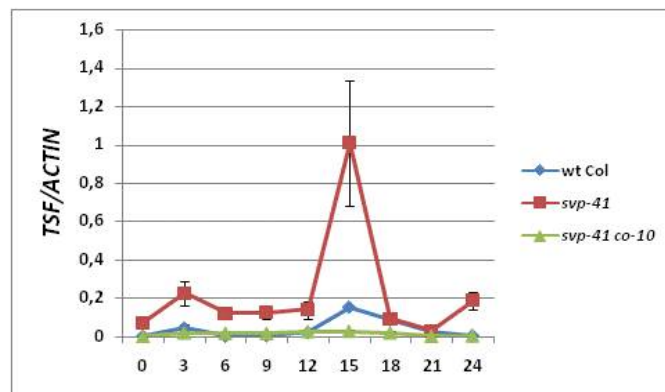
Fig. 46. Quantitative real time PCR of mRNA of genes whose expression is altered by *SVP* in different genetic backgrounds. Panel A and B: seedlings were grown in LD and leaves were collected after 12 days. Panel C and D: Seedlings were grown in LD and leaves or aerial parts enriched in meristems (apex) were collected after 10 days. All samples were collected at ZT8.

To have a more precise description of the expression patterns of *FT* and *TSF* in the *svp* background, the diurnal expression patterns of these two genes during a 24 hours cycle under LD was followed in wild-type, *svp-41*, and *svp-41 co-2*, with a resolution of three hours (**Fig. 47, A, B**). *FT* and *TSF* show their expected diurnal expression pattern, with a peak at the end of the light period in LD, and another smaller peak just after dawn (Suárez-López et al., 2001; Yamaguchi et al., 2005). This pattern is conserved also in *svp* background, but the level of expression is higher, especially for the peak at ZT15 (for *FT* and *TSF*) and the lower peak at ZT3. Another two independent experiments were performed in the same conditions and they show essentially the same results (data not shown).

A



B



C

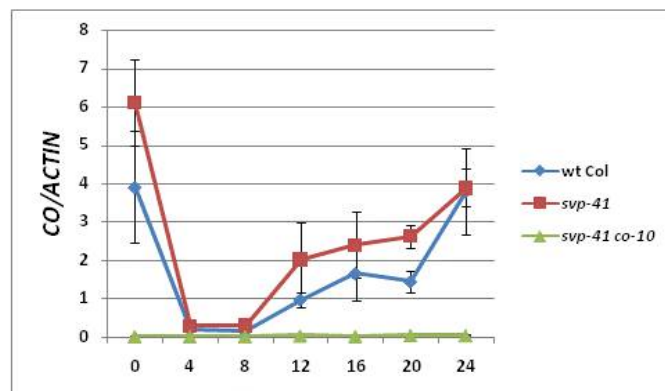


Fig. 47. Diurnal patterns of *FT*, *TSF* and *CO* mRNA levels in presence or absence of a functional *SVP* allele, measured by quantitative real time PCR. Seedlings were grown in LD for 10 days and then collected during the following 24 hours. Aerial parts of the plants were used for RNA extraction. Samples at ZT8 were collected in light, samples at ZT24 were collected in dark. Samples at ZT16 (for panel A and B) were collected in light.

Results

In one of these experiments, in which samples were collected at the resolution of 4 hours, *CO* expression pattern was also tested. No significant difference in the pattern of *CO* expression was found between wild-type and *svp* (**Fig. 47, C**). Therefore, the up-regulation of both *FT* and *TSF* is not due to a higher level of *CO* mRNA in the *svp* background. In addition, *FT* and *TSF* expression in the *svp co* background is very low (**Fig. 47, A, B**), without the characteristic peaks, indicating that *CO* is needed for the up-regulation of *FT* and *TSF* in the *svp* mutant.

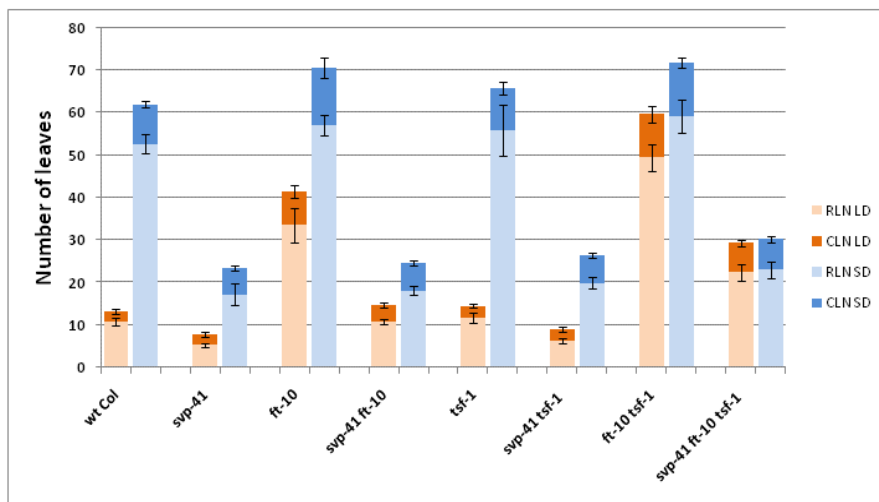


Fig. 48. Flowering times of plants carrying loss of function alleles of *SVP*, *FT*, or *TSF*. Flowering time was scored as number of leaves both in long-days (LD) and short-days (SD). RLN: number of rosette leaves. CLN: number of cauline leaves.

All these expression data suggest that *SVP* represses not only *FT* but also *TSF* in the leaf.

In order to further test this hypothesis, *svp-41* was crossed with *ft-10 tsf-1* double mutant and *svp-41 ft-10 tsf-1* triple mutants were obtained, together with all the other double mutant combinations. Flowering time was scored both in LD and SD conditions (**Fig. 48**). The effect of the *tsf* mutation in *svp* background is minimal (similar to *ft* mutation), while *ft tsf* double mutant combinations cause a larger delay in flowering time in the *svp* background. Nevertheless, the triple mutant still flowers much earlier than the double mutant *ft tsf*, so the early flowering effect of *svp* is still very strong.

Taken together, these results strongly suggest that *SVP* has a role in repressing the expression of *FT* and *TSF* in the leaf, but the effect of *SVP* cannot be explained only by repressing these two genes in the leaf. Therefore since activation of *FT* and *TSF* are the last known events in the leaf there is likely an additional effect that occurs at the apical meristem. Indeed, the triple mutant is

photoperiodic insensitive, and shows a flowering time similar to that of the *svp* mutant in SD, which suggests that the early flowering phenotype of *svp ft tsf* would be dependent on genes that are downstream of *FT* and *TSF*, such as *SOC1*.

5.2.2 *SOC1* in relation to *SVP*, *FT* and *TSF*.

Because the increase of expression of *SOC1* in *svp* background can be due either to a direct effect of the loss of function of *SVP* or to an indirect effect of the up-regulation of *FT*, or to a combination of both, the different contributions on *SOC1* expression need to be separated using different genetic backgrounds. Therefore the pattern of expression of *SOC1* was investigated in the *svp ft tsf* triple mutants and compared to that in wild-type, *svp*, and *ft tsf*.

In situ hybridisations on wild-type Col, as described previously, show that when plants are shifted from SD to LD *SOC1* expression in the meristem is dramatically increased, while *SVP* expression follows the opposite trend (see **Fig. 11**). The expression of these two genes was followed again by *in situ* hybridisation on wild-type Col during a time course in LD. Under these conditions *SVP* starts to decrease in expression in the inflorescence meristem (**Fig. 49, A, B**) and *SOC1* starts to increase at the time of the floral transition (**Fig. 49, D, E**). At a later stage, *SVP* is also expressed in the floral meristems arising from the inflorescence, where *SOC1* is excluded (**Fig. 49, C, F**). The two genes thus have an opposite pattern of expression.

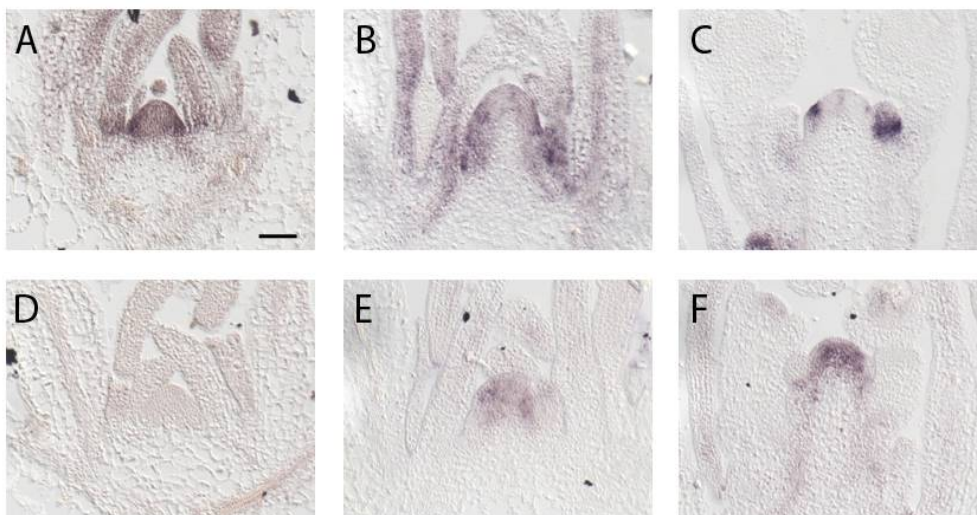


Fig. 49. *SVP* and *SOC1* mRNA expression patterns in wild-type Col plants grown in LD. *In situ* hybridisations were performed on apices using RNA probes for *SVP* (A, B, C) or *SOC1* (C, D, E). Plants were grown in LD for 10 days (A, D), 12 days (B, E) and 15 days (C, E) and harvested at ZT8. Scale bar is 50 μ m.

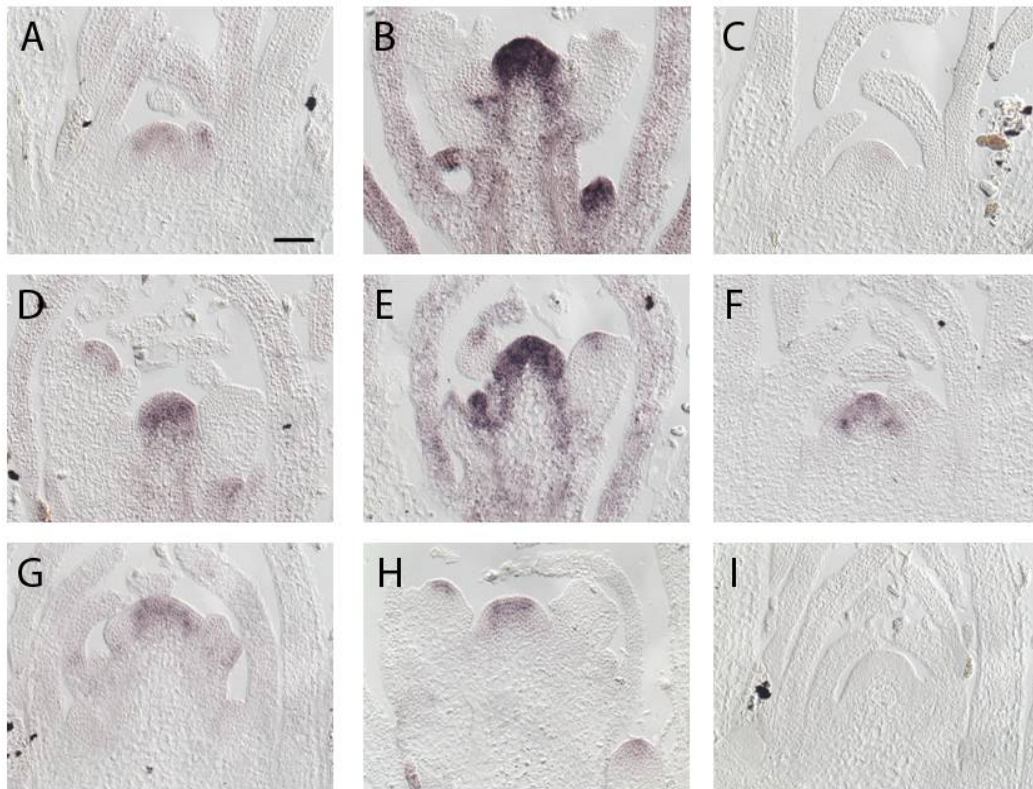


Fig. 50. Expression of *SOCI* mRNA in plants carrying loss of function alleles of *SVP*, *FT* or *TSF*. *In situ* hybridisations were performed on apices using RNA probes for *SOCI*. Wild-type Col (A, D), *svp-41* (B, E), *svp-41 ft-10 tsf-1* (C, F, G, H) and *ft-10 tsf-1* (I) were compared. Plants were grown in LD for 12 days (A, B, C), 15 days (D, E, F), 17 days (G), 20 days (H), and 24 days (I), and harvested at ZT8. Scale bar is 50 μ m.

Anyway, only from the expression pattern, it is not possible to conclude whether there is a direct interaction between *SVP* and *SOCI*, since the increase in *SOCI* expression in the meristem could be an indirect effect caused by *FT* up-regulation in the leaves. It was already observed, both by *in situ* hybridisation and real-time-PCR (see above), that *SOCI* mRNA levels in *svp ft* double mutants are lower than in *svp* mutants, but even in the absence of *FT* they were higher than in wild-type (**Fig. 46, C**). Because this remaining activation could be due to the presence of *TSF*, *svp ft tsf* were tested in comparison with *svp*, wild-type, and *ft tsf* by *in situ* hybridization on a time course in LD (**Fig. 50**). This experiment showed that *SOCI* is expressed in *svp ft tsf* with a delay (**Fig. 50, C, F, G, H**) in respect to wild-type (**Fig. 37, A, D**), and with less intensity than in *svp* single mutants (**Fig. 50, B, E**). Nevertheless in these triple mutants *SOCI* mRNA is still clearly detectable at the SAM, and increases progressively during the time course. On the contrary in *ft tsf* double mutants no *SOCI*

Results

mRNA is detected even later in the time course at 24 LD (**Fig. 50, I**), but it starts to be detectable at 30 LD (**Fig. 51, I**).

The results from *in situ* hybridisation match with the flowering time data of the corresponding genotypes, suggesting that the cause of the residual early flowering of the *svp ft tsf* triple mutants compared to *ft tsf* both in LD and SD is due to *SOCI* expression at the SAM. The *svp* single mutants flower even earlier in LD than the triple mutant likely because of the additional contribution of *FT* and *TSF*.

All these results demonstrate that *SOCI* is still up-regulated in *svp* mutant background even in the absence of both *FT* and *TSF* function and the photoperiodic cascade is not needed to activate *SOCI* in absence of *SVP* repression.

The down-regulation of *SVP* during the floral transition, coinciding with the up-regulation of *SOCI*, indicates the presence of a mechanism that represses specifically *SVP*. Whether this mechanism is based on a response to photoperiod or on developmental changes at the SAM is still not known. In order to get some insight into the mechanism repressing *SVP*, the expression of this gene was followed by *in situ* hybridisation comparing apices from wild-type Col with *ft tsf* double mutants (**Fig. 51**). In the case of plants grown 2 weeks in SD and then shifted to LD, *SVP* mRNA level decreases during the first 3 LD of the shift (**Fig. 11** and **Fig. 51, A, B**). This decrease does not occur in *ft tsf* double mutants (**Fig. 51, C**), and at the third LD the pattern of expression of *SVP* resembles the one before the shift to LD. However, this experiment focuses on a short time after the shift to LD, and since *ft tsf* double mutants are not responsive to LD, it could be that *SVP* does not decrease because these plants are still completely vegetative rather than because *FT/TSF* are upstream of *SVP*. Another experiment in which plants were grown directly in LD shows that while *SVP* clearly decreases in the center of the inflorescence meristem in wild-type Col between 10 and 15 days after germination (**Fig. 51, D-F**), there is still some remaining expression in the center of the *ft tsf* inflorescence meristem between 24 and 30 LD (**Fig. 51, G, H**), even when these mutants start to flower, and when *SOCI* is still very weak (**Fig. 51, I**). However, *SVP* signal in this case is not very strong, and weaker than in the developing floral buds. Overall the data suggest that *SVP* repression does not occur as strongly in the absence of *FT/TSF*, however it is still difficult to determine how direct this effect is and there is clearly some down-regulation of *SVP* even in the absence of *FT/TSF*.

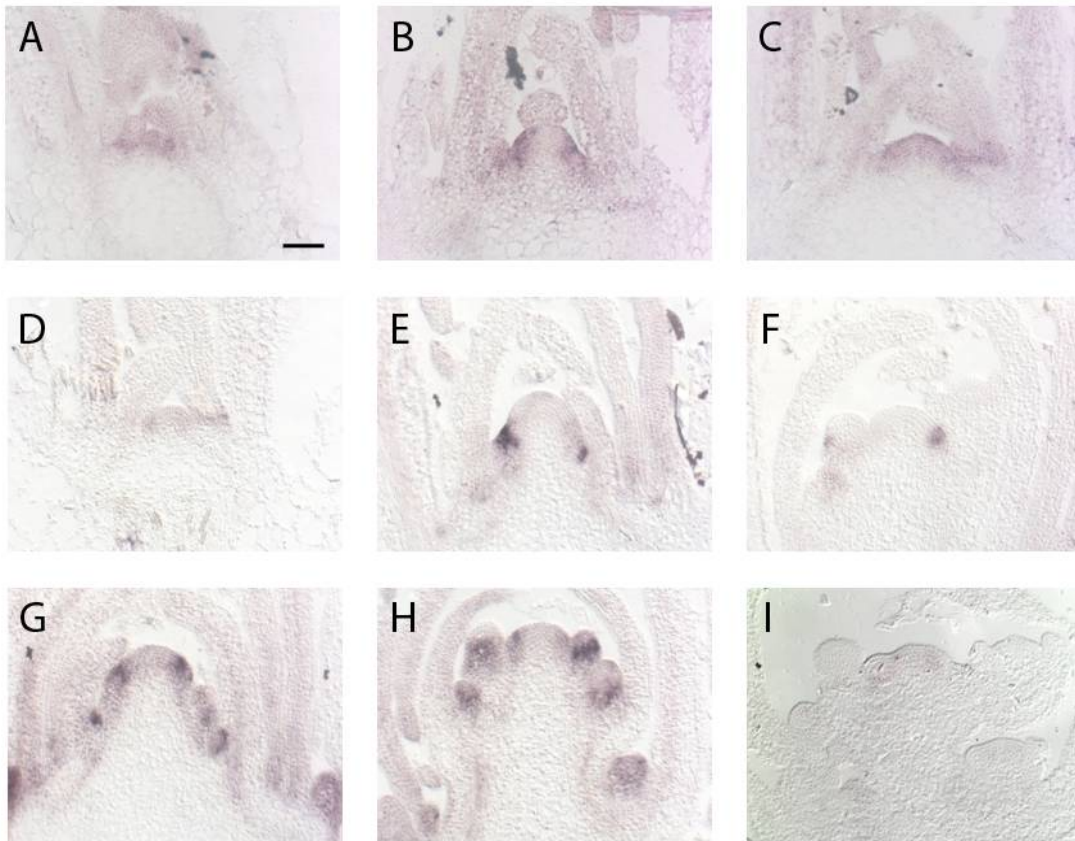


Fig. 51. Expression patterns of *SVP* and *SOC1* mRNAs in wild-type and *ft tsf* double mutants. *In situ* hybridisations were performed on apices using RNA probes for *SVP* (A-H) and *SOC1* (I). Wild-type Col plants were grown for 2 weeks in SD and collected before induction (A) and after +3 LD (B), and *ft-10 tsf-1* was also collected after +3 LD (C). Wild-type Col plants were grown in LD for 10 days (D), 12 days (E) and 15 days (F), while *ft-10 tsf-1* plants were grown in LD for 24 days (G) and 30 days (H, I). All the samples were harvested at ZT8. Scale bar is 50 μ m.

5.2.3 Mis-expression of *SVP* in the leaf vasculature

In order to monitor the effect of mis-expressing *SVP* in the leaf, the gene was specifically expressed in the vascular tissue of *svp-41* mutant using a heterologous promoter. A *SUC2::SVP* construct, which uses the *SUC2* promoter to specifically express the gene in the companion cells of the phloem (Stadler and Sauer, 1996), was constructed and introduced into *svp-41* using *Agrobacterium*. In **Fig. 52**, flowering times under LD and SD of 9 independent lines transformed with this construct are shown. There is some variability in the flowering time of those lines, but most of them flower slightly later than the *svp* mutant, while a few of the strongest ones flower at a similar time to wild-type Col under LD (**Fig. 52, A**). *SUC2::SVP* had a weaker effect under SD and most of the transgenic lines flowered at a similar time to *svp-41* (**Fig. 52, B**). The effect of the mis-

Results

expression is then not strong, especially if it is compared with the *35S::SVP* line, which over-expresses the gene in every tissue and causes markedly late flowering (Fig. 52, A, B).

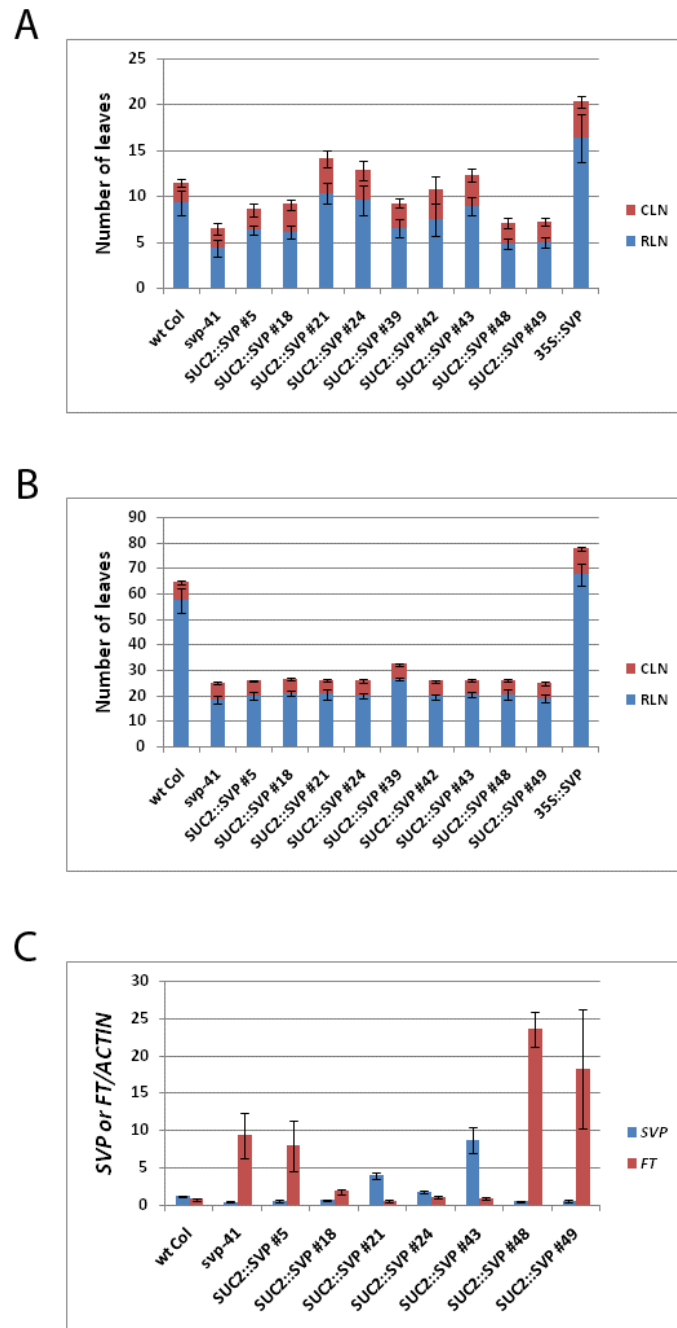


Fig. 52. Effect of mis-expression of *SVP* in the leaves. Flowering times of *SUC2::SVP* mis-expressing lines (in *svp-41* background) were scored in LD (Panel A) and SD (Panel B). *SVP* and *FT* mRNA levels were measured by quantitative real time PCR (Panel C) in the same mis-expressing lines. The mRNAs of the two genes were measured in two separate reactions and plotted in the same graph. Seedlings were grown in LD and collected after 10 days at ZT8 for RNA extraction.

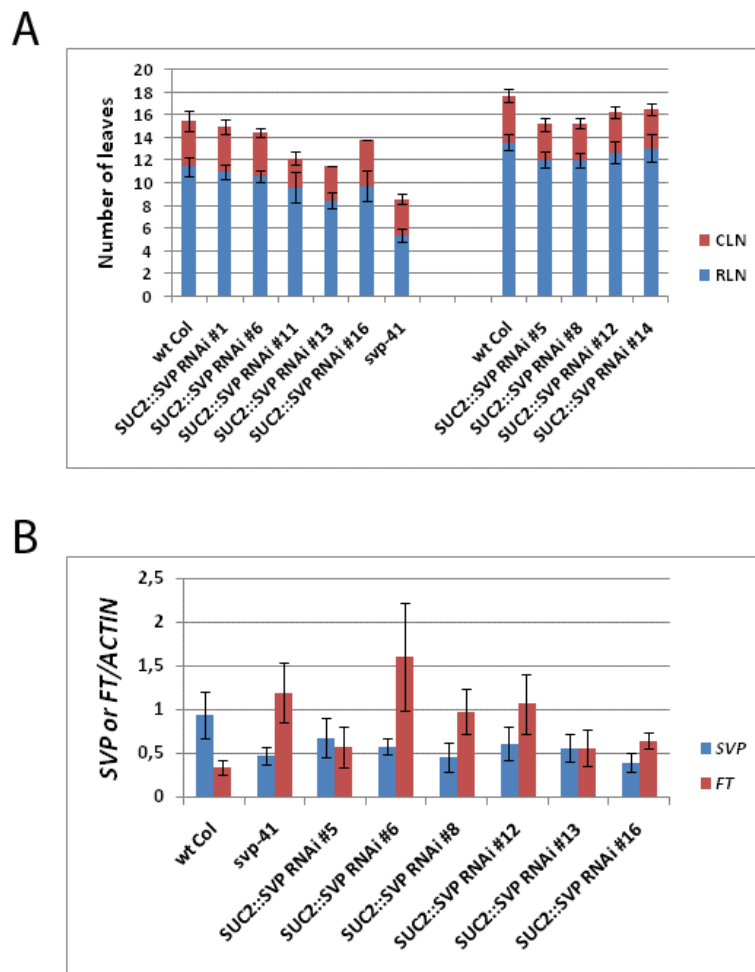


Fig. 53. Effect of reducing *SVP* expression in the leaves. Flowering time of *SUC2::SVP* dsRNAi lines (in wild-type Col background) was scored in LD (Panel A). *SVP* and *FT* mRNA levels were measured by quantitative real time PCR (Panel B) in the same lines as in A. The two mRNAs were measured in two separate reactions and plotted in the same graph. Seedlings were grown in LD for 10 days and leaves were collected at ZT15 for RNA extraction.

Level of expression of *SVP* and *FT* has been checked under LD in some of these transformed lines (**Fig. 52, C**). *SVP* mRNA levels are higher in the lines that show later flowering (e.g. lines 21 and 43), suggesting a direct effect of the mis-expression of *SVP* on flowering time. *FT* levels are generally higher in the earlier flowering lines, where the *SVP* levels are lower, confirming the inverse correlation between *SVP* and *FT* expression in the leaf tissue, with only line 39 being an exception to this rule. In general, the effect of *SUC2::SVP* on flowering was more pronounced in LD (**Fig. 52, A**), while in SD the effect is milder and very similar among all the independent lines (**Fig. 52, B**), which is also consistent with a direct effect on *FT* expression.

The effect of decreasing the level of *SVP* gene expression only in leaf vasculature was also

monitored using RNA interference (dsRNAi) constructs targeting *SVP* driven by the *SUC2* promoter and transformed into wild-type Col. Nine independent transgenic lines were identified and some showed early flowering compared to wild-type in LD (**Fig. 53**) and SD (data not shown), but none were as early flowering as *svp-41*. *SVP* and *FT* mRNA levels in leaves were measured from these plants, and again a negative correlation between the two gene products was found, although less clear than in the case of the *SUC2::SVP* mis-expressing lines and only in some lines.

Therefore, the effect of increasing or decreasing *SVP* in the leaves through transgenic approaches results in a direct effect on *FT* expression and on flowering time. However, it suggests that *SVP* does not only act in the vascular tissue to repress *FT*. These results are in agreement with genetic data shown in the previous sections.

5.3. *SVP* and the meristem: genetic and spatial interactions

5.3.1 Role of *SVP* in the SAM and relation to *SOC1* and *FUL*

To explore the possibility that *SVP* also has a role in repressing flowering in the meristem, the effect of the *svp* mutation on expression of genes that act in the SAM to regulate flowering was also examined.

As previously indicated, *SOC1* has been already reported to be regulated by *SVP* (Li et al., 2008). A gene that shares some features with *SOC1* is *FRUITFULL* (*FUL*). Both genes have been shown to increase at the SAM during the floral transition, around the time at which *SVP* is down-regulated. Moreover, redundant functions of these two genes were demonstrated by studying *soc1 ful* double mutants (Melzer et al., 2008).

The expression of *SOC1* and *FUL* mRNAs were followed by *in situ* hybridisation on a time course in LD. Wild-type and *svp-41* plants grown for 8-10-12-14 LD were collected at ZT3 and hybridised with RNA probes (**Fig. 54**). Both *SOC1* and *FUL* moderately increase in expression in wild-type Col during the time course, while they show a marked increase in expression in *svp* mutants for the corresponding time points. Because the mutants were already flowering, compared to wild-type that were still vegetative, and this increase in *SOC1* and *FUL* expression could be indirect due to an increase of the *FT* levels in the *svp* background, the level of *SOC1* and *FUL* were compared also in the *svp ft* double mutant, which flowers later and lacks an active *FT*. Nevertheless, even in this background the expression of *SOC1* and *FUL* is higher than in wild-type (intermediate between wild-type and *svp* mutant), suggesting also a more direct effect of *SVP* on these two genes that is not mediated by *FT*. On the same genotypes, real time PCR was performed on RNA extracted from

Results

apices (apices enriched in SAM removing older leaves) of seedlings grown under LD condition for 10 days, and the level of *SOC1* mRNA was measured. This independent experiment demonstrated the same trend as the *in situ* hybridisation, confirming a higher expression of *SOC1* mRNA in *svp* compared to wild-type, and an intermediate level in the *svp ft* double mutant (see **Fig. 46, C**).

In order to test the effect of *SVP* on *SOC1* and *FUL* gene expression in the meristem and to investigate the interaction among these MADS-box genes, crosses were done to obtain an *svp soc1 ful* triple mutant and all the combinations of the loss of function alleles of these genes, both in Col and *Ler* ecotypes. Double and triple mutants have been obtained and flowering time has been scored in LD and SD conditions for the Col genotypes (**Fig. 55**).

In terms of flowering time, *soc1-2 ful-2* double mutants flower as late as the *soc1-2* single mutant in LD, therefore with a moderate late flowering phenotype, while in SD they flower extremely late (around 80 rosette leaves and 20 cauline leaves). For most of the individuals the number of cauline leaves in SD could not be scored, since in that condition the plants grow in a very bushy and compact architecture and do not extend the main stem enough before they die. They also show an additional unusual phenotype. When *soc1 ful* double mutants grow in LD, after they have already flowered and very late in development they show a sort of “reversion” to vegetative development. Once mature siliques are formed, instead of dying the plants start another vegetative phase on top of the main apex of the plant (**Fig. 56**), they flower again and repeat this cycle several times. The effect was also recently independently shown by another group (Melzer et al., 2008).

The triple mutant *svp soc1 ful* still flowers earlier than the *soc1 ful* double mutant. Combining *soc1* with *ful* mutation in *svp* background slightly delays flowering time in comparison with *svp soc1* and *svp ful* double mutants. Therefore, when combined with *soc1 ful*, the *svp* mutation still confers an early flowering phenotype both in LD and SD.

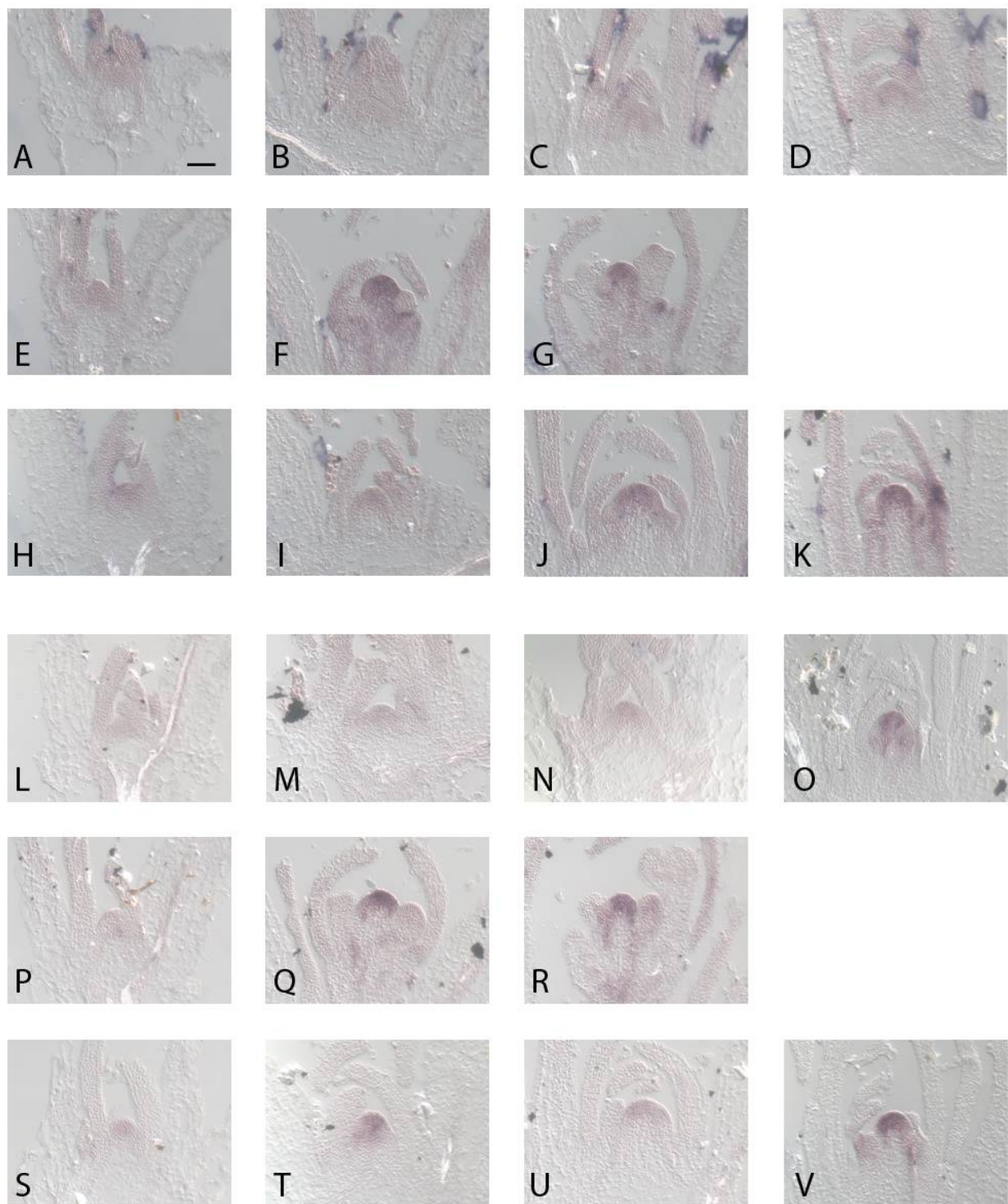


Fig. 54. Expression of *SOCI* and *FUL* mRNA during floral transition in presence or absence of a functional *SVP* allele. *In situ* hybridisation on a time course in LD using probes for *SOCI* (Panels A-K) and *FUL* (Panels L-V) mRNA. Wild-type Col (A-D, L-O) is compared to *svp-41* (E-G, P-R) and *svp-41 ft-10* (H-K, S-V). Plants were grown in LD for 8 days (A, E, H, L, P, S), 10 days (B, F, I, M, Q, T), 12 days (C, G, J, N, R, U) and 14 days (D, K, O, V). All the samples were harvested at ZT3. Scale bar is 50 μ m.

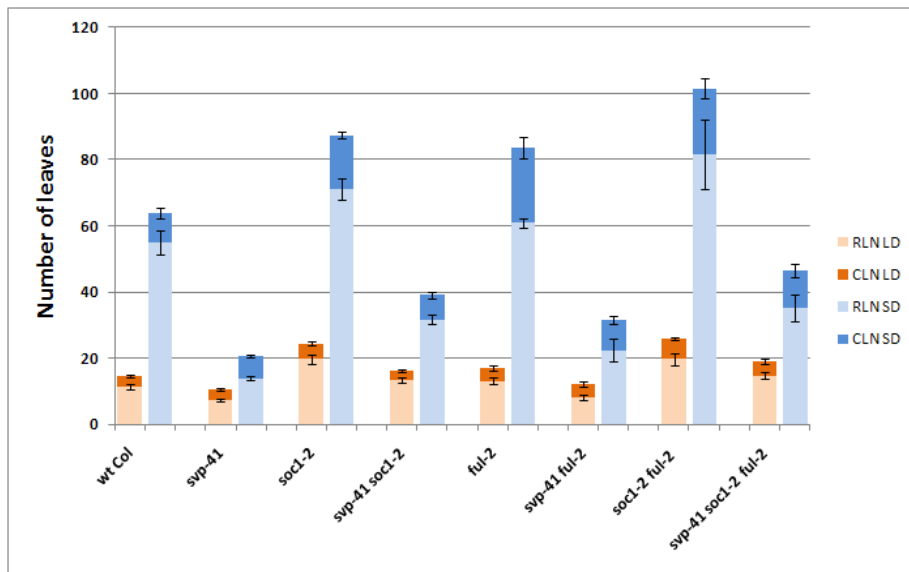


Fig. 55. Flowering times of plants carrying loss of function alleles of *SVP*, *SOC1* or *FUL*. Flowering time was scored as number of leaves both in long-days (LD) and short-days (SD). RLN: number of rosette leaves. CLN: number of cauline leaves.

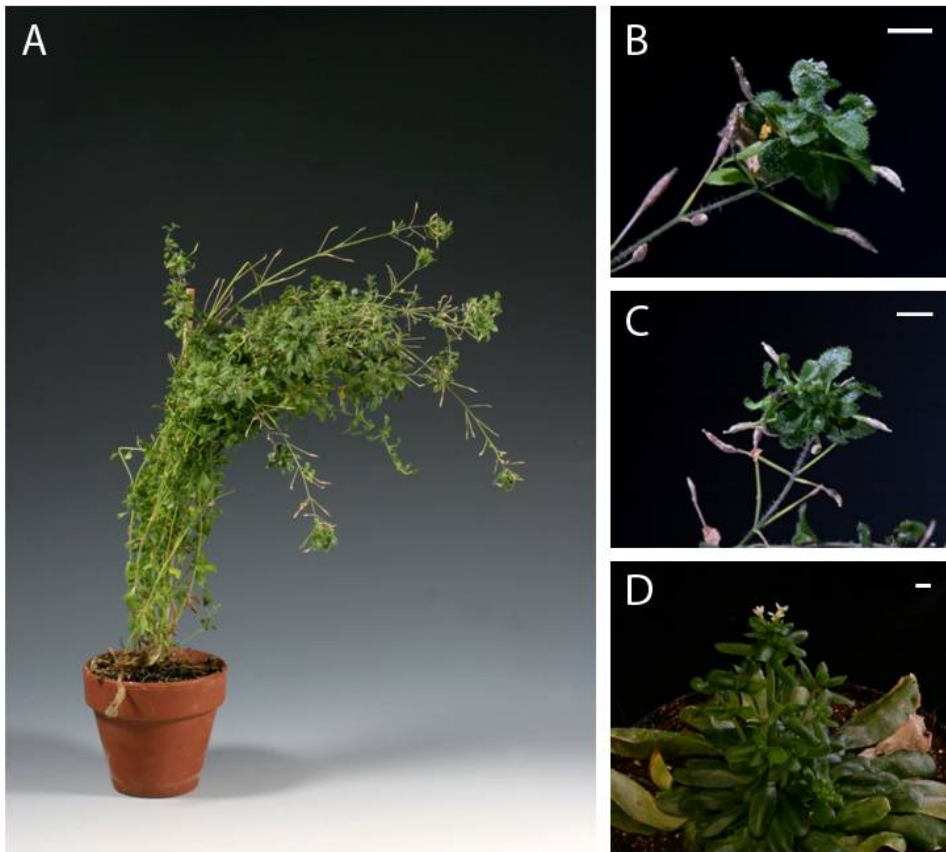


Fig. 56. Phenotype of the *soc1-2 ful-2* double mutant. Plants were grown in LD (A, B, C) or SD (D). A: general view of the plant architecture after flowering. B and C: detailed view of new vegetative shoots grown on the inflorescences after formation of mature siliques. D: bushy architecture of the double mutants grown under continuous SD. Wild-type Col did not show any of these phenotypes under the same growth conditions (data not shown). Scale bar is 5 mm.

These data indicate that as for *FT* and *TSF* in the leaf, *SVP* represses expression of both *SOC1* and *FUL* in the meristem, but the effect of *SVP* cannot be explained only by the repression of these genes. This result complements our previous results of the role of *SVP* in the leaf.

In addition, it was observed that the *svp* mutation suppresses the “reversion” phenotype of the *soc1 ful* double mutant. Thus in a *soc1 ful* double mutant *SVP* must have an important function in facilitating the reversion to vegetative growth observed in these plants.

5.3.2 Mis-expression of *SVP* in the meristem

The approach of mis-expressing or knocking down *SVP* in a tissue-specific manner, as seen above for the leaf, was also followed to assess the function of *SVP* in the meristem. The *KNAT1* promoter can be used to express a gene in the SAM (Lincoln et al., 1994). *KNAT1::SVP* constructs were

Results

introduced into *svp-41* mutants and flowering time of 7 independent lines was scored both in LD and SD (Fig. 57). Most of these lines, similar to mis-expression with *SUC2* promoter, show a slightly later flowering compared to *svp-41* under LD, which does not fully complement the loss of function of *SVP*. In this case, the effect of *KNATI::SVP* on flowering in SD is stronger than the effect of *SUC2::SVP* (see above), consistent with a role of *SVP* in repressing genes at the meristem such as *SOCI*, which has a major role in floral induction.

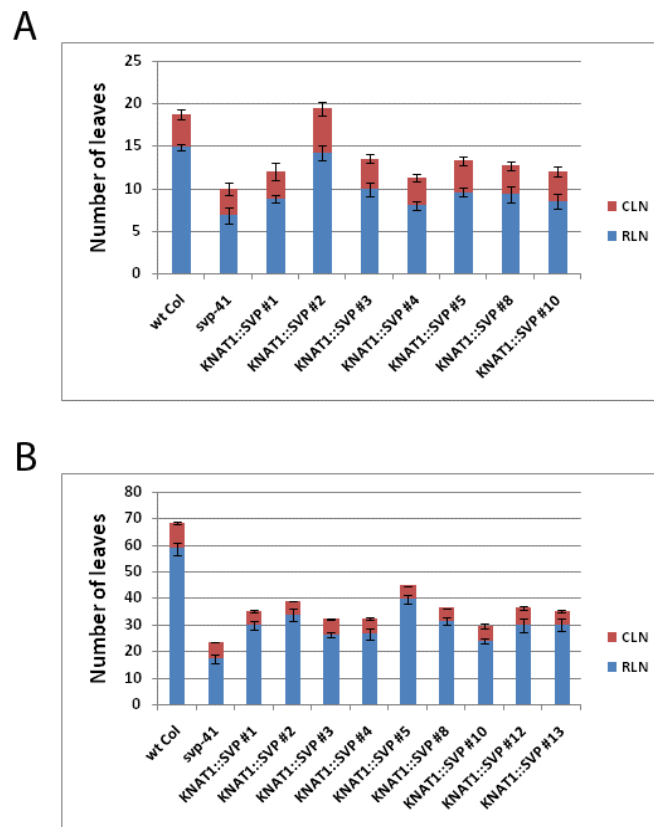


Fig. 57. Effect of mis-expression of *SVP* in the shoot apical meristem. Flowering time of *KNATI::SVP* mis-expression lines (in *svp-41* background) was scored in LD (Panel A) and SD (Panel B).

Interestingly, most of the *KNATI::SVP* lines show an additional floral phenotype. A variable number of flowers, depending on the line and on the growth condition, have additional organs, such as 5-6 sepals, and 5-6-7-8 petals. An example is given in Fig. 58 for line 5, which shows the strongest floral phenotype and the latest flowering in SD.

Because *KNATI* should be expressed only in the SAM (Lincoln et al., 1994), a floral phenotype was not initially expected. However, although *KNATI* transcript was not detected in sepals, petals and

Results

stamens, it was detected in cells encircling the base of the floral primordia (Lincoln et al., 1994). It may be that this effect is caused by a deregulation of the *KNATI* promoter itself in the *svp* mutant background, which would lead *KNATI::SVP* to be expressed in the floral meristem causing floral abnormalities. The expression of *SVP* was followed by *in situ* hybridisation comparing wild-type Col, *svp-41* and most of the *KNATI::SVP* lines (**Fig. 59**). Plants were grown in LD for 10 days and collected at ZT8. Wild-type apices show the typical strong expression of *SVP* in the SAM before floral transition (**Fig. 59, A**), while *svp-41* mutants are already flowering and show a residual weak expression of *SVP* transcript at the floral primordia (**Fig. 59, B**). This signal is probably caused by the fact that this mutant allele is generated by a transposon and part of the coding sequence could be still transcribed, although not functional. The *KNATI::SVP* lines are in different developmental stages, from vegetative (for example **Fig. 59, C, D, G**) to a flowering stage very similar to the one of *svp* mutants (**Fig. 59, F, I**). For most of the lines, the situation depicted in the *in situ* hybridisations correlates with the corresponding flowering time of these lines, especially for the data in SD. Line 5 is the only one with a convincing strong expression of *SVP* at the SAM, while the others mainly show expression near or on the floral primordia. It is not then clear whether this expression is caused by *KNATI* promoter in the SAM, by the deregulation of *KNATI* in the flowers, or if this is the residual expression of *SVP* that is present in the *svp-41* background.



Fig. 58. Effect on the flowers of mis-expression of *SVP* by *KNATI::SVP*. Examples from *KNATI::SVP* (in *svp-41*) line #5 are shown. Flowers with 5 petals (D), 6 petals (E, F), and 7 petals (A, B, C) are shown. Scale bar is 3 mm.

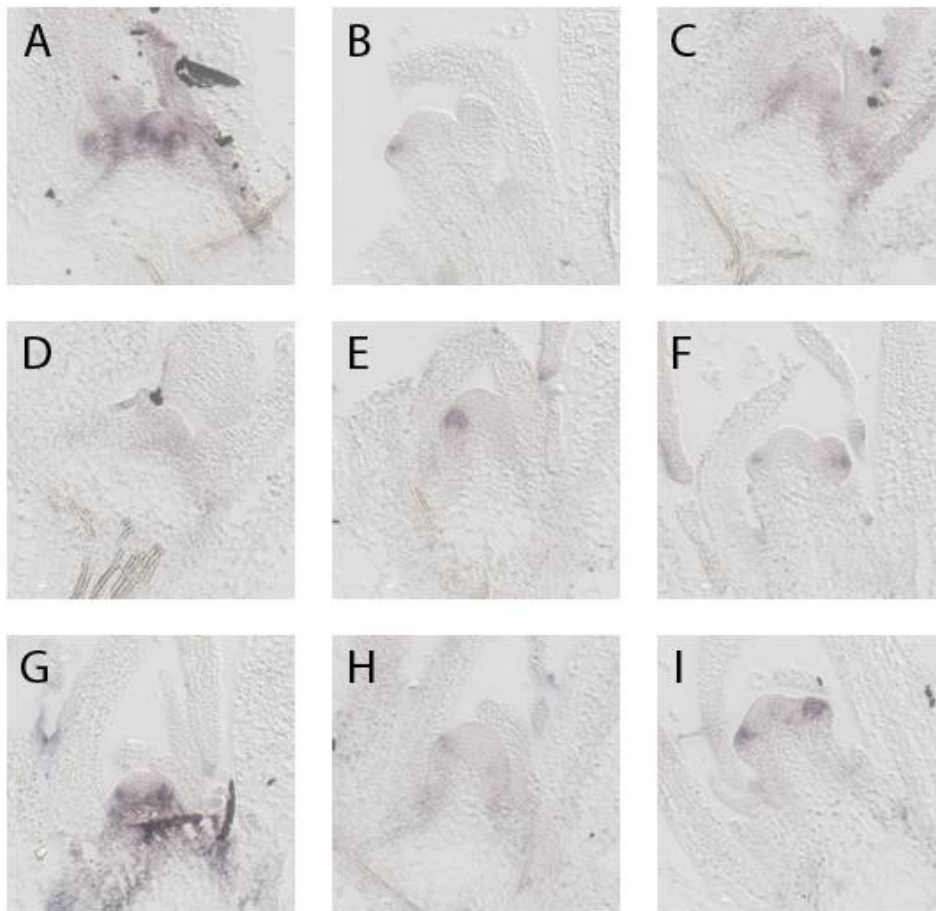


Fig. 59. *SVP* mRNA expression in *KNATI::SVP* lines. *In situ* hybridisations with RNA probe for *SVP* mRNA were performed to detect the level of expression and the spatial pattern of *SVP* transcribed under the *KNATI* promoter. Wild-type Columbia (A), *svp-41* (B), and *KNATI::SVP* (in *svp-41* background) lines #1 (C), #2 (D), #3 (E), #4 (F), #5 (G), #8 (H), #10 (I) are compared. Plants were grown in LD for 10 days and apices collected at ZT8.

KNATI::SVP dsRNAi constructs expressed in wild-type Col seem to have a weak effect on flowering time (**Fig. 60**). It could be that the *KNATI* promoter is not strong enough to have a significant effect on silencing *SVP*. The level of expression of *SVP* mRNA at the meristem of these lines was not measured. Additionally, *UFO::SVP dsRNAi* constructs were also generated. *UFO* is another promoter that has a specific expression pattern in the meristem and in flowers (Ingram et al., 1995), although it is more expressed in the later phases of the floral transition. It is therefore useful for expressing genes in the floral meristem. One of the *UFO::SVP dsRNAi* lines shows slight early flowering in LD, but because only two lines were generated, there is not strong support for this effect (**Fig. 60**). Nevertheless, considering that only a few of the *KNATI::SVP dsRNAi* line showed early flowering, this suggests again that the weakness of the *KNATI* promoter may be a

Results

problem. This, together with the possible de-regulation of the *KNATI* promoter itself in the *svp-41* background, which will be further investigated, suggests that it would be better to test also another independent promoter to express *SVP* specifically in the SAM. Mis-expression of *SVP* was then performed also with the *FD* promoter. In order to test the efficiency of the *FD* promoter to express flowering time genes at the SAM, the same vector was used to produce a *FD::FT* promoter fusion, and transformed into wild-type Col. Several lines transformed with this construct at T1 stage show early flowering phenotype (data not shown), demonstrating the effectiveness of this construct and postulating a possible alternative for the mis-expression of *SVP* in the SAM. *FD::SVP* in *svp-41* background, at the level of T1 transformants, did not show a clear effect on flowering. The effect of these constructs need to be further investigated in the T3 generation.

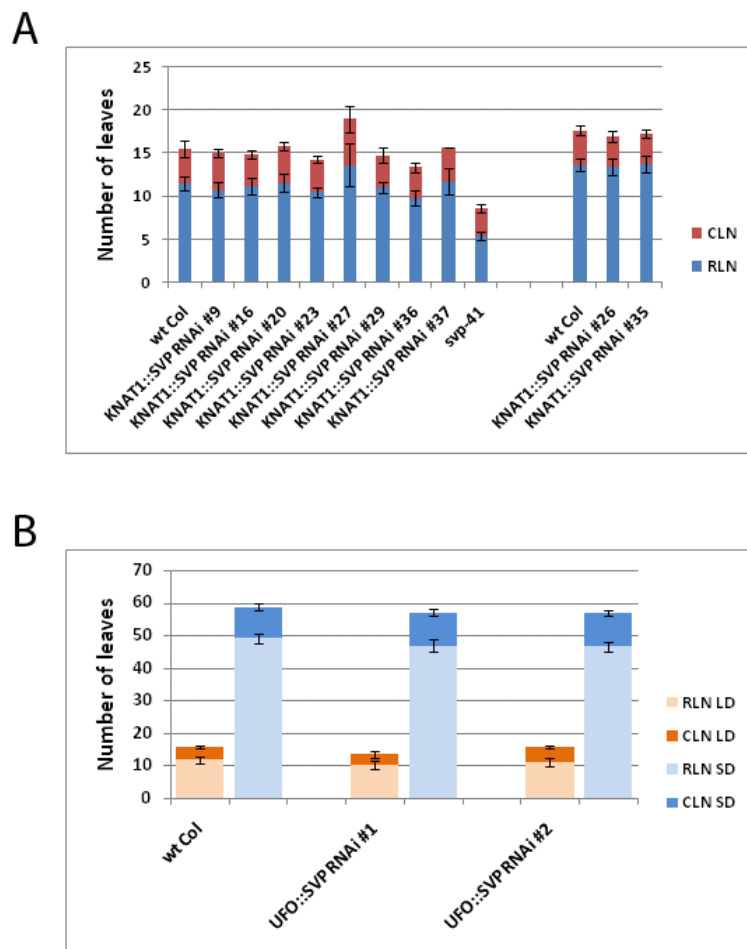


Fig. 60. Effect of reducing *SVP* expression in the shoot apical meristem. Flowering times of *KNATI::SVP* dsRNAi (in wild-type Col background) lines were scored in LD (Panel A). Additionally, flowering times of *UFO::SVP* dsRNAi (in wild-type Col background) lines were scored in LD and SD (Panel B).

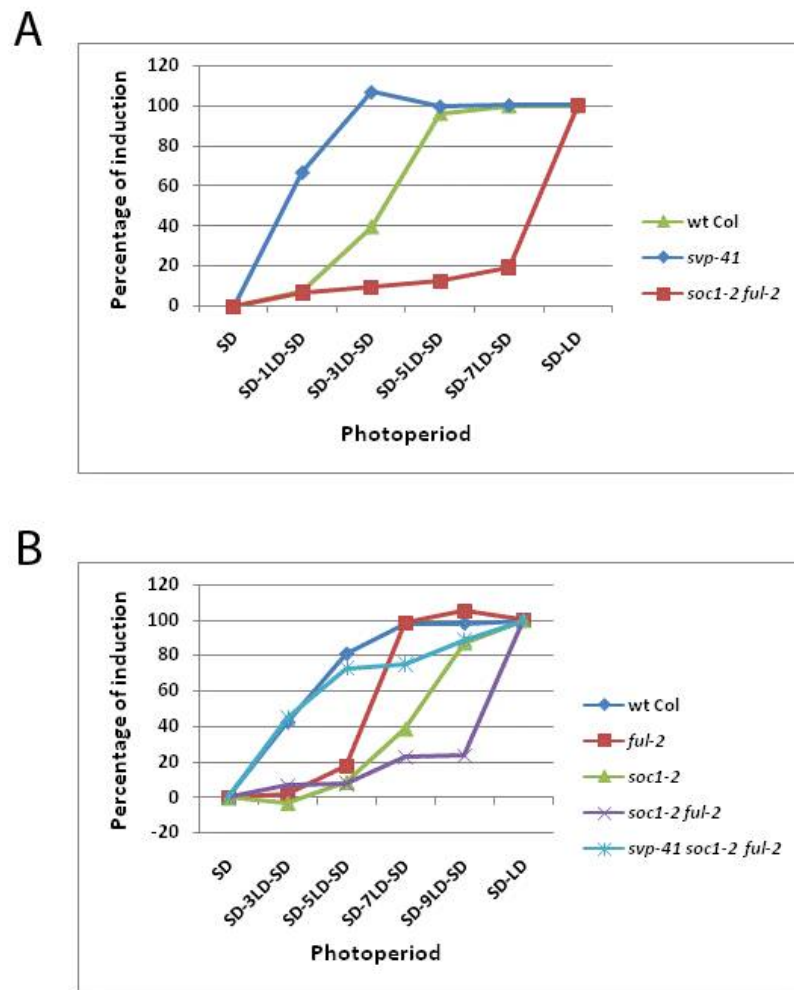


Fig. 61. Flowering times of wild-type and mutants scored after “double shift” experiments. Plants were grown initially in short days (SD) for 2 weeks (except for *svp-41* (Panel A), which was grown for 1 week in SD), shifted to long days (LD, the number of LDs is indicated in the X axis) and then shifted back to SD. Flowering time was scored as number of rosette leaves (RLN) plus number of cauline leaves (CLN), and percentage of induction was calculated with a formula described in the Methods.

5.3.3 Double shift experiments with mutants in flowering time genes

As previously introduced, wild-type Col plants grown for two weeks in SD need 5 LD of induction to be fully committed to flower and 3 LD to be only partially committed, thus accelerating their flowering time compared to plants only grown in SD. It has also been shown how several parameters can affect the number of days required for a plant to be induced or committed to flower. Another example of altering this response is to use mutants instead of wild-type plants in these experiments. Plants carrying mutations in genes required to promote or repress flowering might also

Results

have a different response to LD in terms of floral commitment compared to wild-type. Both cases of loss of components of the photoperiodic signal from the leaf or loss of components of the response to the signal in the meristem might affect this response.

Mutants lacking a functional *SVP* gene flower earlier than wild-type, and they respond faster to induction by LD. A functional *SVP* gene, which is a strong repressor of flowering, is probably a decisive factor in delaying the commitment to flower, as suggested by the *SVP* expression pattern in “double shift” experiments shown before (**Fig. 13**, **Fig. 14**). Indeed, in our conditions *svp-41* mutants grown only one week in SD needed exposure to only 3 LD to be fully committed to flower and needed only 1 LD to accelerate flowering. Although this experiment shows that the meristem responds earlier in the *svp* mutant compared to wild-type, it does not explain whether this is due to a stronger inductive signal coming from the leaf or to a higher sensitivity of the meristem to the stimulus from the leaf, or to both. In all cases, lack of repression from *SVP* decreases the threshold required for the response, either acting in the leaf or in the meristem, or in both.

Double shift experiments were performed with *soc1-2*, *ful-2*, *soc1-2 ful-2*, *svp-41 soc1-2 ful-2* plants, to study the role of *SOCI* and *FUL* in contributing to the effect of the *svp* mutation on the commitment to flower. *ft tsf* double mutants and *svp ft tsf* triple mutants were not used to study the contribution in the leaf, because they are not sensitive to photoperiod so a transient exposure to LD would not have a significant effect on flowering time. Moreover, the “standard” 2 weeks of vegetative growth in SD before the LD induction could not be used for the *svp* mutant because the flowering processes are highly accelerated in this background and so that these mutants would already show a partial induction before the shift. So only 1 week in SD was used for this mutant, while 2 weeks were used for the other ones. The response of the different genotypes was compared using the protocol introduced in section 3.1.1 (see also Methods). In one experiment, wild-type Col, *svp* and *soc1 ful* genotypes are compared. As expected, *svp* responds to fewer LDs than wild-type, while *soc1 ful* shows the opposite effect. Surprisingly, while the double mutant does not exhibit a strong delay in flowering when shifted permanently to LD, it only responds weakly to transient exposure to LD, at least until 7 LD in our condition (**Fig. 61, A**). In another experiment wild-type Col, *soc1*, *ful*, *soc1 ful*, and *svp soc1 ful* were compared (**Fig. 61, B**). *soc1* single mutants are significantly less responsive than wild-type, since 9 LD are needed to have a complete response. Conversely, *ful* mutants are more responsive than *soc1*, although less than wild-type. This is in agreement with the flowering time phenotype of these mutants. *soc1 ful* double mutants, like for the flowering time in LD, show a synergistic effect compared to the single mutants. But again, although

in this experiment also 9 LD of transient induction were included, there was a strongly reduced effect of a transient induction in LD compared to SD. This is in agreement with the idea that these two genes play redundant roles in the response to photoperiod at the SAM. *svp soc1 ful* triple mutants are able to recover a higher degree of induction compared to *soc1 ful* double mutants, since after 5 LD the plants behave similarly to wild-type. The triple mutants have increased levels of *FT* mRNA in the leaf, due to the loss of *SVP*, but this may not be the direct cause of the higher response. Indeed, *soc1 ful* double mutants induced with more LD, resulting in more *FT* expression, do not respond once shifted back to SD. Moreover, the effect of over-expressing *FT* in *soc1 ful* double mutants did not have a strong effect on flowering (Melzer et al., 2008). So it seems more likely than in the triple mutant the induction to LD is restored by a gene or a set of genes that are up-regulated at the SAM in *svp* background and can partially suppress the requirement for *SOC1* and *FUL*.

These results are clearly not fully conclusive, but suggest that *SVP* has a major role at the SAM in delaying floral commitment. Such an effect is consistent with the reduced reversion phenotype observed in *svp soc1 ful* plants compared to *soc1 ful* (see section 5.3.1).

5.4 Dual role of *SVP*: leaf and meristem

In the previous sections, it was shown that the effect on flowering time of *SVP* when active only in the leaf or only in the meristem is mild, although significant. The mild effect on flowering of *SVP* when active in only one of these tissues could be due to it having an additive effect in both tissues to completely fulfill its function. To test this idea mutations in genes acting downstream of *SVP* either in the leaf or the meristem were combined in the *svp* background. Also the transgenic lines mis-expressing *SVP* in the leaf were crossed to those mis-expressing *SVP* in the meristem.

5.4.1 Quintuple mutant

A *soc1 ful* double mutant grown in SD condition does not express *FT* and *TSF*, because these genes are only induced in LD. A *svp soc1 ful* triple mutant in SD shows only a weak expression of *FT* and *TSF*, due to relieving the repression by *SVP*. However, this up-regulation is not strong, since *svp* mutants and *svp ft tsf* triple mutants show only a mild difference in flowering time in SD, of around 5 leaves (see above). Perhaps therefore *svp soc1 ful* triple mutants grown in SD would flower late. However, this triple mutant in SD is still remarkably earlier than the *soc1 ful* double mutant (**Fig. 55**). Therefore introducing *svp* mutation into *soc1 ful* double mutants suppresses the late flowering

Results

phenotype. To test whether this might be due to *FT* and *TSF* the quintuple mutant *svp ft tsf soc1 ful* was made.

The *svp-41 ft-10 tsf-1* plants were crossed to *svp-41 soc1-2 ful-2* in order to generate a quintuple mutant *svp-41 ft-10 tsf-1 soc1-2 ful-2* and the other mutant combinations in the *svp* background. Moreover, *ft-10 tsf-1* were crossed to *soc1-2 ful-2* in order to generate a quadruple mutant *ft-10 tsf-1 soc1-2 ful-2* and the other mutant combinations in the presence of a functional *SVP* gene.

Only a few individuals homozygous for the 5 mutations were identified, therefore a complete flowering time experiment could not yet be performed. However, the estimated average number of total leaves at flowering for this quintuple mutant was around 55-60 (**Fig. 62**). We still do not have a *ft tsf soc1 ful* quadruple mutant to compare with the quintuple, but we already generated a triple mutant *ft tsf soc1*. The triple mutant flowers with around 70 total leaves (**Fig. 62**), so even later than *ft tsf*. Since we do not expect *ft tsf soc1 ful* quadruple mutants to flower earlier than *ft tsf soc1*, we assume that the *svp ft tsf soc1 ful* quintuple mutant would flower earlier than the *ft tsf soc1 ful* quadruple mutant, at least by 5-10 leaves.

We can then conclude that *SVP* has further other targets in addition to *FT*, *TSF*, *SOC1* and *FUL*, and other genes need to be mutated to fully suppress early flowering in an *svp* background.

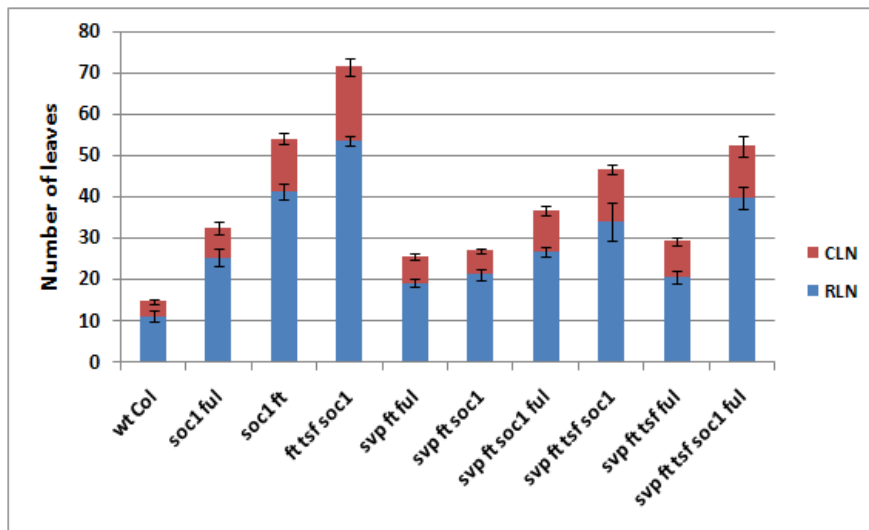


Fig. 62. Flowering times of plants carrying loss of function alleles of *SVP*, *FT*, *TSF*, *SOC1* or *FUL*. Flowering time was scored as number of leaves both in long-days (LD) and short-days (SD). RLN: number of rosette leaves. CLN: number of cauline leaves.

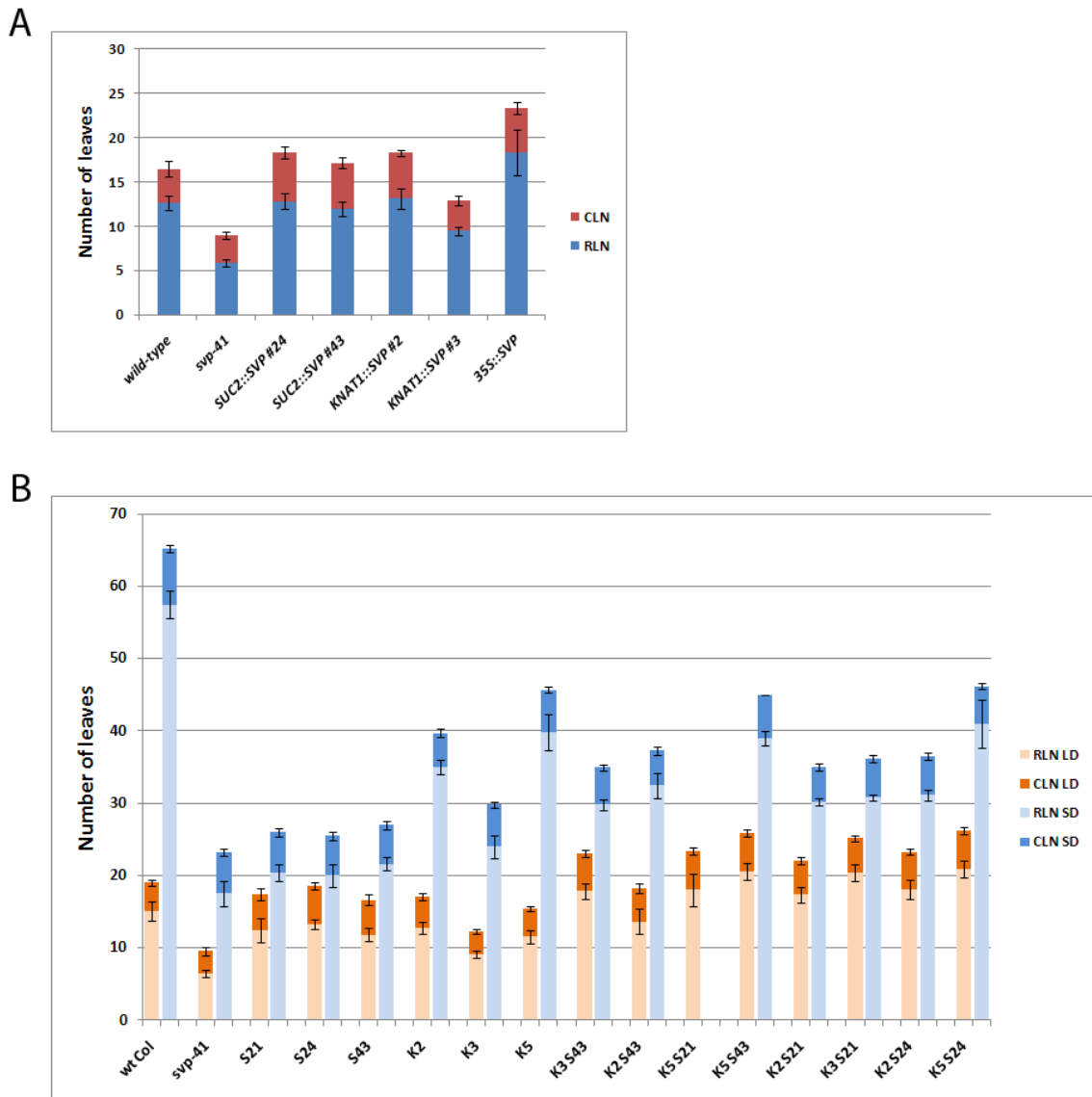


Fig. 63. Combined effect of mis-expression of *SVP* in leaves and meristem. Flowering time was scored for wild-type Col, *svp-41*, *35S::SVP*, *SUC2::SVP* and *KNAT1::SVP* (in *svp-41* background) mis-expression lines, and *SUC2::SVP* crossed to *KNAT1::SVP* (F1, in *svp-41* background). S and K indicate *SUC2* and *KNAT1* respectively. Panel A: flowering time was scored in LD. Panel B: flowering time was scored in LD and SD.

5.4.2 Combined effect of mis-expression

In order to cross *SUC2::SVP* lines with *KNAT1::SVP* lines, 3 independent lines made with each of the constructs were selected and they were crossed in all possible combinations (only one of the combinations failed). The parental lines were selected based on the expression of the transgene and

on the late flowering time phenotype, considering both LD and SD conditions.

Flowering time was scored both in LD and SD for the parental mis-expressing lines and the F1 progeny of the crosses between the different parental lines, together with *svp-41* mutant and wild-type. Because both *SUC2::SVP* and *KNAT1::SVP* are in *svp-41* background, the F1 progeny of the crosses can be used to test the effect of combining the two transgenes. Also the transgenes exert a dominant effect in heterozygosis. The flowering times of some of the parental mis-expressing lines were also previously compared to *35S::SVP* (see **Fig. 52, A, B**, and **Fig. 63, A**).

Combining the two transgenes resulted in significantly later flowering compared to the parental lines, for the vast majority of cases. In LD, this effect is comparable to the effect of over-expressing *SVP* using the *35S* promoter, and for most of the F1 crosses results in slightly later flowering compared to wild-type Col (**Fig. 63, B**). In SD, conversely, none of the combinations of transgenes led to the strong effect of the *35S* ectopic expression, and all the lines flowered significantly earlier than wild-type Col (**Fig. 63, B**). However, all lines carrying combinations of transgenes were much later than *svp-41* mutants.

This result shows that combining the mis-expression of *SVP* in leaf and meristem has an additive effect. This complements all the previous results and further demonstrates an independent role for *SVP* in the leaf and in the meristem to control flowering time.

The combination of transgenes in the F1 generation completely restores the effect of *SVP* in LDs, while it partially restores it in SD. Selection of progeny of F2 plants homozygous for both the transgenes will clarify if this partial effect is due to a quantitative effect of *SVP* expression in the *svp-41* background.

5.5 Mis-expression of *SVP.2* in different tissues

In TAIR database (version 9) there are two splicing variants annotated as products of *SVP*. Together with the conventional form used in the current literature as the product of *SVP*, there is another one which was also found from cDNA libraries. This alternative splicing variant is referred to here as *SVP.2*. This form is longer than the previous one, because it includes an intron (between exon 6 and 7). Within this intron there is a stop codon in frame with the coding sequence so that the predicted protein product is truncated before it reaches the following exon (see **Fig. 64, A**). In this truncated protein the last part of the K-box domain and the C-terminal part of *SVP* would be missing. We tested whether this form has a biological significance and possibly a function in the floral transition. As for the conventional *SVP*, *SVP.2* coding sequence was cloned into binary vectors under the

Results

control of different promoters: *35S* promoter for ectopic expression, *SUC2* promoter for the leaves, and *FD* promoter for the meristem. *svp-41* mutants were transformed with these constructs and 20 independent lines carrying the transgene were obtained for each of the constructs. Only preliminary results were obtained, because only the *35S::SVP.2* was followed so far. At the T2 stage, among the different independent lines there is a significant variation in flowering time. While the majority of transformants are similar to *svp-41* mutants, a few lines flower significantly later than *svp-41* (**Fig. 64, B**), although far less than *35S::SVP* over-expressing lines. Further analysis is needed to characterize the function of this second splicing form of *SVP*.



Fig. 64. Alternative splicing of *SVP* gene. Panel A: The coding region of the *SVP* genomic locus is shown on top. The two alternative splicing forms as indicated in TAIR database are indicated below, as *SVP.1* (the conventional form) and *SVP.2* (another for present in TAIR based on EST collection). The scheme was taken from Gbrowse in the TAIR database (Poole, 2007) and adapted. Panel B: *SVP.2* form was expressed under the *35S* promoter in *svp-41* background. Two lines are shown among all the independent transgenic lines, an early flowering one (line #5) and a later flowering one (line #2).

6. Discussion

PART1

6.1 Known genes and novel mechanisms that regulate the floral transition

A global gene expression profiling of the *Arabidopsis* SAM during the floral transition was performed in this study. The general aims were to identify genes that were not previously known to have functions in floral induction and to place these within a temporal hierarchy of events in the SAM. Prior to the sampling, a detailed analysis of the stages of the floral transition was done. Indeed, while for example for flower development a detailed description of the various stages has been compiled (Smyth et al., 1990), together with a thorough knowledge of the molecular markers of the different stages, a similar formalization is still lacking for the floral transition. Previous indications of the expression kinetics of known genes, such as *SOCI*, *FUL*, *AGL24*, *FD*, *SVP* and *API* have been confirmed in this study and some information further extended. Particularly, a combination of expression studies on key genes upon shift from SD to LD, and flowering time results of double shift experiments have better defined the stages involved in the floral transition and the boundaries of this process. A “transition meristem” is an intermediate state between the vegetative meristem, which did not initiate floral induction, and an inflorescence meristem, which is already induced and bears floral meristems on its flanks. A transition meristem can still be reverted to a vegetative meristem by removing the inductive photoperiod, although I demonstrated that it retains some memory of exposure to inductive conditions, depending on the level of induction. Because my interest in floral induction includes this transition meristem state, I set up a system in which it is possible to induce this state by shifting plants grown for 2 weeks in SD to 1 or 3 consecutive LDs. Exposure to 1 LD activates *FT* expression in the leaf (Corbesier et al., 2007) but only a few molecular events connected to floral induction are induced in the meristem, without any consequence on flowering time. 3 LD partially activates the floral transition. Exposure to an additional 2 LD cause this meristem to be fully committed to flowering at +5 LD, and to reach the inflorescence state with production of floral meristems.

So far, two main families of transcription factors have been shown to play a role in the floral transition at the SAM, the MADS-box (Melzer et al., 2008; Michaels et al., 2003; Samach et al., 2000) and SPL families (Fornara and Coupland, 2009). In the MADS-box family, *SOCI* and *FUL* play key roles in the response to the inductive photoperiod at the SAM. Activation of expression of both genes depends on FT and FD (Schmid et al., 2003; Searle et al., 2006; Wang et al., 2009a),

Discussion

although it is not known how direct this activation is. In our experimental conditions *soc1 ful* double mutants are still responsive to LD and their late flowering phenotype in LD is quite mild (around 10 total leaves more than wild-type) suggesting that although these genes are expressed early during the floral transition other genes that can partially compensate for their loss of function are also expressed at this time. *API* is another MADS-box gene, and it is considered to be a direct target of FT and FD (Abe et al., 2005; Wigge et al., 2005). However, *API* is not a flowering time gene *per se*, because *apl* mutants are not late flowering, rather it plays a function in the determination of the floral meristem and in the establishment of the early floral organs (Irish and Sussex, 1990; Mandel et al., 1992). This conclusion is consistent with its expression pattern, which is specific to floral meristems. The last MADS-box gene is *AGL24*, which is also involved in the floral transition, but its role in response to photoperiod seems to be less clear and more accessory to the function of *SOC1* (Liu et al., 2008; Michaels et al., 2003; Yu et al., 2002).

In this study, I showed that *SOC1* and *FUL* expression patterns differ in their response to photoperiod. While *SOC1* decreases in expression once induced plants are shifted back to non-inductive conditions, *FUL* expression is stably maintained once the meristems are committed to flower, regardless of the photoperiod. This is a new aspect, because there are not any other reports on flowering time genes that are stably maintained during the floral transition when inductive conditions are removed. On the other hand, this has been reported for floral meristem identity (Adrian et al., 2009), where positive loops sustain the expression of meristem identity genes once they are activated, (like the loop *API-LFY* (Bowman et al., 1993; Liljegren et al., 1999; Wagner et al., 1999)), thereby avoiding floral reversion. In addition, feedback regulation suppresses genes that confer inflorescence activity ensuring these are not expressed in floral meristems and avoiding reversion (like *API* to *TFL1/AGL24/SOC1/SVP/FUL* (Liljegren et al., 1999; Liu et al., 2009a; Mandel and Yanofsky 1995a; Ratcliffe et al., 1999)). Similarly, floral activity is suppressed in the inflorescence meristem to avoid floral termination (like *TFL1* to *API* (Ratcliffe et al., 1998)). The only known positive loop in the case of the floral transition is the one involving *SOC1* and *AGL24* (Liu et al., 2008), but the *in situ* hybridisation analysis suggested that this loop is not maintained in our experimental conditions in the absence of inductive photoperiods. A role for *FUL* and *SOC1* in determination and maintenance of floral induction has been proposed on the basis of the phenotype of *soc1 ful* double mutants, in which a phenotypic reversion to vegetative growth occurs after flowering (Melzer et al., 2008). I independently confirmed this effect. It can be related to the results of my double shift experiments in which the *soc1 ful* double mutants never acquired stable floral

Discussion

induction upon transient exposure to up to 9 LD, while the *soc1* and *ful* single mutants are only delayed compared to wild-type. Experiments with more than 9 LD of transient induction are needed to exclude the possibility that *soc1 ful* is only further delayed compared to the single mutants. Particularly, *ful* mutant is only slightly delayed, while *soc1* responds later. This, together with the results of the *in situ* hybridisation on wild-type plants in double shift experiments, suggests that *SOC1* is more important to rapidly respond to LD induction, while *FUL* is required to stably maintain this induction at the meristem. This model implies that there should be a mechanism to maintain *FUL* expression when the plants are returned to SD non-inductive conditions, which is not true for *FT* or *SOC1*. Such a role could be played by *AGL24*. Indeed, it remains to be determined whether there is an interplay between *FUL* and *AGL24*, which would maybe better clarify how the transition meristem is fully committed to the production of flowers. Moreover, the stable decrease of *SVP* mRNA in the SAM at the commitment stage might be important in allowing the increase of *FUL* expression. Again, we do not know what is the upstream mechanism that drives the down-regulation of *SVP*. The other possible candidate as a positive regulator of *FUL* at this commitment stage is *SPL3*, since it has been shown to directly activate *FUL* (Yamaguchi et al., 2009).

The *SPL* genes also play important roles in the floral transition, inducing floral meristem identity genes. In addition, they respond to photoperiodic induction, although they are probably only accelerated in their function by *FT*/*FD*, and not dependent on them. They are more important for the age dependent pathway, which acts in parallel to the photoperiodic pathway (Wang et al., 2009a).

It is very likely that many other regulatory genes are involved in the floral transition at the SAM, while in addition most of the genes regulated by *SOC1*, *FUL* and the *SPLs* remain to be identified.

Many genetic screens carried out in the last years failed to identify new genes involved in the floral transition at the SAM and activated in response to *FT*. These difficulties could be due to these putative genes having only a minor effect on flowering when inactivated. This could be because they play a relatively minor role in the floral transition, that they have family members that are genetically redundant or they might be important for earlier steps in plant development and have been excluded in genetic screens because of the pleiotropic effect of the mutations.

6.2 Next-generation sequencing for global gene expression analysis

Global gene expression analysis performed by next-generation sequencing on laser-dissected material was a challenging experiment. This was one of the first examples of this kind of approach, and at the time that the experiment was set up and performed, there was no other attempt reported in

literature. Therefore, many of the technical steps were still not optimised, from how to recover suitable RNA and DNA material for the sequencing, until the bioinformatics and statistics to analyze the data. The latter part relating to quantification of gene expression is still under development in the scientific community (Wang et al., 2009c; Wilhelm and Landry, 2009). Despite these difficulties the approach has the advantages of analyzing gene expression specifically in the meristem and utilizing the extreme sensitivity of Solexa sequencing. The output of this experiment is a gene expression profile, in which much of the data show correlation in terms of biological replicates, a good correlation with previously published data and allowed the confirmation of newly identified genes with interesting temporal and spatial expression patterns.

6.2.1 Comparison with available microarray data

Comparing my dataset with the microarray data previously published for shoot apices (Schmid et al., 2003), identifies both interesting similarities and differences. Comparison of different global gene expression experiments is difficult, even if performed in a similar way, due to the variability caused by different experimental conditions (Allison et al., 2006; Grant et al., 2007). In this case, the experiments have also some intrinsic differences, such as a different time in which the plants were grown in SD before shift to LD, the difference in the tissues collected and methods for sampling the tissue, different procedures for extraction and amplification of the RNA, and finally a different technology for gene expression analysis and statistical procedures for data analysis. Moreover, the focus of the previous report was on the late stages of floral induction, at +7 LD after shift, by which time floral primordia are already present. Very few genes, even considering the time point +3 LD after the shift for both datasets, have a similar pattern in both datasets. Examples of similarities are *SOC1*, *FUL*, and *SPL9*. Several genes closely similar in sequence to other members of the same family, such as the *SPL3-4-5* or *AGL42*, were not identified by our approach probably because the reads corresponding to these genes led to an ambiguous assignation, and were considered “promiscuous tags” so that they were discarded.

The number of genes identified as differentially expressed by the two approaches is quite similar. In the microarray, for the comparison between time point +0 LD and +7 LD the top 500 genes were considered for both *Ler* and *Col* experiments. Those common between the two ecotypes were recovered, resulting in a total of 332 genes, 101 up-regulated and 231 down-regulated. I show, with the final clustering approach, 339 genes up-regulated and 82 down-regulated, which is in the same range. However, in their case the quantity of down-regulated genes is larger than the up-regulated,

while in my case the trend is opposite. Interestingly, using the same cut-off in the microarray data, comparing +0 LD to +3 LD instead of +7 LD, results in a lower number of differentially expressed genes (about half).

Importantly, many genes that I identified as differentially expressed, showed a ratio of around 1 in expression between time points +3 LD and +0 LD in the microarray experiment, so that those genes were not identified as differentially expressed in that experiment. This could be due to the greater specificity of the LCM in sampling the SAMs, which prevented a dilution of the meristem tissue in the whole apex. *SOCI* and *FUL* are exceptions to this phenomenon, as they were identified also in the microarrays. In addition to their spatial pattern of expression, which extends to the leaves as well as the SAM, this is probably due to the very strong up-regulation of *SOCI* and *FUL* mRNAs in the SAM, so that a dilution of their signal in the entire apex does not prevent their identification. Another exception was *C23*, which is also up-regulated in the microarray data, again probably because of the strong up-regulation of this gene in the central region of the SAM. However, this gene is considered as up-regulated only at + 3 LD, while in the later time points this up-regulation is not significant.

6.2.2 General features of the data

A set of genes that shows a consistent change in expression upon photoperiodic induction was identified. Some of these were chosen as candidates and also tested by *in situ* hybridisation. For the up-regulated genes, some of them were confirmed by this method. For the down-regulated genes, none of them showed a convincing pattern by *in situ* hybridisation (data not shown). There are many possible explanations for this difference. One possibility is that the level of detection by *in situ* hybridisation for all the down-regulated genes was very low. Another possibility is that some of them were false positives. Anyhow, it seems quite challenging to find genes that consistently decrease in expression upon floral transition using our method. Indeed, no genes are so far known to be strongly decreased in expression at this stage. *SVP* is considered to be down-regulated, but only locally, and its transcript is re-distributed on the flanks of the SAM (Hartmann et al., 2000). Consistent with this its expression value is overall constant in my dataset. *SMZ* and *SNZ*, which were identified as down-regulated from the apex RNA microarray data (Schmid et al., 2003), were later shown to be genes mainly acting in the vascular tissue of leaves (Mathieu et al., 2009). The presence of putative false positive down-regulated genes in my dataset could be due to an artifact of the RNA amplification process. Indeed, those genes present a high number of counts in +0LD

sample and very low or even 0 in the +3LD sample. Because the +0LD is the sample with least initial material, less quality in terms of data, and which suffered more of the bias of the amplification procedure, it could be more prone to produce unbalanced values for some genes, leading to very high values in the +0LD sample.

6.3 Classification of the genes selected from the dataset

Analysis of the gene expression data from the SAM transcriptome dataset and the further studies by *in situ* hybridisation for some known and some selected novel genes revealed different patterns of gene expression following the shift from non-inductive SD to inductive LD photoperiod. Genes identified as differentially expressed can be classified according to different criteria:

- response to the photoperiod: how quickly their expression changes upon shift to LD
- spatial pattern of expression: where they are expressed, how the pattern changes upon induction, how specific the signal is for the meristem
- molecular function and biological process in which they are involved
- response to FT/TSF: whether their up-regulation is dependent on *FT* or *TSF* function

These issues are described in the following sections.

6.4 Time of the response to the inducing photoperiod

My major interest was to identify genes induced during the early events of the floral transition. Several genes were found to be up-regulated already after the first LD of induction, although the exact number depended on the criteria used to define up-regulation. All of these genes are potential targets of the very early photoperiodic activation at the SAM, either responding directly to FT protein or to some other signal. *SOCI* follows this response, as shown by several reports, and this was confirmed also by this study. Indeed, *SOCI* activation is also dependent on FT and FD (Searle et al., 2006). *FUL* should follow the same pattern (Schmid et al., 2003), although in our conditions it is less strongly induced during the first LD, as demonstrated by *in situ* hybridisations and data from the transcriptome analysis. Therefore, it is also important to take into account the genes that increase in expression only after 3 LD of induction, because some of them may require more time to respond, depending on which threshold has to be reached for their activation. Indeed, although *FT* is already up-regulated upon shift to LD, 3 LD are necessary to activate a complete floral induction in *Ler*, and *FT* mRNA level in the leaves increases progressively during the 3 LDs (Corbesier et al., 2007). This gradual accumulation of the *FT* transcript, which would lead to the accumulation of FT

protein at the apex, correlates with the gradual increase of *SOCI* mRNA in the apex, and with the fact that *API* is activated even later, presumably after 3 LD in *Ler* and 5 LD in *Col*, although *API* is a direct target of FT/FD.

Moreover, activation of genes at +3LD rather than +1LD may be an indirect effect of FT activating early acting genes like *SOCI* or *FUL*. This would be remarkable since not so much is known about target genes of *SOCI*, besides *LFY* (Lee et al., 2008b) and probably the *CBF* genes (Seo et al., 2009). Similarly almost nothing is known about targets of *FUL*, although it was reported that *LFY* expression may also depend on this gene (Ferrándiz et al., 2000). Interestingly, from the gene expression data, most of the selected candidate genes showed a similar up-regulation from +0LD to +1LD and from +0LD to +3LD, which means that the major up-regulation occurs during the first LD, and this is in agreement in most cases with the results of the *in situ* hybridisations. Nevertheless, for some genes the signal in the *in situ* appears later, at +3LD, suggesting that these genes are likely activated later during floral induction. Typical case is *C11*, which is lowly expressed and restricted to the primordia area. In the case of genes with very low expression levels, it can be useful to probe a later time point such as +5LD, because if there is a progressive increase in its expression under LD, there is more chance that the transcript is detected after 5 LD. Moreover, this revealed more clearly the expression pattern of some genes, that have to reach that developmental stage of the floral commitment to clearly show their specific pattern. Our global gene analysis did not include +5LD but some selected genes were tested at that stage and this should be repeated for all of them.

Other genes respond later at +3LD, and there was agreement between the expression data and *in situ* hybridisation. For example *D13* and *C23* mRNAs increased already at +1LD, but the up-regulation at +3LD is much higher. *C23* could be a possible target of *SOCI* or *FUL*, and this needs to be tested. *D13* does not seem to be a target of *SOCI* and *FUL*, because it is up-regulated independently of *FT* and *TSF*, which are upstream of *SOCI* and *FUL*. Indeed, in the *ft tsf* double mutant, when *D13* strongly increases in expression at +3LD, very low mRNA level of both *SOCI* and *FUL* is present.

6.5 Spatial pattern of expression

Several patterns of gene expression were described by *in situ* hybridisation experiments in this study, both for known and previously undescribed genes (see **Fig. 65** for a scheme). The typical pattern of expression for genes implicated in floral promotion is a broad expression in the whole

Discussion

dome of the SAM upon induction. This pattern is shown by *SOCI*, *FUL* and *AGL24*. *SVP* is also broadly expressed, and then it disappears from the center of the SAM upon floral induction. *SPLs* are emerging as genes with a more complex expression pattern, probably because they regulate several processes and are also related to juvenile/adult vegetative trait transitions (Fornara and Coupland, 2009). *API*, which marks the beginning of the floral meristem, and its homolog *CAL*, have a restricted pattern in the floral meristem, and these genes are not involved in the transition from the vegetative to the inflorescence meristem but are expressed after this has occurred (Kempin et al., 1995).

Interestingly, while some novel genes found in this screen have a similar expression pattern to *SOCI* (*D37*, *D55*, *D31*, *C25*, *C27*), some of them show differences. *C11* is expressed in a restricted region at the primordia before the floral meristems arise, and subsequently in the boundary with the floral organ. *C4* is expressed broadly but excluded from the most external layer L1 (and maybe L2). Strikingly, *C23* and *D13* are expressed in the center of the transition meristem (**Fig. 65**), in a region that is included within the “central zone” (Lyndon, 1998). This results in a novel pattern, because although genes like *WUS* are expressed in this region (Schoof et al., 2000), they are already present at the vegetative phase of the SAM. *TFL1* is the only flowering-related gene known to be expressed specifically in that part of the inflorescence meristem, although it is also already expressed at the vegetative phase (Bradley et al., 1997). This suggests there might be an interaction between *TFL1* and these novel genes, as they at least function in a common tissue and at the same stage. These possible interactions still have to be tested at the expression and genetic levels. *C23*, a gene encoding an unknown protein, is especially interesting because its mRNA seems to be restricted only to that particular region, and only upon floral induction, while *D13* for example is expressed also in external layers of the youngest leaves in the apex. Additionally, the strong signal of *C23* disappears in the absence of *FT* and *TSF*, suggesting that this gene is downstream of the known photoperiodic flowering cascade. Additional hybridisation signals are found after 5 LD of induction in regions that could be developing axillary meristems. This is another common feature with *TFL1* (Bradley et al., 1997).

Interestingly, *C19* and *D13* are strongly and broadly expressed in the inflorescence meristem at +5LD but are not expressed in floral primordia (**Fig. 65**). This feature is also shown by flowering time genes like *SOCI* and *FUL*. Also a gene involved in meristem maintenance, *STM* (Long et al., 1996), is expressed in the SAM but not in the incipient primordia, both leaf and floral, while its expression returns in the later floral meristems (Long et al., 1996).

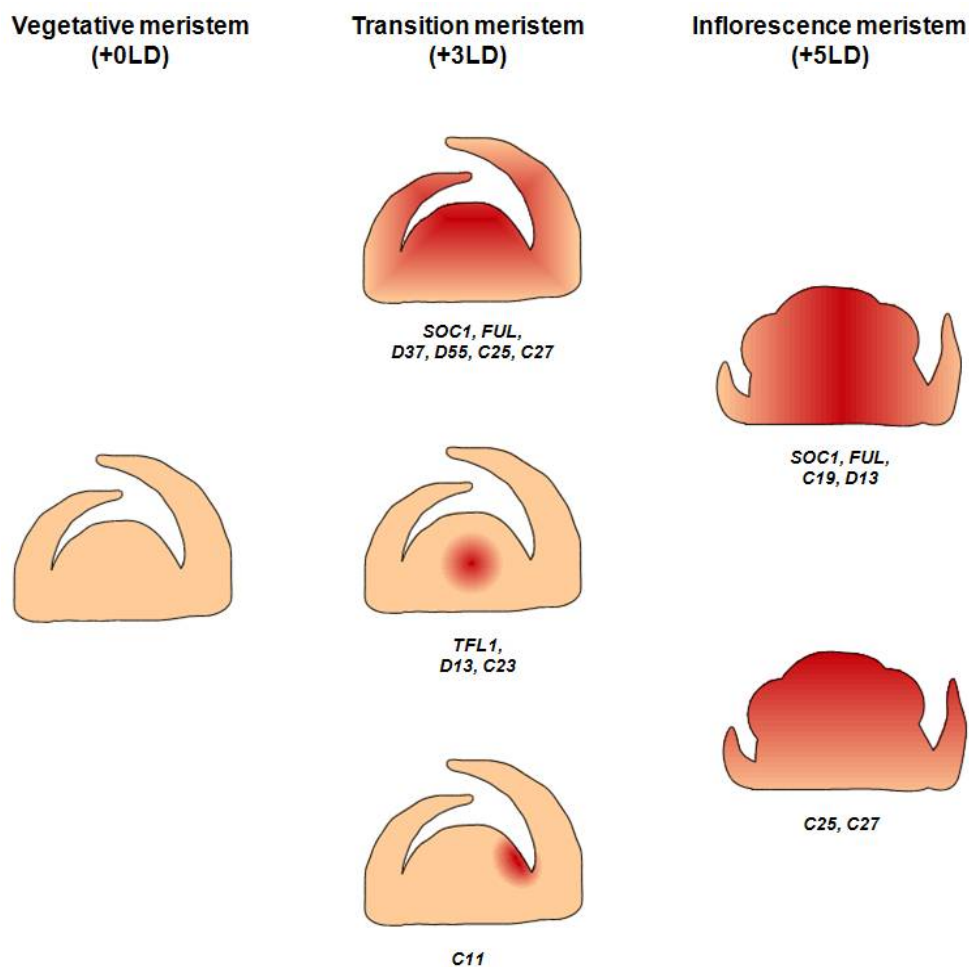


Fig 65. A schematic representation of spatial expression patterns of some known and newly identified genes. The simplified patterns are representations of the results of *in situ* hybridisation experiments. See text for details.

6.6 Biological and molecular functions of the genes up-regulated during the floral transition

6.6.1 Transcription factors and proteins involved in signaling

Transcription factors and other types of regulatory proteins are essential for many developmental switches, like the floral transition. The majority of genes encoding these types of proteins in the Solexa dataset present extremely low expression values, so that only a few of them were tested by *in situ* hybridisation.

Examples are *C4*, which encodes a putative bZIP transcription factor, *D37*, which encodes a dof-type zinc finger transcription factor, and *C29*, which encodes a GATA transcription factor. Among these, *C4* and *D37* present expression patterns that are restricted to the SAM. This contrasts with, for example, *FD*, a crucial gene for the floral transition, which also encodes a bZIP transcription

Discussion

factor, because *FD* expression pattern does not completely overlap with the one of *C4*. Other members of the dof family are the CDFs, which are involved in flowering but they regulate *CO* transcription in the leaf vascular tissue (Sawa et al., 2007; Fornara et al., 2009). *C20*, which encodes a protein with a RING finger-like zinc finger motif, is more broadly expressed in the whole apex. This gene is part of the *SHI* family, and although it was isolated as a gene expressed in the roots as *LATERAL ROOT PRIMORDIUM1 (LRP1)* (Smith and Fedoroff, 1995), loss of function of this gene enhances the defects in the gynoecium when combined with other mutants of the other members of the *SHI* family (Kuusk et al., 2006).

C21 mRNA is barely detectable, although among the regulatory genes identified here it is the only one that has been previously reported to be implicated in the floral transition. *C21* encodes *ATHB16*, a homeodomain-leucine zipper class I protein, involved in plant growth and response to light (Wang et al., 2003). Altering the level of *ATHB16* mRNA in transgenic plants affects flowering time, leaf expansion and shoot elongation. Compared to wild-type, *35S::ATHB16* plants are later flowering in LD, while slightly earlier in SD. Therefore, the over-expressor lines show less responsiveness to photoperiod. Conversely, lines carrying an antisense construct for *ATHB16* have enhanced responsiveness to photoperiod compared to wild-type, since they flower slightly early in LD and significantly late in SD. My data together with these genetic experiments suggest that induction of *ATHB16* expression in the SAM in response to inductive photoperiod may feedback to reduce responsiveness to photoperiod.

However, two putative regulatory genes on which I focused most were *C19* and *C11*, and these are described in the next sections.

6.6.1.1 *C19*

C19 encodes *FLOR1*, which has been classified as a leucine-rich repeat (LRR) protein (Gamboa et al., 2001). LRR proteins, which form a very large family in *Arabidopsis*, are transmembrane receptors involved in signaling, and have several roles mainly in plant development and defense to pathogens (Diévert and Clark, 2004, for a review). In this group, several members were shown to play pivotal roles in developmental processes, like *CLAVATA1* (Clark et al. 1997), *ERECTA* (Torii et al., 1996), and *BRASSINOSTEROID INSENSITIVE1* (Li and Chory, 1997).

There are already two reports on *FLOR1*. This protein was shown to interact *in vitro* with *AGAMOUS* (Gamboa et al., 2001). The pattern of expression was also previously investigated by *in situ* hybridisation (Acevedo et al., 2004), although a major focus was given to its expression

Discussion

during flower development, because this gene was proposed to have a role in the flower. However, no experimental evidence for such a role has yet been provided. The pattern of expression previously reported for this gene in the inflorescence meristem closely resembles the pattern shown in my study in the SAM at vegetative and early stages of floral induction. The signal is strong in the L3 layer in the peripheral zone, less intense in the central zone and not present in the L1 and L2 layers. Moreover, the pattern of the protein was shown to be less restricted than the mRNA and to spread all over the inflorescence meristem, including a further complication (Acevedo et al., 2004). In my study, the expression of this gene is clearly excluded from early floral meristems, as it also seems to be in the previous report.

Interestingly, the LRR proteins that are most closely related in terms of sequence to FLOR1 are the polygalacturonase inhibiting proteins (PGIP). Although the function of PGIP1 and PGIP2 were mostly related to pathogen defense (Ferrari et al., 2006), a PGIP-like protein was shown to regulate floral organ number in rice (Jang et al., 2003).

I showed that the late flowering of *soc1 ful* is enhanced by mutation in *FLOR1*. This suggests a role of this protein in the floral transition, rather than in floral development. It could be that, in addition to AGAMOUS, FLOR1 is able to interact with other MADS-box proteins, related to the floral transition, like SOC1, FUL or AGL24. This was not tested in the previous reports, and needs to be investigated.

Another candidate gene encoding a LRR protein is *C15*. However, its expression seems to be quite broad in the apex, even before induction. *D31* encodes a heptahelical protein (HHP) called HHP3. The proteins of this family are predicted to have 7 transmembrane helices, and could act as receptors in plant cells. *HHP3*, like the other members, is increased in expression upon light treatment, primarily through the effect of photosynthetic products (Hsieh and Goodman, 2005). Interestingly, although barely detectable, *D31* mRNA seems to be present at +3LD after the shift to LD and to be restricted to small areas of the SAM, while being absent in the *ft tsf* double mutants.

6.6.1.2 *C11*

C11 is part of the *Arabidopsis* zinc finger-homeodomain (ZF-HD) family. While other related gene families, such as the Class I *KNOX* genes (Scofield and Murray, 2006), the *WOX* class (van der Graaff et al., 2009), and the class III HD-Leu zipper proteins (Elhiti and Stasolla, 2009), contain members that are well studied since several years, the ZF-HD is still not well functionally

Discussion

characterized. However, there is a report in which a general study of the entire family, consisting of 14 members, named *ATHB20-34*, has been carried out (Tan and Irish, 2006). In this study, the authors reported the phylogenetic relationships among these genes, their expression by northern-blot analysis, and the physical interactions among their protein products. Particularly, these proteins can interact with each other in yeast two-hybrid assays, with a preference for heterodimerization, suggesting that these proteins form complexes to regulate transcription. *ATHB33* has been found to interact also with *AP1* by yeast two-hybrid (Tan and Irish, 2006). The expression pattern of the different *ZF-HD* genes varies in different plant tissues, but all the members are strongly expressed in flowers, and almost all of them in inflorescence.

Because *ATHB31* was isolated from my screen as *C11*, and the loss of function mutant of this gene does not have a phenotype, I tried to silence *C11* and the most related genes in the same plants. I generated two constructs: *amiRNAh21/31*, which silences *ATHB21* and *ATHB31*, and *amiRNAh22/25*, which silences *ATHB22* and *ATHB25*. These two pairs of genes, not only are closely related in terms of sequence, but they are also present in two blocks of conserved synteny, suggesting that they originated from genomic duplications. Moreover, *ATHB21*, *ATHB25* and *ATHB31* are more highly expressed in younger flowers, suggesting an earlier temporal role in floral initiation, more related to the onset of *API* expression than to floral development. Detailed phenotypic screening of the transformants will be needed to test if a decrease of the expression of these genes is related to an effect on the response to photoperiod, but the later flowering of the transformants is encouraging and suggests they play a role in the floral transition.

Both *ATHB31* and *ATHB25* are expressed at the primordia at +3LD, and later at +5LD *ATHB31* is expressed at the boundary between the SAM and floral primordia. An intriguing possibility is that *ATHB31* and *ATHB25* are expressed at a time that immediately precedes floral primordia determination, in a tissue that is not yet determined as floral primordia but will be re-specified with floral meristem character during floral induction. It was reported that at the stage of floral transition there is a restricted period of time in which there is an overlap between development of the last leaf and the first flower, and this overlap can occur in a single primordium on the primary shoot axis (Hempel and Feldman, 1995). This leads to the formation of a chimeric shoot, with both flower and leaf characteristics. The frequency of chimeric shoot formation depends on the growth conditions, but it appeared to be significantly higher in plants shifted from SD to LD than in plants continuously grown in LD. The authors hypothesized a partial re-specification of the leaf anlage by the floral stimulus, and they speculated that primordia in *Arabidopsis* can be specified also during

their development. If this is correct, some genes should be devoted to regulate this transition. Possibly members of the ZF-HD family participate in this process. Alternatively, they could have a role in the specification of the boundary between the SAM and the arising organs. Many transcription factors are known to play a role in this specific developmental process (Aida and Tasaka, 2006, for a review). However, it is perhaps unlikely that such a process would be under photoperiodic control.

6.6.2 Additional layers of regulation

Other proteins that may play pivotal roles in the floral transition, although they are not transcription factors, are protein modifiers that regulate the activity of transcription factors by post-translational modifications. For example the transcription factor AP1 is a target of farnesylation, and the over-expression of a mutated form of AP1 lacking the farnesylation site does not exhibit the typical terminal flower of the complete AP1 coding region but only causes early flowering and additional novel phenotypes (Yalovsky et al., 2000b). The *Arabidopsis eral* (for “enhanced response to abscisic acid”) is a mutant in the β subunit of a farnesyltransferase, which presents several developmental anomalies in meristems, organs and flowers, as well as late flowering (Yalovsky et al., 2000a). Over-expression of wild-type *API* in *eral* background also causes early flowering but not meristem termination (Yalovsky et al., 2000b).

Recently it was reported that a peptidyl-prolyl *cis/trans* isomerase encoded by *Pin1At* gene is involved in flowering (Wang et al., 2010). Pin1At protein was proposed to exert its effect on flowering through post-translational regulation of two key flowering time proteins promoting the floral transition at the SAM, SOC1 and AGL24, by phosphorylation-dependent *cis/trans* isomerization of these two MADS-box transcription factors. *Pin1At* plays an important function in the floral transition since lines expressing an antisense suppressor of this gene (*Pin1At-AS*) show delayed flowering, and over-expression of this gene promotes early flowering. Early flowering of *35S::SOC1* and *35S::AGL24* plants was significantly delayed in *Pin1At-AS* background, and the early flowering of *35S::Pin1At* is completely suppressed in the *soc1 agl24* double mutant background. In this study, both SOC1 and AGL24 proteins were demonstrated to be phosphorylated *in planta*, and Pin1At protein interacted with their phosphorylated forms, catalyzing conformational changes by isomerization and thus affecting their function at the post-translational level. The expression of *Pin1At* was detected in all tissues, including the SAM, and generally increased during floral transition. Interestingly, this was also detected in our gene expression dataset, where Pin1At

is in the list of the up-regulated genes identified by the clustering approach (see **Appendix II**). Consistent with this scenario, a specific kinase called Meristematic receptor-like kinase (MRLK) could be implicated in phosphorylation of AGL24 protein (Fujita et al., 2003). AGL24 was isolated by yeast two-hybrid screen as a physical interactor of MRLK, and then shown to be phosphorylated by this kinase. MRLK is expressed especially in apical meristems (Fujita et al., 2003).

Another gene identified in our dataset, *C27*, encodes a putative calcium-dependent protein kinase. I showed that the expression of this gene strongly increases at the SAM during induction in LD, and that this increase is strongly suppressed in the *ft tsf* double mutant. In tobacco a related protein, a calcium/calmodulin-binding protein kinase named NtCBK1, was reported to be involved in flowering (Hua et al., 2004). However, this gene was strongly expressed in tobacco SAM in the vegetative phase, and its expression decreased upon floral transition. Indeed, *NtCBK1* has a floral repressive function, as over-expression of this gene in tobacco causes late flowering.

6.6.3 Genes involved in metabolism

Metabolism has a role in all basal cellular processes and as many of these are likely to change in the meristem during the floral transition it is not surprising to find many genes connected to metabolic pathways among the up- or down-regulated genes in my dataset. However, the significant enrichment shown in the GO term analysis of processes like "biosynthetic process", "macromolecule metabolic process", "cellular metabolic process" and "primary metabolic process", gives an indication that metabolism plays a major role in the SAM during floral transition. There are two reasons that can account for this enrichment. One is that the floral transition involves a change in the SAM identity so that different structures are produced that sustain new organs, with a considerable energetic consumption. This is reasonable considering the extensive growth undergone by the SAM during the 3 LD of induction that I monitored and the resulting change in the SAM size. The other reason is that the shift from SD to LD implies also a longer exposure of the plants to light, which is reflected by more photosynthetic activity. The result of the photosynthesis, which takes place in the leaves, probably also has consequences at the SAM, which acts as a stronger sink for nutrients as more growth occurs. Transient exposure to red-rich light LD condition at high light intensity promotes flowering in *Arabidopsis*, while it does not have such an effect at low light intensity (King et al., 2008). The effect of high intensity red-rich light correlates with *FT* induction, and increase in expression of *SUC2*, a photosynthetically regulated gene. Blocking photosynthesis by transiently removing atmospheric CO₂ delayed flowering and the activation of *FT* by LD.

Discussion

Moreover, *ft* mutants did not respond to floral activation by high-intensity red-rich LD (King et al., 2008). This suggests that photosynthesis, perhaps by increasing sugar concentration, has a promotive effect on flowering in LD through *FT*. Furthermore, higher light intensity promoted flowering even in SD, but independently of *FT* (King et al., 2008).

From the set of genes which were up-regulated upon shift to LD, *C25* encodes an uncoupling mitochondrial protein (UCP) called UCP1 (or PUMP1). Uncoupling proteins are integral to the inner mitochondrial membrane and dissipate the proton gradient. Loss of function of this gene impacts photosynthesis, as the *ucp1* mutant has a significant decrease in the rate of CO₂ assimilation, and restriction in photorespiratory flux (Sweetlove et al., 2006).

Another gene, *D29*, encodes a plastid glyceraldehyde-3-phosphate dehydrogenase (GAPCP-1). Loss of GAPCP-1 and GAPCP-2 enzymes cause drastic changes in sugar and amino acid balance resulting in arrested root development, dwarfism and sterility (Muñoz-Bertomeu et al., 2009). Male sterility of *gapcp1 gapcp2* double mutants is caused by defects in pollen development, and is likely due to modifications in sugar signaling, particularly by an increase in trehalose (Muñoz-Bertomeu et al., 2010).

There are several publications that implicate sugar metabolism in floral transition processes. In the *pgi1* mutant, which has a highly reduced plastidial phosphoglucose isomerase enzyme activity, leaf starch synthesis is impaired (Yu et al., 2000). Also mutants in phosphoglucomutase (*pgm1*) and ADP-glucose pyrophosphorylase (*adgl*) have low starch content. All three mutants *pgi1*, *pgm1* and *adgl* show a slight delay in flowering in LD compared to wild-type and a more pronounced delay in shorter photoperiods of 12 hours light-12 hours dark (Yu et al., 2000). Additionally, supplementing the medium with 1% sucrose, glucose or fructose restored the flowering time of *pgi1* mutant to that of the wild-type. Sugar concentration has been shown to be correlated with the floral transition (Corbesier et al., 1998), although with opposite effects depending on the concentration and on the genetic background (Ohto et al., 2001).

Mutants in trehalose-6-phosphate synthase1 (*tps1*) are embryonic lethal in the homozygous state, but with a DEX-inducible system for TPS1 in the *tps1* mutant it is possible to generate viable seeds (van Dijken et al., 2004). Interestingly, these lines flower only if they are induced with DEX, otherwise they remain in the vegetative state for about six months until they die. Upon DEX application, TPS function is restored, and the floral transition occurs, although it is still strongly delayed compared to wild-type. These lines also show other phenotypes related to retarded growth (van Dijken et al., 2004).

Discussion

Another two candidate genes, *D35* and *D19*, are only very weakly detectable by *in situ* hybridisation, although they seem to be quite specific for the SAM and not visible before +3LD. *D35* encodes NIA2, a nitrate reductase. The *nia1 nia2* double mutant has an early flowering phenotype (Seligman et al., 2008), which has been attributed to a decrease in nitric oxide production, since this molecule has a repressing action on the floral transition (He et al., 2004). *NIA1* mRNA was also detected in our gene expression dataset, and it was identified as up-regulated by the clustering approach (see **Appendix II**). *D19* encodes AIM1, an enzyme in the pathway of β -oxidation of fatty acids (Richmond and Bleecker, 1999). Several abnormalities affect the inflorescence meristems of *aim1* mutants. Moreover, the normal structure and the fertility of the flowers is severely compromised in these mutants. The presence of *AIM1* mRNA in many tissues, including inflorescence meristems and flowers, was confirmed by *in situ* hybridisation (Richmond and Bleecker, 1999). There are other candidate genes that are related to fatty acid metabolism. *D55* encodes a phospholipid/glycerol acyl transferase, which is expressed strongly after +3LD, and it has a putative role in membrane metabolism (Stålberg et al., 2009). *C22* encodes a putative hydrolase/lipase, which is also detected at +3LD, and quite specifically at the SAM. Finally *D13*, encodes a fatty acid desaturase, which I will discuss in a later section.

6.6.4 Growth is a key process for the floral transition

6.6.4.1 Meristem growth

As already mentioned, meristem growth is a striking aspect of the transition to an inflorescence meristem. Even before the floral primordia arise, remarkable growth of the meristem occurs in all three dimensions. This is immediately visible from sections of the SAMs of plants shifted from SD to LD (**Fig. 11** and **Fig. 18**).

This growth must require increases in metabolic and cellular processes. This is in agreement with the significant enrichment in expression of genes with the GO terms “cellular component organization and biogenesis” and other terms concerning ribosomes, protein metabolism and translation. I already discussed the possible role of metabolism in the transition in the earlier section. The contributions of cell division and cell elongation to this growth have not been thoroughly measured but it seems likely that increased cell cycle activity must play an important role in the meristem transition.

Past studies tried to make a link between meristem transitions and meristem growth, and to describe this by measuring various parameters, including the cell cycle in different sub-domains of the SAM

Discussion

(Kwiatkowska, 2008 for a review). However, the small size of the *Arabidopsis* meristem precluded extensive research on this model plant, and other species were mainly studied. Intrinsic species-specific differences in SAM growth and inflorescence architecture allow only a limited extrapolation of this knowledge to *Arabidopsis*. Moreover, there is not always a clear agreement between different reports concerning the dynamics of these parameters during the floral transition.

Many studies have shown that in *Arabidopsis* the meristem increases in size during the transition to flowering. For *Ler*, it was reported that the vegetative meristem measures around 53 μm at the base and 13 μm in height, and expands to 70 μm at the base and 15 μm in height as an inflorescence meristem (Laufs et al., 1998). In the inflorescence meristem the cell size increases from the outer layer to the inner regions, so that cells in L1 layer are smaller than in L3. Mitotic index for both L1 and L2 layers in the center is lower than in periphery (Laufs et al., 1998), in agreement with the central zone (CZ) consisting of stem cells and the peripheral zone (PZ) consisting of cells forming the organs. Also *in vivo* imaging showed that, at the surface, cells at the center of the SAM grow slower than at the periphery (Grandjean et al., 2004).

In another report, upon shift from SD (after 2 months of growth) to LD, the mitotic index at the transition meristem was 2-3 fold higher than at the vegetative meristem. Considering the central and peripheral zones, the increase was seen especially in the peripheral part (Jackmard et al., 2003). However, slight activation of cell division occurred also at the rib zone. Upon floral induction the SAM grows both in width and height, but because of the higher increase in height relative to width it becomes more domed. This process is also immediately followed by elongation of the apical internodes on the stem (Jackmard et al., 2003).

Recently, a comparison between vegetative, transition, and inflorescence meristems was carried out taking also into account marker genes of the different meristem zones (Geier et al., 2008). The size of the transition meristem was around twice that of the vegetative meristem, correlating also with the width of *STM* expression domain. Inflorescence meristems were intermediate in terms of size between the other two meristem stages. The mitotic index also increased from the vegetative to the transition meristem, both in the CZ and in the PZ. Interestingly, the size of the organizing center and the stem cell region did not directly follow the growth of the overall meristem size (Geier et al., 2008).

6.6.4.2 *FT*, “florigen”, and growth

The remarkable growth of the SAM of wild-type plants upon the shift from SD to LD does not take

Discussion

place in the *ft tsf* double mutant. Although this can be simply explained by the fact that without *FT* (and *TSF*) there is not any response to photoperiodic induction, it raises interesting points on the function of the FT protein at the SAM in the transition to flowering. In this sense, FT could be seen as a general inducer of growth, because increasing the concentration of this at the meristem causes an increase in growth.

A role for the “florigen” as a regulator of growth was proposed from studies in tomato (Shalit et al., 2009). The tomato ortholog of *FT* is *SINGLE FLOWER TRUSS (SFT)*. The *sft* mutant is late flowering and presents altered architecture and flower morphology (Lifschitz et al., 2006). Both *SFT* and *FT* when over-expressed cause early flowering even in tobacco and tomato, which are day-neutral-flowering plants. Over-expression of *SFT* induces early flowering also in a short-day strain of tobacco as well as long-day *Arabidopsis*, suggesting conservation of the function and mechanism of action. *SFT* is also graft-transmissible. However, over-expression of *SFT* leads to terminal inflorescences and retardation of growth (Lifschitz et al., 2006). Conversely *SELF PRUNING (SP)*, the homolog of *Arabidopsis TFL1*, promotes growth and represses flowering (Pnueli et al., 1998). Besides its role in flowering, *SFT* requires *SP* for its role in sympodial and flower meristems (Shalit et al., 2009). High *SFT/SP* ratio causes growth restriction at the SAM and in lateral leaflet meristems, leading to reduced leaf complexity, while still higher ratios (for example in *35S::SFT sp*) cause complete suppression of both vegetative and inflorescence meristems (Shalit et al., 2009). Therefore, the authors propose *SFT/SP* to regulate the balance of growth processes, and the florigen as a general growth hormone. The negative role of *SFT* on growth in tomato seems to contrast with the situation in *Arabidopsis*. However, this could be due to differences in life strategy and plant architecture of these two species.

Another example comes from poplar, where *PtFT1*, the ortholog of *Arabidopsis FT*, plays a role both in flowering and bud set (Böhlenius et al., 2006). In autumn, in response to SD, growth terminates and bud dormancy is initiated in this tree species. However, over-expression of *PtFT1* in poplar causes not only early flowering, but also suppresses the growth cessation induced by SD and bud set, so that transgenic trees do not terminate growth in SD. So in this case FT would promote growth, as appears to be the case in *Arabidopsis* meristems. Also in slow-growing conifers an *FT* orthologue was correlated with photoperiodic bud setting (Gyllenstrand et al., 2007).

However, this does not exclude that the putative “growth factor” is something downstream of FT, which is activated by FT protein, either together with FD or independently of it. *SOCI* and *FUL*, putative early targets of FT, could mediate this function, since they are transcription factors. *FUL*

has been associated with functions in the cell cycle (Gu et al., 1998). Moreover, in a recent report, *FT*, *SOC1* and *FUL* were connected to growth processes in addition to flowering control (Melzer et al., 2008). For example, *ft ful* double mutants show extreme indeterminacy of the apical meristem and grow up to 1 meter tall with only a few branches, reverting to vegetative growth. The *soc1 ful* double mutants show several rounds of reversion to vegetative growth after flowering. *35S::FT* in *soc1 ful* grows with a short inflorescence, a few terminating co-inflorescences, and a reiteration of vegetative growth (Melzer et al., 2008).

6.7 Response to FT/TSF and responsiveness of *ft tsf*

In principle, classes of genes can be identified based on how much their induction upon shift to LD is dependent on *FT/TSF*. This can be done comparing the induction of a gene in wild-type to the induction in *ft tsf* double mutant. However, it is not possible to quantify this difference by *in situ* hybridisation, and other techniques are necessary to determine the level of gene expression in each genotype. Furthermore, in this study only very few genes were tested in the double mutant. Nevertheless, some qualitative information was gained from a series of genes. *C11* and *C23* are genes that convincingly respond to photoperiod and this response is dependent on *FT* or *TSF*, since they are clearly induced by LD in wild-type but not in the double mutant (**Fig. 37** and **Fig. 44**).

A series of other genes have been shown to be expressed in the meristem, and while in wild-type they are up-regulated upon the shift to LD, they remain constant in the double mutant (see *C19* and *C4*) (**Fig. 39** and **Fig. 42**).

Another set of genes seems to partially respond to *FT/TSF*. They increase in their expression in the double mutant, but clearly less than in wild-type (see *C25* and *C27*) (**Fig. 43**). From the microarray data of the shoot apices (Schmid et al., 2003), genes like *SOC1*, *FUL*, and several *SPLs*, show a marked increase in expression upon shift to LD in wild-type. This increase is strongly delayed in *co* and *ft* mutants, but the increase is still detectable, suggesting a residual effect of the photoperiod.

This increase could be due to other factors rather than a response to the photoperiodic flowering pathway. A shift from SD to LD is a dramatic environmental change that plants never experience in nature because they gradually pass from a SD-like to a LD-like condition during the changing seasons. Therefore, many genes could be induced in expression because of this shift, not only due to the floral response to photoperiod. Genes related to stress, especially abiotic, or to temperature change, may be induced due to a direct consequence of a higher exposure of the plants to light. These genes would be expected to be expressed very similarly in the *ft tsf* double mutant. Moreover,

photosynthetic activity is higher in LD than SD, and this can also trigger processes that are related to energy production, as discussed before.

The *ft tsf* double mutants, although un-responsive to photoperiod in terms of induction of flowering, seem to be still responsive to LD for growth. Although the size of the SAM upon floral induction in our experimental condition has not yet been quantified in detail, it is possible to recognize a certain degree of growth at +3LD after photoperiodic induction even in the double mutant. This residual growth may depend on the sugars produced upon photosynthesis and transported to the meristem. The size of the meristem of both wild-type and *ft tsf* during the floral transition needs to be compared, and the mechanism of this residual growth can then be investigated.

From the novel genes isolated in my screen, the only one that seems to be induced by LD completely independently of *FT/TSF* is *D13*.

6.8 A novel signal identified in response to shift in photoperiod

D13, a gene encoding a putative stearoyl-acyl-carrier-protein (ACP) desaturase, has been shown to be strongly induced upon shift to LD in a region at the center of the inflorescence meristem. This induction occurs not only in wild-type, but also in *ft tsf* double mutant, with the same dynamics and a very similar pattern (**Fig. 32, G-L** and **Fig. 33**). This induction is unlikely to be due to direct detection of photoperiod in the meristem, as this is strongly shaded by young leaves. Therefore, I postulated that another signal distinct from *FT/TSF* is likely to trigger *D13* expression. To date, there are no reports of genes rapidly induced by LD in the SAM in the absence of the photoperiodic pathway. Some hypotheses can be made on the identity of this signal.

One possibility is that the photosynthesis, which would create a metabolic signal through the production of sugars could be involved. As discussed before, shift from SD to LD increases the exposure to light and boosts photosynthesis. This possibility could be tested for example using so-called Extended Short Days (ESD) instead of LD. ESD consists of initial 8 hours of light with the complete spectrum, then 8 hours of exposure to far-red light that is perceived as photoperiodically active but is not photosynthetically active, and finally 8 hours of dark.

Another possibility is a hormonal signal. Gibberellins for example are also involved in triggering flowering independently of *FT*, although some studies report possible connections between the two pathways (Hisamatsu and King, 2008). Moreover, some responses to GA are similar to those caused by exposure to LD (Gocal et al., 2001), and gibberellins were reported to be a possible moving signal (Eriksson et al., 2006), although additional reports are needed to clearly support this

Discussion

hypothesis. Another critical point is that for both sugars and gibberellins, and to a certain extent cytokinins (Corbesier et al., 2003), a role in the floral transition has been proposed as well as possible movement from leaf to apex. However, it is not known whether their roles are causal or a consequence of the floral transition. In other words, we do not know if these possible signals would be active in a *ft tsf* double mutant, which does not undergo the transition readily upon shift to LD.

The experiment with the inducible system that activates CO also indicates that *D13* induction occurs independently of the *CO-FT* module, and links *D13* more clearly to the response to LD (**Fig. 35**). The *tfl1* mutant shows an increase of *D13* expression, or a premature expression of this gene, compared to wild-type, at the moment of the floral transition (**Fig. 34**). This suggests that this gene is somehow connected to the floral transition of the SAM. It could be that upon shift to LD a signal triggers the expression of *D13*, which contributes to the transition, independently of FT. Expression of *D13* cannot be sufficient to induce flowering, because it is expressed normally in *ft tsf* double mutants, although these are very late flowering. However, *D13* might still contribute to the early flowering caused by FT/TSF in wild-type plants. Insertion lines carrying a T-DNA within the locus are not available, and the RNAi against *D13* did not efficiently decreased its expression. Possibly a feedback regulation causes this enzyme to be up-regulated once its concentration decreases, making RNAi approaches more challenging. Moreover, the over-expression of *D13* did not show any visible phenotype, consistent with what has been shown for other members of the same gene family (Kachroo et al., 2007).

What could be then the function of *D13* at the SAM? Stearoyl-ACP desaturases are enzymes that catalyze the conversion of stearic acid (18:0) to oleic acid (18:1), to regulate polyunsaturated fatty acid content. Plants can adjust the membrane lipid fluidity by changing levels of unsaturated fatty acids mainly by regulating the activity of fatty acid desaturases. This has been related mainly to the response of abiotic stresses such as changes in temperature (Upchurch, 2008, for a review). Particularly, desaturase activity would maintain higher membrane fluidity when the temperature is very low. Therefore, this function could be connected to the floral transition, in which higher fluidity of the membrane would perhaps facilitate the growth of the meristem. Moreover, *TFL1*, which is expressed in a similar region, was reported to be implicated in endomembrane trafficking, and fractionation of protoplasts showed that TFL1 protein was associated with the membrane fraction (Sohn et al., 2007).

These enzymes can also be involved in pathogen defense responses (Kachroo et al., 2001). *D13* is part of a family of 7 stearyl-ACP desaturase in *Arabidopsis*. Loss of function mutants of one of the

Discussion

members of this family, *SSI2/FAB2*, causes a dwarf phenotype, constitutive activation in salicylic acid-mediated signaling and repression in certain jasmonic acid-mediated responses, with several consequences in defense responses (Kachroo et al., 2001). Therefore, signals derived from fatty acids modulate crosstalk between different defense signaling pathways, revealing an interesting possible role of these enzymes in signaling mechanisms. A general description of this gene family has been published and showed a certain degree of tissue-specificity of the various members *in planta*, although *DI3* was not detected and not considered in this study (Kachroo et al., 2007). Knock-out lines for 3 out of the 7 members of this family were not viable when homozygotic, while for the other 2 members no visible mutant phenotype was detected (Kachroo et al., 2007). However, *DI3* is the most divergent member of this family, as demonstrated by phylogenetic analysis. Its expression pattern, specific for a particular region in the SAM in inductive photoperiods, could account for a unique function of this gene which cannot be predicted from the information on the other *Arabidopsis* ACP-desaturases.

PART2

6.9 SVP represses many genes

Although *SVP* was first described in 2000 (Hartmann et al., 2000), it only recently became of interest to many groups. Several reports underlined the importance of this transcription factor in the control of the floral transition, together with roles in floral meristem determination. A repressive effect of *SVP* on *FT* transcription has been reported by several studies, together with this study (Lee et al., 2007b; Li et al., 2008; Jang et al., 2009). Moreover, I showed that this repression is exerted during the 24 hours of a daily cycle, so that part of the early flowering of the *svp* mutant can be explained by up-regulation of *FT* and not, for example, by a shift in the phase of *FT* expression. I demonstrated the same for *TSF*, adding another similarity between *FT* and *TSF* at the level of their regulation (Jang et al., 2009).

Repression of *SOCI* by *SVP* was also reported, together with this study, by another group (Li et al., 2008). Moreover, a direct repression of *SOCI* by *SVP* was demonstrated by showing that *SVP* binds to the *SOCI* promoter (Li et al., 2008). In addition, I showed that in *svp* mutant, *SOCI* still rises in expression, even in the absence of *FT* and *TSF*. Therefore, in absence of inducers and the *SVP* repressor, there is still activation of *SOCI*. A similar phenomenon was also shown in various double mutant combinations, in which in the absence of repressor (*SVP*) and inducer (*CO* or *FT*) activities there was still activation of the target (*FT* or *SOCI*, respectively), as measured by real-

Discussion

time PCR. It could be that *SOCI* in *svp ft tsf*, in absence of functional photoperiod pathway, is induced by other pathways such as the GA pathway. This can be tested in the future.

Another point is that the *svp co* double mutant flowers slightly but significantly earlier than *svp ft tsf*. Considering *FT* and *TSF* as the only significant targets of *CO* for floral induction, it is expected that these two mutant combinations show the same phenotype. Indeed, I showed that in *svp co* during a day cycle of 24 hours the level of *FT* and *TSF* is very low. However, this reflected the situation of only 1 day at a precise developmental stage (from 10 to 11 days in LD condition), so it could be that there is a slight up-regulation of *FT/TSF* in *svp co* double mutants at another stage. Indeed, another real time PCR experiment showed that at 12 days in *svp co* the expression of both *FT* and *TSF* is significantly higher than in *co*, and even slightly higher than in wild-type. This result suggests that other activators can promote *FT* expression in an *svp co* double mutants.

It is not yet clear how direct is the repression of *FUL* by *SVP*. In *svp ft* double mutants *FUL* is still quite strongly expressed in early stages of the floral transition, suggesting a direct control of *SVP* on *FUL*. However, the *svp soc1 ful* triple mutant does not significantly differ from the *svp soc1* double mutant in terms of flowering time. Hence, other experiments need to be done to investigate the relation between *SVP* and *FUL*. As reported previously, *FUL* is ectopically expressed in *ap1 cal* double mutants, because it lacks the repression exerted by *API* (Mandel and Yanofsky, 1995a). In another report, *FUL* mRNA was measured in the *ap1 agl24 svp* triple mutant and found to be up-regulated even significantly more than in *ap1 cal* (Gregis et al., 2008). The mutation in *SVP* could account for this further up-regulation of *FUL*, suggesting that *FUL* is normally repressed by *SVP*.

6.10 Is *SVP* a general repressor or is it downstream of photoperiodic induction?

I showed that several floral promoter genes are increased in expression in the *svp* mutant and they could also be targets of *SVP*. An alternative view is that, in addition, *SVP* is genetically downstream of some floral promoter genes. Indeed, *SVP* shows a decrease in expression at the center of the SAM during the floral transition, and it is still not known if a floral promoter gene is upstream of *SVP* and negatively regulates it to allow the floral transition to occur. Moreover, the two views are not mutually exclusive, and it is possible that some factors are repressed by *SVP* and then when they are activated, for example by the photoperiod, they in turn repress *SVP*. A similar hypothesis was suggested for *FLC*, where *FLC* represses *SOCI* but *SOCI* would then down-regulate *FLC* (Seo et al., 2009). A previous report excluded that the photoperiodic pathway influences *SVP* expression, since the expression level of this gene did not change in mutants of genes within this genetic

pathway (Li et al., 2008).

6.11 Double action leaf-meristem

I demonstrated that *SVP* has a role in repressing floral promoting genes expressed in the leaves, and a role in repressing floral promoting genes expressed in the meristem. *FLC* is obviously a similar case, since this MADS-box protein has the same dual function in these tissues (Searle et al., 2006). Also the two repressors share many target genes and likely act in a complex. However, in the meantime it is emerging that more and more genes in the flowering time network show this kind of dual function in these two tissues. For example both *SOCI* and *FUL* cause an acceleration of flowering when over-expressed in leaf or meristem, although the major contribution is in the meristem (Searle et al. 2006; Wang et al., 2009a). The same approach with *SPL3* gave similar results (Wang et al., 2009a).

Interestingly, the contribution of *SVP* on flowering seems to be equally important in leaf and meristem, since more or less the same effect is obtained using *SUC2* and *KNATI* promoters, and the combination of the two transgenes restores a phenotype similar to the wild-type. This is similar to what has been observed with *FLC* (Searle et al 2006). However, the combination of the two transgenes for *SVP* does not fully complement the flowering time phenotype in SD. This might be due to the strength of the promoters, which might not be enough to suppress the effect of the *svp* mutation, or to the fact that the transgenes are single copy and heterozygotic. Analysis of the F2 generation when the plants are homozygotic will clarify whether the number of transgene copies makes a difference for the flowering time.

The basis of the floral phenotype of *KNATI::SVP* mis-expressing lines remains to be explained. Over-expression of *SVP* in all tissues using the *35S* promoter leads to a dramatic effect of homeotic transformation on flowers (Masiero et al., 2004). It could be that the tissue where this promoter causes this effect partially overlaps with that of *KNATI* expression. Independent transformations of *svp-41* mutant with *35S::SVP* constructs that I performed show a range of floral phenotypes (data not shown), indicating that the level of expression is also important for the effect. Alternatively, in the *svp* background *KNATI* is de-regulated. This remains to be tested.

6.12 *SVP* and *FLC*

Recently, *SVP* and *FLC* have been shown to be closely related in function. However, these genes also show notable differences.

Discussion

At the level of targets, *FT*, *TSF* and *SOC1* are shared between them. Additionally, *FLC* could be involved in the repression of *FUL*, since *FRI-FLC* lines strongly suppress the photoperiodic induction of *FUL* (Schmid et al., 2003). At the level of regulation, *SVP* and *FLC* are both targets of temperature changes and the autonomous pathway, and they are not directly affected by photoperiod (Lee et al., 2007b; Li et al., 2008; Michaels and Amasino, 1999). Finally, they are both down-regulated in the inflorescence apex (Hartmann et al., 2000; Michaels and Amasino, 1999).

There are also major differences at the level of regulation. While the GA pathway affects only *SVP*, vernalization has an effect only on *FLC* (Li et al., 2008; Michaels and Amasino, 1999). Regarding the target genes, a direct binding of SVP protein to the *FT* promoter has been reported only once, and that experiment was performed in a transient assay with protoplasts (Lee et al., 2007b). It remains possible that the repression by SVP could not be direct, or could involve other specific factors, such as TFL2, that is also a repressor of *FT* and was shown to be recruited to the *SEP3* locus by SVP to establish its repression (Liu et al., 2009b).

The fact that SVP and FLC proteins physically interact does not necessarily explain the possible complexity of the regulation of their target genes. MADS-box transcription factors usually form different complexes with several partners, depending on the developmental stage and the specific tissue (Rijpkema et al, 2007). For example, in the flower SVP interacts with AP1 and AGL24 (and maybe with SOC1) (Liu et al, 2009a, for a review), but probably not with FLC. Because AGL24 and SOC1 proteins are present in the meristem also before floral initiation, interactions of SVP with these proteins to regulate transcription cannot be excluded and needs to be tested.

Other similarities or differences still wait to be tested, such as the epigenetic regulation, which is well known for the *FLC* locus and the regulation through antisense transcripts, which has just been discovered for *FLC* (Swiezewski et al., 2009; Liu et al., 2010). Neither of these aspects has been studied for *SVP*.

Finally, the presence of an alternative shorter differentially spliced form of *SVP* was discussed. Preliminary experiments showed a modest but significant effect on flowering for this form, when over-expressed with the *35S* promoter, while the complete form strongly delays flowering and has also a dramatic effect on flower development. Interestingly, while the function that *SVP* has in *Arabidopsis* is well conserved in closely related species, such as *Brassica campestris* (Lee et al., 2007a), in other species there are important differences. In rice, the *SVP-like* genes still show a conserved role in meristem identity and they have a major role in brassinosteroid signaling, but they are not involved in the floral transition (Lee et al., 2008a). When over-expressed in *Arabidopsis*,

they do not delay flowering but they cause floral reversion similar to the endogenous *SVP* (Fornara et al., 2008). Also in barley, several *SVP*-like genes were isolated, and they also generate floral reversions when over-expressed, both in barley and *Arabidopsis*, while only one member caused late flowering (Trevaskis et al., 2007). Several isoforms of this protein may have arisen during evolution in different species, and alternative splicing may contribute in *Arabidopsis* to keeping more than one function encoded by the same genomic locus. Whether the alternative form of *SVP* mRNA is biologically relevant or just coding for a truncated inactive protein needs to be investigated in more detail.

6.13 A quintuple mutant reveals additional targets of SVP

The generation of the *svp ft tsf soc1 ful* quintuple mutant, and possibly all the other combinations of the different mutations, is a valuable tool to verify the genetic interactions among all these genes. Indeed, it is not yet clear, for example, how much *SOC1* and *FUL* are functionally redundant. It is also not known what would be the effect of combining these mutations into a quadruple mutant *ft tsf soc1 ful*. A triple mutant *ft tsf soc1* is already very late flowering in LD, but it has to be tested if the quadruple mutant can still easily flower.

However, I already showed that the quintuple mutant flowers slightly earlier than *ft tsf soc1* triple mutant, therefore presumably earlier than the *ft tsf soc ful* quadruple mutant, which still has to be generated. This demonstrates that, in absence of *FT*, *TSF*, *SOC1* and *FUL*, *svp* still promotes significant early flowering. This suggests that an additional gene which is normally repressed by *SVP*, promotes early flowering in the quintuple mutant.

What could this unknown gene be? *AGL24* is a possible target, although the *svp* mutation was reported to be epistatic to *agl24* (Gregis et al., 2006). If the effect of the loss of *AGL24* was masked by the up-regulation of the other floral promoter genes in the *svp* background, this would be a reason why this gene was not identified as a possible target of *SVP*. Another floral pathway integrator, *LFY*, could also be downstream of *SVP*. Possible other targets are the *SPL* genes, for which the genetic interactions with *SVP* have not been tested so far. Finally, another gene is *SEP3*, since it has been reported to be a possible direct target of *SVP* during the flower development. Moreover, a role in promoting flowering was never reported for the *SEP* genes. It is possible that in absence of many other known floral promoters *SEP3* would significantly promote the floral transition. Therefore, *SVP* might control one or more genes that are still not reported to have a role in the floral transition. This has to be further investigated.

Conclusions

I set up a system in which the early phase of the floral transition in *Arabidopsis* can be induced and monitored in a controlled and synchronized way by shifting plants from SD to LD. I then collected shoot apical meristems (SAM) from wild-type Columbia with high tissue specificity by laser microdissection creating a time course during floral transition, and used the extracted RNA for global gene expression analysis through next generation sequencing.

Around 300 genes were identified as up-regulated during this process in 3 independent experiments. Global analysis highlighted a high enrichment in metabolic activity, especially for the protein synthesis processes. A group of novel genes from different functional categories were chosen to validate the gene expression data by *in situ* hybridisation. These experiments confirmed the increase in expression upon floral induction for several candidates, and showed novel spatial and temporal expression patterns in some cases. Particularly, I started to characterize four candidates among these novel genes by further experiments (see model in **Fig. 66**).

One is *C19*, a gene encoding a LRR protein, which is expressed broadly in the SAM but seems to respond to floral induction increasing in expression at the SAM. In the *ft tsf* double mutant, the increase in expression of this gene is strongly attenuated. Moreover, a putative loss of function of this gene, when crossed to *soc1 ful* double mutant, enhances the late flowering phenotype. Therefore, *C19* could be involved in the perception of the floral stimulus or in the response to it at the SAM. The second gene is *C11*, which encodes a member of the zinc finger homeodomain protein family, and is specifically up-regulated at the primordia on the flanks of the SAM, only in the presence of functional *FT* and *TSF*. This suggests that this gene is downstream of the photoperiodic cascade. Preliminary results with transgenic lines knocking-down several members of this homeodomain family show a moderate late flowering, that would suggest a redundant role played by *C11* together with other homologue genes in the control of the floral transition. The third is *D13*, a gene encoding a lipid desaturase, expressed in the center of the SAM upon photoperiodic induction. This gene is up-regulated independently of the presence of functional *FT* and *TSF* genes, suggesting the presence of a signal responding to inductive photoperiod that does not pass through the classical pathway activated by long-day. Additionally a fourth gene, *C23*, which does not have similarity to any known gene, is also expressed in the center of the meristem in a very restricted area upon photoperiodic induction, and this up-regulation is totally dependent on *FT/TSF*. Since some of the genes isolated by this approach were not previously identified by other global gene

Conclusions and perspectives

expression studies, the use of laser microdissection resulted in a successful method to increase sensitivity toward lowly expressed genes.

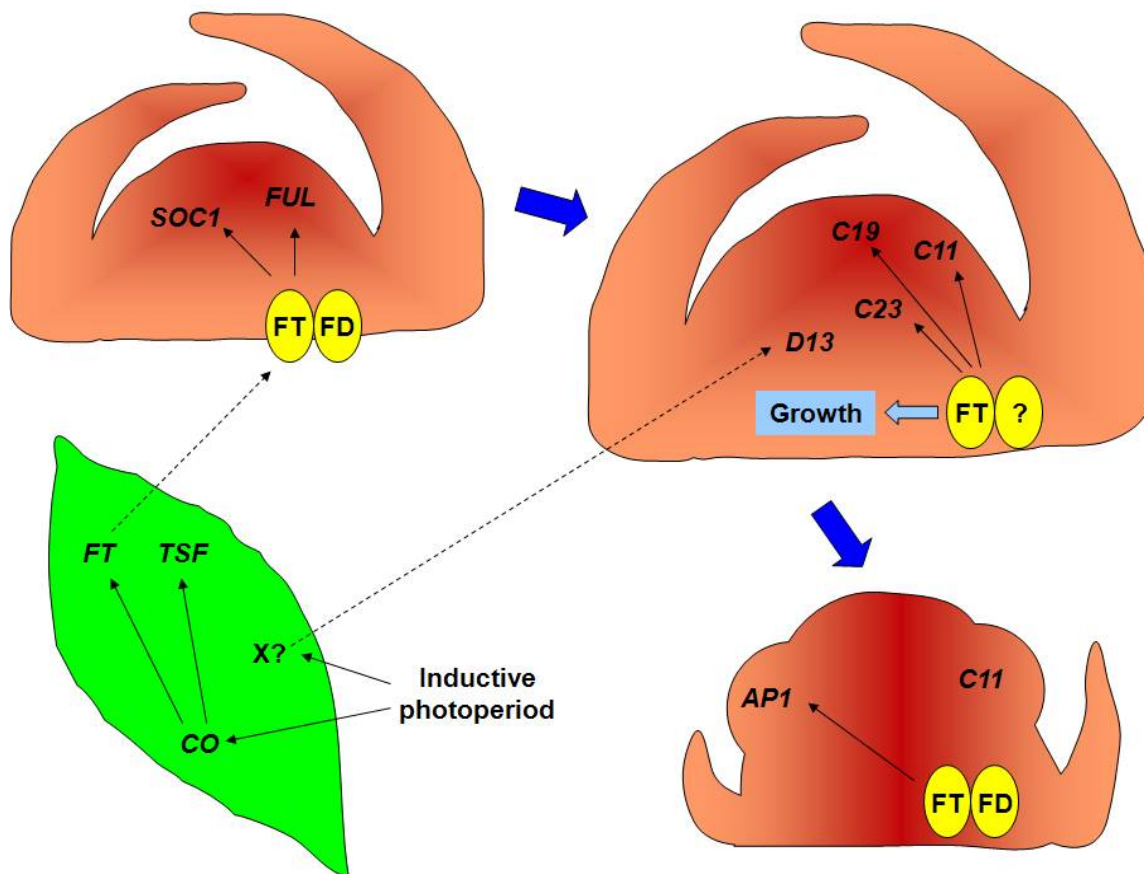


Fig 66. A model of the possible temporal and spatial interactions between flowering time genes and novel genes identified by this study. See text for details.

I also showed by genetic and expression studies that *SVP* transcription factor represses several floral promoter genes. These included *FT* and *SOC1*, as shown by other studies, and *TSF* and *FUL*, which are novel targets. In addition, I showed the spatial relationship of *SVP* with these genes: *FT* and *TSF* are repressed in the leaf, *SOC1* and *FUL* in the SAM. Furthermore, I found that in absence of *SVP* the presence of *FT* and *TSF* is not necessary to activate *SOC1*, but it only probably enhances this activation. I confirmed the dual role of *SVP* in leaf and meristem in repressing flowering using lines that mis-express this transcription factor in one or the other tissue. *SVP* activity in either organ

Conclusions and perspectives

has a partial effect on flowering, but these activities are synergistic so when combined in the same background much later flowering occurs. Finally, an *svp ft tsf soc1 ful* quintuple mutant showed that the absence of *SVP* still promotes flowering in this genetic background, and demonstrates that an additional or more unknown genes are repressed by *SVP* (see model in **Fig. 67**).

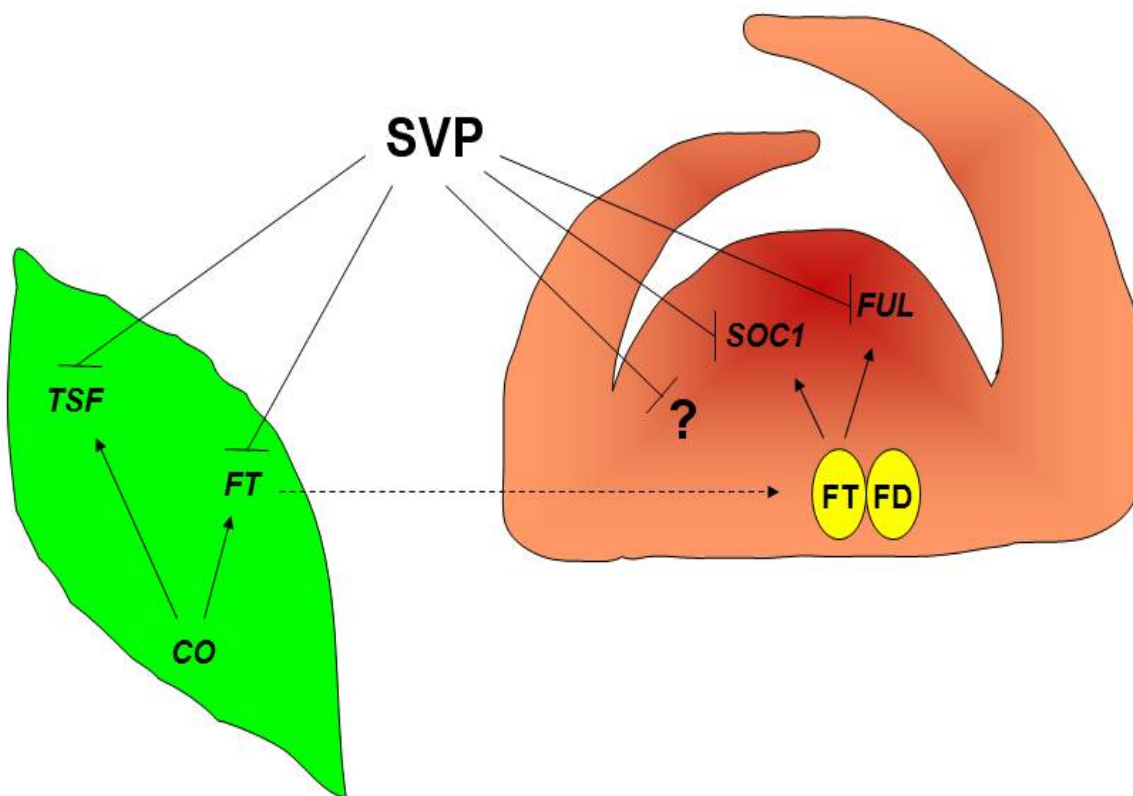


Fig 67. A model of the genetic and spatial interactions of the transcription factor *SVP* with floral promoter genes. See text for details.

Perspectives

In general, many loss of function mutations do not cause a phenotype due to genetic redundancy. Similarly, the redundant nature of the flowering pathways in *Arabidopsis* often makes it necessary to combine mutations in different loci to cause a clear phenotypic effect. Furthermore, because floral induction occurs late in plant development, mutation affecting earlier steps in development

Conclusions and perspectives

can have pleiotropic effects on flowering, confounding the identification of genes with a more direct effect. Therefore, identifying new genes involved in the floral transition in *Arabidopsis* can be a challenging task. Nonetheless, global gene expression analysis combined with genetic approaches can be very powerful. The initial approach that will be used on the most promising genes identified in this study, is to try to place them in the genetic hierarchy of the flowering pathways, testing their expression level and spatial pattern in mutants. Together with *ft tsf* double mutants, also *soc1 ful* double mutants, *svp*, and *tfl1* will be used, to reveal if there are epistatic interactions with these novel genes during the early phases of the floral induction. This will pinpoint which genes are likely to participate in the flowering network and place them relative to one another. Also transgenic approaches are in progress to ectopically express these genes using specific promoters, in order to investigate whether their over-expression is sufficient to cause a flowering phenotype. More detailed phenotypic analysis of meristem morphology during the floral transition in wild-type, mutants and transgenic plants may show that some of these genes do not affect flowering time but still have significant effects on meristem growth or development. A particular interest is also on the unknown signal that I proposed leads to a molecular response at the SAM when plants are shifted to inductive photoperiod in the absence of *FT* and *TSF*. Experimental approaches, together with the use of specific mutants, will be employed to identify the nature of this putative novel signal.

Another unknown factor to identify is the further gene or genes regulated by *SVP* in addition to *FT*, *TSF*, *SOC1* and *FUL*. Global gene expression analysis comparing the *svp ft tsf soc1 ful* quintuple mutant to the *ft tsf soc1 ful* quadruple mutant is a possible approach to try to address this question, in order to gain insight on possible novel genes involved in the floral transition.

References

- Abe M, Kobayashi Y, Yamamoto S, Daimon Y, Yamaguchi A, Ikeda Y, Ichinoki H, Notaguchi M, Goto K, Araki T. (2005) FD, a bZIP protein mediating signals from the floral pathway integrator FT at the shoot apex. *Science* 309, 1052-1056.
- Acevedo FG, Gamboa A, Paéz-Valencia J, Jiménez-García LF, Izaguirre-Sierra M, Alvarez-Buylla ER (2004) FLOR1, a putative interaction partner of the floral homeotic protein AGAMOUS, is a plant-specific intracellular LRR. *Plant Science* 167, 225-231.
- Adrian J, Torti S, Turck F (2009) From decision to commitment: the molecular memory of flowering. *Molecular Plant* 2, 628-642.
- Ahn JH, Miller D, Winter VJ, Banfield MJ, Lee JH, Yoo SY, Henz SR, Brady RL, Weigel D (2006) A divergent external loop confers antagonistic activity on floral regulators FT and TFL1. *The EMBO Journal* 25, 605-614.
- Aida M, Tasaka M (2006) Morphogenesis and patterning at the organ boundaries in the higher plant shoot apex. *Plant Mol Biol.* 60, 915-928.
- Alabadi D, Oyama T, Yanovsky MJ, Harmon FG, Más P, Kay SA (2001) Reciprocal regulation between TOC1 and LHY/CCA1 within the Arabidopsis circadian clock. *Science* 293, 880-883.
- Allison DB, Cui X, Page GP, Sabripour M (2006) Microarray data analysis: from disarray to consolidation and consensus. *Nature Reviews* 7, 55-65.
- Alonso JM, Strepanova AN, Leisse TJ, Kim CJ, Chen H, Shinn P, Stevenson DK, Zimmerman J, Barajas P, Cheuk R, et al. (2003) Genome-wide insertional mutagenesis of Arabidopsis thaliana. *Science* 301, 653-657.
- Al-Shahrour F, Minguez P, Tárraga J, Montaner D, Alloza E, Vaquerizas JMM, Conde L, Blaschke C, Vera J, Dopazo J (2006) BABELOMICS: a systems biology perspective in the functional annotation of genome-scale experiments. *Nucleic Acids Research* 34, W472-W476
- Altschul SF, Madden TL, Schäffer AA, Zhang J, Zhang Z, Miller W, Lipman DJ (1997) Gapped BLAST and PSI-BLAST: a new generation of protein database search programs. *Nucleic Acids Res.* 25, 3389-3402.
- An H, Roussot C, Suárez-López P, Corbesier L, Vincent C, Piñeiro M, Hepworth S, Mouradov A, Justin S, Turnbull C, Coupland G. (2004) CONSTANS acts in the phloem to regulate a systemic signal that induces photoperiodic flowering of Arabidopsis. *Development* 131, 3615-26.
- Aoyama T, Chua N-H (1997) A glucocorticoid-mediated transcriptional induction system in transgenic plants. *The Plant Journal* 11, 605-612
- The Arabidopsis genome initiative (2000) Analysis of the genome sequence of the flowering plant Arabidopsis thaliana. *Nature* 408, 796-815.
- Asano T, Masumura T, Kusano H, Kikuchi S, Kurita A, Shimada H, Kadowaki K (2002) Construction of a specialized cDNA library from plant cells isolated by laser capture microdissection: toward comprehensive analysis of the genes expressed in the rice phloem. *The Plant Journal* 32, 401-408
- Aukerman MJ, Sakai H (2003) Regulation of flowering time and floral organ identity by a microRNA and its APETALA2-like target genes. *Plant Cell* 15, 2730-2741.
- Ausin I, Alonso-Blanco C, Jarillo JA, Ruiz-García L, Martínez-Zapater JM (2004) Regulation of flowering time by FVE, a retinoblastoma-associated protein. *Nature Genetics* 36, 162-166.
- Ausín I, Alonso-Blanco C, Martínez-Zapater JM (2005) Environmental regulation of flowering. *Int J Dev Biol.* 49, 689-

References

705.

Balasubramanian S, Sureshkumar S, Lempe J, Weigel D (2006) Potent induction of *Arabidopsis thaliana* flowering by elevated growth temperature. *PLoS Genetics* 2, e106.

Bäurle I, Dean C (2006) The timing of developmental transitions in Plants. *Cell* 125, 655-664.

Bastow R, Mylne JS, Lister C, Lippman Z, Martienssen RA, Dean C (2004) Vernalization requires epigenetic silencing of FLC by histone methylation. *Nature* 427, 164-167.

Bennett S, Barnes C, Cox A, Davies L, Brown C (2005) Toward the 1,000 dollars human genome. *Pharmacogenomics* 6, 373-382.

Blázquez MA, Ahn JH, Weigel D (2003) A thermosensory pathway controlling flowering time in *Arabidopsis thaliana*. *Nat Genet.* 33, 168-71.

Blázquez MA, Ferrándiz C, Madueño F, Parcy F (2006) How floral meristem are built. *Plant Molecular Biology* 60, 855-870.

Blázquez MA, Green R, Nilsson O, Sussman MR, Weigel D (1998) Gibberellins promote flowering of *Arabidopsis* by activating the LEAFY promoter. *Plant Cell* 10, 791-800.

Blázquez MA, Soowal LN, Lee I, Weigel D (1997) LEAFY expression and flower initiation in *Arabidopsis*. *Development* 124, 3835-3844.

Blázquez MA, Weigel D. (2000) Integration of floral inductive signals in *Arabidopsis*. *Nature* 404, 889-892.

Borner R, Kampmann G, Chandler J, Gleissner R, Wisman E, Apel K, Melzer S. (2000) A MADS domain gene involved in the transition to flowering in *Arabidopsis*. *Plant J.* 24, 591-9.

Boss PK, Bastow RM, Mylne JS, Dean C (2004) Multiple pathways in the decision to flower: enabling, promoting, and resetting. *Plant Cell* 16, S18-31.

Bowman JL, Alvarez J, Weigel D, Meyerowitz EM, Smyth DR (1993) Control of flower development in *Arabidopsis thaliana* by APETALA1 and interacting genes. *Development* 119, 721-743.

Böhlenius H, Huang T, Charbonnel-Campaa L, Brunner AM, Jansson S, Strauss SH, Nilsson O (2006) CO/FT regulatory module controls timing of flowering and seasonal growth cessation in trees. *Science* 312, 1040-1043.

Bradley D, Ratcliffe O, Vincent C, Carpenter R, Coen E (1997) Inflorescence commitment and architecture in *Arabidopsis*. *Science* 275, 80-83.

Brenner S, Johnson M, Bridgham J, Golda G, Lloyd DH, Johnson D, Luo S, McCurdy S, Foy M, Ewan M, et al. (2000) Gene expression analysis by massively parallel signature sequencing (MPSS) on microbead arrays. *Nat. Biotechnol.* 18, 630-634.

Brooks III L, Strable J, Zhang X, Ohtsu K, Zhou R, Sarkar A, Hargreaves S, Elshire RJ, et al. (2009) Microdissection of shoot meristem functional domains. *PLoS Genetics* 5, e1000476.

Bünning E (1936) Die endogene Tagesrhythmie als Grundlage der photoperiodischen Reaktion. *Ber. Dtsch. Bot. Ges.* 54, 590-607.

Cardon G, Höhmann S, Klein J, Nettekheim K, Saedler H, Huijser P (1999) Molecular characterization of the *Arabidopsis* SBP-box genes. *Gene* 237, 91-104.

Cardon GH, Höhmann S, Nettekheim K, Saedler H, Huijser P (1997) Functional analysis of the *Arabidopsis thaliana* SBP-box gene SPL3: a novel gene involved in the floral transition. *The Plant Journal* 12, 367-377.

References

- Carles CC, Fletcher JC (2003) Shoot apical meristem maintenance: the art of a dynamic balance. *Trends Plant Sci.* 8, 394-401.
- Castillejo C, Pelaz S (2008) The balance between CONSTANS and TEMPRANILLO activities determines FT expression to trigger flowering. *Current Biology* 18, 1338-1343.
- Cerdan PD, Chory J (2003). Regulation of flowering time by light quality. *Nature* 423, 881–885.
- Chardon F, Damerval C (2005) Phylogenomic analysis of the PEBP gene family in cereals. *J. Mol. Evol.* 61, 579-590.
- Chen X (2004) A microRNA as a translational repressor of APETALA2 in Arabidopsis flower development. *Science* 303, 2022-2025.
- Chiang GCK, Barua D, Kramer EM, Amasino RM, Donohue K (2009) Major flowering time gene, FLOWERING LOCUS C, regulates seed germination in Arabidopsis thaliana. *Proc. Natl. Acad. Sci. USA* 106, 11661-11666.
- Chuck G, Cigan AM, Saeteurn K, Hake S (2007) The heterochronic maize mutant Corngrass1 results from overexpression of a tandem microRNA. *Nature Genetics* 39, 544-549.
- Clark SE (2001) Cell signalling at the shoot meristem. *Nat. Rev. Mol. Cell. Biol.* 2, 276-284.
- Clark SE, Williams RW, Meyerowitz EM (1997) The CLAVATA1 gene encodes a putative receptor kinase that controls shoot and floral meristem size in Arabidopsis. *Cell* 89, 575-585.
- Cloonan N, Forrest ARR, Kolle G, Gardiner BBA, Faulkner GJ, Brown MK, Taylor DF, Steptoe AL, et al. (2008) Stem cell transcriptome profiling via massive-scale mRNA sequencing. *Nature Methods* 5, 613-619.
- Clough SJ, Bent AF (1998) Floral dip: a simplified method for Agrobacterium-mediated transformation of Arabidopsis thaliana. *Plant J.* 16,735-743.
- Coen ES, Meyerowitz EM (1991) The war of the whorls: genetic interactions controlling flower development. *Nature* 353, 31-37.
- Conti L, Bradley D (2007) TERMINAL FLOWER1 is a mobile signal controlling Arabidopsis architecture. *The Plant Cell* 19, 767-778.
- Corbesier L, Coupland G (2005) Photoperiodic flowering of Arabidopsis: integrating genetic and physiological approaches to characterization of the floral stimulus. *Plant, Cell and Environment* 28, 54-66.
- Corbesier L, Coupland G. (2006) The quest for florigen: a review of recent progress. *J. Exp. Bot.* 57, 3395-403.
- Corbesier L, Gadiisseur I, Silvestre G, Jacquard A, Bernier G (1996) Design in Arabidopsis thaliana of a synchronous system of floral induction by one long day. *The Plant Journal* 9, 947-952.
- Corbesier L, Lejeune P, Bernier G (1998) The role of carbohydrates in the induction of flowering in Arabidopsis thaliana: comparison between the wild type and a starchless mutant. *Planta* 206, 131-137.
- Corbesier L, Prinsen E, Jacquard A, Lejeune P, Van Onckelen H, Périlleux C, Bernier G (2003) Cytokinin levels in leaves, leaf exudate and shoot apical meristem of Arabidopsis thaliana during floral transition. *J. Exp. Bot.* 54, 2511-2517.
- Corbesier L, Vincent C, Jang S, Fornara F, Fan Q, Searle I, Giakountis A, Farrona S, Gissot L, Turnbull C, Coupland G. (2007) FT protein movement contributes to long-distance signaling in floral induction of Arabidopsis. *Science* 316, 1030-1033.
- Czechowski T, Stitt M, Altmann T, Udvardi MK, Scheible W-R (2005) Genome-wide identification and testing of superior reference genes for transcript normalization in Arabidopsis. *Plant Physiology* 139, 5-17.

References

- Danilevskaya ON, Meng X, Selinger DA, Deschamps S, Hermon P, Vansant G, Gupta R, Ananiev EV, Muszynski MG. (2008) Involvement of the MADS-box gene ZMM4 in floral induction and inflorescence development in Maize. *Plant Physiology* 147, 2054-2069.
- Davis SJ (2009) Integrating hormones into the floral-transition pathway of *Arabidopsis thaliana*. *Plant Cell Environ.* 32, 1201-1210.
- Diévert A, Clark SE (2004) LRR-containing receptors regulating plant development and defense. *Development* 131, 251-261.
- Dodsworth S (2009) A diverse and intricate signalling network regulates stem cell fate in the shoot apical meristem. *Developmental Biology* 336, 1-9.
- Edwards K, Johnstone C, Thompson C (1991) A simple and rapid method for the preparation of plant genomic DNA for PCR analysis. *Nucleic Acids Research* 19, 1349.
- Elhiti M, Stasolla C (2009) Structure and function of homodomain-leucine zipper (HD-Zip) proteins. *Plant Signal Behav.* 4, 86-88.
- Eriksson S, Böhlenius H, Moritz T, Nilsson O (2006) GA₄ is the active gibberellin in the regulation of LEAFY transcription and *Arabidopsis* floral initiation. *Plant Cell* 18, 2172-2181.
- Ferrándiz C, Gu Q, Martienssen R, Yanofsky MF (2000) Redundant regulation of meristem identity and plant architecture by FRUITFULL, APETALA1 and CAULIFLOWER. *Development* 127, 725-34.
- Ferrari S, Galletti R, Vairo D, Cervone F, De Lorenzo G (2006) Antisense expression of the *Arabidopsis thaliana* AtPGIP1 gene reduces polygalacturonase-inhibiting protein accumulation and enhances susceptibility to *Botrytis cinerea*. *Mol. Plant Microbe Interact.* 19, 931-936.
- Fornara F, Coupland G (2009) Plant phase transitions make a SPLash. *Cell* 138, 625-627.
- Fornara F, Gregis V, Pelucchi N, Colombo L, Kater M (2008) The rice StMADS11-like genes OsMADS22 and OsMADS47 cause floral reversions in *Arabidopsis* without complementing the *svp* and *agl24* mutants. *J Exp Bot.* 59, 2181-2190.
- Fornara F, Panigrahi KCS, Gissot L, Sauerbrunn N, Rühl M, Jarillo JA, Coupland G (2009) *Arabidopsis* DOF transcription factors act redundantly to reduce CONSTANS expression and are essential for a photoperiodic flowering response. *Developmental Cell* 17, 75-86.
- Fowler S, Lee K, Onouchi H, Samach A, Richardson K, Morris B, Coupland G, Putterill J (1999) GIGANTEA: a circadian clock-controlled gene that regulates photoperiodic flowering in *Arabidopsis* and encodes a protein with several possible membrane-spanning domains. *EMBO Journal* 18, 4679-4688.
- Fujita H, Takemura M, Tani E, Nemoto K, Yokota A, Kohchi T (2003) An *Arabidopsis* MADS-box protein, AGL24, is specifically bound to and phosphorylated by meristematic receptor-like kinase (MRLK). *Plant Cell Physiol.* 44, 735-742.
- Fullwood MJ, Wei C-L, Liu ET, Ruan Y (2009) Next-generation DNA sequencing of paired-end tags (PET) for transcriptome and genome analyses. *Genome Research* 19, 521-532.
- Fujiwara S, Oda A, Yoshida R, Niinuma K, Miyata K, Tomozoe Y, Tajima T, Nakagawa M, Hayashi K, Coupland G, Mizoguchi T. (2008) Circadian Clock Proteins LHY and CCA1 Regulate SVP Protein Accumulation to Control Flowering in *Arabidopsis*. *The Plant Cell* 20, 2960-2971.
- Gandikota M, Birkenbihl RP, Hohmann S, Cardon GH, Saedler H, Huijser P (2007) The miRNA156/157 recognition element in the 3' UTR of the *Arabidopsis* SBP box gene SPL3 prevents early flowering by translational inhibition in seedlings. *The Plant Journal* 49, 683-693.

References

- Gamboa A, Paéz-Valencia J, Acevedo GF, Vázquez-Moreno L, Alvarez-Buylla RE (2001) Floral transcription factor AGAMOUS interacts in vitro with a leucine-rich repeat and an acid phosphatase protein complex. *Biochem. Biophys. Res. Commun.* 288, 1018-1026.
- Geier F, Lohmann JU, Gerstung M, Maier AT, Timmer J, Fleck C (2008) A quantitative and dynamic model for plant stem cell regulation. *PLoS One* 3, e3553.
- Gendall AR, Levy YY, Wilson A, Dean C. (2001) The VERNALIZATION 2 gene mediates the epigenetic regulation of vernalization in Arabidopsis. *Cell* 107, 525-35.
- Gentleman R, Carey VJ, Huber W, Irizarry RA, Dudoit S (2005) Bioinformatics and computational biology solutions using R and Bioconductor. Springer Verlag.
- Giakountis A., Coupland G. (2008) Phloem transport of flowering signals. *Current Opinion in Plant Biology* 11, 1-8.
- Ginsberg SD. (2005) RNA amplification strategies for small sample populations. *Methods* 37, 229-37.
- Gocal GFW, Sheldon CC, Gubler F, Moritz T, Bagnall DJ, MacMillan CP, Li SF, Parish RW, Dennis ES, Weigel D, King RW (2001) GAMYB-like genes, flowering, and gibberellin signaling in Arabidopsis. *Plant Physiology* 127, 1682-1693.
- Grandjean O, Vernoux T, Laufs P, Belcram K, Mizukami Y, Traas J (2004) In vivo analysis of cell division, cell growth, and differentiation at the shoot apical meristem in Arabidopsis. *Plant Cell* 16, 74-87.
- Grant GR, Manduchi E, Stoeckert CJ Jr (2007) Analysis and management of microarray gene expression data. *Curr Protoc Mol Biol.* Chapter 19, Unit 19.6.
- Greb T, Mylne JS, Crevillen P, Geraldo N, An H, et al. (2007) The PHD finger protein VRN5 functions in the epigenetic silencing of Arabidopsis FLC. *Current Biology* 17, 73-78.
- Gregis V, Sessa A, Colombo L, Kater MM (2006) AGL24, SHORT VEGETATIVE PHASE, and APETALA1 redundantly control AGAMOUS during early stages of flower development in Arabidopsis. *The Plant Cell* 18, 1373-1382.
- Gregis V, Sessa A, Colombo L, Kater MM. (2008) AGAMOUS-LIKE24 and SHORT VEGETATIVE PHASE determine floral meristem identity in Arabidopsis. *The Plant Journal* 56, 891-902.
- Gregis V, Sessa A, Dorca-Fornell C, Kater MM (2009) The Arabidopsis floral meristem identity genes AP1, AGL24 and SVP directly repress class B and C floral homeotic genes. *The Plant Journal* 60, 626-637.
- Gu Q, Ferrándiz C, Yanofsky MF, Martienssen R. (1998) The FRUITFULL MADS-box gene mediates cell differentiation during Arabidopsis fruit development. *Development* 125, 1509-17.
- Gustafson-Brown C, Savidge B, Yanofsky MF (1994) Regulation of the Arabidopsis floral homeotic gene APETALA1. *Cell* 76, 131-143.
- Gyllenstrand N, Clapham D, Källman T, Lagercrantz U (2007) A Norway spruce flowering locus T homolog is implicated of control of growth rhythm in conifers. *Plant Physiol.* 144, 248-257.
- Haerizadeh F, Wong CE, Singh MB, Bhalla PL. (2008) Genome-wide analysis of gene expression in soybean shoot apical meristem. *Plant Mol. Biol.* 69, 711-727.
- Halliday K, Salter MG, Thingnaes E, Whitelam GC. (2003). Phytochrome control of flowering is temperature sensitive and correlates with expression of the floral integrator FT. *Plant J.* 33, 875-885.
- Hanzawa Y, Money T, Bradley D. (2005) A single amino acid converts a repressor to an activator of flowering. *Proc Natl Acad Sci U S A* 102, 7748-53.

References

- Harmer SL (2009) The circadian system in higher plants. *Annu. Rev. Plant Biol.* 60, 357-377.
- Hartmann U, Höhmann S, Nettekheim K, Wisman E, Saedler H, Huijser P (2000) Molecular cloning of SVP: a negative regulator of the floral transition in Arabidopsis. *The Plant Journal* 21(4), 351-360.
- He Y, Michaels S, Amasino MR (2003) Regulation of flowering time by histone acetylation in Arabidopsis. *Science* 302, 1751-1754.
- He Y, Tang RH, Hao Y, Stevens RD, Cook CW et al. (2004) Nitric oxide represses the Arabidopsis floral transition. *Science* 305, 1968-1971.
- Helliwell CA, Wood CC, Robertson M, Peacock WJ, Dennis ES (2006) The Arabidopsis FLC protein interacts directly in vivo with SOC1 and FT chromatin and is part of a high-molecular-weight protein complex. *The Plant Journal* 46, 183-192.
- Hempel FD, Feldman LJ (1995) Specification of chimeric flowering shoots in wild-type Arabidopsis. *Plant Journal* 8, 725-731.
- Hempel FD, Weigel D, Mandel MA, Ditta G, Zambryski PC, Feldman LJ, Yanofsky MF. (1997) Floral determination and expression of floral regulatory genes in Arabidopsis. *Development* 124, 3845-3853.
- Hepworth SR, Valverde F, Ravenscroft D, Mouradov A, Coupland G (2002) Antagonistic relation of flowering-time gene SOC1 by CONSTANS and FLC via separate promoter motifs. *EMBO Journal* 21, 4327-4337.
- Hisamatsu T, King RW (2008) The nature of floral signals in Arabidopsis. II. Roles for FLOWERING LOCUS T (FT) and gibberellin. *J. Exp. Bot.* 59, 3821-3829.
- Hong RL, Hamaguchi L, Busch MA, Weigel D (2003) Regulatory elements of the floral homeotic gene AGAMOUS identified by phylogenetic footprinting and shadowing. *Plant Cell* 15, 1296-1309.
- Hsieh MH, Goodman HM (2005) A novel gene family in Arabidopsis encoding putative heptahelical transmembrane proteins homologous to human adiponectin receptors and progesterin receptors. *J Exp Bot.* 56, 3137-3147.
- Hua W, Zhang L, Liang S, Jones RL, Lu Y-T (2004) A tobacco calcium/calmodulin-binding protein kinase functions as a negative regulator of flowering. *J. Biol. Chem.* 279, 31483-31494.
- Huq E, Tepperman JM, Quail PH. (2000) GIGANTEA is a nuclear protein involved in phytochrome signaling in Arabidopsis. *Proc Natl Acad Sci U S A.* 97, 9789-94.
- Imaizumi T (2010) Arabidopsis circadian clock and photoperiodism: time to think about location. *Current Opinion in Plant Biology* 13, 83-89.
- Imaizumi T, Tran HG, Swartz TE, Briggs WR, Kay SA. (2003) FKF1 is essential for photoperiodic-specific light signalling in Arabidopsis. *Nature* 426, 302-6.
- Inada N, Wildermuth MC. (2005) Novel tissue preparation method and cell-specific marker for laser microdissection of Arabidopsis mature leaf. *Planta* 221, 9-16.
- Ingram GC, Goodrich J, Wilkinson MD, Simon R, Haughn GW, Coen ES (1995) Parallels between UNUSUAL FLORAL ORGANS and FIMBRIATA, genes controlling flower development in Arabidopsis and Antirrhinum. *Plant Cell* 7, 1501-1510.
- Irish VF, Sussex IM. (1990) Function of the apetala1 gene during Arabidopsis floral development. *Plant Cell* 2, 741-753.
- Jack T (2001) Relearning our ABCs: new twists on an old model. *Trends Plant Sci.* 6, 310-316.
- Jacqumard A, Gadisseur I, Bernier G (2003) Cell division and morphological changes in the shoot apex of Arabidopsis

References

- thaliana during floral transition. *Annals of Botany* 91, 571-576.
- Jacobsen SE, Olszewski NE (1993) Mutations at the SPINDLY locus of Arabidopsis alter gibberellin signal transduction. *Plant Cell* 5, 887-896.
- Jaeger KE, Wigge P (2007) FT protein acts as a long-range signal in Arabidopsis. *Current Biology* 17, 1050-1054.
- Jang S, Lee B, Kim C, Kim SJ, Yim J, Han JJ, Lee S, Kim SR, An G (2003) The OsFOR1 gene encodes a polygalacturonase-inhibiting protein (PGIP) that regulates floral organ number in rice. *Plant Mol Biol.* 53, 357-369.
- Jang S, Marchal V, Panigrahi KCS, Wenkel S, Soppe W, Deng X-W, Valverde F, Coupland G. (2008) Arabidopsis COP1 shapes the temporal pattern of CO accumulation conferring a photoperiodic flowering response. *The EMBO journal* 27, 1277-1288.
- Jang S, Torti S, Coupland G (2009) Genetic and spatial interactions between FT, TSF, and SVP during the early stages of floral induction in Arabidopsis. *The Plant Journal* 60, 614-625.
- Jiao Y, Tausta SL, Gandotra N, Sun N, Liu T, Clay NK, Ceserani T, et al. (2009) A transcriptome atlas of rice cell types uncovers cellular, functional and developmental hierarchies. *Nature Genetics* 41, 258-263.
- Johanson U, West J, Lister C, Michaels S, Amasino R, Dean C. (2000) Molecular analysis of FRIGIDA, a major determinant of natural variation in Arabidopsis flowering time. *Science* 290, 344-7.
- Jung J-H, Seo Y-H, Seo PJ, Reyes JL, Yun J, Chua N-H, Park C-M (2007) The GIGANTEA-regulated microRNA172 mediates photoperiodic flowering independent of CONSTANS in Arabidopsis. *The Plant Cell* 19, 2736-2748.
- Kachroo A, Shanklin J, Whittle E, Lapchyk L, Hildebrand D, Kachroo P (2007) The Arabidopsis stearoyl-acyl carrier protein-desaturase family and the contribution of leaf isoforms to oleic acid synthesis. *Plant Molecular Biology* 63, 257-271.
- Kachroo P, Shanklin J, Shah J, Whittle E, Klessig DF (2001) A fatty acid desaturase modulates the activation of defense signaling pathways in plants. *Proc Natl Acad Sci U S A* 98, 9448-9453.
- Kardailsky I, Shukla VK, Ahn JH, Dagenais N, Christensen SK, Nguyen JT, Chory J, Harrison MJ, Weigel D. (1999) Activation tagging of the floral inducer FT. *Science* 286, 1962-5.
- Kehr J (2003). Single cell technology. *Current Opinion in Plant Biology* 6, 617-621.
- Kempin SA, Savidge B, Yanofsky MF. (1995) Molecular basis of the cauliflower phenotype in Arabidopsis. *Science* 267, 522-525.
- Kerk NM, Ceserani T, Tausta SL, Sussex IM, Nelson TM (2003) Laser Capture Microdissection of cells from plant tissues. *Plant physiology* 132, 27-35.
- Kim D-H, Doyle MR, Sung S, Amasino RM (2009) Vernalization: winter and the timing of flowering in plants. *Annu. Rev. Cell Dev. Biol.* 25, 277-299.
- Kim WY, Fujiwara S, Suh SS, Kim J, Kim Y, Han L, David K, Putterill J, Nam HG, Somers DE. (2007) ZEITLUPE is a circadian photoreceptor stabilized by GIGANTEA in blue light. *Nature* 449, 356-360.
- King RW, Hisamatsu T, Goldschmidt EE, Blundell C (2008) The nature of floral signals in Arabidopsis. I. Photosynthesis and a far-red photoresponse independently regulate flowering by increasing expression of FLOWERING LOCUS T (FT). *J. Exp. Bot.* 59, 3811-3820.
- Knott JE. (1934) Effect of a localized photoperiod on spinach. *Proc. Am. Soc. Hort. Sci.* 31, 152-4.
- Kobayashi Y, Kaya H, Goto K, Iwabuchi M, Araki T. (1999) A pair of related genes with antagonistic roles in mediating flowering signals. *Science* 286, 1960-2.

References

- Kobayashi Y, Weigel D (2007) Move on up, it's time for change--mobile signals controlling photoperiod-dependent flowering. *Genes Dev.* 21, 2371-2384.
- Koornneef M, Alonso-Blanco C, Blankestijn-de Vries H, Hanhart CJ, Peeters AJ. (1998) Genetic interactions among late-flowering mutants of *Arabidopsis*. *Genetics* 148, 885-92.
- Koornneef M, Hanhart CJ, van der Veen JH. (1991) A genetic and physiological analysis of late flowering mutants in *Arabidopsis thaliana*. *Mol Gen Genet.* 229, 57-66.
- Koornneef M, Meinke D (2010) The development of *Arabidopsis* as a model plant. *Plant J.* 61, 909-921.
- Koornneef M, Van der Veen JH (1980) Induction and analysis of gibberellin sensitive mutants in *Arabidopsis thaliana* (L) Heynh. *Theoretical and Applied Genetics* 58, 257-263.
- Kotake T, Takada S, Nakahigashi K, Ohto M, Goto K (2003) *Arabidopsis* TERMINAL FLOWER 2 gene encodes a Heterochromatin Protein 1 homolog and represses both FLOWERING LOCUS T to regulate flowering time and several floral homeotic genes. *Plant Cell Physiology* 44, 555-564.
- Krizek BA, Fletcher JC (2005) Molecular mechanisms of flower development: an armchair guide. *Nat. Rev. Genet.* 6, 688-698.
- Kuusk S, Sohlberg JJ, Magnus Eklund D, Sundberg E (2006) Functionally redundant SHI family genes regulate *Arabidopsis* gynoecium development in a dose-dependent manner. *Plant J.* 47, 99-111.
- Kwiatkowska D (2008) Flowering and apical meristem growth dynamics. *Journal of Experimental Botany* 59, 187-201.
- Larsson AS, Landberg K, Meeks-Wagner DM (1998) The TERMINAL FLOWER 2 (TFL2) gene controls the reproductive transition and meristem identity in *Arabidopsis thaliana*. *Genetics* 149, 597-605.
- Laubinger S, Marchal V, Gentilhomme J, Wenkel S, Adrian J, Jang S, Kulajta C, Braun H, Coupland G, Hoecker U (2006) *Arabidopsis* SPA proteins regulate photoperiodic flowering and interact with the floral inducer CONSTANS to regulate its stability. *Development* 133, 3213-3222.
- Laufs P, Grandjean O, Jonak C, Kiêu K, Traas J (1998) Cellular parameters of the shoot apical meristem in *Arabidopsis*. *Plant Cell* 10, 1375-1389.
- Laux T, Mayer KFX, Berger J, Jurgens G (1996) The WUSCHEL gene is required for shoot and floral meristem integrity in *Arabidopsis*. *Development* 122, 87-96.
- Lee I, Aukerman MJ, Gore SL, Lohman KN, Michaels SD, Weaver LM, John MC, Feldmann KA, Amasino RM (1994) Isolation of LUMINIDEPENDENS: a gene involved in the control of flowering time in *Arabidopsis*. *Plant Cell* 6, 75-83.
- Lee H, Suh SS, Park E, Cho E, Ahn JH, Kim SG, Lee JS, Kwon YM, Lee I. (2000) The AGAMOUS-LIKE 20 MADS domain protein integrates floral inductive pathways in *Arabidopsis*. *Genes Dev.* 14, 2366-2376.
- Lee H, Yoo SJ, Lee JH, Kim W, Yoo SK, Fitzgerald H, Carrington JC, Ahn JH (2010) Genetic framework for flowering-time regulation by ambient temperature-responsive miRNAs in *Arabidopsis*. *Nucleic Acids Research*, ahead of print.
- Lee JH, Park SH, Lee JS, Ahn JH (2007a) A conserved role of SHORT VEGETATIVE PHASE (SVP) in controlling flowering time of Brassica plants. *Biochim. Biophys. Acta* 1769, 455-461.
- Lee JH, Yoo SJ, Park AH, Hwang I, Lee JS, Ahn JH (2007b) Role of SVP in the control of flowering time by ambient temperature in *Arabidopsis*. *Genes & Development* 21, 397-402.
- Lee S, Choi SC, An G (2008a) Rice SVP-group MADS-box proteins, OsMADS22 and OsMADS55, are negative

References

- regulators of brassinosteroid responses. *Plant J.* 54, 93-105.
- Lee J, Oh M, Park H, Lee I. (2008b) SOC1 translocated to the nucleus by interaction with AGL24 directly regulates LEAFY. *Plant Journal* 55, 832-843.
- Lenhard M, Bohnert A, Jurgens G, Laux T (2001) Termination of stem cell maintenance in Arabidopsis floral meristems by interactions between WUSCHEL and AGAMOUS. *Cell* 105, 805-814.
- Levy YY, Mesnage S, Mylne JS, Gendall AR, Dean C. (2002) Multiple roles of Arabidopsis VRN1 in vernalization and flowering time control. *Science* 297, 243-6.
- Li J, Chory J (1997) A putative leucine-rich repeat receptor kinase involved in brassinosteroid signal transduction. *Cell* 90, 929-938.
- Li H, Durbin R (2009) Fast and accurate short read alignment with Burrows-Wheeler transform. *Bioinformatics* 25, 1754-1760.
- Li D, Liu C, Shen L, Wu Y, Chen H, Robertson M, Helliwell CA, Ito T, Meyerowitz E, Yu H. (2008) A Repressor Complex Governs the Integration of Flowering Signals in Arabidopsis. *Developmental Cell* 15, 110-120.
- Lifschitz E, Eviatar T, Rozman A, Shalit A, Goldschmidt A, Amsellem Z, Alvarez JP, Eshed Y (2006) The tomato FT ortholog triggers systemic signals that regulate growth and flowering and substitute for diverse environmental stimuli. *Proc Natl Acad Sci U S A* 103, 6398-6403.
- Liljegren SJ, Gustafson-Brown C, Pinyopich A, Ditta GS, Yanofsky MF (1999) Interactions among APETALA1, LEAFY, and TERMINAL FLOWER1 specify meristem fate. *Plant Cell* 11, 1007-1018.
- Lim M-H, Kim J, Kim Y-S, Chung K-S, Seo Y-H, Lee I, Kim I, Kim J, Hong CB, Kim H-J, Park C-M (2004) A new Arabidopsis gene, FLK, encodes an RNA binding protein with K homology motifs and regulates flowering via FLOWERING LOCUS C. *Plant Cell* 16, 731-740.
- Lin MK, Belanger H, Lee YJ, Varkonyi-Gasic E, TaokaKI, Miura E, Xaconostle-Cázares B, Gendler K, Jorgensen RA, Phinney B, Lough TJ, Lucas WJ. (2007) FLOWERING LOCUS T protein may act as the long-distance florigenic signal in the Cucurbits. *Plant Cell* 19, 1488-1506.
- Lincoln C, Long J, Yamaguchi J, Serikawa K, Hake S (1994) A knotted1-like homeobox gene in Arabidopsis is expressed in the vegetative meristem and dramatically alters leaf morphology when overexpressed in transgenic plants. *Plant Cell* 6, 1859-1876.
- Liu C, Hongyan C, Hong LE, Hui MS, Kumar PP, Han J-H, Yih CL, Hao Y. (2008) Direct interaction of AGL24 and SOC1 integrates flowering signals in Arabidopsis. *Development* 135, 1481-1491.
- Liu C, Thong Z, Yu H (2009a) Coming into bloom: the specification of floral meristems. *Development* 136, 3379-3391.
- Liu C, Xi W, Shen L, Tan C, Yu H (2009b) Regulation of floral patterning by flowering time genes. *Developmental Cell* 16, 711-722.
- Liu C, Zhou J, Bracha-Drori K, Yalovsky S, Ito T, Yu H (2007) Specification of Arabidopsis floral meristem identity by repression of flowering time genes. *Development* 134, 1901-1910.
- Liu F, Marquardt S, Lister C, Swiezewski S, Dean C (2010) Targeting 3' processing of antisense transcripts triggers Arabidopsis FLC chromatin silencing. *Science* 327, 94-96.
- Locke JC, Southern MM, Kozma-Bognar L, Hibberd V, Brown PE, et al. (2005) Extension of a genetic network model by iterative experimentation and mathematical analysis. *Mol. Syst. Biol.* 1, 2005.0013.
- Lohmann JU, Hong RL, Hobe M, Busch MA, Parcy F, Simon R, Weigel D (2001) A molecular link between stem cell regulation and floral patterning in Arabidopsis. *Cell* 105, 793-803.

References

- Long J, Barton MK. (2000) Initiation of axillary and floral meristems in Arabidopsis. *Dev Biol.* 218, 341-53.
- Long JA, Moan EI, Medford JI, Barton MK (1996) A member of the KNOTTED class of homeodomain proteins encoded by the STM gene of Arabidopsis. *Nature* 379, 66-69.
- Lyndon RF (1998) The shoot apical meristem: its growth and development. Cambridge University Press, Cambridge.
- Macknight R, Bancroft I, Page T, Lister C, Schmidt R, Love K, Westphal L, Murphy G, Sherson S, Cobbett C, Dean C (1997) FCA, a gene controlling flowering time in Arabidopsis, encodes a protein containing RNA-binding domains. *Cell* 89, 737-745.
- Macknight R, Duroux M, Laurie R, Dijkwel P, Simpson G, Dean C (2002) Functional significance of the alternative transcript processing of the Arabidopsis floral promoter FCA. *Plant Cell* 14, 877-888.
- Mandel MA, Gustafson-Brown C, Savidge B, Yanofsky MF. (1992) Molecular characterization of the Arabidopsis floral homeotic gene APETALA1. *Nature* 360, 273-277.
- Mandel MA, Yanofsky MF. (1995a) The Arabidopsis AGL8 MADS box gene is expressed in inflorescence meristems and is negatively regulated by APETALA1. *The Plant Cell* 7, 1763-1771.
- Mandel MA, Yanofsky MF (1995b) A gene triggering flower formation in Arabidopsis. *Nature* 377, 522-524.
- Mardis ER. (2008) Next-Generation DNA Sequencing Methods. *Annu. Rev. Genomics Hum. Genet.* 9, 387-402.
- Margulies M, Egholm M, Altman W, Attiya S, Bader J, Bemben L, Berka J, Braverman M, Chen Y, Chen Z, et al. (2005) Genome sequencing in microfabricated high-density picolitre reactors. *Nature* 437, 376-380.
- Marioni JC, Mason CE, Mane SM, Stephens M, Gilad Y. (2008) RNA-Seq: An assessment of technical reproducibility and comparison with gene expression arrays. *Genome Res.* 18, 1509-1517.
- Masiero S, Li MA, Will I, Hartmann U, Saedler H, Huijser P, Schwarz-Sommer Z, Sommer H (2004) INCOMPOSITA: a MADS-box gene controlling prophyll development and floral meristem identity in *Antirrhinum*. *Development* 131, 5981-5990.
- Mathieu J, Yant LJ, Mürdter F, Küttner F, Schmid M (2009) Repression of flowering by the miR172 target SMZ. *PLOS Biology* 7, e1000148.
- Mathieu J, Warthmann N, Küttner F, Schmid M (2007) Export of FT protein from phloem companion cells is sufficient for floral induction in Arabidopsis. *Current Biology* 17, 1055-1060.
- Mayer KFX, Schoof H, Haecker A, Lenhard M, Jurgens G, Laux T (1998) Role of WUSCHEL in regulating stem cell fate in the Arabidopsis shoot meristem. *Cell* 95, 805-815.
- Melzer S, Majewski DM, Apel K. (1990) Early Changes in Gene Expression during the Transition from Vegetative to Generative Growth in the Long-Day Plant *Sinapis alba*. *Plant Cell* 2, 953-961.
- Melzer S, Lens S, Gennen J, Vanneste S, Rohde A, Beeckman T. (2008) Flowering-time genes modulate meristem determinacy and growth form in Arabidopsis thaliana. *Nature Genetics* 40, 1489-1492.
- Meyers BC, Tej SS, Vu TH, Haudenschild CD, Agrawal V, Edberg SB, Ghazal H, Decola S. (2004) The use of MPSS for whole-genome transcriptional analysis in Arabidopsis. *Genome research* 14, 1641-1653.
- Michaels SD, Amasino RM. (1999) FLOWERING LOCUS C encodes a novel MADS domain protein that acts as a repressor of flowering. *Plant Cell* 11, 949-56.
- Michaels SD, Amasino RM. (2001) Loss of FLOWERING LOCUS C activity eliminates the late-flowering phenotype of FRIGIDA and autonomous pathway mutations but not responsiveness to vernalization. *Plant Cell* 13, 935-941.

References

- Michaels SD, Ditta G, Gustafson-Brown C, Pelaz S, Yanofsky M, Amasino RM. (2003) AGL24 acts as a promoter of flowering in Arabidopsis and is positively regulated by vernalization. *Plant J.* 33, 867-74.
- Michaels SD, Himelblau E, Kim SY, Schomburg FM, Amasino RM (2005) Integration of flowering signals in winter-annual Arabidopsis. *Plant Physiology* 137, 149-156.
- Mizoguchi T, Wheatley K, Hanzawa Y, Wright L, Mizoguchi M, Song HR, Carré IA, Coupland G (2002) LHY and CCA1 are partially redundant genes required to maintain circadian rhythms in Arabidopsis. *Dev Cell.* 2, 629-641.
- Mizoguchi T, Wright L, Fujiwara S, Cremer F, Lee K, Onouchi H, Mouradov A, Fowler S, Kamada H, Putterill J, Coupland G. (2005) Distinct roles of GIGANTEA in promoting flowering and regulating circadian rhythms in Arabidopsis. *Plant Cell* 17, 2255-70.
- Mizukami Y, Ma H (1997) Determination of Arabidopsis floral meristem identity by AGAMOUS. *Plant Cell* 9, 393-408.
- Mockler TC, Yu X, Shalitin D, Parikh D, Michael TP, Liou J, Huang J, Smith Z, et al. (2004) Regulation of flowering time in Arabidopsis by K homology domain proteins. *Proc. Natl. Acad. Sci. USA* 101, 12759-12764.
- Moon J, Suh S-S, Lee H, Choi K-R, Hong CB, Paek N-C, Kim S-G, Lee I. (2003) The SOC1 MADS-box gene integrates vernalization and gibberellin signals for flowering in Arabidopsis. *The Plant Journal* 35, 613-623.
- Mortazavi A, Williams BA, McCue K, Schaeffer L, Wold B. (2008) Mapping and quantifying mammalian transcriptomes by RNA-Seq. *Nature Methods* 5, 621-628.
- Mouradov A, Cremer F, Coupland G. (2002) Control of flowering time: interacting pathways as a basis for diversity. *Plant Cell* 14, S111-30.
- Muñoz-Bertomeu J, Cascales-Miñana B, Mulet JM, Baroja-Fernández E, Pozueta-Romero J, Kuhn JM, Segura J, Ros R (2009) Plastidial glyceraldehyde-3-phosphate dehydrogenase deficiency leads to altered root development and affects the sugar and amino acid balance in Arabidopsis. *Plant Physiol.* 151, 541-558.
- Muñoz-Bertomeu J, Cascales-Miñana B, Irlés-Segura A, Mateu I, Nunes-Nesi A, Fernie AR, Segura J, Ros R (2010) The plastidial glyceraldehyde-3-phosphate dehydrogenase is critical for viable pollen development in Arabidopsis. *Plant Physiol.* 152, 1830-1841.
- Mutasa-Göttgens E, Hedden, P (2009) Gibberellin as a factor in floral regulatory networks. *J. Exp. Bot.* 60, 1979-1989.
- Nakazono M, Qiu F, Borsuk LA, Schnable PS (2003) Laser-Capture Microdissection, a tool for the global analysis of gene expression in specific plant cell types: identification of genes expressed differentially in epidermal cells or vascular tissues of maize. *The Plant Cell* 15, 583-596.
- Nelson T, Tausta SL, Gandotra N, Liu T (2006) Laser Microdissection of plant tissue: what you see is what you get. *Annu. Rev. Plant. Biol.* 57, 181-201.
- Nilsson O, Lee I, Blázquez MA, Weigel D. (1998) Flowering-time genes modulate the response to LEAFY activity. *Genetics* 150, 403-10.
- Noh B, Lee SH, Kim HJ, Yi G, Shin EA, et al. (2004) Divergent roles of a pair of homologous jumonji/zinc-finger-class transcription factor proteins in the regulation of Arabidopsis flowering time. *Plant Cell* 16, 2601-2613.
- Nygaard V, Hovig E. (2006) Options available for profiling small samples: a review of sample amplification technology when combined with microarray profiling. *Nucleic Acids Res.* 34, 996-1014.
- O'Malley RC, Ecker JR (2010) Linking genotype to phenotype using the Arabidopsis unimutant collection. *Plant J.* 61, 928-940.

References

- Ohto M, Onai K, Furukawa Y, Aoki E, Araki T, Nakamura K (2001) Effects of sugar on vegetative development and floral transition in *Arabidopsis*. *Plant Physiol.* 127, 252-261.
- Ohtsu K, Smith MB, Emrich SJ, Borsuk LA, Zhou R, Chen T, Zhang X, Timmermans MCP, Beck J, Buckner B, Janick-Buckner D, Nettleton D, Scanlon MJ, Schnable PS. (2007) Global gene expression analysis of the shoot apical meristem of maize (*Zea mays* L.). *The Plant Journal* 52, 391-404.
- Onouchi H, Igeño MI, Périlleux C, Graves K, Coupland G (2000) Mutagenesis of plants overexpressing *CONSTANS* demonstrates novel interactions among *Arabidopsis* flowering-time genes. *Plant Cell* 12, 885-900.
- Ossowski S, Schneeberger K, Clark RM, Lanz C, Warthmann N, Weigel D (2008a) Sequencing of natural strains of *Arabidopsis thaliana* with short reads. *Genome Res.* 18, 2024-2033.
- Ossowski S, Schwab R, Weigel D (2008b) Gene silencing in plants using artificial microRNAs and other small RNAs. *Plant J.* 53, 674-690.
- Parcy F, Bomblies K, Weigel D (2002) Interaction of *LEAFY*, *AGAMOUS* and *TERMINAL FLOWER1* in maintaining floral meristem identity in *Arabidopsis*. *Development* 129, 2519-2527.
- Parcy F, Nilsson O, Busch MA, Lee I, Weigel D. (1998) A genetic framework for floral patterning. *Nature* 395, 561-6.
- Park DH, Somers DE, Kim YS, Choy YH, Lim HK, Soh MS, Kim HJ, Kay SA, Nam HG (1999) Control of circadian rhythms and photoperiodic flowering by the *Arabidopsis* *GIGANTEA* gene. *Science* 285, 1579-1582.
- Peiffer JA, Kaushik S, Sakai H, Arteaga-Vazquez M, Sanchez-Leon N, Ghazal H, Vielle-Calzada JP, Meyers BC. (2008) A spatial dissection of the *Arabidopsis* floral transcriptome by MPSS. *BMC Plant Biology* 8, 43.
- Pittendrigh CS, Minis DH. (1964) The entrainment of circadian oscillations by light and their role as photoperiodic clocks. *Am. Nat.* 98, 261-322.
- Pnueli L, Carmel-Goren L, Hareven D, Gutfinger T, Alvarez J, Ganai M, Zamir D, Lifschitz E (1998) The *SELF-PRUNING* gene of tomato regulates vegetative to reproductive switching of sympodial meristems and is the ortholog of *CEN* and *TFL1*. *Development* 125, 1979-1989.
- Poethig RS (2003) Phase change and the regulation of developmental timing in plants. *Science* 301, 334-336.
- Poole RL (2007) The TAIR database. *Methods Mol Biol.* 406, 179-212.
- Putterill J, Robson F, Lee K, Simon R, Coupland G. (1995) The *CONSTANS* gene of *Arabidopsis* promotes flowering and encodes a protein showing similarities to zinc finger transcription factors. *Cell* 80, 847-57.
- Quesada V, Macknight R, Dean C, Simpson GG (2003) Autoregulation of *FCA* pre-mRNA processing controls *Arabidopsis* flowering time. *EMBO J.* 22, 3142-3152.
- Ratcliffe OJ, Amaya I, Vincent CA, Rothstein S, Carpenter R, Coen ES, Bradley DJ (1998) A common mechanism controls the life cycle and architecture of plants. *Development* 125, 1609-1615.
- Ratcliffe OJ, Bradley DJ, Coen ES (1999) Separation of shoot and floral identity in *Arabidopsis*. *Development* 126, 1109-1120.
- Rédei GP. (1962) Supervital Mutants of *Arabidopsis*. *Genetics.* 47, 443-60.
- Reeves PH Coupland G (2001) Analysis of flowering time control in *Arabidopsis* by comparison of double and triple mutants. *Plant Physiol.* 126, 1085-1091.
- Rhoades MW, Reinhart BJ, Lim LP, Burge CB, Bartel B, Bartel DP (2002) Prediction of plant microRNA targets. *Cell* 110, 513-520.

References

- Richmond TA, Bleecker AB (1999) A defect in β -oxidation causes abnormal inflorescences development in Arabidopsis. *Plant Cell* 11, 1911-1923.
- Rijpkema AS, Gerats T, Vandenbussche M. (2007) Evolutionary complexity of MADS complexes. *Curr Opin Plant Biol.* 10, 32-8.
- Robson F, Costa MM, Hepworth SR, Vizir I, Piñeiro M, Reeves PH, Putterill J, Coupland G. (2001) Functional importance of conserved domains in the flowering-time gene CONSTANS demonstrated by analysis of mutant alleles and transgenic plants. *Plant J.* 28, 619-31.
- Ruiz-García L, Madueño F, Wilkinson M, Haughn G, Salinas J, Martínez-Zapater JM (1997) Different roles of flowering-time genes in the activation of floral initiation genes in Arabidopsis. *Plant Cell* 9, 1921-1934.
- Sablowski R (2007) Flowering and determinacy in Arabidopsis. *J. Exp. Bot.* 58, 899-907.
- Saddic LA, Huvermann B, Bezhani S, Su Y, Winter CM, Kwon CS, Collum RP, Wagner D (2006) The LEAFY target LMI1 is a meristem identity regulator and acts together with LEAFY to regulate expression of CAULIFLOWER. *Development* 133, 1673-1682.
- Salomé PA, McClung CR. (2004) The Arabidopsis thaliana clock. *J Biol Rhythms* 19, 425-35.
- Samach A, Onouchi H, Gold SE, Ditta GS, Schwarz-Sommer Z, Yanofsky MF, Coupland G. (2000) Distinct roles of CONSTANS target genes in reproductive development of Arabidopsis. *Science* 288, 1613-6.
- Sawa M, Nusinow DA, Kay SA, Imaizumi T. (2007) FKF1 and GIGANTEA Complex Formation is required for Day-Length Measurement in Arabidopsis. *Science* 318, 261-265.
- Schmid M, Uhlenhaut NH, Godard F, Demar M, Bressan R, Weigel D, Lohman JU (2003) Dissection of floral induction pathways using global expression analysis. *Development* 130, 6001-6012.
- Schomburg FM, Patton DA, Meinke DW, Amasino RM (2001) FPA, a gene involved in floral induction in Arabidopsis, encodes a protein containing RNA-recognition motifs. *Plant Cell* 13, 1427-1236.
- Schoof H, Lenhard M, Haecker A, Mayer KF, Jürgens G, Laux T (2000) The stem cell population of Arabidopsis shoot meristems is maintained by a regulatory loop between the CLAVATA and WUSCHEL genes. *Cell* 100, 635-644.
- Schultz EA, Haughn GW (1991) LEAFY, a homeotic gene that regulates inflorescence development in Arabidopsis. *Plant Cell* 3, 771-781.
- Schwab R, Ossowski S, Riester M, Warthmann N, Weigel D (2006) Highly specific gene silencing by artificial microRNAs in Arabidopsis. *Plant Cell* 18, 1121-1133.
- Schwab R, Palatnik JF, Riester M, Schommer C, Schmid M, Weigel D (2005) Specific effects of microRNAs on the plant transcriptome. *Developmental Cell* 8, 517-527.
- Schwartz S, Grande AV, Bujdoso N, Saedler H, Huijser P (2008) The microRNA regulated SBP-box genes SPL9 and SPL15 control shoot maturation in Arabidopsis. *Plant Mol. Biol.* 67, 183-195.
- Scofield S, Murray JA (2006) KNOX gene function in plant stem cell niches. *Plant Mol Biol.* 60, 929-946.
- Scortecci E, Michels SD, Amasino RM (2001) Identification of a MADS-box gene, FLOWERING LOCUS M, that represses flowering. *The Plant Journal* 26, 229-236.
- Scortecci E, Michels SD, Amasino RM (2003) Genetic interaction between FLM and other flowering-time genes in Arabidopsis thaliana. *Plant Molecular Biology* 52, 915-922.
- Searle I, He Y, Turck F, Vincent C, Fornara F, Kröber S, Amasino RA, Coupland G (2006) The transcription factor FLC confers a flowering response to vernalization by repressing meristem competence and systemic signalling in

References

Arabidopsis. *Genes & Development* 20, 898-912

Seligman K, Saviani EE, Oliveira HC, Pinto-Maglio CA, Salgado I (2008) Floral transition and nitric oxide emission during flower development in *Arabidopsis thaliana* is affected in nitrate reductase-deficient plant. *Plant Cell physiology* 49, 1112-1121.

Seo E, Lee H, Jeon J, Park H, Kim J, Noh Y-S, Lee I (2009) Crosstalk between cold response and flowering in *Arabidopsis* is mediated through the flowering-time gene *SOC1* and its upstream negative regulator *FLC*. *Plant Cell* 21, 3185-3197.

Shalit A, Rozman A, Goldschmidt A, Alvarez JP, Bowman JL, Eshed Y, Lifschitz E (2009) The flowering hormone florigen functions as a general systemic regulator of growth and termination. *Proc. Natl. Acad. Sci. USA* 106, 8392-8397.

Shannon S, Meeks-Wagner DR. (1991) A Mutation in the *Arabidopsis* *TFL1* Gene Affects Inflorescence Meristem Development. *Plant Cell* 3, 877-892.

Simon R, Igeño IM, Coupland G (1996) Activation of floral meristem identity genes in *Arabidopsis*. *Nature* 384, 59-62.

Simpson GG (2004) The autonomous pathway: epigenetic and post-transcriptional gene regulation in the control of *Arabidopsis* flowering time. *Curr. Opin. Plant Biol.* 7, 570-574.

Simpson GG, Dean C. (2002) *Arabidopsis*, the Rosetta stone of flowering time? *Science* 296, 285-9.

Simpson GG, Dijkwel PP, Quesada V, Henderson I, Dean C (2003) *FY* is an RNA 3' end processing factor that interacts with *FCA* to control the *Arabidopsis* floral transition. *Cell* 113, 777-787.

Smith DL, Fedoroff NV (1995) *LRP1*, a gene expressed in lateral and adventitious root primordia of *Arabidopsis*. *Plant Cell* 7, 735-745.

Smyth DR, Bowman JL, Meyerowitz EM (1990) Early flower development in *Arabidopsis*. *Plant Cell* 2, 755-767.

Sohn EJ, Rojas-Pierce M, Pan S, Carter C, Serrano-Mislata A, Madueno F, Rojo E, Surpin M, Raikhel NV. (2007) The shoot meristem identity gene *TFL1* is involved in flower development and trafficking to the protein storage vacuole. *Proc. Natl. Acad. Sci. USA* 104, 18801-18806.

Sridhar VV, Surendrarao A, Gonzalez D, Conlan RS, Liu Z (2004) Transcriptional repression of target genes by *LEUNIG* and *SEUSS*, two interacting regulatory proteins for *Arabidopsis* flower development. *Proc Natl Acad Sci U S A*. 101, 11494-11499.

Stadler R, Sauer N (1996) The *Arabidopsis thaliana* *AtSUC2* gene is specifically expressed in companion cells. *Bot. Acta* 109, 299-306.

Stålberg K, Ståhl U, Stymne S, Ohlrogge J (2009) Characterization of two *Arabidopsis thaliana* acyltransferases with preference for lysophosphatidylethanolamine. *BMC Plant Biol.* 9, 60.

Strayer CA, Kay SA. (1999) The ins and outs of circadian regulated gene expression. *Curr Opin Plant Biol.* 2, 114-20.

Suárez-López P, Wheatley K, Robson F, Onouchi H, Valverde F, Coupland G. (2001) *CONSTANS* mediates between the circadian clock and the control of flowering in *Arabidopsis*. *Nature* 410, 1116-20.

Sung S, Amasino RM. (2004) Vernalization in *Arabidopsis thaliana* is mediated by the PHD finger protein *VIN3*. *Nature* 427, 159-64.

Sung S, Schmitz RJ, Amasino RM (2006) A PHD finger protein involved in both the vernalization and photoperiodic pathways in *Arabidopsis*. *Genes Dev.* 20, 3244-3248.

Sweetlove LJ, Lytovchenko A, Morgan M, Nunes-Nesi A, Taylor NL, Baxter CJ, Eickmeier I, Fernie AR (2006)

References

- Mitochondrial uncoupling protein is required for efficient photosynthesis. *Proc. Natl. Acad. Sci. USA* 103, 19587-19592.
- Swiezewski S, Liu F, Magusin A, Dean C (2009) Cold-induced silencing by long antisense transcripts of an Arabidopsis Polycomb target. *Nature* 462, 799802.
- Takada S, Goto K (2003) TERMINAL FLOWER2, an Arabidopsis homolog of HETEROCHROMATIN PROTEIN1, counteracts the activation of FLOWERING LOCUS T by CONSTANS in the vascular tissues of leaves to regulate flowering time. *The Plant Cell* 15, 2856-2865.
- Tamaki S, Matsuo S, Wong HL, Yokoi S, Shimamoto K. (2007) Hd3a protein is a mobile flowering signal in rice. *Science* 316,1033-1036.
- Tan Q K-G, Irish VF (2006) The Arabidopsis zinc finger-homeodomain genes encode proteins with unique biochemical properties that are coordinately expressed during floral development. *Plant Physiology* 140, 1095-1108.
- Teper-Bamholker P, Samach A. (2005) The Flowering Integrator FT Regulates SEPALLATA3 and FRUITFULL Accumulation in Arabidopsis Leaves. *The Plant Cell* 17, 2661-2675.
- Theissen G, Saedler H (2001) Plant biology. Floral quartets. *Nature* 409, 469-471.
- Thomashow, MF (1999) Plant cold acclimation: freezing tolerance genes and regulatory mechanisms. *Annu. Rev. Plant Physiol. Plant Mol. Biol.* 50, 571-599.
- Tooke F, Ordidge M, Chiurugwi T, Battey N. (2005) Mechanisms and function of flower and inflorescence reversion. *J Exp Bot.* 56, 2587-2599.
- Torii KU, Mitsukawa N, Oosumi T, Matsuura Y, Yokoyama R, Whittier RF, Komeda Y (1996) The Arabidopsis ERECTA gene encodes a putative receptor protein kinase with extracellular leucine-rich repeats. *Plant Cell* 8, 735-746.
- Trevaskis B, Tadege M, Hemming MN, Peacock WJ, Dennis ES, Sheldon C (2007) Short Vegetative Phase-like MADS-box genes inhibit floral meristem identity in barley. *Plant Physiol.* 143, 225-235.
- Turck F, Fornara F, Coupland G (2008) Regulation and identity of florigen: FLOWERING LOCUS T moves center stage. *Annu. Rev. Plant Biol.* 59, 573-594.
- Upchurch RG (2008) Fatty acids unsaturation, mobilization, and regulation in the response of plants to stress. *Biotechnol. Lett.* 30, 967-977.
- Valverde F, Mouradov A, Soppe W, Ravenscroft D, Samach A, Coupland G. (2004) Photoreceptor regulation of CONSTANS protein in photoperiodic flowering. *Science* 303, 1003-6.
- van der Graaff E, Laux T, Rensing SA (2009) The WUS homeobox-containing (WOX) protein family. *Genome Biol.* 10, 248.
- Van Dijken AJH, Schlupe H, Smeekens SCM (2004) Arabidopsis trehalose-6-phosphate synthase 1 is essential for normal vegetative growth and transition to flowering. *Plant Physiol.* 135, 969-977.
- Wagner D, Sablowski RWM, Meyerowitz EM (1999) Transcriptional activation of APETALA1 by LEAFY. *Science* 285, 582-584.
- Wang J-W, Czech B, Weigel D (2009a) miR156-regulated SPL transcription factors define an endogenous flowering pathway in Arabidopsis thaliana. *Cell* 138, 738-749.
- Wang J-W, Schwab R, Czech B, Mica E, Weigel D (2008) Dual effects of miR156-targeted SPL genes and CYP78A5/KLUH on plastochron length and organ size in Arabidopsis thaliana. *Plant Cell* 20, 1231-1243.
- Wang R, Farrona S, Vincent C, Joecker A, Schoof H, Turck F, Alonso-Blanco C, Coupland G, Albani MC (2009b)

References

- PEP1 regulates perennial flowering in *Arabis alpina*. *Nature* 459, 423-427.
- Wang Z, Gerstein M, Snyder M (2009c) RNA-Seq: a revolutionary tool for transcriptomics. *Nat Rev Genet.* 10, 57-63.
- Wang Y, Henriksson E, Söderman E, Henriksson KN, Sundberg E, Engström P (2003) The *Arabidopsis* homeobox gene, *ATHB16*, regulates leaf development and the sensitivity to photoperiod in *Arabidopsis*. *Developmental Biology* 264, 228-239.
- Wang Y, Liu C, Yang D, Yu H, Liou Y-C (2010) *Pin1At* encoding a peptidyl-prolyl *cis/trans* isomerase regulates flowering time in *Arabidopsis*. *Molecular Cell* 37, 112-122.
- Weigel D, Alvarez J, Smyth DR, Yanofsky MF, Meyerowitz EM. (1992) *LEAFY* controls floral meristem identity in *Arabidopsis*. *Cell* 69, 843-859.
- Weigel D, Jürgens G (2002) Stem cells that make stems. *Nature* 415, 751-754.
- Weigel D, Nilsson O (1995) A developmental switch sufficient for flower initiation in diverse plants. *Nature* 377, 495-500.
- Wigge PA, Kim MC, Jaeger KE, Busch W, Schmid M, Lohman JU, Weigel D (2005) Integration of spatial and temporal information during floral induction in *Arabidopsis*. *Science* 309, 1056-1059.
- Wilhelm BT, Landry JR (2009) RNA-Seq-quantitative measurement of expression through massively parallel RNA-sequencing. *Methods* 48, 249-257.
- William DA, Su Y, Smith MR, Lu M, Baldwin DA, Wagner D (2004) Genomic identification of direct target genes of *LEAFY*. *Proc. Natl. Acad. Sci. USA* 101, 1775-1780.
- Wilson RN, Heckman JW, Somerville CR (1992) Gibberellin is required for flowering in *Arabidopsis thaliana* under short days. *Plant Physiol.* 100, 403-408.
- Wong CE, Bhalla PL, Ottenhof H, Singh MB. (2008a) Transcriptional profiling of the pea shoot apical meristem reveals processes underlying its function and maintenance. *BMC Plant Biology* 8:73.
- Wong CE, Singh MB, Bhalla PL. (2008b) Molecular processes underlying the floral transition in the soybean shoot apical meristem. *The Plant Journal* 57, 832-845.
- Wu G, Park MY, Conway SR, Wang J-W, Weigel D, Poethig RS (2009) The sequential action of *miR156* and *miR172* regulates developmental timing in *Arabidopsis*. *Cell* 138, 750-759.
- Wu G, Poethig RS (2006) Temporal regulation of shoot development in *Arabidopsis thaliana* by *miR156* and its target *SPL3*. *Development* 133, 3539-3547.
- Xie K, Wu C, Xiong L (2006) Genomic organization, differential expression, and interaction of *SQUAMOSA* promoter-binding-like transcription factors and *microRNA156* in rice. *Plant Physiol.* 142, 280-293.
- Yalovsky S, Kulukian A, Rodríguez-Concepción M, Young CA, Grissem W (2000a) Functional requirement of plant farnesyltransferase during development in *Arabidopsis*. *Plant Cell*, 12, 1267-1278.
- Yalovsky S, Rodríguez-Concepción M, Bracha K, Toledo-Ortiz G, Grissem W (2000b) Prenylation of the floral transcription factor *APETALA1* modulates its function. *Plant Cell* 12, 1257-1266.
- Yamaguchi A, Kobayashi Y, Goto K, Abe M, Araki A (2005) *TWIN SISTER OF FT (TSF)* acts as a floral pathway integrator redundantly with *FT*. *Plant Cell Physiol* 46, 1175-1189.
- Yamaguchi A, Wu M-F, Yang L, Wu G, Poethig RS, Wagner D (2009) The microRNA-regulated SBP-box transcription factor *SPL3* is a direct upstream activator of *LEAFY*, *FRUITFULL*, and *APETALA1*. *Developmental Cell* 17, 268-278.

References

- Yanovsky MJ, Kay SA. (2002) Molecular basis of seasonal time measurement in Arabidopsis. *Nature* 419, 308-12.
- Yoo SK, Chung KS, Kim J, Lee JH, Hong SM, Yoo SJ, Yoo SY, Lee JS, Ahn JH (2005) CONSTANS activates SUPPRESSOR OF OVEREXPRESSION OF CONSTANS 1 through FLOWERING LOCUS T to promote flowering in Arabidopsis. *Plant Physiology* 139, 770-778.
- Yoshida R, Fekih R, Fujiwara S, Oda A, Miyata K, Tomozoe Y, Nakagawa M, Niinuma K, Hayashi K, Ezura H, Coupland G, Mizoguchi T (2009) Possible role of EARLY FLOWERING 3 (ELF3) in clock-dependent floral regulation by SHORT VEGETATIVE PHASE (SVP) in Arabidopsis thaliana. *New Phytologist* 182, 838-850.
- Yu H, Ito T, Wellmer F, Meyerowitz EM. (2004) Repression of AGAMOUS-LIKE 24 is a crucial step in promoting flower development. *Nat Genet.* 36, 157-61.
- Yu H, Xu Y, Tan EL, Kumar PP. (2002) AGAMOUS-LIKE 24, a dosage-dependent mediator of the flowering signals. *Proc Natl Acad Sci U S A* 99, 16336-41.
- Yu Y, Lashbrook CC, Hannapel DJ (2007) Tissue integrity and RNA quality of laser microdissected phloem of potato. *Planta* 226, 797-803.
- Yu T-S, Lue W-L, Wang S-M, Chen J (2000) Mutation of Arabidopsis plastid phosphoglucose isomerase affects leaf starch synthesis and floral initiation. *Plant Physiol.* 123, 319-325.
- Zeevaart JAD (1976) Physiology of flower formation. *Annu. Rev. Plant Physiol.* 27, 321-48.
- Zeilinger MN, Farre EM, Taylor SR, Kay SA, Doyle FJ, et al. (2006) A novel computational model of the circadian clock in Arabidopsis that incorporates PRR7 and PRR9. *Mol. Syst. Biol.* 2, 58.
- Zhang X, Madi S, Borsuk L, Nettleton D, Elshire RJ, Buckner B, Janick-Buckner D, Beck J, Timmermans M, Schnable PS, Scanlon MJ (2007) Laser microdissection of narrow sheath mutant maize uncovers novel gene expression in the shoot apical meristem. *PLoS Genetics* 3(6): e101 doi:10.1371/journal.pgen.0030101.
- Zhang Z, Schwartz S, Wagner L, Miller W (2000) A greedy algorithm for aligning DNA sequences. *J Comput Biol.* 7, 203-214.

Appendix I. List of primers used in this study

-RT-PCR

SOC1

T003 SOC1small-R GTGATCTCCACTCAACAAAA
T004 SOC1small-R CAACAAGAGAGAAGCAGCTTTA

TUBULIN

F041 TUB-F CAACTCTGACCTCCGAAAGC
F042 TUB-R CACATTCAGCATCTGCTCGT

ACTIN2

T032 qRT-ACT-F GGTAACATTGTGCTCAGTGGTGG
T033 qRT-ACT-R AACGACCTTAATCTTCATGCTGC

SOC1

SOC1-RTAn-F GGATCGAGTCAGCACCAAACCG
SOC1-RTAn-R CTTGAAGAACAAGGTAACCAATGAACAAT

C19 (upstream T-DNA)

T151 C19-F3 GCATCCACACATAATCACGA
T181 C19-R3 GTGTGGCAGGTAGCTGAAAT

C19 (downstream T-DNA)

T070 C19-F TCTACGGGAAGATAACACCA
T071 C19-T7-R TAATACGACTCATTATAGGGAAGGGAGTTCACAAAGAC

-Real-time PCR

TSF

T030 TSF-F-RT CTCGGGAATTCATCGTATTG
T031 TSF-R-RT CCCTCTGGCAGTTGAAGTAA

ACTIN2

T032 qRT-ACT-F GGTAACATTGTGCTCAGTGGTGG
T033 qRT-ACT-R AACGACCTTAATCTTCATGCTGC

SVP

T074 SVP-RT-F AAGAGAACGAGCGACTTGG
T075 SVP-RT-R ATACGGTAAGCCGAGCCTAA

FT

T144 FT-F-PLC191 CGAGTAACGAACGGTGATGA
T145 FT-R-PLC192 CGCATCACACTATATAAGTAAAACA

TFL1

A07-FW-TFL1 RT GGCAAAGAGGTGGTGAAGCTA
A08-RE-TFL1 RT AAGATCATACTCGACCGCAAA

SOC1

T003 SOC1small-R GTGATCTCCACTCAACAAAA
T004 SOC1small-R CAACAAGAGAGAAGCAGCTTTA

SOC1

SOC1-RTAn-F GGATCGAGTCAGCACCAAACCG
SOC1-RTAn-R CTTGAAGAACAAGGTAACCAATGAACAAT

CO

F191 CO-qRT-F TAAGGATGCCAAGGAGGTG
F192 CO-qRT-R CCCTGAGGAGCCATATTTGA

D13

T094 D13-F CCCGATGCTATTCGAACATT
T188 D13-R TCTCTCGTCTGCACGCTCT

-Cloning

SVP CDS

T001 SVPattB1-F GGGGACAAGTTTGTACAAAAAAGCAGGCTTCATGGCGAGAGAAAAGATTC
T002 SVPattB2-R GGGGACCACTTTGTACAAGAAAGCTGGGTCAACCACATACGGTAAGC

SVP RNAi

T008 SVPRNAi-F GGGGACAAGTTTGTACAAAAAAGCAGGCTTATTTCTCTGGCTTCTTCTTC
T009 SVPRNAi-R GGGGACCACTTTGTACAAGAAAGCTGGGTGAAGCAAGAGAGAGAGCTTAGGT

D13 RNAi

T149 D13i-F GGGGACAAGTTTGTACAAAAAAGCAGGCTGTGTGGGTAGCTCAGAGGA
T150 D13i-R GGGGACCACTTTGTACAAGAAAGCTGGGTCAAGAAACGGAGAAA

amiRNAh21/31

T189 ARNA1_I gaTAGTAATGTCGTTATTACCAGTctctctcttttgtattcc
T190 ARNA1_II gaCTGGTAATAACGACATTACTAtcaaagagaatcaatga
T191 ARNA1_III gaCTAGTAATAACGAGATTACTTtcacaggtcgtgatatg
T192 ARNA1_IV gaAAGTAATCTCGTTATTACTAGTctacatatatattcct

amiRNAh22/25

T193 ARNA2_I gaTCCTTGCGGTGGAAGTCGCGAtctctctcttttgtattcc
T194 ARNA2_II gaTCGCGACTTCCACCGCAAGGAtcaaagagaatcaatga
T195 ARNA2_III gaTCACGACTTCCACCGCAAGGTtcacaggtcgtgatatg
T196 ARNA2_IV gaACCTTGCGGTGGAAGTCGTGAtctacatatatattcct

D13 CDS

T203 D13-GW-F GGGGACAAGTTTGTACAAAAAAGCAGGCTTCATGCTTGCACACAAGTCTCT
T204 D13-GW-R GGGGACCACTTTGTACAAGAAAGCTGGGTCTTACACACTAATCTGCTTATCGAAGA

-Genotyping

T166 SALKLB TGGTTCACGTAGTGGGCCATCG
T187 GKLB CCCATTTGGACGTGAATGTAGACAC

svp-41

F208 SVP-1F (wt) GACCCACTAGTTATCAGCTCAG
F209 SVP-1R (wt) AAGTTATGCCTCTCTAGGAC
F210 SVP-2R (mut) AAGTTATGCCTCTCTAGGTT

soc1-2

SOC1-F TTCTTCTCCCTCCAGTAATGC
SOC1-R GAGTTTTGCCCTCACCATA
SALKLB

ful-1

T012 AGL8PG TGTATTCACGTACATACCG
T013 AGL8MG CTCATGAGCTTCTTGAGC
T014 GUS3 CTTGTAACGCGCTTTCCC

ful-2

T026 ful2-1F AATGTTGTAGGAAAATTGG
T027 ful2-1R TTATGAGGATCCAAGACACA
T028 ful2-2F CCAATGTTGTAGGAAAATTA
T029 ful2-2R ATGAGGATCCAAGACACAA

svp-3 (followed by digestion with HgaI)

T080 svp3F_dicap TTATTGGAATGTGTTTATATTATGAC
T020 svp3-2 TTGGTAATTCAACGGAGTAA

soc1-1 (followed by digestion with AvaII)

T081 soc1F_dicap TCGTTATCTGAGGCATACTAAGGAC
T077 SOC1WT-R TTCATCATGTTTGCTGCTTC

ft-10

FT-F-Fer TAAGCAGAGTTGTTGGAGAC
FT-R-Fer GTCTTCTTCGTCCGCA
T187 GKLB

tsf-1
 TSF-F-Fer CACGAGGTTGGTCTCTCTTAAG
 TSF-R-Fer CTGGCAGTTGAAGTAAGAG
 SALKLB

c19
 T151 C19-F3 GCATCCACACATAATCACGA
 T071 C19-T7-R TAATACGACTCACTATAGGGAAGGGGAGTTCACAAAGAC
 SALKLB-F

d13
 T234 D13-LP AAGGGTGTGATCATCGTCTG
 T235 D13-RP TCAACCATAAGATCCAATGGC

35S promoter
 F195 35S-For CTTCGCAAGACCCTTCCT

SUC2
 F067 pSUC2-1F CGAATTTCTCGCTTCATGGT

FD promoter
 F353 pFD-2F TCCCTCTCTGCGGTAGGA

KNAT1 promoter
 T005 KNAT1-F GAAGTAGCCGCGAAGACCTA

SVP.2 (intron)
 T205 SVP-i-R GGGGTGTGTACGTTAATGGT

amiRNAh21/31
 T238 pIIARNA1 CTGGTAATAACGACATTACTA

amiRNAh22/25
 T239 pIIARNA2 TCGCGACTTCCACCGCAAGGA

-Templates for *in situ* hybridisation

SVP
 SVPT3-F ATTAACCCTCACTAAAGGGAATGAAGGAAGTCCTAGAGAGGCATAAC
 SVPT7-R TAATACGACTCACTATAGGGAGAATTCACTACTTAGACATTGTCTC

SOC1
 SOC1T3-F ATTAACCCTCACTAAAGGGAATCGAGGAGCTGCAACAGAT
 SOC1T7-R TAATACGACTCACTATAGGGTTGACCAAACCTTCGCTTTCA

AGL24
 T015 AGL24-F GGATGAGAATAAGAGACTGAGGGATAAAC
 T016 AGL24-T7R TAATACGACTCACTATAGGGGACCAATAACACGTACAATATCTGAAAC

WUS
 T175 WUS-F ACAACAACGTAGGTGGAGGA
 T176 WUS-T7-R TAATACGACTCACTATAGGGCACCGTTGATGTGATCTTCA

FD
 F094 FDT7-2R TAATACGACTCACTATAGGGaccagagcctcgaaagaggt
 F095 FDT3-2F ATTAACCCTCACTAAAGGGAAtttcatcctcatcaccatcg

FUL
 F096 FULT7-R TAATACGACTCACTATAGGGacgtctcgacaacggagttc
 F097 FULT3-F ATTAACCCTCACTAAAGGGAagggggaagatcttgattcgt

Candidate genes:

C4
 T040 C4-F TTCAATCCAACGGTGACG
 T041 C4-T7-R TAATACGACTCACTATAGGGCATTAGCCATAATGGGTTGG

C11
 T054 C11-F CAATGTTGATCTGTCCGGTA

T055 C11-T7-R TAATACGACTCACTATAGGGCGAGAGATAGCGAAATGAGC

C15

T062 C15-F ATTTTCAGGCAACACAGAGC

T063 C15-T7-R TAATACGACTCACTATAGGGCAGCTTCTTCTCCATTTC

C19

T070 C19-F TCTACGGGAAGATACCACCA

T071 C19-T7-R TAATACGACTCACTATAGGGAAGGGGAGTTCACAAAGAC

C20

T072 C20-F GGATCGTAGGGTCTCAACAA

T073 C20-T7-R TAATACGACTCACTATAGGGCCTCCACTGCCGTTACTCTA

D3

T084 D3-F AAGCCTCTTGGTTCTGATCG

T085 D3-T7-R TAATACGACTCACTATAGGGATTTAGCTGGAGGCCAAAT

D13

T094 D13-F CCCGATGCTATTGCAACATT

T095 D13-T7-R TAATACGACTCACTATAGGGTCTCTCGTCTGCACGCTCT

D13_2

T147 D13-2F GTGTGGGTTAGCTCAGAGGA

T148 D13-T7-2R TAATACGACTCACTATAGGGCAAGAAACGGAGAAAGGAAA

D19

T100 D19-F TGT TTTCTGGGCAGACACTG

T101 D19-T7-R TAATACGACTCACTATAGGGTTCAGCCTCTCCTTCTGCAT

D27

T108 D27-F ACAAGCCAAGGGAGGTGAG

T109 D27-T7-R TAATACGACTCACTATAGGGATCGTTTGGGGGATAATAGC

D29

T110 D29-F TGACAACGTCCACGCAACT

T111 D29-T7-R TAATACGACTCACTATAGGGCGTAAGAGGCACCCCTTCTCA

D31

T112 D31-F GGTGCTCTTGCTCATTGTGT

T113 D31-T7-R TAATACGACTCACTATAGGGCAAAATCAAGTCTCGGTTTCAA

D35

T116 D35-F AAACGTTAAGTCGTCAAAAAGC

T117 D35-T7-R TAATACGACTCACTATAGGGCGCAGAAAATTC AATGTACG

D37

T118 D37-F GTCAAGAAGAGGGGTCCAGT

T119 D37-T7-R TAATACGACTCACTATAGGGCTCCAAAACCAACAGATTG

D55

T136 D55-F CACGCCACATTTTATTCCTT

T137 D55-T7-R TAATACGACTCACTATAGGGTTGTGCTAAGTCCCAACTC

C21

T208 C21-F GAGGGCAAAGGTGGAATAAT

T209 C21-T7-R TAATACGACTCACTATAGGGCAGACTTAAGGGTCAAACG

C22

T210 C22-F GAGACTGCTAACGCCATTGT

T211 C22-T7-R TAATACGACTCACTATAGGGATCAATTGTGACCGGTTTTT

C23

T212 C23-F ATTCAGCAGAAGATGCAAGG

T213 C23-T7-R TAATACGACTCACTATAGGGTCTCCTCAAGAAATCGTACTAAAAA

C25

T216 C25-F CTTGGCTCATGGAACGTAAT

T217 C25-T7-R TAATACGACTCACTATAGGGCCGAAAACAATATTCGACCA

C26

T218 C26-F TCAAAGACAAGTTGCTTCCAG

T219 C26-T7-R TAATACGACTCACTATAGGGACAAAAGTCAAAGAACTTT CACA

C27

T220 C27-F CATGACCTAAGCGAAATCGT

T221 C27-T7-R TAATACGACTCACTATAGGGTCTTTTTGGAATTTTCTTTTTTCA

C29

T224 C29-F GGAAGGTTTTTAAAGGAGCAG
T225 C29-T7-R TAATACGACTCACTATAGGGTCTGAAAATTAATGCGAAACA

C30

T226 C30-F CTGTGGCTCATTGCTCTTT
T227 C30-T7-R TAATACGACTCACTATAGGGATCTGCAGGTCCTTCTCCT

ATHB21

T177 ATHB21-F CAGCTTTGTCAAGAGATTGGA
T178 ATHB21-T7-R TAATACGACTCACTATAGGGAACAACAATCTGAACTTAACTAAGGA

ATHB25

T179 ATHB25-F ACCACCACAGTCTTCGTTC
T180 ATHB25-T7-R TAATACGACTCACTATAGGGCCAACATCATCAACATCATCA

PGIP2

T182 PGIP2-F GCATCCCCAAAGGAGAGTAT
T183 PGIP2-T7-R TAATACGACTCACTATAGGGGCTAAAACATTGGTTCATGCT

Appendix II. Lists of genes from the Solexa gene expression data

Genes identified as up-regulated by the clustering approach.

AGI	A 0LD	A 1LD	A 3LD	B 0LD	B 1LD	B 3LD	C 0LD	C 1LD	C 3LD	AVG 0LD	AVG 1LD	AVG 3LD	code	Annotation
AT1G02330	0.00	8.04	49.01	0.00	50.61	65.47	52.12	74.17	281.11	17.37	44.27	131.86	0	
AT1G02780	1094.22	1101.64	1646.75	514.65	648.06	1332.44	1933.08	3025.64	3633.26	1190.65	1591.78	2170.82		emb2386 (embryo defective 2386); structural constituent of ribosome
AT1G02800	0.00	16.08	19.80	0.00	7.03	11.55	1.83	1.40	10.50	0.61	8.17	13.88		ATCEL2; cellulase/hydrolase, hydrolyzing O-glycosyl compounds
AT1G03170	0.00	0.00	59.81	0.00	0.00	14.83	0.00	1.40	86.29	0.00	0.47	53.91	C23	unknown protein
AT1G03780	9.20	32.16	29.41	10.29	26.30	25.42	2.29	4.20	87.02	7.26	20.66	40.62		targeting protein-related
AT1G04520	9.20	32.16	107.82	30.88	39.36	98.26	45.72	158.14	205.20	28.60	76.66	133.10		DLP2 (PLASMODESMATA-LOCATED PROTEIN 2)
AT1G06670	48.98	120.62	89.22	61.47	123.30	85.49	32.46	125.85	294.97	43.30	122.86	152.89		NIH (NUCLEAR DEH-BOXHELICASE); DNA binding / DNA helicase
AT1G06680	18.39	233.19	245.05	41.17	82.94	284.95	838.68	3206.17	2182.37	268.75	1174.10	897.46		PSSP-1 (PHOTOSYSTEM II SUBUNIT P-1); poly(U) binding
AT1G06740	0.00	8.04	29.41	0.00	2.81	11.55	0.00	9.80	50.51	0.00	6.98	30.49		transposable element gene
AT1G07705	56.17	88.46	88.22	61.78	84.06	124.00	5.49	27.99	37.42	40.81	60.37	83.21		transcription regulator
AT1G07770	1213.76	1841.43	1891.80	1245.46	1031.92	2284.40	909.84	2461.66	2233.78	1123.02	1778.30	2138.66		RPS16A (ribosomal protein s16a); structural constituent of ribosome
AT1G08560	174.71	353.81	362.68	174.98	223.51	268.80	170.89	344.27	272.67	173.56	307.20	301.38		unknown protein
AT1G08760	0.00	16.08	39.21	0.00	23.90	23.88	5.03	0.00	24.06	1.68	13.33	29.04		unknown protein
AT1G08845	0.00	0.00	29.41	0.00	26.71	21.57	9.60	0.00	16.24	3.20	8.90	22.40		structural constituent of ribosome
AT1G09380	0.00	0.00	19.80	0.00	16.87	29.27	0.00	2.80	178.90	0.00	6.66	76.26	C22	GDSL-motif lipase/hydrolase family protein
AT1G09430	0.00	8.04	49.01	0.00	7.03	12.32	0.81	0.00	10.14	0.30	5.02	23.82		ACLA-3; ATP citrate synthase
AT1G09640	211.48	426.18	529.31	216.15	354.26	563.77	194.31	326.08	512.78	207.32	368.94	531.95		elongation factor 1B-gamma, putative / eEF-1B gamma, putative
AT1G11380	0.00	0.00	19.80	0.00	15.46	10.78	0.00	2.80	23.06	0.00	6.09	17.82		unknown protein
AT1G13870	0.00	16.08	19.80	0.00	7.03	28.50	3.66	5.60	36.34	1.22	9.57	28.15		DRL1 (DEFORMED ROOTS AND LEAVES 1); cam bind. / purine bind.
AT1G14440	0.00	160.82	117.83	20.69	32.33	36.20	0.46	4.20	52.22	7.01	65.78	69.68	C11	AHB31 (ARABIDOPSIS THALIANA HOMEBOX PROTEIN 31);
AT1G14687	0.00	0.00	39.21	0.00	4.22	11.55	6.86	38.39	53.83	2.29	13.53	34.87		AHB32 (ARABIDOPSIS THALIANA HOMEBOX PROTEIN 32);
AT1G14830	36.78	40.21	78.42	82.34	147.60	170.21	103.79	92.38	172.27	74.30	93.39	140.30		ADL1C (ARABIDOPSIS DYNAMIN-LIKE PROTEIN 1C); GTP bind. / GTPase
AT1G15370	36.78	64.33	225.45	20.69	47.80	144.03	14.17	36.39	108.16	23.86	49.50	159.68		0
AT1G15490	0.00	0.00	49.01	0.00	22.48	17.71	0.00	2.80	61.28	0.00	8.43	26.85		hydrolase, alpha/beta fold family protein
AT1G15570	9.20	48.25	49.01	10.29	19.68	26.19	12.34	71.37	81.28	10.61	46.43	45.49		CYCA2.3 (CYCLIN A2.3); cyclin-dependent protein kinase regulator
AT1G15930	1029.86	1801.22	1774.18	1595.42	1481.98	3036.11	989.85	2128.59	2071.74	1205.04	1797.26	2264.01		40S ribosomal protein S12 (RPS12A)
AT1G19880	110.34	225.15	186.24	72.05	112.46	120.92	28.98	71.37	98.79	99.79	136.33	135.32		regulator of chromosome condensation (RCC1) family protein
AT1G20300	9.20	8.04	19.80	10.29	21.09	25.42	10.97	8.40	45.49	10.15	12.51	30.17		penicillipeptide (PPR) repeat-containing protein
AT1G21720	91.95	80.41	178.44	51.47	184.15	268.03	59.89	62.88	120.05	67.77	109.18	188.17		PBC1 (PROTEASOME BETA SUBUNIT C1); peptidase
AT1G22060	9.20	8.04	19.80	0.00	8.43	10.01	2.29	0.00	18.84	3.83	5.49	16.15		0
AT1G22920	285.06	490.51	754.76	319.08	222.11	479.83	156.36	193.13	379.09	263.50	301.92	537.89		PFL (POINTED FIRST LEAVES); RNA bind / struct. constituent ribosome
AT1G25260	91.95	506.59	372.48	247.03	282.56	495.89	154.08	208.62	343.91	194.35	332.66	374.10		CSN6A (COP9 SIGNALOSOME 5A)
AT1G25280	73.56	56.29	117.83	61.76	46.39	96.27	40.23	107.76	160.97	58.52	70.15	124.96		acidic ribosomal protein P0-related
AT1G28070	9.20	40.21	39.21	0.00	5.62	13.09	2.74	9.80	189.94	3.98	18.54	74.08		ATL10 (TUBBY LIKE PROTEIN 10); phosphoric diester hydrolase/ T.F.
AT1G30470	73.56	104.54	137.23	72.05	104.03	185.59	20.12	22.38	97.17	55.24	76.98	133.33		0
AT1G30950	0.00	8.04	29.41	0.00	7.03	16.17	22.40	34.98	198.01	7.47	16.93	81.63		SIT4 phosphatase-associated family protein
AT1G31420	9.20	48.25	49.01	20.69	35.14	77.79	6.86	0.00	23.51	12.21	27.80	50.10		UFO (UNUSUAL FLORAL ORGANS); T. F. binding / ubiquitin-protein ligase
AT1G32190	9.20	8.04	19.80	0.00	0.00	15.40	0.46	2.80	33.56	3.22	3.81	22.86		FEI1 (FEI 1); ATP binding / kinase/ protein serine/threonine kinase
AT1G35560	45.98	56.29	88.22	20.69	77.32	133.23	41.61	155.34	236.51	36.06	96.32	149.32		0
AT1G43800	0.00	8.04	509.71	0.00	1.41	251.85	0.46	2.80	332.70	0.15	4.08	364.75	D13	CINV1 (cytosolic invertase 1); beta-fructofuranosidase
AT1G44900	36.78	144.74	156.83	61.76	92.78	154.81	278.89	615.76	532.43	125.81	284.43	281.36		acyl-(acyl-carrier-protein) desaturase, putative / stearyl-ACP desaturase, put.
AT1G47420	36.78	32.16	78.42	10.29	32.33	97.04	138.89	104.98	418.03	62.02	56.49	197.83		ATP binding / DNA binding / DNA-dependent ATPase
AT1G48140	9.20	8.04	88.22	10.29	36.56	40.82	6.86	18.79	83.35	8.78	20.46	70.80		0
AT1G48280	9.20	8.04	88.22	0.00	5.62	26.19	4.11	0.00	84.97	4.44	4.55	68.46		dolichol-phosphate mannosyltransferase-related
AT1G48420	0.00	0.00	29.41	10.29	18.27	54.68	1.37	15.39	40.56	7.32	19.26	44.82		hydroxyproline-rich glycoprotein family protein
AT1G48820	0.00	0.00	29.41	10.29	18.27	23.11	9.14	0.00	74.38	6.48	6.09	42.30		D-CDES (D-CYSTEINE DESULFHYDRASE);
AT1G52905	9.20	16.08	19.80	0.00	9.84	10.01	0.91	1.40	16.60	3.37	9.11	15.41		ATMTK (ARABIDOPSIS THALIANA S-METHYL-5-THIORIBOSE KINASE);
AT1G53310	18.39	24.12	58.81	20.69	15.46	45.44	18.00	123.15	89.28	18.33	54.25	64.51		unknown protein
AT1G53460	9.20	32.16	29.41	10.29	9.84	23.11	79.65	168.54	172.18	33.01	69.51	74.80		ATPPC1 (PHOSPHOENOLPYRUVATE CARBOXYLASE 1);
AT1G54630	91.95	209.07	372.48	144.10	127.92	250.31	185.23	331.67	338.47	143.76	222.89	319.75		ACP3 (ACYL CARRIER PROTEIN 3); acyl carrier

AT1G56340	82.76	201.03	245.05	41.17	61.86	136.64	32.00	160.64	174.42	51.98	141.27	186.04	unknown protein
AT1G57600	0.00	24.12	19.60	0.00	7.03	10.01	1.83	33.59	71.51	0.61	21.58	33.71	membrane bound O-acyl transferase (MBOAT) family protein
AT1G57800	82.76	192.99	186.04	113.22	97.00	250.31	471.38	1024.41	1675.11	222.45	438.13	673.82	60S ribosomal protein L21
AT1G60940	18.39	46.25	39.21	0.00	23.90	23.98	0.46	2.80	36.28	6.28	24.98	32.78	unknown protein
AT1G62970	0.00	8.04	19.60	20.59	60.45	50.06	8.69	15.39	16.78	9.76	27.96	28.82	DNAJ heat shock N-terminal domain-containing protein
AT1G63050	0.00	0.00	19.60	0.00	0.00	23.11	0.46	9.80	46.75	0.16	3.27	29.82	membrane bound O-acyl transferase (MBOAT) family protein
AT1G63260	9.20	6.04	58.81	0.00	7.03	15.40	8.23	0.00	13.64	5.81	5.02	29.28	ribulose-1,5-bisphosphate carboxylase, put. / pentose-5-P 3-epimerase, put.
AT1G64670	18.39	64.33	137.23	30.88	26.71	49.29	6.40	18.19	225.39	18.56	36.41	137.30	BDG31 (BODYGUARD1); hydrolase
AT1G65290	524.12	1286.59	1509.52	688.75	608.69	1333.98	539.50	657.75	936.24	674.13	851.01	1260.91	mIACP2 (mitochondrial acyl carrier protein 2); acyl carrier/ metal ion binding
AT1G67250	27.59	64.33	107.82	20.69	44.98	121.99	63.55	244.91	271.06	37.24	118.07	166.88	proteasome maturation factor UMP1 family protein
AT1G67350	64.37	120.82	168.04	123.52	220.70	343.51	86.87	449.23	396.67	91.58	283.52	312.07	unknown protein
AT1G68410	0.00	16.08	19.60	0.00	2.81	19.25	1.37	0.00	10.14	0.46	6.30	16.33	protein phosphatase 2C-related / PP2C-related
AT1G68040	0.00	8.04	235.25	20.69	36.14	136.32	16.00	200.12	173.71	12.20	81.10	181.78	ACR4 (ACT REPEAT 4); amino acid binding
AT1G69360	0.00	8.04	19.60	0.00	53.42	63.16	4.57	0.00	57.33	1.52	20.49	46.70	unknown protein
AT1G69620	1314.91	3980.33	3059.25	1616.01	1678.47	3221.73	1546.72	2135.58	2651.45	1482.55	2586.14	2977.14	RPL34 (RIBOSOMAL PROTEIN L34); structural constituent of ribosome
AT1G69740	18.39	64.33	58.81	61.78	81.53	135.55	35.20	60.18	77.88	38.46	68.68	90.75	HEMB1; catalytic/ metal ion binding / porphobilinogen synthase
AT1G70600	488.95	699.58	725.36	452.89	538.40	833.35	335.13	244.91	1296.53	418.90	404.30	951.41	structural constituent of ribosome
AT1G71010	73.56	128.86	117.83	10.29	44.98	70.86	9.60	18.19	35.71	31.15	63.95	74.73	phosphatidylinositol-4-phosphate 5-kinase family protein
AT1G71180	0.00	16.08	49.01	0.00	11.25	26.19	5.03	8.40	27.01	1.68	11.91	34.07	6-phosphogluconate dehydrogenase NAD-binding domain-containing protein
AT1G71780	9.20	8.04	68.61	0.00	19.68	30.81	2.29	2.80	10.59	3.83	10.17	36.67	unknown protein
AT1G74050	432.17	619.17	891.99	452.89	448.43	759.41	245.98	225.31	576.98	377.01	430.97	743.79	60S ribosomal protein L6 (RPL6C)
AT1G74270	91.95	184.95	343.07	154.40	229.14	321.94	325.99	463.22	801.78	190.78	282.44	488.93	60S ribosomal protein L35a (RPL35aC)
AT1G74470	36.78	160.82	178.44	61.78	54.82	118.61	151.79	198.72	249.34	83.44	138.12	181.48	geranylgeranyl reductase
AT1G74920	73.56	90.41	127.43	51.47	78.72	140.18	66.75	96.56	270.61	63.93	85.23	179.40	ALDH10A8; 3-chloroalyl aldehyde dehydrogenase/ oxidoreductase
AT1G76110	9.20	72.37	88.22	30.88	70.29	80.10	10.52	15.39	79.14	16.86	52.68	82.49	high mobility group (HMG1/2) family protein / ARID/BRIGHT DNA-binding
AT1G77350	27.59	40.21	88.22	41.17	81.53	132.47	6.40	11.20	67.26	25.06	44.31	98.00	unknown protein
AT1G77780	9.20	16.08	29.41	0.00	1.41	15.40	5.94	0.00	15.07	5.06	5.83	19.68	NIA1 (NITRATE REDUCTASE 1); nitrate reductase
AT1G78180	0.00	32.16	29.41	0.00	7.03	12.32	1.37	5.60	20.19	0.46	14.93	20.64	binding
AT1G79530	202.29	385.98	303.88	113.22	334.57	380.48	105.61	513.60	368.50	140.38	411.38	350.65	D29 GAPCP-1 (GLYCERALDEHYDE-3-P DEHYDROGENASE OF PLASTID 1);
AT1G79850	18.39	96.49	88.61	41.17	84.35	136.32	15.54	37.79	135.57	25.04	72.87	113.60	RAD23; damaged DNA binding
AT1G80920	18.39	32.16	88.22	0.00	43.58	39.20	10.52	20.99	17.86	9.64	32.24	47.42	ribosomal protein S15 family protein
AT1G80950	9.20	8.04	49.01	0.00	2.81	29.27	0.91	1.40	20.73	3.37	4.08	33.00	D55 phospholipid/sterol acyltransferase family protein
AT2G01250	1590.76	3144.10	3528.75	2140.95	2027.09	3911.82	1020.02	3105.41	2318.65	1583.91	2758.87	3253.41	60S ribosomal protein L7 (RPL7B)
AT2G02050	36.78	128.86	117.83	61.78	106.84	141.72	17.83	111.66	84.16	38.79	115.82	114.60	NADH-ubiquinone oxidoreductase B18 subunit, putative
AT2G03120	9.20	32.16	117.83	10.29	30.93	50.83	11.89	23.79	22.07	10.46	28.86	63.51	ATSP (ARABIDOPSIS SIGNAL PEPTIDE PEPTIDASE);
AT2G03150	18.39	46.25	49.01	0.00	12.85	23.88	2.74	7.00	77.25	7.04	22.83	50.05	emb1579 (embryo defective 1579); binding / calcium ion binding
AT2G03350	18.39	32.16	49.01	10.29	14.06	52.37	59.44	205.72	137.37	29.37	83.88	79.58	unknown protein
AT2G05210	0.00	8.04	19.60	0.00	15.46	30.81	0.91	0.00	15.34	0.30	7.83	21.92	APOT1a (Protection of Telomeres 1a); telomeric DNA binding
AT2G07060	45.98	168.36	176.44	72.05	222.11	200.25	123.90	97.96	265.94	90.64	162.98	214.21	minichromosome maintenance family protein / MCM family protein
AT2G10410	229.88	402.06	627.33	133.81	261.47	241.84	23.32	54.68	102.84	129.00	239.37	323.64	transposable element gene
AT2G16090	110.34	112.58	176.44	144.10	106.43	236.45	127.56	93.76	541.58	127.33	103.92	318.16	KCS8 (3-KETOACYL-COA SYNTHASE 8); acyltransferase/ catalytic
AT2G18110	46.98	96.49	78.42	30.88	97.00	95.50	33.83	32.19	133.15	36.90	75.23	102.38	PIN1AT (PEPTIDYLPROLYL CIS/TRANS ISOMERASE, NIMA-INTERACT. 1;
AT2G18330	18.39	72.37	78.42	30.88	74.50	74.71	224.03	169.34	458.34	91.10	105.40	203.15	elongation factor 1-beta, putative / EF-1-beta, putative
AT2G18730	682.05	1198.13	1048.82	627.88	556.68	1312.41	1701.28	7239.43	8250.44	697.06	2988.08	3537.23	AAA-type ATPase family protein
AT2G20260	27.59	46.25	127.43	30.88	63.26	81.64	22.40	142.75	119.60	26.96	84.75	109.69	60S ribosomal protein L28 (RPL28A)
AT2G20280	118.54	192.99	254.85	61.78	57.64	120.92	148.59	155.34	303.45	108.96	135.32	228.41	PSAE-2 (photosystem I subunit E-2); catalytic
AT2G23080	36.78	40.21	58.81	0.00	22.49	37.74	9.60	51.78	191.92	15.46	38.16	96.16	unknown protein
AT2G24765	18.39	24.12	58.81	10.29	33.74	23.88	64.01	53.18	117.81	30.90	37.01	66.83	casein kinase II alpha chain, putative
AT2G25610	18.39	16.08	78.42	0.00	18.27	35.43	37.03	27.99	61.46	18.47	20.78	58.44	ARF3 (ADP-RIBOSYLATION FACTOR 3); protein binding
AT2G26200	0.00	0.00	29.41	10.29	9.84	27.73	0.91	5.60	55.09	3.74	5.15	37.41	H4-transferring two-sector ATPase, C subunit family protein
AT2G26780	0.00	24.12	19.60	0.00	16.87	13.86	5.94	15.39	27.81	1.98	18.80	20.43	unknown protein
AT2G27730	101.15	128.86	441.09	82.34	74.50	147.88	55.32	110.66	148.66	79.60	104.57	246.21	SCP151 (SERINE CARBOXYPEPTIDASE-LIKE 51);
AT2G27920	9.20	16.08	58.81	10.29	19.68	21.57	5.03	0.00	26.11	8.17	11.92	35.60	zinc finger (CCH-type) family protein
AT2G28450	9.20	40.21	58.81	0.00	4.22	13.09	8.23	7.00	31.86	5.81	17.14	34.59	ATP binding / ATP-dependent helicase/ nucleic acid binding
AT2G28800	18.39	56.29	39.21	10.29	15.46	60.08	1.83	72.77	90.08	10.17	48.17	63.12	

AT2G030060	27.59	56.29	58.81	20.59	68.88	77.79	4.11	5.60	20.91	17.43	43.59	52.50
AT2G032060	395.39	981.02	725.38	370.55	410.48	1020.51	561.45	1144.78	1611.54	442.46	845.42	1119.14
AT2G032810	0.00	8.04	29.41	0.00	21.09	22.34	0.46	9.80	24.67	0.16	12.87	25.47
AT2G033255	9.20	32.16	68.61	10.29	21.09	38.51	39.58	39.19	111.17	18.98	30.81	72.78
AT2G034160	27.59	40.21	49.01	20.59	40.77	40.82	4.11	0.00	22.25	17.43	26.99	37.38
AT2G034560	18.39	64.33	89.22	20.59	16.87	40.05	7.32	7.00	26.79	15.43	29.40	52.69
AT2G035470	0.00	16.08	49.01	0.00	6.62	23.88	5.49	18.19	18.20	1.93	13.30	30.70
AT2G036300	9.20	24.12	19.80	0.00	14.06	16.94	11.89	30.78	29.43	7.03	22.99	21.99
AT2G036580	56.17	96.49	178.44	154.40	186.56	689.37	43.43	393.25	504.79	84.33	225.10	423.73
AT2G036620	286.05	587.01	499.91	298.50	298.02	687.78	704.09	1714.34	1408.68	429.21	866.46	865.46
AT2G037470	46.98	305.56	235.25	216.15	196.97	372.77	187.91	811.69	608.96	150.01	434.74	405.68
AT2G038460	441.37	707.82	901.79	370.55	556.27	1008.98	969.53	1055.20	1764.97	592.32	772.70	1225.24
AT2G041160	0.00	0.00	0.00	0.00	6.62	11.55	0.91	0.00	23.42	0.30	1.87	24.73
AT2G042200	0.00	16.08	19.60	0.00	9.84	16.94	0.91	0.00	31.67	0.30	8.64	22.74
AT2G042240	0.00	8.04	39.21	10.29	7.03	19.25	5.03	4.20	53.92	5.11	6.42	37.46
AT2G042310	331.03	643.29	659.74	380.84	351.44	700.98	73.81	197.32	396.22	281.93	397.35	584.61
AT2G042710	56.17	184.95	245.05	61.76	140.58	197.17	65.32	71.37	101.39	57.42	132.30	181.20
AT2G043160	0.00	0.00	0.00	0.00	14.06	23.88	3.86	16.79	72.77	1.22	10.28	45.28
AT2G043460	542.51	554.94	1009.82	494.07	477.96	1457.98	776.79	1367.28	4156.04	604.46	800.02	2207.88
AT2G043750	0.00	40.21	78.42	20.59	30.93	46.21	12.80	64.38	97.08	11.13	45.17	73.90
AT2G043770	82.78	88.45	168.64	72.05	57.64	109.37	49.84	67.17	152.98	68.21	71.09	142.89
AT2G044160	27.59	24.12	49.01	20.59	40.77	50.06	17.83	34.36	34.36	22.00	38.42	44.48
AT2G045270	18.39	32.16	39.21	10.29	7.03	16.94	8.69	0.00	50.07	12.46	13.06	35.41
AT2G045660	0.00	402.06	284.06	10.29	176.72	232.00	5.94	61.59	148.58	5.41	213.12	225.08
AT2G045850	9.20	72.37	49.01	10.29	36.14	40.05	11.89	11.20	23.96	10.46	39.57	37.87
AT2G048540	45.98	104.54	195.04	92.64	78.72	191.78	123.45	135.75	303.09	87.35	106.34	230.30
AT2G047240	9.20	16.08	19.80	0.00	5.62	10.78	9.23	0.00	25.66	5.81	7.24	18.68
AT2G047500	18.39	16.08	39.21	0.00	8.43	18.48	3.20	23.79	36.43	7.20	16.10	31.37
AT2G047820	0.00	0.00	19.80	0.00	7.03	16.17	0.00	11.20	28.61	0.00	6.07	21.80
AT2G013330	0.00	8.04	49.01	10.29	36.56	28.50	0.00	15.39	18.39	3.43	19.99	31.97
AT3G002080	796.98	2677.71	2234.88	1816.01	1196.27	2493.99	593.45	1113.97	971.81	1003.15	1680.32	1900.19
AT3G002640	73.56	182.99	215.65	113.22	91.37	187.93	22.40	30.79	102.64	69.73	105.05	168.74
AT3G002920	9.20	24.12	19.80	10.29	11.25	23.11	60.35	95.16	127.05	26.91	43.51	69.59
AT3G004920	551.71	924.73	931.20	689.63	690.90	1037.45	769.48	792.10	3426.06	670.27	759.24	1797.90
AT3G005560	682.05	1188.13	1509.52	782.27	612.91	1498.03	397.31	556.99	1072.57	613.98	789.34	1360.04
AT3G006680	56.17	184.95	188.24	102.83	96.59	178.99	289.50	300.88	490.65	146.97	193.81	281.88
AT3G007140	0.00	8.04	29.41	0.00	11.25	35.43	21.49	37.79	59.40	7.16	19.02	41.41
AT3G008680	137.93	184.95	372.48	82.34	82.94	297.30	277.88	281.29	826.18	166.08	183.06	498.65
AT3G103320	9.20	8.04	19.80	0.00	8.43	19.25	1.37	1.40	11.66	3.52	5.96	16.84
AT3G115110	836.76	972.98	1342.89	905.79	811.12	1736.02	664.04	1095.78	1603.56	812.19	959.96	1560.82
AT3G119400	294.24	981.02	823.38	483.77	470.93	980.46	680.20	1388.68	1727.11	478.41	640.21	1178.98
AT3G146110	0.00	0.00	19.80	0.00	1.41	10.78	0.91	2.80	24.67	0.30	1.40	18.35
AT3G160800	174.71	434.22	695.95	463.19	399.23	900.36	1229.22	3085.82	5844.30	624.37	1306.43	2480.20
AT3G181400	27.59	24.12	49.01	30.88	35.14	52.37	35.20	149.74	176.13	31.22	69.67	82.50
AT3G187400	1167.78	2404.31	3038.65	1898.35	1657.38	2868.11	669.55	1726.54	1570.27	1174.23	1929.08	2492.38
AT3G193400	0.00	80.41	89.22	10.29	32.33	36.97	24.69	41.98	43.26	11.96	51.58	56.15
AT3G211400	27.59	64.33	58.81	10.29	70.29	47.75	15.09	11.20	70.34	17.86	48.60	58.97
AT3G222300	340.22	924.73	901.79	535.24	518.72	1115.24	1213.88	887.28	3636.22	696.45	776.91	1984.42
AT3G233900	432.17	1383.03	1195.86	864.62	1128.82	2039.48	667.08	859.27	1211.91	654.82	1123.72	1482.41
AT3G237400	0.00	8.04	49.01	10.29	8.43	28.50	7.32	16.79	23.51	5.87	11.09	33.67
AT3G252300	27.59	32.16	117.63	10.29	96.97	146.85	75.44	170.73	236.12	37.77	97.62	168.46
AT3G255200	918.51	1752.98	1499.72	761.69	946.07	1852.32	601.68	800.37	1948.01	760.96	1099.81	1769.68
AT3G256600	0.00	8.04	19.80	0.00	4.22	62.99	0.46	0.00	23.78	0.16	4.09	35.28
AT3G259400	0.00	16.08	29.41	20.59	47.80	41.59	67.21	167.94	163.39	29.27	77.27	78.13
AT3G269800	239.07	337.73	598.52	102.93	238.98	398.96	68.75	54.58	116.30	136.25	210.43	360.93

Ran-binding protein 1b (RanBP1b)
40S ribosomal protein S12 (RPS12C)
BGAL9 (Beta galactosidase 9);
catalytic/hydrolase/ phosphoglycolate phosphatase
xanthine/uracil permease family protein
katanin, putative
unknown protein
integral membrane Yip1 family protein
pyruvate kinase, putative
RPL24A (ribosomal protein L24); structural constituent of ribosome
histone H2B, putative
unknown protein
RPL23AA (RIBOSOMAL PROTEIN L23AA);
unknown protein
SPL9 (SQUAMOSA PROMOTER BINDING PROTEIN-LIKE 9); T. F.
nucleic acid binding / nucleotide binding
unknown protein
ribosomal protein L1 family protein
ribonuclease P family protein
80S ribosomal protein L35 (RPL38A)
OASB (O-ACETYL SERINE (THIOL) LYASE B); cysteine synthase
transducin family protein / WD-40 repeat family protein
MTHFR2 (METHYLENETETRAHYDROFOLATE REDUCTASE 2);
glycoprotein M22 family protein
AGL20 (AGAMOUS-LIKE 20); transcription factor
DNA-binding family protein
unknown protein
long-chain-fatty-acid-CoA ligase family protein
ATP binding / microtubule motor
unknown protein
DEL3 (DP-E2F-LIKE PROTEIN 3); DNA binding / transcription factor
40S ribosomal protein S19 (RPS19A)
unknown protein
replication protein-related
40S ribosomal protein S24 (RPS24A)
80S ribosomal protein L22-2 (RPL22B)
80S ribosomal protein L29 (RPL29B)
GPI transamidase component Gpi18 subunit family protein
unknown protein
transferase, transferring glycosyl groups
40S ribosomal protein S14 (RPS14B)
ATP55A (RIBOSOMAL PROTEIN 5A); structural constituent of ribosome
CYP72A7; electron carrier/ heme bind. / iron bind. / monooxygenase/
80S ribosomal protein L37 (RPL37C)
transducin family protein / WD-40 repeat family protein
80S ribosomal protein L30 (RPL30C)
0
FMN binding
80S ribosomal protein L27 (RPL27B)
80S ribosomal protein L36a/L44 (RPL36aA)
unknown protein
ATL5 (A. THALIANA RIBOSOMAL PROTEIN L5);
ROF1 (ROTAMASE FKBP 1); FK506 bind./cam bind./peptidyl-prolyl e.-t. isom.
calcium ion binding
transcription factor S-II (TFIS); domain-containing protein
mitotic spindle checkpoint protein, putative (MAD2)

AT3G27190	0.00	24.12	49.01	10.29	40.77	73.17	19.20	32.19	48.81	9.83	32.36	57.00	uracil phosphoribosyltransferase, put. /
AT3G27906	0.00	0.00	19.60	18.27	22.34	23.34	0.46	0.00	32.93	3.58	6.09	24.96	unknown protein
AT3G28730	91.95	152.78	245.05	20.59	101.21	105.52	233.17	485.61	397.48	115.24	246.54	249.35	ATHMG (ARABIDOPSIS THALIANA HIGH MOBILITY GROUP); T. F.
AT3G42062	0.00	8.04	29.41	0.00	15.46	11.55	0.46	0.00	77.16	0.16	7.83	39.37	transposable element gene
AT3G43960	0.00	56.29	98.02	30.88	74.50	142.49	31.09	100.78	410.58	20.86	77.18	217.03	40S ribosomal protein S29 (RPS29A)
AT3G44340	0.00	16.08	19.60	0.00	23.90	33.89	1.83	2.80	28.35	0.61	14.26	27.28	CE5 (clone eighty-four); protein binding / transporter/ zinc ion binding
AT3G47640	0.00	24.12	19.60	0.00	12.65	20.03	1.37	0.00	32.21	0.46	12.26	23.95	basic helix-loop-helix (bHLH) family protein
AT3G47730	0.00	0.00	19.60	0.00	14.06	36.97	1.83	0.00	11.04	0.61	4.89	22.54	ATATH1; ATPase, coupled to T. M. movement of substances / transporter
AT3G48930	1103.42	2420.39	2705.38	1554.25	1443.71	3189.39	860.48	2653.38	2259.98	1172.71	2172.49	2721.55	EMB1080 (embryo defective 1080); structural constituent of ribosome
AT3G49890	18.39	40.21	58.81	20.59	36.55	55.53	7.32	18.19	48.27	15.43	31.85	55.21	K1CP-02; ATP binding / microtubule motor
AT3G50240	0.00	16.08	19.60	0.00	19.28	17.71	1.37	7.00	25.12	0.46	14.25	20.81	zinc finger (GATA type) family protein
AT3G51080	0.00	8.04	19.60	0.00	4.22	13.86	0.46	0.00	35.17	0.15	4.09	22.88	C29 male sterility MS5, putative
AT3G51280	91.95	112.58	178.44	51.47	52.01	100.13	21.95	180.53	231.57	55.12	115.04	169.41	ATG2; aminopeptidase/ metalloexopeptidase
AT3G51450	0.00	0.00	19.60	0.00	8.43	13.96	2.29	0.00	46.57	0.76	2.81	28.68	ATG2; aminopeptidase/ metalloexopeptidase
AT3G51800	248.27	1045.35	960.61	236.74	309.27	659.98	264.26	926.45	696.48	249.76	760.35	769.02	unknown protein
AT3G52040	156.32	385.98	352.88	174.98	251.53	361.22	439.83	528.66	708.38	257.04	421.52	474.16	UBQ1 (UBIQUITIN EXTENSION PROTEIN 1); protein bind./struct. of ribosome
AT3G52560	585.49	1083.60	1440.91	792.69	596.04	1434.10	1747.89	2836.71	2748.44	1042.98	1508.78	1874.48	STV1 (SHORT VALVE1); structural constituent of ribosome
AT3G53020	2307.98	3783.27	4714.81	2758.54	2221.08	4809.87	1150.78	2353.90	3493.87	2072.43	2779.42	4339.62	pectate lyase family protein
AT3G53160	228.88	273.40	529.31	504.36	357.06	825.95	357.08	1773.12	1858.73	363.77	501.19	1071.23	40S ribosomal protein S21 (RPS21B)
AT3G53980	312.64	667.42	1019.42	864.62	667.73	1639.75	1527.98	1273.51	3569.72	901.74	869.65	2075.63	mitochondrial substrate carrier family protein
AT3G53990	18.39	32.16	58.81	10.29	32.74	41.59	10.97	23.78	17.32	13.22	29.80	39.24	PUMP1 (PLANT UNCOUPLING MITOCHONDRIAL PROTEIN 1);
AT3G54110	9.20	80.41	68.81	20.59	52.01	100.90	34.29	92.38	136.83	21.36	74.93	102.11	C25
AT3G54500	18.39	16.08	29.41	0.00	23.90	39.97	0.00	26.59	51.50	6.13	22.19	39.29	C30
AT3G54560	606.88	868.45	1146.85	761.89	539.81	1275.44	475.49	1795.51	1715.98	614.89	1067.92	1379.42	HTA11; DNA binding
AT3G55260	18.39	40.21	29.41	0.00	1.41	10.78	22.40	95.16	94.03	13.90	45.59	48.01	unknown protein
AT3G55380	82.76	194.95	147.03	51.47	88.56	180.20	87.78	72.77	145.53	74.00	115.43	150.92	UBC14 (ubiquitin-conjugating enzyme 14); ubiquitin-protein ligase
AT3G55390	18.39	40.21	29.41	0.00	8.43	10.78	0.00	7.00	13.64	6.13	18.55	17.94	integral membrane family protein
AT3G57610	56.17	94.33	186.24	102.93	108.24	189.48	115.67	274.30	200.44	91.26	148.96	189.39	ADSS (ADENYLOSUCCINATE SYNTHASE); adenylosuccinate synthase
AT3G58540	9.20	8.04	19.60	0.00	7.03	22.34	0.81	0.00	138.80	3.37	5.02	60.25	C31 unknown protein
AT3G58660	0.00	0.00	19.60	0.00	25.30	29.27	81.84	95.16	143.83	27.28	40.16	64.23	protein kinase family protein
AT3G58950	211.49	578.96	637.14	524.95	440.00	841.92	318.67	782.30	893.52	351.70	600.42	787.49	60S ribosomal protein L38 (RPL38B)
AT3G59690	36.78	104.54	127.43	30.88	42.17	89.26	24.23	38.19	51.59	30.83	61.96	89.43	dihydrodipicolinate reductase family protein
AT3G62140	9.20	16.08	19.60	0.00	2.81	22.34	5.03	0.00	72.32	4.74	6.30	38.09	unknown protein
AT3G62760	82.76	56.29	215.65	41.17	46.39	143.26	61.38	131.55	227.54	88.44	78.08	195.48	NADH-ubiquinone oxidoreductase-related
AT3G63280	45.98	84.33	147.03	61.78	111.05	97.04	5.94	55.98	51.05	37.89	77.12	99.38	ATMRK1; kinase/ protein serine/threonine/tyrosine kinase
AT3G63340	110.34	206.07	168.64	51.47	84.36	130.93	84.58	205.72	208.43	92.13	166.38	169.67	APG1 (ALBINO OR PALE GREEN MUTANT 1); methyltransferase
AT4G00400	0.00	16.08	19.60	10.29	11.26	16.17	2.74	0.00	15.34	4.36	9.11	17.04	GPAT8 (glycerol-3-phosphate acyltransferase 8);
AT4G01150	36.78	88.45	188.24	61.78	71.98	155.35	148.59	130.15	276.98	82.38	96.77	208.52	unknown protein
AT4G01525	0.00	8.04	98.02	10.29	43.58	73.17	0.00	5.60	59.94	3.43	19.07	77.04	transposable element gene
AT4G02860	18.39	201.03	198.04	41.17	63.26	124.77	31.55	96.56	215.43	30.37	120.28	179.75	0 chloroplast thylakoid lumen protein
AT4G02950	9.20	16.08	88.61	10.29	23.90	25.50	9.14	16.79	131.27	9.54	18.92	76.13	catalytic
AT4G09060	9.20	48.26	49.01	10.29	11.26	26.96	9.60	0.00	14.98	6.63	3.75	30.32	unknown protein
AT4G09140	18.39	32.16	29.41	10.29	37.96	32.35	21.95	50.38	60.74	16.88	40.17	40.83	MLH1 (MUTL-HOMOLOGUE 1); protein binding, bridging
AT4G10270	46.98	84.33	480.30	10.29	44.58	350.44	1.83	8.40	1297.55	19.37	39.24	709.10	wound-responsive family protein
AT4G10320	82.76	192.99	294.06	133.81	175.72	259.56	195.23	891.48	744.18	137.26	420.06	432.60	isoleucyl-tRNA synthetase, putative / isoleucine--tRNA ligase, putative
AT4G10610	46.98	48.26	117.63	10.29	132.14	119.38	16.46	82.57	58.05	24.24	87.85	98.35	CID12; RNA binding
AT4G10920	285.06	287.32	627.33	154.40	378.16	432.85	75.44	250.50	195.24	171.63	295.32	418.47	KELF; DNA binding / transcription coactivator/ transcription regulator
AT4G11120	45.98	32.16	188.24	20.59	61.85	73.17	47.55	107.76	225.86	38.04	67.26	161.69	ribosomal elongation factor Ts (EF-Ts), putative
AT4G12600	156.32	418.14	294.06	228.45	272.72	412.82	102.87	481.42	420.54	181.98	380.76	375.81	translational protein L7Ae/L30e/S12e/Gad645 family protein
AT4G13615	0.00	32.16	78.42	20.59	68.88	49.29	64.47	86.77	119.24	28.36	62.80	82.32	four F5 protein-related / 4F5 protein-related
AT4G14600	0.00	24.12	39.21	0.00	40.77	29.27	2.74	15.39	14.80	0.91	26.76	27.78	0
AT4G14720	9.20	16.08	29.41	0.00	14.06	21.57	6.40	8.90	13.64	5.20	12.85	21.54	PPD2; dioxygenase/ metal ion binding
AT4G14770	0.00	0.00	19.60	0.00	7.03	10.78	5.94	0.00	37.68	1.98	2.34	22.69	TCX2 (TESMIN/TSO1-LIKE CXC 2); transcription factor
AT4G15680	18.39	16.08	39.21	10.29	9.84	35.51	20.57	25.19	61.36	18.42	17.04	39.69	ESD4 (EARLY IN SHORT DAYS 4); SUMO-specific protease
AT4G17260	0.00	112.58	137.23	10.29	15.46	131.70	4.11	7.00	62.90	4.80	45.01	110.61	L-lactate dehydrogenase, putative

AT4G17300	0.00	16.08	29.41	0.00	9.84	15.40	1.93	2.80	29.61	0.81	9.57	24.81
AT4G17410	0.00	8.04	19.60	0.00	12.65	18.48	4.57	0.00	75.64	1.52	6.00	37.91
AT4G17520	211.49	682.88	401.89	226.45	376.74	407.43	176.02	348.87	536.30	204.85	429.83	448.21
AT4G17650	110.34	128.66	188.24	61.76	42.17	134.78	33.38	182.34	135.30	68.48	111.06	162.11
AT4G18730	422.98	611.13	754.76	442.60	469.52	659.08	632.77	771.10	1552.50	499.45	617.25	1088.98
AT4G19180	0.00	0.00	19.60	0.00	9.84	10.78	0.00	0.00	36.97	0.00	3.28	22.45
AT4G19360	18.38	16.08	29.41	10.29	12.65	18.48	19.20	18.19	92.60	15.96	15.64	48.83
AT4G22120	27.59	24.12	68.61	0.00	46.39	33.12	1.93	0.00	66.09	9.80	23.50	58.94
AT4G25225	0.00	0.00	29.41	0.00	7.03	12.32	0.00	0.00	80.47	0.30	2.34	34.07
AT4G26240	73.56	285.36	205.84	72.05	73.10	156.35	12.34	13.89	29.52	52.86	117.48	130.67
AT4G26250	193.10	488.55	450.80	288.21	278.74	517.57	685.91	978.23	1696.26	389.04	585.51	887.91
AT4G26640	9.20	32.16	29.41	20.59	75.91	61.85	12.90	67.17	64.87	14.19	58.42	61.88
AT4G28220	36.78	32.16	78.42	10.29	11.25	22.34	16.46	32.19	34.54	21.18	25.20	45.10
AT4G29360	56.17	144.74	137.23	92.64	158.85	189.48	44.35	152.64	178.36	64.05	152.04	172.02
AT4G29390	487.34	932.78	960.61	658.75	470.93	1137.58	501.10	1478.23	1529.71	649.05	960.98	1209.30
AT4G29460	91.96	192.99	158.83	61.78	81.53	136.32	158.19	284.09	530.18	103.97	186.20	274.45
AT4G29560	9.20	8.04	19.60	0.00	11.25	23.88	2.29	5.60	24.14	3.83	8.30	22.64
AT4G31200	73.56	96.49	176.44	10.29	46.39	79.33	18.75	20.89	98.61	34.20	54.63	118.13
AT4G31985	248.27	916.99	1283.88	844.03	738.02	1383.27	1102.32	4286.58	3085.80	731.54	1890.42	1914.32
AT4G32330	45.98	80.41	78.42	10.29	36.56	39.28	17.37	30.79	73.75	24.56	49.25	63.82
AT4G32420	9.20	8.04	19.60	10.29	23.90	22.34	6.40	0.00	23.06	8.83	10.65	21.67
AT4G33910	0.00	32.16	38.21	20.59	18.27	66.24	6.40	5.60	33.47	9.00	18.88	46.30
AT4G34450	56.17	40.21	88.22	30.88	39.36	61.82	121.16	173.13	350.11	69.07	93.90	168.65
AT4G35070	27.59	32.16	88.22	0.00	2.81	30.81	37.95	123.15	104.71	21.94	52.71	74.58
AT4G35550	0.00	24.12	19.60	0.00	7.03	10.78	2.74	7.00	64.96	0.91	12.72	31.78
AT4G35940	0.00	0.00	19.60	0.00	12.65	15.40	0.91	0.00	80.30	0.30	4.22	38.44
AT4G36420	18.38	56.29	58.81	0.00	16.87	25.42	5.94	8.40	53.83	8.11	27.18	48.02
AT4G36920	46.58	225.15	245.05	123.62	167.28	191.78	79.55	194.63	259.93	83.02	195.65	232.25
AT4G37760	193.10	402.06	362.68	257.62	319.11	425.92	164.14	635.36	425.29	208.28	452.17	404.63
AT4G37830	220.08	514.83	627.33	205.88	266.69	509.87	64.01	142.75	128.31	163.52	307.89	421.84
AT4G38200	0.00	24.12	58.81	10.29	28.12	30.81	6.86	11.20	22.70	5.72	21.14	37.44
AT4G38220	64.37	56.29	117.63	10.29	23.90	34.86	11.89	20.89	118.80	28.85	33.73	80.38
AT4G39630	0.00	40.21	49.01	10.29	14.06	27.73	85.50	189.93	196.94	31.93	81.06	77.86
AT4G39760	18.38	32.16	29.41	10.29	19.68	30.81	10.97	144.14	96.45	13.22	65.33	52.22
AT4G39820	0.00	0.00	39.21	10.29	30.93	67.78	15.54	65.77	46.48	8.81	32.23	51.15
AT4G40060	294.24	619.17	627.33	391.14	393.61	606.14	265.59	648.65	771.09	313.85	563.11	868.19
AT5G02610	0.00	64.33	88.22	0.00	12.65	30.81	4.11	5.60	195.60	1.37	27.53	104.88
AT5G03850	156.32	488.55	546.82	185.27	161.66	315.78	184.71	127.35	355.94	175.43	262.52	408.88
AT5G04930	8.20	24.12	39.21	20.59	42.17	339.86	5.94	0.00	18.48	11.91	22.10	132.45
AT5G05010	257.46	434.22	401.89	154.40	208.46	312.70	140.82	388.25	425.56	184.23	343.31	380.05
AT5G05240	9.20	16.08	19.60	0.00	16.87	35.43	3.20	141.35	136.20	4.13	58.10	63.75
AT5G08650	9.20	24.12	38.21	0.00	19.68	23.11	1.93	1.40	14.80	3.87	15.07	25.71
AT5G07060	652.86	1310.71	1333.09	771.98	891.41	1483.40	647.98	1251.12	1781.92	690.90	1147.75	1526.13
AT5G10110	27.59	32.16	78.42	10.29	42.17	31.58	21.03	50.38	70.79	19.64	41.57	60.26
AT5G11160	0.00	64.33	49.01	61.47	44.98	101.87	20.12	13.88	38.76	23.86	41.10	63.15
AT5G14250	18.38	176.91	168.64	41.17	42.17	174.06	202.08	537.39	412.02	87.22	252.16	260.60
AT5G14920	18.38	24.12	49.01	30.88	23.90	56.99	10.08	16.79	98.70	19.78	21.60	68.23
AT5G14960	9.20	8.04	29.41	0.00	21.09	14.83	6.40	0.00	36.80	5.20	9.71	26.81
AT5G15200	2674.64	3613.99	4498.36	1410.15	1311.57	3706.18	1608.16	3441.28	3476.11	1863.85	2755.61	3890.65
AT5G16080	56.17	104.54	88.22	20.59	46.39	85.49	28.80	249.10	386.53	34.95	133.34	188.75
AT5G16250	174.71	345.77	264.68	113.22	143.39	353.52	138.08	156.74	378.56	142.00	215.30	332.24
AT5G17240	0.00	0.00	19.60	0.00	5.62	25.42	5.94	34.99	72.14	1.98	13.54	39.05

NS1: asparagine-tRNA ligase
zinc ion binding
nuclear RNA-binding protein, putative
DNA-binding family protein
RPL16B: structural constituent of ribosome
nucleoside phosphatase family protein / GDA1/CD39 family protein
EMB3006 (embryo defective 3006)
early-responsive to dehydration protein-related / ERD protein-related
unknown protein
SKS1 (SKU5 SIMILAR 1): copper ion binding / oxidoreductase
60S ribosomal protein L31 (RPL31B)
WRKY20: transcription factor
NDB1 (NAD(P)H dehydrogenase B1);
PFN2 (PROFILIN 2); actin binding / protein binding
40S ribosomal protein S30 (RPS30B)
mitochondrial ATP synthase g subunit family protein
methyltransferase
SWAP (Suppressor-of-White-A-Picot)/surp domain-containing protein
60S ribosomal protein L39 (RPL39C)
peptidyl-prolyl cis-trans isomerase cyclophilin-type family protein
oxidoreductase, 2OG-Fe(II) oxygenase family protein
coatomer gamma-2 subunit, put. /
0
WOX13 (WUSCHEL-RELATED HOMEBOX 13): DNA binding / T. F.
unknown protein
ribosomal protein L12 family protein
AP2 (APETALA 2); transcription factor
ANT (AINTEGUMENTA); DNA binding / transcription factor
cytochrome c oxidase-related
guanine nucleotide exchange family protein
aminoacylase, putative / N-acyl-L-amino-acid amidohydrolase, putative
unknown protein
unknown protein
binding
ATHB16 (ARABIDOPSIS THALIANA HOMEBOX PROTEIN 16);
60S ribosomal protein L35 (RPL35D)
40S ribosomal protein S28 (RPS28B)
ALA1 (aminophospholipid ATPase1); ATPase
TOC34: GTP binding
clathrin adaptor complexes medium subunit-related
0
unknown protein
40S ribosomal protein S4 (RPS4B)
unknown protein
ATER
ATVAMP713 (VESICLE-ASSOCIATED MEMBRANE PROTEIN 713
pentapeptide (FPP) repeat-containing protein
COP13 (CONSTITUTIVE PHOTOMORPHOGENIC 13); protein binding
gibberellin-regulated family protein
GMII (GOLGI ALPHA-MANNOSIDASE II); alpha-mannosidase
40S ribosomal protein S9 (RPS9B)
0
unknown protein
SDG40 (SET DOMAIN GROUP 40)

AT5G17620	18.39	16.08	68.81	41.17	30.93	75.48	19.20	13.98	33.38	26.26	20.33	59.19	0	IRNA (guanine-N7)-methyltransferase
AT5G17660	0.00	0.00	29.41	0.00	0.00	10.78	4.57	0.00	13.46	1.52	0.00	17.89		binding / protein binding
AT5G17930	18.39	24.12	98.02	30.88	50.61	81.62	26.52	86.77	229.52	25.26	53.83	129.72		RAN-1; GTP binding / GTPase/ protein binding
AT5G20010	286.66	337.73	470.50	308.78	258.66	657.62	102.41	98.38	158.27	225.95	231.92	385.47		unknown protein
AT5G20130	0.00	16.08	19.60	10.29	8.84	38.51	21.03	18.16	47.64	7.01	14.71	35.25		adaplin family protein
AT5G22780	0.00	56.29	78.42	10.29	21.09	137.86	8.23	7.00	14.63	6.17	28.12	78.97		HCF139; protein binding
AT5G23120	0.00	24.12	19.60	10.29	8.43	10.78	3.20	0.00	12.46	1.07	10.85	14.44		disease resistance family protein / LRR family protein
AT5G23400	0.00	32.16	68.81	10.29	26.71	25.42	1.37	22.39	61.46	3.89	27.09	51.83		RPS11-BETA (RIBOSOMAL PROTEIN S11-BETA); struct. of ribosome
AT5G23740	312.64	486.55	617.53	328.38	234.76	690.70	163.22	261.70	570.29	268.44	331.87	582.84		SSI1 (SUPPRESSOR OF SA INSENSITIVITY 1); starch synthase/transferase
AT5G24300	18.39	16.08	49.10	20.69	18.27	38.51	9.14	8.40	27.46	16.04	14.25	38.33		unknown protein
AT5G25480	18.39	24.12	98.02	10.29	23.90	118.61	6.40	7.00	107.49	11.89	18.34	108.04		P-P-bond-hydrolysis-driven protein transmembrane transporter
AT5G27365	36.78	56.29	68.81	10.29	28.12	48.52	14.17	32.18	86.60	20.42	38.86	64.31		seryl-RNA synthetase / serine-RNA ligase
AT5G27470	27.59	176.91	176.44	41.17	116.27	155.58	57.61	141.35	192.06	42.12	144.51	171.38		ribosomal protein L18 family protein
AT5G27620	8.20	24.12	19.60	0.00	14.06	23.88	2.74	11.20	15.07	3.98	16.46	19.62		LSH1 (LIGHT-DEPENDENT SHORT HYPOCOTYLS 1)
AT5G28480	46.98	128.86	441.09	41.17	43.58	143.28	50.28	36.39	76.27	45.81	89.54	220.21		protein binding
AT5G30680	0.00	24.12	29.41	10.29	14.06	20.80	3.20	4.20	12.65	4.50	14.13	20.95		RIO1 family protein
AT5G37660	8.20	8.04	68.81	10.29	7.03	20.03	33.38	48.18	91.43	17.82	20.42	60.02		NADP-dependent oxidoreductase, putative
AT5G38000	0.00	0.00	29.41	0.00	18.27	20.03	1.37	7.00	36.80	0.46	8.42	28.41		forkhead-associated domain-containing protein / FHA domain-containing
AT5G38840	18.39	24.12	98.02	20.69	32.33	45.44	12.80	37.78	66.89	17.26	31.41	66.78		80S ribosomal protein L5 (RPL5B)
AT5G39740	1075.83	1684.52	1783.98	948.98	951.69	2171.95	518.84	1438.55	1482.42	846.48	1351.62	1808.12		unknown protein
AT5G39860	0.00	0.00	39.21	0.00	4.22	42.38	0.00	2.80	16.78	0.00	2.34	32.78		unknown protein
AT5G40480	0.00	0.00	29.41	0.00	8.43	11.55	4.57	0.00	41.18	1.52	2.81	27.38		unknown protein
AT5G42780	0.00	24.12	19.60	0.00	5.62	10.78	3.66	0.00	14.00	1.22	9.82	14.79		AHB27 (ARABIDOPSIS THALIANA HOMEBOX PROTEIN 27); leucine-rich repeat transmembrane protein kinase, putative
AT5G43020	56.17	192.99	235.25	41.17	67.48	146.34	16.00	145.64	235.08	37.46	195.34	205.69		80S ribosomal protein L11 (RPL11D)
AT5G45775	275.85	486.39	460.70	329.38	288.77	643.11	484.64	3013.95	2291.12	363.29	1255.40	1131.64		mAOP3 (mitochondrial acyl carrier protein 3); acyl carrier/ cofactor binding
AT5G47630	8.20	32.16	68.81	20.69	33.74	52.37	14.83	9.60	85.86	14.80	25.23	62.28		unknown protein
AT5G47700	1728.69	3083.89	3205.23	1648.89	2780.90	4241.47	362.11	998.22	111.06	1245.89	2274.80	2785.94		FKBP15-2; FK506 binding / peptidyl-prolyl cis-trans isomerase
AT5G48480	1131.00	3312.96	3714.93	1564.54	1731.89	3106.97	669.35	1051.00	1248.54	1121.63	2031.95	2989.50		sterile alpha motif (SAM) domain-containing protein
AT5G48580	18.39	16.08	39.21	10.29	8.43	28.50	7.32	8.40	88.46	12.00	10.97	62.39		unknown protein
AT5G49100	18.39	56.29	68.81	41.17	64.66	90.88	48.48	89.57	130.56	36.01	70.17	98.68		ATCF1 (Ca ²⁺ -binding protein 1); calcium ion binding
AT5G49480	0.00	0.00	19.60	0.00	8.43	10.01	3.20	0.00	11.48	1.07	2.81	13.70		F-box family protein
AT5G51380	6.20	24.12	39.21	0.00	4.22	23.11	1.37	0.00	27.10	3.52	9.45	29.80		unknown protein
AT5G51510	45.98	40.21	88.22	30.88	49.20	102.44	4.11	8.40	88.11	26.99	32.60	82.92		40S ribosomal protein S10 (RPS10C)
AT5G52860	524.12	1157.93	1059.83	689.05	574.95	1362.48	468.35	773.60	1178.98	553.17	835.80	1200.03		MRE11 (meiotic recombination 11); nuclease/ hydrolase /ion binding/ phosphat.
AT5G53160	18.39	24.12	49.01	0.00	7.03	36.20	9.80	26.59	18.30	9.33	19.25	34.50		RNA recognition motif (RRM)-containing protein
AT5G54260	8.20	16.08	29.41	0.00	7.03	19.25	0.00	5.60	16.69	3.07	9.57	21.78		HSP81-3; ATP binding / unfolded protein binding
AT5G54580	91.95	72.37	168.83	20.69	84.66	90.10	9.80	90.97	303.99	40.71	76.00	180.31		HSP81-2 (HEAT SHOCK PROTEIN 81-2); ATP binding
AT5G56010	349.42	619.17	597.93	483.77	331.76	778.67	264.72	408.64	395.40	365.97	463.19	591.00		zinc finger (C3HC4-type RING finger) family protein
AT5G56030	303.44	804.12	705.75	411.72	317.70	646.19	203.00	177.73	351.27	306.05	433.18	567.74		40S ribosomal protein S30 (RPS30C)
AT5G56340	9.20	8.04	19.60	30.88	26.71	54.68	2.74	7.00	17.82	14.27	13.92	82.04		80S ribosomal protein L31 (RPL31C)
AT5G56530	18.39	24.12	39.21	0.00	32.33	56.22	7.32	15.39	18.56	8.57	23.95	38.33		APO2 (ACCUMULATION OF PHOTOSYSTEM ONE 2)
AT5G56670	533.32	864.94	931.20	699.93	641.02	1099.07	339.33	327.47	733.95	523.86	644.48	921.40		ORP3C (OSBP(OXYSTEROL BINDING PROTEIN)-RELATED PROTEIN 3C)
AT5G56710	708.03	1611.74	1421.30	761.69	732.40	1576.69	1185.07	962.07	3072.53	894.93	1035.40	2023.47		unknown protein
AT5G57930	18.39	24.12	49.01	10.29	7.03	40.05	2.74	7.00	14.89	10.48	12.72	34.65		VP2 (VIRE2 INTERACTING PROTEIN2); protein bind. /transcription regulator
AT5G58420	8.20	8.04	39.21	10.29	26.71	29.27	9.23	0.00	27.55	9.24	11.58	32.01		40S ribosomal protein S15A (RPS15aF)
AT5G58500	0.00	16.08	68.81	10.29	12.66	20.80	4.57	27.89	76.36	4.96	18.81	55.28		elongation factor 1-alpha / EF-1-alpha
AT5G58613	174.71	297.52	578.32	72.05	192.59	398.18	1178.39	1864.98	1912.66	474.38	784.73	959.72		replication protein, putative
AT5G58710	36.78	120.62	127.43	20.69	30.93	83.95	63.08	49.98	199.28	40.15	66.84	136.89		40S ribosomal protein S19 (RPS19C)
AT5G59650	597.68	1141.85	1107.64	905.79	951.69	1837.69	271.59	540.19	1023.67	591.68	877.91	1323.00		TUB3; GTP binding / GTPase/ structural molecule
AT5G60390	1508.00	3329.04	3381.53	1638.59	1521.02	2613.27	3548.64	6269.80	6245.10	2230.38	3706.56	4083.30		
AT5G60640	0.00	40.21	78.42	0.00	28.12	33.89	8.40	11.20	10.14	2.13	26.51	40.81		
AT5G61000	18.39	40.21	98.02	61.47	40.77	102.44	176.94	123.16	476.09	82.26	88.04	225.18		
AT5G61170	123.78	2790.29	3138.67	1358.68	1310.16	3095.38	464.98	554.19	704.16	1012.47	1551.55	2302.07		
AT5G62300	275.85	1157.93	1146.85	422.01	365.66	895.74	368.23	337.26	737.72	365.36	628.81	926.77		
AT5G62700	441.37	554.84	862.78	411.72	302.24	713.20	216.28	251.90	395.51	356.45	389.86	853.83		

AGI	A0LD	A1LD	A3LD	B0LD	B1LD	B3LD	C0LD	C1LD	C3LD	AVG 0LD	AVG 1LD	AVG 3LD	code	Annotation
AT5G62930	9.20	16.08	19.60	20.59	14.06	39.28	2.74	0.00	0.00	84.97	10.84	10.05	47.65	GDSL-motif lipase/hydrolase family protein
AT5G65440	0.00	32.16	39.21	0.00	9.84	20.50	22.40	48.98	37.96	7.47	30.33	32.65	63.09 C1	zinc finger (C3HC4-type RING finger) family protein
AT5G66930	0.00	16.08	39.21	10.29	15.46	40.05	5.49	39.19	52.04	5.26	23.58	43.77	287.82 C2	ATDAD1 (DEFENDER AGAINST APOPTOTIC DEATH 1)
AT5G66980	0.00	8.04	39.21	0.00	15.46	13.36	0.91	0.00	12.47	0.30	7.83	#N/A C4	#N/A	
AT5G68030	18.39	40.21	29.41	10.29	43.58	50.06	21.49	37.79	214.26	16.72	40.52	97.91	68.59 C5	bZIP transcription factor family protein
AT5G68570	73.58	410.10	323.47	92.64	136.36	271.11	29.80	48.98	128.22	65.00	168.48	240.83	68.69 C11	ATHB31 (ARABIDOPSIS THALIANA HOMEBOX PROTEIN 31); T. F.
AT5G67510	27.59	104.54	127.43	20.59	50.81	101.97	37.03	155.34	187.88	28.40	103.49	139.89	182.24 C15	leucine-rich repeat family protein
AT5G67540	0.00	0.00	19.60	0.00	4.22	10.01	2.74	2.80	83.52	0.91	2.34	31.05	446.88 C19	FLR1: enzyme inhibitor/transcription factor binding
													179.64 C20	LRP1 (LATERAL ROOT PRIMORDIUM 1); protein homodimerization

Genes for which probes were tested on wild-type apices by *in situ* hybridisation.

AGI	A0LD	A1LD	A3LD	B0LD	B1LD	B3LD	C0LD	C1LD	C3LD	AVG 0LD	AVG 1LD	AVG 3LD	code	Annotation
AT5G64560	9.20	88.45	88.61	10.29	116.27	27.73	8.23	208.92	9.33	9.24	137.88	35.22 D1	364.75 D13	acyl-acyl-carrier-protein) desaturase, putative / stearyl-ACP desaturase, put.
AT4G19160	18.39	176.91	88.61	10.29	205.24	71.93	4.57	4.20	8.08	11.09	128.78	49.44 D3	86.59 D15	unknown protein
AT5G20810	202.29	0.00	0.00	102.93	7.03	19.25	22.40	81.58	16.51	109.21	22.87	11.92 D4	17.00 D20	transcription factor jumonji (jmi)C) domain-containing protein
AT5G23340	0.00	104.54	0.00	0.00	123.71	15.40	10.08	0.00	7.45	3.35	76.08	7.82 D5	0	
AT5G16820	239.07	0.00	29.41	113.22	2.81	3.08	16.00	0.00	0.00	122.77	0.94	10.83 D7	10.83 D7	HSF3 (HEAT SHOCK FACTOR 3); DNA binding / transcription factor
AT1G67280	286.66	8.04	9.80	216.15	64.66	8.47	39.88	15.39	6.82	173.89	29.37	8.39 D8	8.39 D8	lactoylglutathione lyase, putative / glyoxalase I, putative
AT4G16190	137.93	321.85	9.80	228.45	351.44	13.09	60.75	0.00	0.09	138.37	224.36	7.68 D10	7.68 D10	cysteine proteinase, putative
AT3G21720	4801.01	932.78	137.23	2865.90	1117.57	186.36	521.67	1.40	1.35	2698.19	693.92	101.65 D11	101.65 D11	ICL (ISOCITRATE LYASE); catalytic/ isocitrate lyase
AT1G12805	0.00	0.00	245.05	0.00	0.00	151.73	0.00	1.40	6.37	0.00	0.47	134.39 D12	134.39 D12	nucleotide binding
AT1G43800	0.00	8.04	509.71	0.00	1.41	251.95	0.46	2.80	332.70	0.15	4.08	364.75 D13	364.75 D13	acyl-acyl-carrier-protein) desaturase, putative / stearyl-ACP desaturase, put.
AT2G38940	18.39	0.00	98.22	30.88	2.81	45.44	8.69	102.16	31.78	19.32	34.99	55.14 D14	55.14 D14	COI1 (CORONATINE INSENSITIVE 1); protein binding / ubiquitin-protein ligase
AT4G33560	0.00	0.00	166.64	0.00	0.00	92.42	0.00	0.00	0.72	0.00	0.00	86.59 D15	86.59 D15	unknown protein
AT4G29010	27.59	104.54	39.21	10.29	129.33	55.45	69.75	13.99	35.89	34.88	82.82	43.52 D19	43.52 D19	AIM1 (ABNORMAL INFLORESCENCE MERISTEM); enoyl-CoA hydratase
AT1G68370	27.59	128.66	9.80	0.00	108.24	20.03	9.80	23.79	21.17	12.40	96.90	17.00 D20	17.00 D20	ARG1 (ALTERED RESPONSE TO GRAVITY 1); cytoskeletal protein binding
AT5G37770	0.00	241.24	0.00	10.29	147.80	54.88	5.03	2.80	8.70	5.11	130.55	21.13 D21	21.13 D21	TCH2 (TOUCH 2); calcium ion binding
AT3G06240	0.00	104.54	0.00	10.29	102.82	10.78	4.11	0.00	2.69	4.80	69.05	4.49 D23	4.49 D23	F-box family protein
AT1G22190	211.49	217.11	9.80	247.03	188.37	53.14	449.06	0.00	3.95	302.19	135.16	22.30 D25	22.30 D25	AP2 domain-containing transcription factor, putative
AT2G17800	36.78	96.49	137.23	20.59	73.10	121.98	55.78	123.15	57.96	37.72	97.58	105.63 D28	105.63 D28	ARAC1; GTP binding
AT1G78920	248.27	570.92	519.51	82.34	427.35	524.50	119.59	237.91	61.46	149.07	412.06	368.49 D27	368.49 D27	ATP binding
AT1G79530	202.29	395.98	303.86	113.22	334.57	380.48	105.61	513.60	398.50	140.38	411.38	350.85 D39	350.85 D39	GAPCP-1 (GLYCERALDEHYDE-3-P DEHYDROGENASE OF PLASTID 1);
AT2G27020	450.56	1029.27	548.92	473.48	943.26	589.97	449.97	512.20	986.61	457.87	828.24	708.60 D30	708.60 D30	PAG1; endopeptidase/ peptidase/ threonine-type endopeptidase
AT2G24150	18.39	0.00	58.81	0.00	7.03	36.51	8.23	2.80	3.32	3.28	3.28	33.65 D31	33.65 D31	HHP3 (heptahelical protein 3); receptor
AT3G09090	36.78	8.04	58.81	30.88	19.68	93.96	11.43	5.60	238.31	26.36	11.11	130.39 D32	130.39 D32	DEX1 (DEFECTIVE IN EXINE FORMATION 1); calcium ion binding
AT1G03710	9.20	8.04	88.61	0.00	9.84	77.79	68.52	2.80	46.57	22.57	6.89	64.32 D33	64.32 D33	0
AT1G37130	0.00	0.00	88.22	10.29	7.03	60.08	10.06	0.00	86.10	6.78	2.34	79.13 D35	79.13 D35	NIA2 (NITRATE REDUCTASE 2); nitrate reductase (NADH)
AT2G15000	27.59	8.04	78.42	10.29	12.65	73.94	31.09	55.98	20.28	22.99	25.56	57.54 D38	57.54 D38	unknown protein
AT1G64620	9.20	8.04	107.82	10.29	15.46	89.34	30.83	121.75	44.23	16.71	48.42	80.47 D37	80.47 D37	Dof-type zinc finger domain-containing protein
AT1G68260	16568.08	894.53	98.02	1152.82	109.65	36.20	6912.09	111.96	77.43	9107.86	368.71	70.55 D39	70.55 D39	unknown protein
AT3G10640	91.95	8.04	19.60	30.88	2.81	40.32	18.75	58.78	6.64	47.19	23.21	22.35 D40	22.35 D40	VPS60.1
AT4G28190	257.46	8.04	9.80	20.59	1.41	13.09	1.37	0.00	10.86	93.14	3.15	11.25 D41	11.25 D41	zinc finger (CCH-type) family protein
AT5G56210	166.51	0.00	19.60	30.88	0.00	20.03	8.69	18.19	23.78	68.36	6.06	21.14 D42	21.14 D42	WIP2 (WPP-domain Interacting Protein 2); protein heterodimerization

AT1G07590	275.85	546.80	9.80	8944.65	10231.06	422.07	67.21	5.60	18.57	3085.91	3594.49	150.15	D45	pentatricopeptide (PPR) repeat-containing protein
AT2G33830	2796.13	876.49	9.80	247.03	46.20	9.24	37.03	102.16	3.59	1023.40	342.82	7.54	D47	dormancy/auxin associated family protein
AT2G40000	321.83	0	0	1543.98	953.1	116.299	36.1192	0	0.08972	633.97	317.70	38.80	D48	HSPRO2 Arabidopsis ortholog of Sugar beet HS1 PRO-1 2
AT5G48180	367.81	1594.11	86.81	4209.85	3453.93	177.14	368.88	51.78	3.95	1686.78	1686.61	83.24	D49	NSP5 (NITRILE SPECIFIER PROTEIN 5)
AT1G55020	137.93	152.78	0.00	555.82	434.38	6.16	7.77	2.80	3.14	233.84	196.65	3.10	D51	LOX1: lipoxygenase
AT2G32510	119.54	0.00	0.00	752.27	317.70	1.54	6.86	7.00	2.78	302.89	108.23	1.44	D52	MAPKKK17: ATP binding / kinase
AT1G15380	56.17	289.48	9.80	638.17	1396.39	32.35	115.22	0.00	0.00	289.52	551.96	14.05	D53	lactoylglutathione lyase family protein / glyoxalase I family protein
AT1G20890	18.39	8.04	127.43	0.00	0.00	23.11	5.94	7.00	12.74	8.11	5.01	54.42	D54	unknown protein
AT1G80950	8.20	8.04	49.01	0.00	2.81	29.27	0.81	1.40	20.73	3.37	4.08	33.00	D55	phospholipid/ glycerol acyltransferase family protein
AT3G15450	36.78	434.22	29.41	1070.48	1672.94	94.73	533.13	32.19	28.08	548.46	713.09	50.74	D57	unknown protein
AT3G29970	0.00	0.00	39.21	0.00	0.00	19.25	0.00	0.00	0.63	0.00	0.00	19.70	D59	germination protein-related
AT4G40060	0.00	64.33	88.22	0.00	12.65	30.81	4.11	5.60	195.60	1.37	27.53	104.88	C21	ATHB16 (ARABIDOPSIS THALIANA HOMEBOX PROTEIN 16); T. F.
AT1G09390	0.00	0.00	19.60	0.00	16.87	29.27	0.00	2.80	176.90	0.00	6.56	76.29	C22	GDSL-motif lipase/hydrolase family protein
AT1G03170	0.00	0.00	58.81	0.00	0.00	14.63	0.00	1.40	88.29	0.00	0.47	53.81	C23	unknown protein
AT3G54110	9.20	90.41	88.81	20.59	52.01	100.90	34.29	92.38	136.93	21.36	74.93	102.11	C25	PUMP1 (PLANT UNCOUPLING MITOCHONDRIAL PROTEIN 1);
AT3G55600	0.00	0.00	9.80	0.00	2.81	8.47	1.83	22.39	86.31	0.61	8.40	28.19	C26	0
AT1G49580	0.00	0.00	9.80	0.00	7.03	6.93	0.46	5.60	52.76	0.15	4.21	23.16	C27	calcium-dependent protein kinase, putative / CDPK, putative
AT2G43190	0.00	0.00	39.21	0.00	14.06	23.88	3.66	16.79	72.77	1.22	10.28	45.29	C28	ribonuclease P family protein
AT3G51080	0.00	8.04	19.60	0.00	4.22	13.86	0.46	0.00	35.17	0.15	4.09	22.89	C29	zinc finger (GATA type) family protein
AT3G54500	18.39	16.08	29.41	0.00	23.90	36.97	0.00	26.59	51.50	6.13	22.19	39.29	C30	0
AT3G58540	9.20	8.04	19.60	0.00	7.03	22.34	0.91	0.00	138.90	3.37	5.02	60.25	C31	unknown protein

Color key:

 confirmed by *in situ* hybridisation

 signal by *in situ* hybridisation, pattern not confirmed

 no signal by *in situ* hybridisation

Appendix III. List of abbreviations

General abbreviations

amiRNA	artificial micro RNA
bp	base pairs
cDNA	complementary DNA
Col	Columbia
CZ	central zone
DNA	deoxyribonucleic acid
dNTP	deoxyribonucleotide triphosphate
dsRNAi	double-stranded RNA interference
GA	gibberellin
GO	gene ontology
kb	kilo bases
LB	Luria-Bertani
LCM	laser capture microdissection
LD	long days
<i>Ler</i>	Landsberg <i>erecta</i>
LRR	LEUCINE-RICH REPEAT
miR	micro RNA
mRNA	messenger RNA
PCR	polymerase chain reaction
PZ	peripheral zone
RNA	ribonucleic acid
RT-PCR	Reverse transcriptase PCR
SAM	shoot apical meristem
SD	short days
UTR	Untranslated region

Name of the genes

AG	AGAMOUS
AGL24	AGAMOUS-LIKE 24
AP1	APETALA1

CAL	CAULIFLOWER
CDF	CYCLING DOF FACTOR
CLV	CLAVATA
CO	CONSTANS
FD	FD
FLC	FLOWERING LOCUS C
FT	FLOWERING LOCUS T
FUL	FRUITFULL
KNAT1	KNOTTED1-LIKE IN ARABIDOPSIS THALIANA
LFY	LEAFY
SMZ	SCHLAFMUTZE
SNZ	SCHNARCHZAPFEN
SOC1	SUPPRESSOR OF OVEREXPRESSION OF CONSTANS
SPL	SQUAMOSA PROMOTER BINDING PROTEIN-LIKE
STM	SHOOTMERISTEMLESS
SUC2	SUCROSE-PROTON SYMPORTER 2
SVP	SHORT VEGETATIVE PHASE
TFL1	TERMINAL FLOWER1
TSF	TWIN SISTER OF FT
UFO	UNUSUAL FLORAL ORGAN
WUS	WUSCHEL

Acknowledgments

I would like to thank first of all my PhD supervisor, Prof. George Coupland, for his supervision, and for giving me the opportunity to work in this project and to learn so much during these years.

I would like to thank Prof. Wolfgang Werr for being my second examiner, Prof. Martin Hülkamp for being head of my committee, and Wim Soppe for being Beisitzer.

Thanks to Peter Huijser, for being my second supervisor during my PhD.

Then I would like to thank many people from the lab, especially Fabio Fornara for his great help in the lab, and Doris Falkenhan for technical assistance.

Antonis Giakountis, Nabil Elrouby, Isabella Nougalli and Mitzi Villajuana for the nice time in the lab (and outside).

Fernando Andrés and Markus Berns for useful discussion and training.

Christiane Kiefer, Tom Colby and Franziska Turck for the nice music breaks.

Aimone Porri for the TFL1 challenge and the funny time.

Alfredo Sanchez for sharing the last “race” of the PhD.

I would also like to thank Prof. Martin Kater, Lucia Colombo and the people from their lab in Milano, Alice Sessa and Carmen Fornell.

Erklärung

“Ich versichere, dass ich die von mir vorgelegte Dissertation selbstständig angefertigt, die benutzten Quellen und Hilfsmittel vollständig angegeben und die Stellen der Arbeit – einschliesslich Tabellen, Karten und Abbildungen-, die anderen Werken Im Wortlaut oder dem Sinn nach entnommen sind, in jedem Einzelfall als Entlehnung kenntlich gemacht habe; dass diese Dissertation noch keener anderen Fakultät oder Universität zur Prüfung vorgelegen hat; dass sie – abgesehen von unten angegebenen Teilpublikationen – noch nicht veröffentlichung vor Abschluss des Promotionsverfahrens nicht vornehmen werde. Die Bestimmungen dieser Promotionsordnung sind mir bekannt. Die von mir vorgelegte Dissertation ist von Prof. Dr. George Coupland betreut worden.”

Köln, den Mai 2008

Teilpublikationen

Jang S, Torti S, Coupland G (2009) Genetic and spatial interactions between *FT*, *TSF*, and *SVP* during the early stages of floral induction in *Arabidopsis*. *The Plant Journal* 60, 614-625.

Lebenslauf

Persönliche Informationen

Name: Torti

Vorname: Stefano

Geburtsdatum: 18.01.78

Geburtsort: Narni

Nationalität: Italienisch

Familienstand: ledig

Ausbildung

- | | |
|-----------|--|
| 1993-1997 | Abitur: Lyceum "G. Galilei", Terni (Italien) |
| 1997-2004 | Studium der Biotechnologie, Universität Bologna (Italien) |
| 2003 | Auslandsaufenthalt am York Structural Biology Laboratory, York (England) |
| 2003 | Diplomarbeit: "Expression, purification, and crystallisation of UreE from <i>Bacillus Pasteurii</i> : structural studies on a Nickel-Chaperonine." |
| 2004 | Abschluss: Diplom Biotechnologie |
| 2005 | Master Kurs für Bio-Informatik, Universität Bologna, mit Auslandsaufenthalt am Gulbenkian Institute, Oeiras (Portugal) |
| 2005-2006 | Stipendium am Universität Bologna in der Arbeitsgruppe von Prof. Claudio Franceschi |
| July 2006 | Beginn der Doktorarbeit am Max-Planck-Institut für Züchtungsforschung, Köln in der Arbeitsgruppe von Prof. Dr. George Coupland. |

